

THE UNIVERSITY OF MANITOBA

ORTHOBARIC VOLUMES AND VAPOR PRESSURES  
OF CERTAIN PURE LIQUIDS AND VAPOR-LIQUID EQUILIBRIA IN  
A BINARY MIXTURE UP TO THE CRITICAL REGION

A Thesis

Presented to

The Faculty of Graduate Studies

in Partial Fulfilment of

the Requirements for the Degree of

Doctor of Philosophy

by

Rabindra Mohan Chatterjee



Winnipeg, Canada

December, 1968

c1968

TO JHARNA

## ACKNOWLEDGEMENTS

I have great pleasure in acknowledging my debt of gratitude to Professor A. N. Campbell for his invaluable advice during the course of this research. I am also indebted to Dr. E. M. Kartzmark for her interest and for many helpful discussions. Both of them provided more intellectual stimulation and personal encouragement than I could hope to repay.

I owe much to many people who, on many counts, contributed in one way or another to the successful completion of this research. I wish to thank Mr. G. Epp and Mr. H. Griffiths for fabricating all the glass apparatus. The assistance extended by Mr. G. Trider and his staff of the Science Technical Workshop is gratefully acknowledged. Special thanks are due to Mr. J. Gould who constructed the shaking mechanism in the vapor-liquid equilibrium determination.

Dr. D. Ambrose, National Physical Laboratory, Division of Chemical Standards, Teddington, England has been most generous, making available to me reprints, computer programs and references he knew would be of interest to me. I am grateful to him and Dr. J. F. Counsell of the same place, for processing my vapor pressure data by KDF 9 computer.

The financial help in the form of a Graduate Fellowship by the University of Manitoba is gratefully acknowledged.

## ABSTRACT

The specific volumes and pressures in the saturated states of the pure liquids acetone, benzene, chloroform, and carbon tetrachloride, and the saturation pressure of 7 mixtures of the binary system acetone-benzene were determined from a temperature of 100°C and a pressure of about 2 atmosphere up to the highest temperature and pressure at which liquid and vapor coexist. The vapor-liquid equilibria of the binary mixtures were independently measured by a static method up to the critical region. The critical temperatures of the pure compounds as well as those of mixtures were determined by the disappearance-of-the-meniscus method. Critical densities of the pure compounds were obtained by the application of the law of rectilinear diameter, and the critical pressures by extrapolation of the  $\log P$  vs  $1/T$  line to the critical temperature.

P-T-x relations at the liquid-vapor phase boundaries of the binary system, as obtained by the determination of the bubble-point-pressure vs temperature curves of a series of mixtures of known composition, did not indicate any existence of an azeotrope in the range of temperature and pressure studied in this research. The binary data obtained were treated thermodynamically to yield the liquid phase activity coefficients. The partial molal volumes in the liquid mixture required for the Poynting correction (effect of pressure on liquid phase properties) for liquid-phase activity coefficients were also obtained. The fugacity coefficient of a component in the vapor mixture was obtained by a modified Redlich-Kwong equation as suggested by Chueh and Prausnitz



(Ind. Eng. Chem. Vol. 60, No. 3, pp. 34-52 (1968)). Following their modification of the van Laar equation, several binary liquid phase parameters such as binary interaction constant, Henry's constant and dilation constant, as required for the solution model for excess Gibbs energy, were calculated with the aid of an IBM 360/65 electronic computer.

## GLOSSARY OF SYMBOLS

- A,B,C,D,E - constants in vapor pressure equations, liquid density equation, also binary parameters defined in equations 58, 65, 66.
- a,b - constants in van der Waals' equation (1) and Redlich-Kwong equation (25).
- $c_v, c_p$  - specific heat at constant volume and constant pressure.
- $f_i$  - fugacity of component i.
- $f_i^o$  - reference fugacity of component i.
- $G^E$  - excess Gibbs free energy.
- H - enthalpy in Table II.
- $H_2(1)$  - Henry's constant for solute 2 in solvent 1 as defined in equation 43.
- $K_T$  - isothermal compressibility.
- $k_{ij}$  - characteristic constant for i-j interaction.
- $n_i$  - number of moles of component i.
- N - number of components.
- P - total pressure.
- $P_c$  - critical pressure.
- $P^r$  - constant reference pressure.
- $P^s$  - saturation vapor pressure.
- $P_0$  - constant reference pressure of zero pressure.
- q - effective molal volume defined by equations 60 and 61.
- R - gas constant.
- S - entropy.
- T - temperature.
- $T_c$  - critical temperature.
- $T_{CM}$  - pseudocritical temperature of a mixture.
- $T_{CM}^{\prime}$  - corrected pseudocritical temperature of a mixture.
- $T_{CT}$  - true experimental critical temperature of a mixture.
- $T_m$  - temperature of disappearance of meniscus.
- $T_R$  - reduced temperature.

$T^*$	- characteristic constant of a binary system, used in correlating dilation constants.
$v$	- molal volume of the liquid phase or vapor phase.
$v_c$	- critical volume.
$v_{cM}$	- pseudocritical volume of a mixture.
$v'_{cM}$	- corrected pseudocritical volume of a mixture.
$v_{cT}$	- true critical volume of a mixture.
$v_R$	- reduced volume.
$v_i^L$	- partial molal volume of component $i$ in the liquid mixture.
$v_l, v_g$	- orthobaric volumes.
$V$	- total volume.
$x$	- mole fraction in the liquid-phase.
$y$	- mole fraction in the vapor phase.
$Z$	- compressibility factor.
$Z_c$	- critical compressibility factor.

#### Subscripts.

$c$	- critical.
$g$	- gas.
$i$	- component $i$ .
$ii (j)$	- $i$ - $i$ interaction in the environment of $j$ .
$ij$	- $i$ - $j$ interaction.
$l$	- liquid.
$M$	- mixture.
$R$	- reduced property.

#### Superscripts.

$E$	- excess property.
$id$	- ideal property.
$L$	- liquid phase.
$(P^0)$	- at constant reference pressure of zero.
$(P^r)$	- at constant reference pressure.
$s$	- at saturation.
$o$	- reference state.
$\infty$	- infinite dilution.

Greek Letters.

- $\alpha, \beta, \gamma, \delta$  - critical exponents defined in Table I.
- $\alpha_{12}$  - interaction constant of molecules 1 and 2.
- $\alpha_{22(1)}$  - self-interaction constant of molecules 2 in the environment of molecules 1.
- $\gamma_i$  - activity coefficient of component i.
- $\eta_{2(1)}$  - dilation constant of solute 2 in solvent 1.
- $\eta^*$  - characteristic constant of a solute, used in correlating dilation constants.
- $\theta$  - surface fraction defined by equation 88.
- $\nu_{ij}$  - correlating parameter for critical volume in equation 90.
- $\rho$  - density.
- $\tau_{ij}$  - correlating parameter for critical temperature in equation 89.
- $\phi_i$  - fugacity coefficient of component i in vapor phase defined by equation 21.
- $\Phi$  - volume fraction defined in equation 55.
- $\omega$  - acentric factor as defined in page 46.
- $\Omega_a, \Omega_b$  - dimensionless constants in Redlich-Kwong equation (25).

TABLE OF CONTENTS

<u>CHAPTER</u>	<u>PAGE</u>
I. GENERAL INTRODUCTION.....	1
THEORETICAL INTRODUCTION .....	2
I. CRITICAL PHENOMENA .....	2
I(a) The Critical Point .....	2
I(b) The Critical Region .....	4
I(c) Classical Liquid-Vapor Transitions .....	8
I(d) Recent Developments in Critical Phenomena ...	13
I(e) Thermodynamics of the Critical Point .....	21
II. THERMODYNAMIC PROPERTIES FROM PVT DATA .....	24
III. VAPOR-LIQUID EQUILIBRIA .....	30
III A. General Equilibrium Equation .....	31
III B. The Representation of Vapor-Phase Fugacity Coefficients .....	36
III B(I). Equation of State .....	36
III B (II). Fugacity Coefficient .....	43
III B (III). Fugacity Coefficients from Revised Redlich-Kwong Equation .....	45
III C. Liquid-Phase Activity Coefficients .....	46
III C (I). Reference States .....	46
III C (II). Gibbs-Duhem Equation .....	48
III C (III). Effect of Composition .....	50
III C (IV). Choice of Reference Pressure .....	52
III C (V). Analytical Representation of Activity Coefficients .....	54
III C (V)(a) Excess Gibbs Energy .....	54
III C (V)(b) A Dilated Van Laar Model for Binary Mixtures .....	56
III C (V)(c) Mixtures of Condensable Components	59
III C (VI) Effect of Pressure .....	61
III C (VI)(a) Partial Molal Volume from an Equation of State .....	62

TABLE OF CONTENTS (Cont'd)

<u>CHAPTER</u>	<u>PAGE</u>
I(c) Chloroform .....	114
I(d) Carbon Tetrachloride .....	114
II. VAPOR PRESSURE .....	121
II(a) Acetone .....	121
II(b) Benzene .....	121
II(c) Chloroform .....	126
II(d) Carbon Tetrachloride .....	126
III. CRITICAL TEMPERATURE .....	126
III(a) Pure Liquids .....	126
III(b) The System Acetone-Benzene .....	126
IV. VAPOR-LIQUID EQUILIBRIUM .....	133
V. DISCUSSION .....	140
I. CORRELATION OF DATA .....	140
I(a) Critical Constants .....	140
I(b) Density .....	160
I(c) Vapor Pressure .....	164
II. THERMODYNAMIC ANALYSIS .....	177
II(a) Vapor-liquid Equilibrium Data .....	177
II(a) I. Analysis of the Binary System where $T_{R_1}$ and $T_{R_2} < 0.93$ .....	178
II(a) II. Thermodynamic Consistency Test and Screening of Data .....	186
II(a) III. Analysis of the Binary System where $T_{R_2} \geq 0.93$ .....	188
SUMMARY AND CONCLUSIONS .....	201
APPENDIX .....	204
BIBLIOGRAPHY .....	207

LIST OF FIGURES

<u>FIGURE</u>	<u>PAGE</u>
1. Plot of Pressure against Volume at Different Temperatures near the Critical Temperature (Mayer's "Derby" Hat) .....	6
2. The Orthobaric Densities of a Typical Pure Substance ..	9
3. Apparatus for Degassing and Preparing Mixtures of Liquid Samples .....	87
4. The Thermostat .....	92
5. Transfer of Sample to the Mercury-Air Manometer .....	101
6. Cross-Sectional View of the Glass and Metal Bombs for Vapor-Liquid Equilibrium Determination .....	107
7. The Metal Bomb in the High-Temperature Bath with the Shaking Mechanism .....	111
8. Orthobaric Densities of Acetone .....	113
9. Orthobaric Densities of Benzene .....	116
10. Orthobaric Densities of Chloroform .....	118
11. Orthobaric Densities of Carbon Tetrachloride.....	120
12. Vapor Pressure of Acetone from 100°C to $T_c$ .....	123
13. Vapor Pressure of Benzene from 100°C to $T_c$ .....	125
14. Vapor Pressure of Chloroform from 100°C to $T_c$ .....	128
15. Vapor Pressure of Carbon Tetrachloride from 100°C to $T_c$	130
16. Gas-Liquid Critical Temperatures of the Benzene-Acetone System as a Function of Mole Fraction and Surface Fraction .....	132
17. Lines of Constant Composition on a Pressure-Temperature Diagram .....	136
18. Liquid-Vapor Composition Equilibrium Curves for the System Benzene-Acetone at 100°, 125°, 150°, 175°, 200°, 225°, 250°, 260°, and 270°C .....	138

LIST OF FIGURES (Cont'd)

<u>FIGURE</u>	<u>PAGE</u>
19. Plot of $d_l$ and $d_v$ versus $(T_c - T)^{1/3}$ for Acetone .....	151
20. Plot of $d_l$ and $d_v$ versus $(T_c - T)^{1/3}$ for Benzene .....	152
21. Plot of $d_l$ and $d_v$ versus $(T_c - T)^{1/3}$ for Chloroform ..	153
22. Plot of $d_l$ and $d_v$ versus $(T_c - T)^{1/3}$ for Carbon Tetrachloride .....	154
23. Plot of Henry's constants $H_2(1)^{(PS)}$ for Acetone (2) in Benzene (1) at 225°, 250°, 260°, and 270°C .....	196



LIST OF TABLES

<u>TABLE</u>		<u>PAGE</u>
I.	Critical Point Exponents for Gas-Liquid Transition ..	12
II.	Dimensionless Form of Thermodynamic Functions .....	25
III.	Summary of Thermodynamic Functions .....	28
IV.	Most Recent Critical Data .....	82
V.	Orthobaric Densities of Acetone .....	112
VI.	Orthobaric Densities of Benzene .....	115
VII.	Orthobaric Densities of Chloroform .....	117
VIII.	Orthobaric Densities of Carbon Tetrachloride .....	119
IX.	Vapor Pressure of Acetone .....	122
X.	Vapor Pressure of Benzene .....	124
XI.	Vapor Pressure of Chloroform .....	127
XII.	Vapor Pressure of Carbon Tetrachloride .....	129
XIII.	Gas-Liquid Critical Temperatures of the System Benzene-Acetone .....	131
XIV.	Experimental Saturation Pressure of the System Benzene-Acetone .....	134
XV.	Experimental Vapor-Liquid Equilibria of the System Benzene-Acetone at Different Isotherms .....	137
XVI.	Density and Refractive Index Data for the System Benzene-Acetone .....	139
XVII.	Statistical Analysis of the Francis Equation for Liquid Density Data .....	162
XVIII.	Statistical Analysis of the Coefficients of the Frost- Kalkwarf Equation .....	168
XIX.	Treatment of Vapor Pressure Data for Benzene by Cox and Cragoe Equations .....	170

LIST OF TABLES (Cont'd)

<u>TABLE</u>		<u>PAGE</u>
XX.	Treatment of Vapor Pressure Data for Carbon Tetrachloride by Cox and Cragoe Equations .....	171
XXI.	Polynomial Expressions for the Vapor Pressure Data of Acetone .....	173
XXII.	Polynomial Expressions for the Vapor Pressure Data of Benzene .....	174
XXIII.	Polynomial Expressions for the Vapor Pressure Data of Chloroform .....	175
XXIV.	Polynomial Expressions for the Vapor Pressure Data of Carbon Tetrachloride .....	176
XXV.	Thermodynamic Analysis of the System Benzene (1) - Acetone (2) up to $T_{R_2} = 0.93$ .....	181
XXVI.	Thermodynamic Analysis of the System Benzene (1) - Acetone (2) for Isotherms at $T_{R_2} \geq 0.93$ .....	189

## CHAPTER I.

### GENERAL INTRODUCTION

During the last two decades many theoretical, computational, and experimental developments have been made in the study of the properties of gases and liquids. It is unfortunate that both theory and practice in the study of liquid mixtures have been separated from the study of pure liquids.

The basic problem in the thermodynamics of liquid mixtures has been to relate the properties of a mixture to those of its components with a minimum amount of experimental information on the mixture itself. The final goal is to predict the properties of the mixture using only pure-component data. While this goal has not been reached even for the simplest mixtures, much progress has been made in recent years, and for a few types of mixtures it is now possible to make good estimates of mixture properties using approximate theories of solutions.

The dependence on the theory of pure fluids has been a feature of most theories of mixtures in the last decade. The practical demands of these theories can only be met by a very detailed knowledge of the equilibrium properties of the pure liquids.

The usefulness of experimental data on the thermodynamic properties of binary systems to test theories or to formulate theories which attempt to predict binary mixture properties from pure-component data is obvious. Another obvious use is the evaluation of parameters characterizing interactions between unlike species, useful not only in the correlation of data for binary mixtures but

also in the prediction of properties for multicomponent systems.

Phase-equilibrium data at high pressures, specially in the critical region, are of considerable interest. Such data are invariably sparse, mainly because of the difficulty of taking into account vapor-phase non-idealities. Present experimental knowledge of equilibrium properties of the critical region is in a rapidly moving state, and the same is true of approximate statistical mechanical theories of the critical region. Any attempt to settle the shape of the coexistence curve experimentally is beset by severe experimental problems and will be commented on in almost all sections of this work. A simplified theory of critical behavior in the liquid-gas transition may be obtained from the van der Waals equation of state. The gas-liquid critical point is the most familiar, but a variety of others exist. A feature of this field is that both experimental data and theoretical insight indicate that critical phenomena in systems as apparently unrelated as gases, binary alloys, and ferromagnets can all be studied from the same point of view. Thus, the disparate fields of physical chemistry, solid-state physics, chemical engineering, and low-temperature physics converge when dealing with critical anomalies.

## THEORETICAL INTRODUCTION

### I. CRITICAL PHENOMENA

#### I(a). The Critical Point

The critical phenomenon was first discovered by de la Tour (1)

in 1822 when he observed that upon heating a liquid in a stationary sealed tube, at a certain temperature the meniscus between the liquid and vapor phases disappeared without ebullition, yielding what appeared by ordinary light to be one homogeneous phase. Upon cooling the tube, the meniscus again appeared but the temperature of re-appearance did not coincide exactly with the temperature of disappearance.

König (2) stated that Schmidt (3) in 1823 predicted the critical point on the basis that the latent heat of vaporization would become zero.

The disappearance of the meniscus was used by Andrews (4 to 7) as the criterion for the critical temperature. Prior to this time, many investigators had tried unsuccessfully to liquefy gases by the application of pressure and had come to the erroneous conclusion that there existed certain "permanent" gases which could not be liquefied.

From Andrews' studies on the gaseous and liquid states of carbon dioxide under various conditions of temperature and pressure, he concluded that each gas has a temperature above which it cannot be liquefied regardless of the applied pressure; but below this temperature, the vapor is condensable by pressure.

Thus, in terms of Andrews' classical experiments, the critical temperature may be defined as the temperature at which the meniscus disappears, or as the minimum temperature above which a gas cannot, as evidenced by the appearance of a meniscus, be liquefied. The pressure (vapor pressure) required to liquefy a gas at this critical temperature is called the critical pressure. The volume of a unit

mass of the substance at the critical temperature and pressure is called the critical volume.

In 1873, van der Waals (8) made an important contribution to the knowledge of liquids and vapors, particularly near the critical point. He was able to give, on grounds at least partly theoretical, the first moderately satisfactory equation which gave a comprehensive description of the behavior of liquids and vapors under varying pressures and temperatures. On the basis of this equation it follows that there is but one temperature at which the pressure and the volume of the gas equal those of the liquid. Successful and widely accepted, the van der Waals' equation has been the starting point for most subsequent studies dealing with equations of state.

On the basis of Andrews' work and van der Waals' equation, it was, therefore, thought that the critical state was a unique point at which the meniscus dividing the vapor and liquid disappeared and the two phases became a single, homogeneous phase. Their work seemed not only to establish the identity of phases at the critical point but to yield the additional fact that liquid could not exist above the critical temperature. These two facts may be said to represent what has come to be known as the classical theory of the critical state.

#### I(b). The Critical Region

The classical theory requires a unique critical point associated with the disappearance of the meniscus and the formation of a completely homogeneous phase. Evidence which conflicted with the van der Waals continuity theory was obtained, however, about

the turn of the century by several investigators.

The concept of a critical region in contrast to a critical point has often been discussed, especially in order to explain various anomalous critical phenomena which apparently were in conflict with the van der Waals equation. Kuenen (9) has reviewed the older literature, especially the effects of gravity and of impurities on the critical phenomena. Objections to, and the limitations of, the van der Waals-Andrews theory have been summarized by Bruhat (10), Clark (11), Traube (12) and Brescia (13).

The only attempt to deduce a critical region from the ideas of van der Waals is by Bakker (14). He pointed out there may be a range in temperature where the thickness of the capillary layer is of the same order as  $v_{\ell}^{1/3} - v_g^{1/3}$ . In this region one would not see a meniscus, although the two phases are still present. This has also been suggested by Mayer and Harrison (15). A review of Mayer's arguments, which are partially formal and partially physical, and are based on the fugacity and virial expansions, is given in a monograph by Mayer and Mayer (16). Mayer's conclusion is that there may be a temperature  $T_m < T_c$  where the meniscus would disappear, although there are still horizontal parts in the isotherms for temperatures between  $T_m$  and  $T_c$ .  $T_c$  is the true critical temperature according to him. In the temperature range  $T_m$  to  $T_c$ , the isotherms enter the two-phase region with a horizontal tangent. Because of the resulting shape of the coexistence curve near the critical point, this region is often referred to as Mayer's derby hat (Figure 1).

FIGURE 1. Plot of Pressure against Volume at Different Temperatures near the Critical Temperature (Mayer's "Derby" Hat).



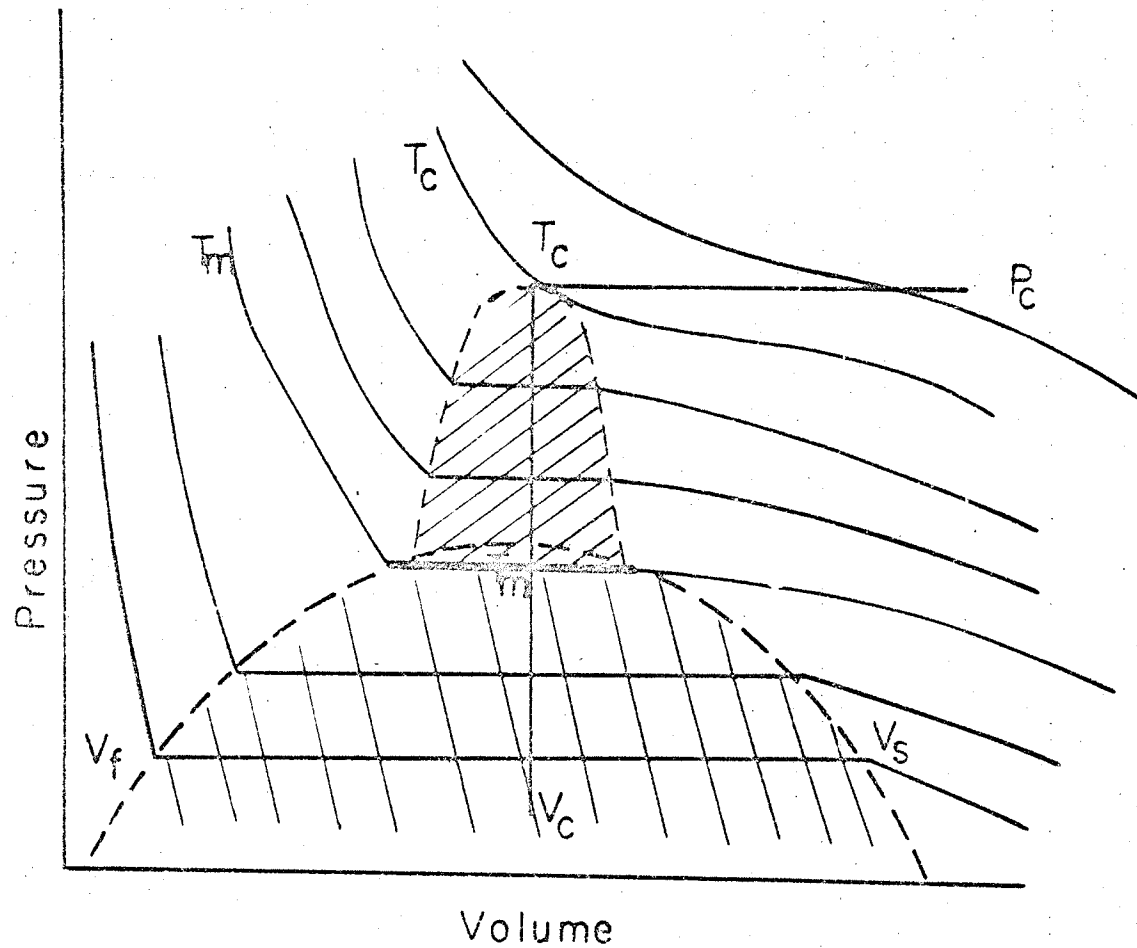


Figure. Plot of pressure against volume at different temperatures near the critical temperature.

Maass and coworkers (17,18,19,20) found viscosity and density hysteresis effects in the region of the critical temperature. It has also been postulated by these investigators that the coexistence curve has a finite horizontal flat segment at  $T_m$  and that a "steam-dome" region is superimposed on the coexistence curve above this flat segment.

In the very careful study of Weinberger and Schneider (21), using very pure Xenon, they extended the density measurements down to temperatures differing from  $T_c$  by only 1 part in 30,000 (i.e.,  $\Delta T/T_c \approx 0.003\%$ ) and down to corresponding density differences of  $(\rho - \rho_c)/2\rho_c \approx 0.04$ . (The temperature was controlled to within  $\pm 0.001^\circ\text{C}$ .) They established the shape of the coexistence curve in bombs of two different lengths, 19 cm. and 1.2 cm. It was found that gravitational effects could account for a large part of the flat-topped segment of the coexistence curve. Experiments near the critical region are very difficult to perform; a long time is needed to establish equilibrium and hysteresis phenomena are difficult to avoid; the system is very susceptible to minute amounts of impurities and, due to the large compressibility, highly sensitive to gravitational fields. Indeed as shown by Weinberger and Schneider (21) it is important to take special precautions to reduce the effects of gravity if the true shape of the coexistence curve is to be measured close to  $T_c$ .

From the experimental point of view the existence of a critical region is still controversial. In recent years, considerable attention has been drawn to the phenomena which occur very near critical points. Several recent conferences (22,23) have presented a wealth of new experimental data and theoretical ideas in this area. These conferences

have established the fact that there are quite marked similarities between apparently very different phase transitions.

At the present time, most (though not all) workers in the field believe that the coexistence curve is rounded. In what follows, the present knowledge of what is actually observed in the neighborhood of the critical temperature is described. Rowlinson (24) has given a very thorough discussion of the classical thermodynamics of the coexistence curve and the critical region, and has also appraised much of the better data on equilibrium properties (of liquids and liquid mixtures). Rice (25,26) has several times reviewed the field of critical phenomena.

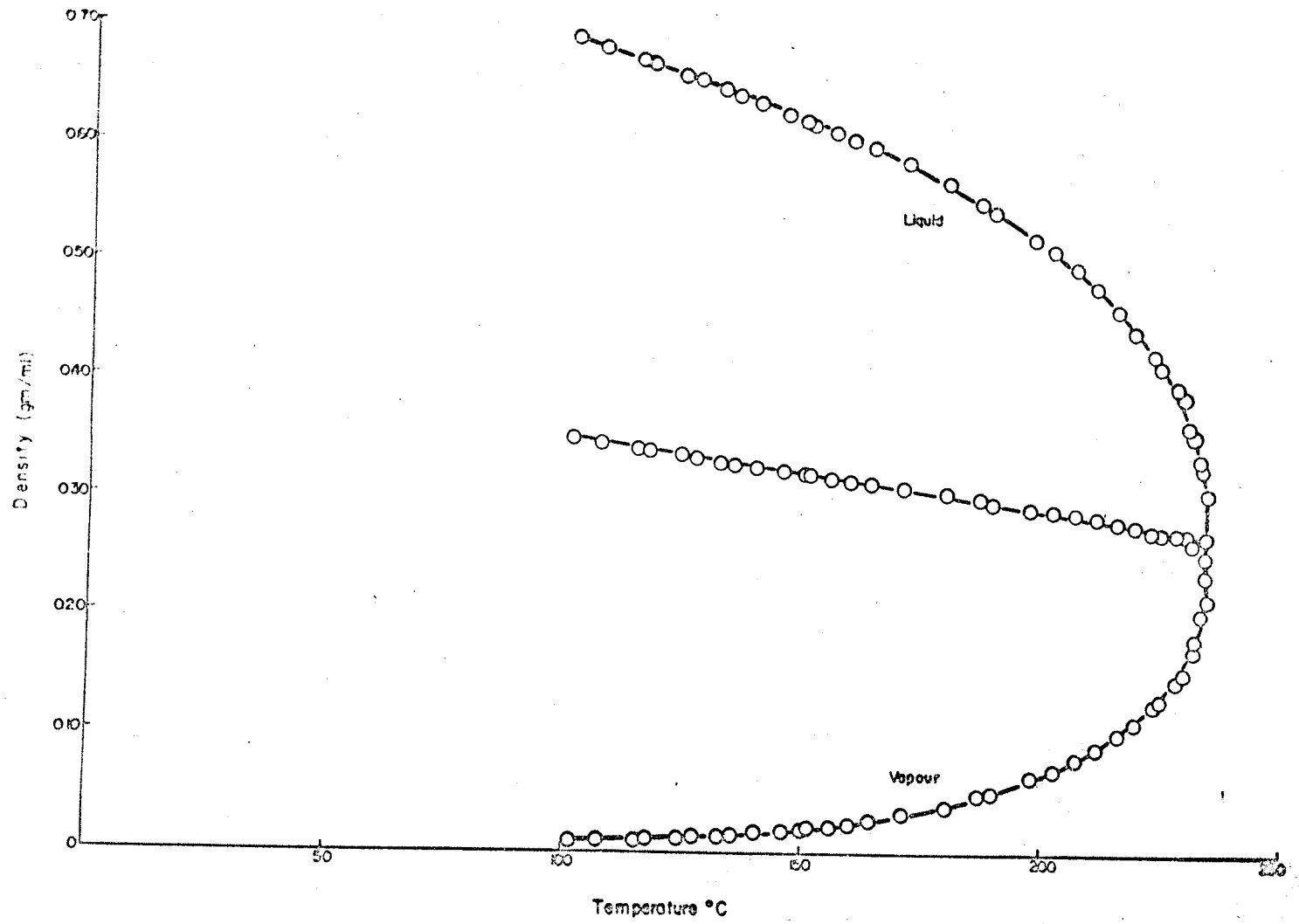
#### I(c). Classical Liquid-Vapor Transitions

Various early attempts were made to understand the occurrence of phase transitions and the anomalies in the vicinity of critical points. In 1873, van der Waals (8) observed that the Boyle-Charles law relating pressure  $P$ , volume  $V$ , and temperature  $T$  of a gas by  $PV = RT$  is correct only when the volume of, and the interaction between, molecules can be neglected. In the liquid state, however, the volume occupied by the molecules is of the order of the macroscopic volume and the heat released during condensation is evidence of the attractive energy between particles. Van der Waals' equation of state is given by

$$(P + a/V^2) (V - b) = RT \quad (1)$$

Van der Waals' law gives a qualitative description of the thermodynamic behavior of gases in the critical region, and notably of the large

FIGURE 2. The Orthobaric Densities of a Typical Pure Substance.



compressibilities observed near the critical point. In particular, this approach implies that:

(a) at the critical temperature, the density minus the critical density is given by

$$\rho - \rho_c \sim (P - P_c)^{1/3} \quad (2)$$

where  $P - P_c$  is the deviation of the pressure from its critical value.

(b) on the coexistence curve (Figure 2), the densities of gas and liquid are given by

$$\rho_{\text{liq.}} - \rho_c = -(\rho_{\text{gas}} - \rho_c) \sim (T_c - T)^{1/2} \quad (3)$$

(c) when  $T > T_c$  and  $\rho = \rho_c$ , the isothermal compressibility  $K_T$  diverges as

$$K_T \equiv \rho^{-1} (\partial \rho / \partial P)_T \sim (T - T_c)^{-1} \quad (4)$$

(d) there is a similar divergence for  $T < T_c$  where

$$K_T \sim (T_c - T)^{-1} \quad (5)$$

on the coexistence curve.

The quadratic coexistence curve, the third degree critical isotherm, and the linearly diverging compressibility are not just consequences of the particular form of van der Waals equation. It can be shown that this behavior is a consequence of a very general assumption---that the free energy behaves analytically around the critical point. This means that the free energy is assumed to have a Taylor series expansion in density and temperature. All classical theories of critical phase transitions have this property as do most of the equations of state in the chemical and engineering literature.

This concept of analyticity plays a decisive role in the theory of critical phenomena.

It is now known that van der Waals' theory cannot be expected to hold in the vicinity of the critical point. The assumption that the potential energy is proportional to the density is a good one, if the interactions between molecules vary slowly with distance and are long-range (i.e., interactions are between molecules whose distances are much larger than those between nearest neighbors, cf. page 13), since in that case each molecule feels the influence of all others in the same way. Kac, Uhlenbeck and Hemmer (27) recently showed that van der Waals' equation holds rigorously in the limit of long-range forces in a one-dimensional gas. The nature of the critical transition, moreover, is independent of the dimensionality of the system for a van der Waals gas, because each molecule is in the range of all others.

With more or less the same reasonings and assumptions as van der Waals, Weiss, and Bragg and Williams formulated their inner field theories on phase transitions of ferromagnets and order-disorder transitions of binary alloys. Since both physical concepts and mathematical structure of the inner field theories of van der Waals, Weiss, and Bragg and Williams are so closely similar, it is not surprising that their predictions for critical behavior are strictly analogous. In emphasizing the great similarity of the three classical theories it must be remembered that they are all based on the assumption that the attractive forces between the molecules which produce the cooperative effects have a very long range, although the derivations are often quite different. All inner-field theories predict a quadratic coexistence curve, a jump discontinuity in  $C_v$ , a third degree critical isotherm, and a linearly diverging compressibility, or susceptibility.

The prediction of the classical theories turns out to be incorrect for most experimental systems, but the concept of analogy is retained.

For theoretical discussions and in the analysis of experimental data it is useful to describe the behavior of properties close to the critical point in terms of power laws. The definitions of the most important critical point exponents for gases may be given as follows:

TABLE I.

Properties	Liquid-gas transition
Coexistence curve.	$ \rho - \rho_c  \sim  T - T_c ^\beta$
Specific heat along critical isochore.	$c_v \sim  T - T_c ^{-\alpha}$
Compressibility along critical isochore.	$K_T \sim  T - T_c ^{-\gamma}$
Critical isotherm.	$ P - P_c  \sim  \rho - \rho_c ^\delta$

The critical behavior of each property is thus characterized by a value of the corresponding exponent. The various exponents, however, are not independent. On the basis of thermodynamic considerations one can conclude that they should satisfy certain inequalities. The best known inequalities given by Fisher (28) are:

$$\alpha + 2\beta + \gamma \geq 2 \quad (6)$$

$$\alpha + \beta(1 + \delta) \geq 2 \quad (7)$$

Both in classical theories and in modern theories, these inequalities are satisfied as equalities (with = replacing  $\geq$ ).



I(d). Recent Developments in Critical Phenomena

A problem of central interest in the study of critical phenomena, both experimentally and theoretically, is the determination of the asymptotic laws governing the approach to a critical point. Some of these, notably the "one-third" power law for the vanishing of the density discontinuity  $\rho_L - \rho_G$  between coexisting liquid and gas as a function of  $T_c - T$  have a fairly long history; others, such as the logarithmic divergence of the specific heat  $C_p$  of helium at the lambda point and the near-logarithmic divergence of  $C_v$  for argon at its critical point, are more recent discoveries. Theories competent to make significant predictions about critical-point behavior have, however, developed mainly in the past decade or two.

The inadequacies of the classical theories are now evident, particularly by comparison with the exact results for plane Ising models (lattice gas). The summaries of the results of the Ising model theories as well as the theoretical and experimental values of the critical point exponents are given in recent reviews by Fisher (28,29), Heller (30), Kadanoff(31), Sengers and Levelt-Sengers (32), and in the recent analysis by Green, Vicentini-Missoni and Levelt-Sengers (33). In the absence of detailed knowledge about the intermolecular forces, it was generally believed that the attractive forces in classical theories had a very long range. But the later development showed more and more clearly that the cooperative forces were not of a very long range, that each atom was influenced by at best a few shells of neighboring atoms. This was realized in the late twenties as a result of the quantum mechanical revolution, when London elucidated the nature

of the van der Waals attractive forces and Heisenberg of the Weiss inner field. In 1925, Ising proposed a simple model. He assumed the magnetic spins to be localized on the lattice sites of a regular array and capable of only two orientations in opposite directions. If located on adjacent sites, parallel spins attracted each other and antiparallel spins repelled each other. All interactions beyond those between nearest neighbors were neglected. The intuitive and approximate approach of the inner field theories was, furthermore, replaced by the methods of statistical mechanics, in which averages were taken over all possible microscopic arrangements.

The concept of analogy among different critical transitions was conserved in an elegant way in the Ising model. When upward-pointing spins, for instance, were replaced by molecules and downward-pointing spins by "holes" or empty sites, the ferromagnetic Ising model was transformed into a model for the gas-liquid transition, the so-called lattice gas. Although this may sound somewhat artificial, the procedure is very fruitful.

Solving the Ising problem without using the inner field concept is a very difficult task, since for any given total energy all possible arrangements of the spins on the lattice must be enumerated. The recent change of view about the nature of the critical point is due to the impact of the solution to the two-dimensional Ising problem by Onsager (34). His finding has dominated the subject for the last 25 years. The most striking result of Onsager is that there is a critical point and that the specific heat is logarithmically diverging there in contrast to the classical result. Fisher and his coworkers (35) have developed

approximation methods for the three-dimensional model and for the two-dimensional model in the presence of a field. Fisher's model shows the nonanalytic behavior at the critical point.

A survey of the experimental situation, as it stands today, in regard to fluids serves to establish the definitions of the various critical exponents  $\alpha$ ,  $\beta$ ,  $\gamma$  ....., and leads to the phenomenological development of the close analogies between different physical systems. These analogies find a firm theoretical foundation in the equivalence of classical-latticegases and Ising-model ferromagnets and of quantal-lattice gases and anisotropic Heisenberg-Ising ferromagnets. Series expansions have been used to obtain numerical information about critical points when exact theories have not been known. A general theoretical understanding of critical phenomena is obtained from relations and 'laws' derived from the "droplet" picture of the critical point and from various 'homogeneity' and 'scaling' hypotheses. It is worthwhile to assess a number of recently developed theoretical ideas which aim at throwing light on the values of the critical singularities. Some of the suggested approaches have tried to establish that only two independent critical exponents are required by a physical system, one for the temperature variation and one for the field (or pressure, etc.) variation. In the light of present knowledge, none of the various theories is fully convincing but it is hoped that they point the way forward to a deeper understanding of the numerical results so far found experimentally and theoretically. Fierz (36) and de Boer (37) have presented ideas to describe a theory of the critical region based on the droplet (or physical-cluster) picture of condensation for the fluid

case ( $L \rightleftharpoons V$ ). Fisher and coworkers (38,39) have pointed out that they can be extended to describe the critical point of liquids. Rice(25) had earlier considered the process of condensation of a vapor from the point of view of associating molecules (clusters).

The basic idea of the "droplet" picture is that in a gas of particles interacting with repulsive cores and short-range attractive forces, the typical configuration at low densities and temperatures will consist of essentially isolated clusters of one, two, three or more particles. A sufficiently large cluster is just a small droplet of the liquid phase at the same temperature. These droplets will be in dynamic equilibrium and the relative proportions of differently sized droplets will change with temperature and pressure. Condensation in this picture corresponds to the growth of a macroscopic droplet of the liquid. Fisher (29) has formulated these ideas mathematically and has also translated the arguments for the fluid case into magnetic terms (28). He has discussed a microscopic picture of the critical point which, perhaps, gives some insight into the magnitudes and interrelations of the critical exponents (29). A more phenomenological macroscopic approach may be followed to show the exponent relations given by equations (6) and (7).

Recently, Widom (40), Kadanoff (31,41) and Griffiths (42) have put forward ideas about the nature of the equation of state in the critical region. It is known that the equilibrium thermodynamic properties of a pure single-component fluid are completely determined by a knowledge of the Helmholtz free energy per unit volume as a function of density and temperature (42). For fluids, Widom (40) has introduced a function

of two variables, one a measure of the density of the system and the other a measure of the temperature. The classical theory is characterized by this function being a constant. By contrast, a real fluid of finite dimensionality is characterized by this function being a homogeneous function of its variables, with a positive degree of homogeneity. It is just this assumption of Widom which leads to the nonclassical compressibility and specific heat. Experimental work of increasing precision--including, but not limited to, heat-capacity measurements--suggests that anomalies near the critical point not present in the classical treatment may be the rule rather than the exception in pure materials.

This so-called scaling-law equation of state exhibits non-classical critical anomalies with proper choice of the suggested function. Green et al (33) have shown that a scaling-law equation of state is also valid in the critical region of gases above and below  $T_c$ , and have proposed a new way of deriving critical exponents from experimental data. Thus, it is evident that the scaling-law can describe the PVT behavior of a variety of gases in a large region around the critical point.

Great emphasis must be given to the experimental situation in order to understand the nature of critical phenomena as it is known today. One can be confident that the deviations now observed between theory and experiment are consequences of over-simplifications of the models (rather than deficiencies of calculation). The widespread appreciation of the difficulties inherent in making truly reliable measurements in the critical region has really been quite recent. New

techniques such as the dielectric constant and refractive index methods have already yielded some remarkable results concerning the behavior of the equation of state of fluids.

Some of the general difficulties inherent in the measurements near the critical point have already been discussed. In some of the experiments involving the critical points in fluids, the data do not seem to settle down to their asymptotic critical behavior until  $\epsilon = \frac{(T-T_c)}{T_c}$  gets smaller than  $10^{-2}$ . A temperature control system must be able to maintain and reproduce temperatures to perhaps one part in  $10^4$  of  $T_c$  in order to provide meaningful data over a two-decade range in  $\epsilon$  within this critical region. Since this control is most easily achieved near room temperature, the most complete data are obtained for the classical gases Xe and  $\text{CO}_2$  ( $T_c = 289.6^\circ\text{K}$  and  $304.0^\circ\text{K}$  respectively).

Given a good temperature control system, the extremely large compressibilities must be contended with when critical conditions are approached. Due to the weight of the fluid, critical pressure is realized only over a very narrow vertical height range in a sample bomb (in theory, of course, only at a single horizontal plane), and what is measured in a PVT measurement is the average condition of the fluid. This may be quite different from the critical condition unless special precautions are taken, and can lead to a flat top in the co-existence curve (43) (liquid-gas density difference as a function of temperature). One of the most elegant methods of dealing with this was devised by Lorentzen (44) as explained below. The remarkable sharpness of the critical point was also demonstrated by the results of a particularly careful series of measurements due to him (43,44). A glass

tube filled with very pure  $\text{CO}_2$  was placed in a thermostat capable of holding the temperature constant to within a fraction of a millidegree for several days. The tube and its contents formed a cylindrical lens, the focal length of which depended on the fluid density. This lens was used to form an image of a pair of vertical slits. The separation between the two slit images provided a measure of the fluid density as a function of height in the tube. By calculating the variation of pressure with height due to gravity, the shape of the  $(P, \rho)$  isotherms could be obtained. All critical exponents except  $\alpha$  (the specific heat exponent) can be determined directly from an experiment of this type.

A further complication arises from the large heat capacity of a fluid near critical conditions (45,46,47). Equilibration times become very long near the critical point as a result of this and other reasons, necessitating waits of perhaps days before it is reasonably certain equilibrium conditions have been attained. Wentorf (48) has asserted that pressure equilibration in the critical region is achieved within 30 min., but that constancy of fluid structure as judged from photographs may require as much as 5 hours.

The most accurately determined parameter for the classical gases is exponent  $\beta$  of the coexistence curve. By the early 1900's it was known that gas-liquid coexistence curves were roughly of the third degree, in contrast to the parabola predicted by van der Waals' equation. All later experiments have essentially confirmed this. The best value of the exponent  $\beta$  is 0.35 for a large variety of gases including even  $^3\text{He}$  and  $^4\text{He}$  (21,22,43).

In binary liquid mixtures ( $L_1 \rightleftharpoons L_2$ ), the precise measurements of Rice and his coworkers (49) indicate  $\beta$  is close to 0.33. Recently there have been some speculations, based on theoretical considerations by Fisher (39), that the density should be linear to  $(T_c - T)^{5/16}$  rather than  $(T_c - T)^{1/3}$ . Rice (49) has tried replotting his results on this basis, but, it appears, these functional forms are so closely similar that, even with the degree of precision he has obtained (temperature control was  $\pm 0.00005^\circ\text{C}$ ), it is impossible to distinguish between them.

It now seems quite well established experimentally that for simple fluids, such as the noble gases, the coexistence curve does not have a significantly "flat top". Rice (50) and Zimm (51) suggested this in 1950 at a symposium on critical phenomena. Rice and his coworkers (52,53,54) in later publications reiterated his even earlier claim (25) of the existence of a flat top without realizing that the temperature control in these measurements was not accurate enough to decide the question. His more recent work with Thompson (49) was undertaken to clarify the behavior of a system first investigated by Zimm (51) who did not find any evidence of a flat top. In this careful study Rice (49) concluded that there was no flat portion of the coexistence curve unless it was within  $0.0001^\circ$  of  $T_c$ . Thus, there is no limit to the accuracy of temperature control to which the measurements should be made.

Critical opalescence of certain systems has been studied by Chu (22,55) by means of visible light scattering. His recent results have been discussed in terms of Debye theory of critical opalescence (56)



and the solubility parameter theory of Hildebrand and Scatchard. The findings substantiate the proposal of Scott (57) on the breakdown of the geometric mean law for fluorocarbon-hydrocarbon systems.

In many respects the behavior of binary fluid mixtures ( $L_1 \rightleftharpoons L_2$ ) such as those investigated by Rice and others which undergo phase separation is closely analogous to the condensation of simple fluids ( $L \rightleftharpoons V$ ) and most of the preceding remarks about the nature of the coexistence curve can be translated directly into such terms (24,26). While it is always possible that measurements taken much closer still to the critical point might yet yield a different value of  $\beta$  (exponent of the coexistence curve) it seems reasonable to conclude that the classical theory does not correspond to reality. The fact that measurements of the phase boundaries of binary fluid mixtures near both their upper and lower critical points are also fitted well by the same cube-root law that applies to simple gases suggests that the behavior close to a critical point is insensitive to the detailed nature of the intermolecular forces.

#### I(e). Thermodynamics of the Critical Point

The classical theory of fluids does not account for the approach of logarithmic heat capacity to infinity along the critical isochore (58) as  $T$  approaches  $T_c$ . Further, classical theory leads to the prediction that the liquid-vapor coexistence curve is quadratic when pressure is expanded about the critical point in a Taylor series in density and temperature. This conflict with the known experimental evidence suggests that a Taylor expansion as usually carried out is not valid.

In order to account for a cubic coexistence curve Rice (26), Widom and Rice (59), and Davis and Rice (60) recognized the singular nature of the critical point and suggested that  $(\frac{\partial^3 P}{\partial \rho^3})_c = 0$  and that  $(\frac{\partial^4 P}{\partial \rho^4})_c$  is discontinuous. Dunlap and Furrow (61) have also suggested this. Widom (40) has given special consideration to the region very close to the critical point and has proposed a theory consistent with the singular behavior of  $C_v$  along the critical isochore. Davis and Rice (60) have assumed that ordinary Taylor expansions may be carried out provided they are made at some increment away from a singular point or point of discontinuity. They have given thermodynamic derivations for a cubic coexistence curve in liquid-vapor systems. They found two separate Taylor series in pressure are necessary to describe the behavior in the gas and liquid single-phase regions of a one-component fluid. Two expressions for the saturation vapor pressure at a certain temperature (up to some arbitrarily small increment away from the coexistence curve) are provided in their thermodynamic treatment, after specifying the densities to be those at the coexistence curve, i.e., the saturation densities. They avoided the data or observations very near the critical point (since it is difficult to obtain reliable data) and discussed methods based on thermodynamics to obtain critical constants  $\rho_c$ ,  $T_c$ , and  $P_c$ . An extensive survey is also given by Rowlinson (24).

In 1873, van der Waals (8) first defined the term "reduced condition" and presented the "theorem of corresponding states" that all pure gases manifest the same compressibility factors when measured at the same reduced conditions of pressure and temperature. This concept

was extended to liquids by Young (62) in 1899. Since then many generalized methods for estimating thermodynamic properties of pure fluids based upon the theorem of corresponding states have been presented. By reason of their very generality, encompassing as they do all substances, the generalized charts cannot begin to be as precise as the measurement of the properties of individual substances. Since a very detailed knowledge of the equilibrium properties of the pure liquids is demanded by most theories of mixtures, wherever possible such experimental measurements should be made instead of depending on the generalized charts.

There is a scarcity of data for vapor pressures above the normal boiling points of substances which are liquids at room temperature, and the exact course of the vapor pressure curve between the boiling and critical points is not usually well known.

Although several papers by Young (63,64,65) dealt with measurements of orthobaric volumes of liquids, the amount of work on this subject published since then has been disappointingly small. The measurement of the gas and liquid densities may be made by finding the volume of a known mass of gas at its bubble-point (the orthobaric liquid-density) and dew-point (the orthobaric gas-density). These measurements are difficult near the critical point, and therefore, most workers have preferred to measure the relative proportions of gas and liquid at two overall-densities lying between those of the coexisting phases. The orthobaric densities can then be found by solving a pair of simultaneous equations. Details have been presented in the experimental section of this thesis.

It is customary to express the PVT properties of fluids by empirical equations designed to fit the experimental data. The complexity of such equations and the number of empirical constants required are dependent on the accuracy of experimental measurements, the precision required, and the experimental range of variables.

Such equations represent a convenient condensation of experimental data and are valuable not only for calculating values of pressure, temperature, volume, and density but also for deriving thermodynamic properties therefrom.

## II. THERMODYNAMIC PROPERTIES FROM P-V-T DATA

For the determination of the thermodynamic properties of pure fluids, both liquid and gaseous, the most common experimental measurements are of P-V-T data for the single phases and of vapor pressures to relate the properties of vapor and liquid phases in equilibrium.

The properties of pure homogeneous fluids may be considered functions of temperature and pressure only. The influence of temperature on thermodynamic properties is not usually considered, for this cannot be determined from compressibility data alone. However, P-V-T data are used to determine the influence of pressure only, so the property changes with pressure of a pure material can be studied along an isotherm.

The thermodynamic properties calculated from PVT data are obtained in the form of deviations of these properties from ideal behavior (ideal gas law). The thermodynamic properties of a substance in the ideal gas state may be calculated from heat capacity data using

the methods of statistical mechanics. The deviations from ideal behavior of the thermodynamic properties are determined in dimensionless form as shown in the following table:

Table II

<u>Function</u>	<u>Dimensionless Form</u>
Volume	$P(V - V_0^{id})/RT$
Internal Energy	$(E - E_0^{id})/RT$
Enthalpy	$(H - H_0^{id})/RT$
Entropy	$(S - S_0^{id})/R$
Gibbs free energy	$(G - G_0^{id})/RT$
Helmholtz free energy	$(A - A_0^{id})/RT$

The general equations relating thermodynamic functions in Table II to pressure by use of compressibility factors (defined by the equation  $Z = PV/RT$ ) can easily be written. For gases at constant temperature, the fugacity coefficient (defined by  $\phi = \frac{f}{P}$ ; equation (21) in "Vapor-liquid equilibria" Section) may be obtained from the experimental compressibility data after integrating the following equation (66)

$$d \ln \phi = \frac{Z - 1}{P} dP \quad (8)$$

Integration at constant T from the zero-pressure state to a state at finite pressure P gives

$$\ln \phi - \ln \phi^* = \int_0^P \frac{(Z - 1)}{P} dP \quad (9)$$

The asterisk indicates the limiting value as P approaches zero, where all gases are assumed to obey the ideal-gas law. Therefore,  $\phi = \frac{f^*}{P^*} = 1$ , and

$$\ln \phi = \int_0^P \frac{(Z - 1)}{P} dP \quad (10)$$

Values of Z as a function of P at a given temperature T can be calculated from PVT data. To determine the values of the integral, the isothermal

values of  $(Z - 1)/P$  are first calculated. These values are fitted to a polynomial in  $P$ , using a least squares procedure, and the resulting expression is integrated analytically to provide values of  $\int_0^P \frac{(Z - 1)}{P} dP$  at various pressures.

The enthalpy deviation, i.e.  $H_0^{id} - H$  is the difference between the enthalpy of an ideal-gas and the enthalpy of the actual gas and is related to the compressibility factor, pressure and temperature (66) by

$$\frac{H - H_0^{id}}{RT} = -T \int_0^P \frac{(\partial Z / \partial T)_P}{P} dP \quad (11)$$

To evaluate the integral, compressibility factors are plotted vs. pressure on a large scale graph. Next a cross plot of the compressibility factors vs. temperature for constant values of pressure is made. These compressibility isobars are then fitted as polynomials in  $T$  using a least squares procedure, and the resulting expressions are differentiated analytically to give values of  $\frac{\partial Z}{\partial T}$  at various pressures. For each isotherm, the values of  $(\partial Z / \partial T)_P / P$  are fitted to polynomials in  $P$  by a least squares procedure, and the resulting expression is integrated analytically to provide values of  $\int_0^P \frac{(\partial Z / \partial T)_P}{P} dP$  at various pressures.

Having obtained the values of  $\ln \phi$  and  $(H^{id} - H)$  as functions of pressure at various constant temperatures, the other functions can be calculated from well-known thermodynamic relationships.

Since by definition  $G = H - TS$ , then also  $G^{id} = H^{id} - TS^{id}$ .

By difference one gets for a given temperature and pressure

$$G^{id} - G = H^{id} - H - T(S^{id} - S) \quad (12)$$

$$\text{or } G^{id} - G = \Delta H - T\Delta S \quad (13)$$

Where  $\Delta S$  is the entropy deviation, defined in a fashion analogous to the enthalpy deviation. Integration of  $dG = RT d \ln f$  at constant temperature from the real-gas state to the ideal-gas state gives

$$G^{id} - G = RT \ln \frac{P}{f} = -RT \ln \phi$$

Therefore, equation (13) becomes

$$-RT \ln \phi = \Delta H - T\Delta S \quad (14)$$

$$\text{or } \Delta S = \frac{\Delta H}{T} + R \ln \phi \quad (15)$$

By equation (15) it is now possible to calculate values of the entropy deviation as a function of pressure for various temperatures from the previously determined values of  $\ln \phi$  and  $\Delta H$ .

The thermodynamic properties of a substance in the ideal-gas state may be calculated from heat capacity data using the methods of statistical mechanics. Values of  $(H - H_0^{id})$  and  $(S - S_0^{id})$  can then be tabulated or plotted as functions of  $T$  and  $P$ . The selection of a numerical value for  $H_0^{id}$  and for  $S_0^{id}$  is arbitrary. Once selected, these values are constant, and do not affect property changes of the material.

All the thermodynamic functions in Table II can now be evaluated. The following table shows the various functions with the integrals to be evaluated for their calculation:

Table III

Summary of Thermodynamic Functions

Volume	$Z - 1$
Internal Energy	$-T \int_0^P \frac{(\partial Z / \partial T)_P}{P} dP - (Z-1)$
Enthalpy	$-T \int_0^P \frac{(\partial Z / \partial T)_P}{P} dP$
Entropy	$-T \int_0^P \frac{(\partial Z / \partial T)_P}{P} dP - \int_0^P \frac{(Z-1)}{P} dP$
Gibbs free energy	$\int_0^P \frac{(Z-1)}{P} dP$
Helmholtz free energy	$\int_0^P \frac{(Z-1)}{P} dP - (Z-1)$
Fugacity Coefficient	$\exp. \int_0^P \frac{(Z-1)}{P} dP$

The methods described are used for gases from the zero-pressure state up to the pressure at which condensation begins, i.e., the dew point. For a pure vapor the dew point occurs at the vapor pressure. When this pressure is reached along an isotherm, the property being represented generally changes abruptly from that observed for the vapor phase to that observed for the liquid phase after condensation at constant temperature and pressure. For example, the specific volume of saturated liquid  $V_\ell$  is very different from that for saturated vapor (gas)  $V_g$ ; there is a discrete enthalpy change from  $H_\ell$  to  $H_g$ , and a discrete entropy change from  $S_\ell$  to  $S_g$ . The exception is the Gibbs



function. It is always given by  $G = g(T,P)$  for systems at equilibrium, and it is known from experience that when a pure material evaporates or condenses at constant temperature, the pressure also remains constant. Thus for such a process  $dG = 0$ , as theory requires for any equilibrium.

The enthalpy of vaporization of a pure material may be calculated from the well-known Clapeyron equation, which can be written

$$\frac{dP}{dT} = \frac{\Delta H^{\text{vap}}}{T\Delta V^{\text{vap}}} \quad (16)$$

where  $dP/dT$  is the slope of the vapor pressure curve at the particular temperature being considered,

$$\Delta H^{\text{vap}} = H_g - H_l, \quad (17)$$

the latent heat of vaporization, and

$$\Delta V^{\text{vap}} = V_g - V_l, \quad (18)$$

the volume change of vaporization.

Although all one component systems having vapor in equilibrium with liquid obey this equation exactly, the rigorous exact differential form is difficult to apply unless PVT data and the rate of change of vapor pressure with respect to temperature are available. Other latent heat prediction methods are based on the theory of corresponding states, Trouton's rule, molal volumes, critical properties, equations of state, and comparisons with a reference compound.

Since  $P$  and  $T$  are constant during the vaporization process, equation (13) becomes  $\Delta H^{\text{vap}} = T\Delta S^{\text{vap}}$ . Hence the entropy of vaporization is given by

$$S_g - S_l = \Delta S^{\text{vap}} = \Delta H^{\text{vap}}/T \quad (19)$$

Thus once the vapor-pressure curve is established and saturated liquid and vapor volumes are measured for a pure material, the enthalpy and entropy values of liquid and vapor are connected by equations (16) and (19).

For the liquid phase equations (10), (11), and (15) are still valid and could be applied to the calculation of liquid properties, but they are not commonly used. This procedure would make the Clapeyron equation for pure materials unnecessary.

Knowing the enthalpies, entropies, volumes and fugacity coefficients of a pure compound in the gas phase, those of the saturated vapor may be obtained by extrapolating each isotherm to the corresponding vapor pressure. The quantities for the saturated liquid are obtained by subtracting the latent heat of vaporization or the entropy of vaporization from the enthalpy or entropy of the saturated vapor.

Thus, these general equations allow calculation of the thermodynamic properties of pure fluids in the gaseous and liquid regions from PVT data, vapor pressure data, and certain equations of statistical mechanics using ideal-gas heat capacities and spectroscopic data. Other methods of calculation from the same data are certainly possible, but none is more direct. From such calculations, tables of thermodynamic data are readily constructed, although other measurements are sometimes used to test the accuracy of results.

### III. VAPOR - LIQUID EQUILIBRIA

It has been customary for many years to subject vapor-liquid

equilibrium data at low pressures to thermodynamic analysis but this custom has rarely been extended to vapor-liquid data at high pressures. Although the chemical literature is fairly rich in experimental studies of the phase behavior of binary mixtures at high pressures, very little attention has been given to the problem of how the experimental results may be meaningfully treated with the aid of suitable thermodynamic functions. That a start has been made in this direction is clear from several publications by Prausnitz et al. quoted in the course of this discussion. Thermodynamic analysis for reduction of high-pressure vapor-liquid equilibrium data is essential to enable one to predict phase-behavior under conditions different from those at which the data were obtained. It also provides empirical techniques for estimating high-pressure vapor-liquid equilibria in multi-component mixtures from a minimum of experimental data (using only the results of binary data reduction).

### III A. General Equilibrium Equation

All the equilibrium properties of each species in multicomponent phase equilibria are described by the chemical potential which was introduced by J. W. Gibbs (67). For the equilibrium of a particular species between any two phases at a given temperature the chemical potential of that species must be the same in both phases. A more meaningful quantity called the fugacity is often convenient to use. It was introduced by G. N. Lewis (68), and can be thought of as a thermodynamic pressure, since in a real mixture it is considered as the partial pressure which has been corrected for imperfection. The

fugacity of a pure substance in any condensed phase is defined as being equal to the fugacity in the gas phase with which it is in equilibrium. Evidently when two condensed phases are in equilibrium with each other the fugacities of an arbitrary  $i^{\text{th}}$  component must be equal in the two phases:

$$f_i^V = f_i^L \quad (20)$$

where the superscripts V and L stand for vapor and liquid.

In order to be able to express the fugacities in terms of experimentally observable quantities two auxiliary functions are introduced. The first of these, the fugacity coefficient  $\phi$ , relates the vapor-phase fugacity  $f_i^V$  to the vapor-phase mole-fraction  $y_i$  and to the total pressure  $P$ . Thus

$$\phi_i = \frac{f_i^V}{y_i P} \quad (21)$$

The activity coefficient  $\gamma$  relates the liquid-phase fugacity  $f_i^L$  to the liquid-phase mole fraction  $x_i$  and to a standard-state fugacity  $f_i^{\text{OL}}$ . Thus

$$\gamma_i = \frac{f_i^L}{x_i f_i^{\text{OL}}} \quad (22)$$

Since for phase equilibrium  $f_i^V = f_i^L$ , from equations (21) and (22), the combined equation for the calculation of vapor-liquid equilibria is obtained as

$$\phi_i y_i P = \gamma_i x_i f_i^{\text{OL}} \quad (23)$$

The usual phase-equilibrium problem is to calculate the

composition of a vapor phase in equilibrium with a liquid phase of given composition or vice versa. Compositions were introduced into equation (20) by the use of the fugacity coefficient of a constituent in solution. This is entirely appropriate, in principle, for high-pressure equilibria, since no assumptions have been made to limit the pressure to which these relationships apply. However, the method is impractical for the liquid phase and will remain so until a satisfactory equation of state is developed for liquid solutions. The concept of activity coefficient was therefore introduced for the liquid phase. The advantage of the activity coefficient is that it relates the fugacity of a constituent in solution to the fugacity of the same constituent in another state (the standard or reference state) for which fugacity values may be more readily determined. In fact, for vapor-liquid equilibria at low pressures, the activity coefficient rather than the fugacity coefficient is used generally in the treatment of both phases. Although it is difficult to relax the restrictions applicable at low pressures, the use of activity coefficients is certainly not inherently limited to these pressures alone.

The direct effect of pressure on liquid properties is usually neglected at normal pressures and the truncated virial equation is usually employed for the vapor phase. At high pressures these simplifying assumptions are not valid to describe the properties of the phases. Even the use of the virial expansion in densities truncated to the third term may not be adequate. Even if it is, the third virial coefficients for solutions are rarely known, and methods of estimation are very crude. One must also have data on the volumetric properties of liquids in order

to take into account correctly the effect of pressure on liquid-phase properties. Thus volumetric data, either directly measured or as given by an adequate equation of state, must be available for both the vapor and liquid phases in addition to phase-equilibrium data themselves if one is to reduce the equilibrium data at high pressures to thermodynamic variables.

A difficult problem comes from the definition of activity coefficient as given by equation (22). The activity coefficient is not completely defined unless the standard-state fugacity  $f_i^{OL}$  is clearly specified. The selection of the standard state represented by  $f_i^{OL}$  is quite arbitrary and it is up to the individual to choose it according to his convenience. At low pressures the standard state for constituent  $i$  is taken to be pure  $i$  at the same temperature as that of the solution, at some fixed composition, and at some specified pressure, usually the pressure of the solution. At high pressures, for both the liquid phase and the vapor phase this normally requires the standard state for one or the other of the constituents to be fictitious or hypothetical. The more volatile constituent exists only as a vapor at the solution temperature and pressure, and the less volatile, only as a liquid. For azeotropic systems both constituents may exist only as vapors or only as liquids. In any event, fictitious states must be employed, and properties in such states can be obtained only by extrapolation. At low pressures, the extrapolation is short, and when the simplest expression of the virial equation is used this is automatic and is always achieved in a consistent fashion. It is seldom possible to fulfill these conditions at high pressures, and

the choice of the variables used in the definition of standard state (namely some fixed composition and some specified pressure) becomes arbitrary. It is strictly for convenience that certain conventions have been adopted in the choice of a standard-state fugacity. These conventions, in turn, result from two important considerations: (i) the necessity for an unambiguous thermodynamic treatment of non-condensable components in liquid solutions, and (ii) the relation between activity coefficients given by the Gibbs-Duhem equation.

A serious situation is encountered from the first of these considerations, that is, when the solution temperature is above the critical temperature of one of the constituents. One then must postulate a liquid state for that constituent in a region where the pure liquid cannot exist, no matter what the pressure is. Therefore, the normalization of activity coefficients for such noncondensable components must be different from that used for condensable (sub-critical) components. The second consideration given above makes it necessary to derive methods to take account of the effect of pressure and composition on activity coefficients and to use adjusted activity coefficients, which are independent of pressure.

On the basis of these two considerations, the key equation for characterization of vapor-liquid equilibrium (equation 23) at high pressures was obtained, by using fugacity coefficients (rather than activity coefficients) only for the vapor phase, and activity coefficients and as-yet-unsettled standard states for the liquid phase. As a consequence of restricting activity coefficients to liquids, the variation of the partial molal free energy with pressure is small, but

in general this is taken into account by an easily computed correction term (Poynting correction). In the vicinity of the critical state, however, and also for dissolved gases, the pressure influence is large and not easily estimated.

For gases, the fugacity coefficient represents the deviation from the perfect gas as well as the deviation of a mixture from the perfect solution. As has been pointed out, the fugacity coefficient is, by definition, dependent on the pressure and the vapor composition (and of course on the temperature). Its values are practically always derived from an equation of state.

Thus in high-pressure systems both phases, vapor and liquid, exhibit large deviations from ideal behavior. Attention is next turned to separate discussions of the individual functions, which describe these non-idealities.

### III B. The Representation of Vapor-Phase Fugacity Coefficients

#### III B. (I) Equation of State.

If it cannot be assumed that the vapor is a perfect gaseous mixture, the fugacity coefficients have to be derived from a suitable equation of state. The very fact that more than a hundred equations of state have been proposed suggests caution. It is necessary to consider only those requirements, which are necessary practically using molecular theory as a helpful guide.

An algebraic formulation appears to be indispensable. Compressibility factors, of course, can never be better represented by an equation with two individual parameters than by the usual



generalized charts. Similarly, an equation with three parameters cannot give better values of  $Z$  than the tables of Pitzer and his coworkers (69) or of Riedel (70). The practical interest in an equation of state however, does not lie in the compressibility factors but in the fugacity coefficients. Here the algebraic equation has the advantage of retaining its definiteness in the necessary steps of integration and differentiation, which lead to loss of accuracy in numerical operations. Since individual fugacity coefficients in mixtures are the real objective, a definite combination rule for the parameters, independent of specific data for the mixtures, is desirable.

An equation of state, or at least its main term, must imply an equation of the third degree in  $Z$ . This conclusion can be drawn from Wegscheider's discussion (71) of the equation of Wohl (72).

Good performance at high pressures is closely connected with the approach of the experimentally well established limiting condition for the reduced volume  $V_r$

$$\lim_{P = \infty} V_r = 0.26 \quad (24)$$

For mixtures, Neusser's rarely quoted condition (73) of additivity of the volumes at high pressure should be satisfied. The obvious interpretation of this condition is the additivity of the proper volume of the molecule. The condition is important, particularly since the volume in general is far from being additive at moderate pressures.

Approach of the perfect gas equation at low pressure and high

temperature is also an obvious condition.

An excellent discussion of the relative merits of dozens of equations has been recently published by Martin (74). The merits and limitations of fourteen of the most common equations of state have been thoroughly discussed by Shah and Thodos (75), for the subcritical, critical and hypercritical regions.

An equation proposed nearly 20 years ago by Redlich and Kwong (76) satisfies the conditions outlined above. It is very similar to van der Waals' equation but represents the compressibility factor of gases much better. Except for the vicinity of the critical point, it gives results fairly close to the data of the generalized charts. However, since it contains only two individual parameters, one cannot expect too much of it, in view of the well-known invalidity of the theorem of corresponding states.

One would hesitate, of course, to compare a two-parameter equation such as Redlich-Kwong's with the eight-parameter equation of Benedict, Webb and Rubin (77) or with the nine-parameter Martin-Hou (78) equation. It goes without saying that the latter equations are much superior in the representation of data in a limited range. Van der Waals and others who followed him, such as Clausius, Dieterici, Berthelot, Wohl, as well as Redlich and Kwong, endeavored to find equations covering the whole range of density from infinitely attenuated gas to compressed liquid, but were willing to accept fairly large deviations from the experimental results. It is interesting to note, however, that Redlich in later papers with other collaborators (79,80) focused attention on higher precision representation and increased the

number of arbitrary constants in his equation from 2 to 44. Independent investigations on pure substances and mixtures, by several workers (81,82,83,84,85,86), during the last few years have led to the conclusion that the crude two-parameter Redlich-Kwong equation is not inferior to the eight-parameter B-W-R equation, and it is generally regarded as the best two-parameter equation now available (75). The remarkable success of the tables of Pitzer (69) or Riedel (70) for compressibility factors prompted Redlich et al. (80) to include Pitzer's "acentric factor" as a third parameter, in addition to the critical temperature and pressure, in their improved equation. Even further development suggested by Redlich and coworkers (79) failed to yield good results for mixtures. The failure of the equation to give consistently good results for mixtures is probably due to the inflexible combination rules for the composition dependence of the equation-of-state constants. Chueh and Prausnitz (87) proposed a modified mixing rule for the constant  $a$ ; this modification incorporated one characteristic binary constant. A somewhat similar treatment, restricted to light hydrocarbon-carbon dioxide mixtures, has been suggested by Joffe and Zudkevitch (88). Other modifications of the Redlich-Kwong equation have been reported by several authors (83,84,85,86).

As has been mentioned earlier only the virial equation has a sound theoretical foundation for representing the properties of pure and mixed gases. When truncated after the third term, the virial equation is useful up to a density nearly corresponding to the critical density. A method for estimating the third virial coefficient of mixtures has been given by Prausnitz and coworkers (89,90,91). For application at

higher densities, an empirical equation of state such as the Redlich-Kwong equation (76) is more reliable. For vapor-phase fugacity coefficients the Redlich-Kwong equation is useful throughout the entire range of density.

The Redlich-Kwong equation is

$$P = \frac{RT}{v-b} - \frac{a}{T^{0.5} v(v+b)} \quad (25)$$

where

$$a = \frac{\Omega_a R^2 T_{ci}^{2.5}}{P_{ci}} \quad (26)$$

$$b = \frac{\Omega_b R T_{ci}}{P_{ci}} \quad (27)$$

The dimensionless constants  $\Omega_a$  and  $\Omega_b$  are, respectively, 0.4278 and 0.0867 if the first and second isothermal derivatives of pressure, with respect to volume, are set equal to zero at the critical point. In vapor-liquid equilibria, however, one is interested in the volumetric behavior of saturated vapors over a relatively wide range of temperature, rather than in the critical region only. Therefore,  $\Omega_a$  and  $\Omega_b$  should be evaluated for each pure component by fitting equation (25) to the volumetric data of the saturated vapor. The temperature range to be used is that from the normal boiling point to the critical temperature. A list of  $\Omega_a$  and  $\Omega_b$  for the saturated vapors of some pure substances has been given by Chueh and Prausnitz (87).

In order to attain the real objective of an equation of state, combination rules for the parameters have to be established. In

general, linear combination is used for the coefficients  $a$  and  $b$  in equations (26) and (27) but, a combination of the attraction coefficients  $a_i$  may also be provided by means of arbitrary interaction coefficients  $a_{ij}$ , which, in general, is chosen by trial so that available data for mixtures are best represented. Chueh and Prausnitz (87) have proposed:

$$b = \sum_{i=1}^N y_i b_i \quad (28)$$

where

$$b_i = \frac{\Omega_{bi} R^T c_i}{P_{ci}} \quad (29)$$

and

$$a = \sum_{i=1}^N \sum_{j=1}^N y_i y_j a_{ij} \quad (a_{ij} \neq \sqrt{a_{ii} a_{jj}}) \quad (30)$$

where

$$a_{ii} = \frac{\Omega_{ai} R^2 T_{ci}^{2.5}}{P_{ci}} \quad (31)$$

$$a_{ij} = \frac{(\Omega_{ai} + \Omega_{aj}) R^2 T_{cij}^{2.5}}{2P_{cij}} \quad (32)$$

$$P_{cij} = \frac{Z_{cij} R^T c_{ij}}{v_{cij}} \quad (33)$$

$$v_{cij}^{1/3} = \frac{1}{2} (v_{ci}^{1/3} + v_{cj}^{1/3}) \quad (34)$$

$$Z_{cij} = 0.291 - 0.08 \left( \frac{\omega_i + \omega_j}{2} \right) \quad (35)$$

$$T_{cij} = \sqrt{T_{cii} T_{cjj}} (1 - k_{ij}) \quad (36)$$

The binary constant  $k_{ij}$  represents the deviation from the geometric mean for  $T_{cij}$ . It is a constant characteristic of the  $i - j$  interaction; to a good approximation  $k_{ij}$  is independent of the temperature, density, and composition. In general,  $k_{ij}$  must be obtained from some experimental information about the binary interaction. Good sources of this information are provided by second virial cross coefficients (92) or by saturated liquid volumes of binary systems (90). Best estimates of  $k_{ij}$  have been reported for some binary systems by Chueh and Prausnitz (87).

The mixing rule proposed by Chueh and Prausnitz (87) for  $a_{ij}$  differs from Redlich's original mixing rule in two respects: (1) introduction of a binary constant  $k_{ij}$ , and (2) combination of critical volumes and compressibility factors to obtain  $a_{ij}$  according to equation (32) through (35). As a result of (2), the mixing rule proposed by Chueh and Prausnitz does not reduce to Redlich's original rule even when  $k_{ij} = 0$ , except when  $v_{ci}/v_{cj}$  is close to unity; in general Redlich's original rule gives a value for  $a_{ij}$  slightly smaller than that given by Chueh and Prausnitz's proposed rule with  $k_{ij} = 0$ .

McGlashan and Potter (93) have used the Lorentz combination (equation 34) for pseudo-critical volumes and the geometric mean rule for pseudo-critical temperatures to obtain remarkable agreement with their experimental interaction virial coefficients. It has long been recognized that for mixtures of substances with widely different molecular sizes the pseudo-critical temperature predicted by the geometric

mean is too large. Several modifications of this combination rule have been proposed. Hudson and McCoubrey (94) have derived an equation which includes first ionization potentials. Fender and Halsey (95) suggested a harmonic mean combination. More recently Dantzler, Knobler and Windsor (96) used these combination rules and obtained too weak an interaction, whereas the geometric mean rule provided results which showed too strong an interaction. Therefore, Chueh and Prausnitz's correlation seems to be the best, since it takes account of the deviation from the geometric mean rule.

### III B. (II) Fugacity Coefficient

The fugacity of a component  $i$  in a gas mixture is related to the total pressure  $P$  and its mole fraction  $y_i$  through the fugacity coefficient  $\phi_i$  as shown in equation (21).

The fugacity coefficient is a function of pressure, temperature, and gas composition; it is related to the volumetric properties of the gas mixture by either of the two exact relations (97,98):

$$RT \ln \phi_i = \int_0^P \left[ \left( \frac{\partial V}{\partial n_i} \right)_{T,P,n_j} - \frac{RT}{P} \right] dP \quad (37)$$

$$RT \ln \phi_i = \int_V^\infty \left[ \left( \frac{\partial P}{\partial n_i} \right)_{T,V,n_j (j \neq i)} - \frac{RT}{V} \right] dV - RT \ln Z \quad (38)$$

where  $V$  is the total molal volume of the gas mixture, and  $Z$  is the compressibility factor of the gas mixture at  $T$  and  $P$ . Since most

equations of state are explicit in pressure, equation (38) is more convenient to use.

For a mixture of ideal gases  $\phi_i = 1$  for all values of  $i$ .

For a gas mixture that follows Amagat's assumption ( $\bar{v}_i = v_{\text{pure } i}$  at the same  $T$  and  $P$  for the entire pressure range from zero to  $P$ ), equation (37) gives the Lewis fugacity rule (99) which says

$$\phi_i = \phi_{\text{pure } i} \quad (\text{at same } T \text{ and } P) \quad (39)$$

This simplifying assumption, however, may lead to large error, especially for components present in small concentrations. The Lewis fugacity rule becomes exact (at any pressure) only in the limit  $y_i \rightarrow 1$ .

The fugacity coefficient of component  $i$  in a gas mixture can be calculated from equations (37) and (38) if sufficient volumetric data are available for the gas mixture. Since such data are not usually available, especially for multicomponent systems, fugacity coefficients are most often calculated by an extension of the theorem of corresponding states or with an equation of state.

The formulation of the corresponding states theorem was done by van der Waals (8) in 1873. This principle was extended by Pitzer (100) in terms of molecular interactions. Longuet-Higgins (101), Scott (102), Brown (103), Prigogine et al. (104), and Wojtowicz et al. (105) have applied the molecular corresponding states equations to ideal fluid mixtures. An alternate corresponding states procedure has recently been presented by Flory and others (106). A review of the extensions of the theorem of corresponding states is provided by Stiel (107). The method of calculating the fugacity coefficients based on



corresponding states has been discussed by Joffe (108) and Leland et al. (109,110).

It is often more accurate to calculate the fugacity coefficients from an equation of state rather than by using the method based on the corresponding states theorem.

### III B. (III) Fugacity Coefficients from Revised Redlich-Kwong Equation.

To obtain numerical results, it is necessary to substitute a particular equation of state into equation (38). By substituting equation (25) and the mixing rules, (equations (28) through (36)), into (38), the fugacity coefficient of component k in the mixture becomes:

$$\ln \phi_k = \ln \frac{v}{v-b} + \frac{b_k}{v-b} - \frac{2 \sum_{i=1}^N y_i a_{ik}}{RT^{3/2} b} \ln \frac{v+b}{v} + \frac{ab_k}{RT^{3/2} b^2} \left[ \ln \frac{v+b}{v} - \frac{b}{v+b} \right] - \ln \frac{Pv}{RT} \quad (40)$$

The molal volume,  $v$ , is that of the gas mixture; it is obtained by solving equation 25 (which is cubic in  $v$ ) and taking the largest real root for  $v$ .

The good agreement between experimental and calculated fugacity coefficients at high pressures, as obtained by Chueh and Prausnitz (87), suggests that the revised Redlich-Kwong equation can be successfully applied to mixtures containing nonpolar or slightly polar gases.

Sometimes, while calculating the fugacity coefficient of a polar molecule from correlations based on the extended corresponding states theory, the value of the acentric factor (111) of the polar component

is taken as that of its homomorph (112). The acentric factor is defined as  $\omega \equiv -\log P_R \Big|_{T_R = 0.7} - 1.000$ , that is the value of  $P_R$  at  $T_R = 0.7$  is used to define this term. A homomorph of a polar molecule is a nonpolar molecule having approximately the same size and shape as those of the polar molecule. For example, the homomorph of acetone is isobutane. Since the corresponding states theory has not been used in this work, no use of such a concept has been made in the calculations of fugacity coefficients of mixtures.

### III C. Liquid-Phase Activity Coefficients.

#### III C. (I) Reference States.

The activity coefficients of the constituents of a liquid solution are functions of composition, temperature, and pressure of the liquid solution and also depend upon the reference state chosen. The choice of reference state determines the normalization of the activity coefficient; when the pressure, temperature and composition which determine  $f_i^L$  in equation (22) are the same as those of the reference state,  $\gamma_i$  must attain a fixed value. When the normalization of activity coefficients is spoken of, a specification of the state wherein the activity coefficient is unity is meant. For condensable components (subcritical), i.e., for components whose critical temperatures are above the temperature of the solution, it is customary to normalize the activity coefficient so that

$$\gamma_i \rightarrow 1 \quad \text{as} \quad x_i \rightarrow 1 \quad (41)$$

For such components, then, the fugacity becomes equal to the mole fraction times the standard-state fugacity as the composition of

the solution approaches that of the pure liquid. Thus, in this case the standard-state fugacity for component  $i$  is the fugacity of pure liquid  $i$ . In many common cases all the components in a liquid mixture are subcritical and equation (41) is therefore used for all components; since all components are, in this case, treated alike, the normalization of activity coefficients is said to follow the symmetric convention.

If, however, the liquid solution contains a noncondensable (supercritical) component, the normalization shown in equation (41) cannot be applied to that component since a pure, supercritical liquid is a physical impossibility. Of course, it is possible to introduce the concept of a pure, hypothetical supercritical liquid and to evaluate its properties by extrapolation and, provided that the component in question is not excessively above its critical temperature, this concept is quite useful. These hypothetical liquids are referred to as condensable components whenever they follow the convention of equation (41). However, for a highly supercritical component the concept of a hypothetical liquid is of little use since the extrapolation of pure liquid properties in this case is so excessive as to lose all its physical significance.

For a noncondensable component  $i$  (the temperature  $T$  of the solution is near or above the critical temperature  $T_{ci}$ ), therefore, it is convenient to use a normalization different from that given by equation (41); in its place equation (42) is used

$$\gamma_i^* \rightarrow 1 \quad \text{as} \quad x_i \rightarrow 0 \quad (42)$$

The purpose of the asterisk is to call attention to the difference in normalization and is a reminder that the unsymmetric convention has been

used for normalization of activity coefficients.

According to equation (42) the fugacity of component  $i$  becomes equal to the mole fraction times the standard-state fugacity of  $i$  when component  $i$  is infinitely dilute. The concentration region where the activity coefficient of a dilute component is (essentially) equal to unity is called the ideal dilute solution or Henry's law region. The characteristic constant for the ideal dilute solution is Henry's constant  $H$  which is defined by

$$H \equiv \lim_{x_i \rightarrow 0} \frac{f_i^L}{x_i} \quad (43)$$

The use of Henry's constant for a standard-state fugacity means that the standard-state fugacity for a noncondensable component depends not only on the temperature but also on the nature of the solvent. It is this feature of the unsymmetric convention, equations (42) and (43), which is its greatest disadvantage and it is as a result of this disadvantage that special care must be exercised in the use of the unsymmetric convention for multicomponent solutions. Since  $H$  depends on the solvent, the most convenient procedure in the case of a mixed solvent is to define the standard-state fugacity of a noncondensable component as Henry's constant for that component in a pure (reference) solvent which is a constituent of the solvent mixture.

### III C. (II) Gibbs-Duhem Equation

The activity coefficients of all the components in a multicomponent solution are not independent but are related by the Gibbs-Duhem equation which at constant temperature and pressure has the form

$$\sum_i x_i d \ln \gamma_i = 0 \quad (44)$$

Now, for a binary two-phase system the phase rule states that at constant temperature it is impossible to vary the composition without also varying the pressure. In thermodynamic analysis of low-pressure vapor-liquid equilibria the small effect of pressure on the activity coefficients is often neglected entirely or it is taken into account approximately. At high pressures, the effect of pressure on the activity coefficient is large and thus, if the Gibbs-Duhem equation at constant temperature and pressure is to be used, all isothermal activity coefficients must be corrected to the same pressure. If the standard state is defined at a fixed pressure, this correction is given by the equation

$$\left( \frac{\partial \ln \gamma_i}{\partial P} \right)_{x,T} = \frac{\bar{v}_i^L}{RT} \quad (45)$$

where  $\bar{v}_i^L$  is the partial molal volume of component  $i$  in the liquid phase at composition  $x$  and at temperature  $T$ .

In order to satisfy equation (44) it is necessary to adjust the activity coefficient through equation (45) in such a way that it is a function only of composition, for if this is done two advantages are obtained. Firstly, the Gibbs-Duhem equation and its various integrated solutions (the van Laar equation or the Margules equation) may be applied to these pressure-independent activity coefficients, thus enabling one to subject them to a test for thermodynamic consistency and to express them analytically by simple mathematical functions. Secondly, by

separating from each other the effects of composition and pressure on the activity coefficient, interpretation and correlation of the equilibrium data are very much facilitated. Therefore, it is useful to define the adjusted (pressure-independent) activity coefficients as given in the next section.

### III C. (III) Effect of Composition

For the heavy (condensable or subcritical) component the adjusted activity coefficient is

$$\gamma_1^{(P^R)} = \frac{f_1}{x_1 f_{1 \text{ pure}}^{(P^R)}} \exp \int_P^{P^R} \frac{\bar{v}_1^L}{RT} dP \quad (46)$$

In equation (46) all quantities are evaluated at the temperature  $T$  of the solution which is well below the critical temperature  $T_{c1}$ . The fugacity  $f_1$  is for component 1 at the composition  $x_1$  and at the total pressure  $P$ , but  $f_{1 \text{ pure}}^{(P^R)}$  is the fugacity of pure liquid component 1 at the (arbitrary) reference pressure  $P^R$  and  $\bar{v}_1^L$  is the partial molal volume of component 1 at the composition  $x_1$ . The adjusted activity coefficient  $\gamma_1^{(P^R)}$  is independent of the total pressure of the solution for any isotherm; it depends only on the composition and always refers to the reference pressure  $P^R$ , which is most conveniently set equal to zero (see subsection III C. (IV)).

From equation (46) it follows that regardless of the choice of  $P^R$

$$\gamma_1^{(P^R)} \rightarrow 1 \quad \text{as} \quad x_1 \rightarrow 1 \quad (47)$$

For the light (non-condensable or supercritical) component the definition of the adjusted, pressure-independent, activity coefficient is

$$\gamma_2^* (P^r) = \frac{f_2}{x_2 H_{2(1)} (P^r)} \exp \int_P^{P^r} \frac{-L}{RT} dP \quad (48)$$

In equation (48) all quantities are evaluated at the temperature  $T$  of the solution which is near or above the critical temperature  $T_{c2}$ . The fugacity  $f_2$  is for component 2 at the composition  $x_2$  and at the total pressure  $P$  while  $H_{2(1)}$  is the standard state fugacity (Henry's law constant) evaluated at the reference pressure  $P^r$ . The partial molal volume of component 2 is evaluated at the composition  $x_2$ . The asterisk indicates that the activity coefficient for component 2, unlike that for component 1, does not approach unity as the mole fraction of component 2 approaches one. The adjusted activity coefficient  $\gamma_2^* (P^r)$  is also independent of the total pressure; for any isotherm it depends only on the composition and always refers to the reference pressure  $P^r$ .

From equation (48) it again follows that

$$\gamma_2^* (P^r) \rightarrow 1 \quad \text{as} \quad x_1 \rightarrow 1 \quad (x_2 \rightarrow 0) \quad (49)$$

regardless of the choice of  $P^r$ .

The normalization relations given by equations (47) and (49) are desirable boundary conditions for integration of the Gibbs-Duhem equation. For a binary system, the isothermal, isobaric Gibbs-Duhem equation, following equation (44), is given by

$$x_1 d \ln \gamma_1^{(Pr)} + x_2 d \ln \gamma_2^* (P^r) = 0 \quad (50)$$

The composition dependence of the activity coefficients defined by equations (46) and (48) can be represented by an integrated form of

equation (50) with the boundary conditions given by equations (47) and (49). These normalization relations (equations 47 and 49) suggest that both activity coefficients approach unity as the liquid solution becomes infinitely dilute with respect to the light component. Through the exponential factors in equations (46) and (48) (the Poynting correction), the effect of pressure is separated from the effect of composition. Sub-section III C. (VI) deals with the effect of pressure on the activity coefficients and a technique for calculating partial molal volumes  $\bar{v}_1^L$  and  $\bar{v}_2^L$ , required in equations (46) and (48), is presented therein.

In equation (48), any ambiguity (see sub-section III C. (I) - Reference States) in the standard state fugacity of the supercritical gas has been avoided by the use of the experimentally accessible Henry's constant

$$H_{2(1)}^{(P^R)} = H_{2(1)}^{(P_1^S)} \int_{P_1^S}^{P^R} \frac{\bar{v}_2^\infty}{RT} dP \quad (51)$$

where  $H_{2(1)}^{(P_1^S)}$  is evaluated by extrapolating to  $x_2 = 0$  a plot of  $\ln f_2/x_2$  vs.  $x_2$ . In equation (51),  $P_1^S$  is the saturation (vapor) pressure of solvent 1 and  $\bar{v}_2^\infty$  is the liquid partial molal volume of component 2 infinitely dilute in solvent 1.

### III C. (IV) Choice of Reference Pressure

In equations (46) and (48), the reference pressure  $P^R$  is completely arbitrary; this arbitrariness, however, in no way influences the fact that the adjusted activity coefficients defined above must satisfy equation (50).



The partial molal volumes in the integrals of equations (46) and (48) are for the liquid phase and thus, for physically meaningful results, the reference pressure  $P^r$  should be such that the liquid phase can exist over the entire pressure range  $P \rightarrow P^r$ ; this means that  $P^r$  must be equal to or larger than the highest observed pressure along the isotherm under consideration.

For practical applications in vapor-liquid equilibria, however, this requirement is not very useful; in performing typical calculations it is easiest to choose as the reference pressure the system pressure when  $x_2 = 0$ , i.e., the saturation (vapor) pressure  $P_1^S$  of the heavier component. This reference pressure is convenient because it is the one at which the Henry's law constant is evaluated; it is a pressure which depends only on the properties of the solvent and not on those of the solute. Unfortunately, however,  $P_1^S$  is the minimum rather than the maximum pressure along a given isotherm and thus the integration path from  $P$  to  $P_1^S$  is in a hypothetical region, since the liquid phase of a given composition cannot exist at any pressure less than the total pressure of the two-phase system. For computation purposes in engineering work this is not a serious deficiency since the partial molal volume is almost never known as a function of pressure and thus, as a matter of necessity, the partial molal volumes in the integrals must be considered as functions of composition and temperature only.

If, however, comparisons are to be made between observed activity coefficients and those predicted by theories of solution, hypothetical regions must be avoided. For convenience, therefore,  $P^r$  has been chosen as zero pressure in this work. Thus, the activity coefficients

can be expressed by simple analytical functions which are solutions of the Gibbs-Duhem differential equation (equation 50) subject to the (arbitrary) boundary conditions which determine the normalizations of the various activity coefficients.

### III C. (V) Analytical Representation of Activity Coefficients

A general technique for obtaining analytical expressions for activity coefficients of liquid mixtures has been given by Wohl (113); the main idea of this technique is to define an excess free energy and then to expand this excess free energy in a series of algebraic functions of the mole fractions. The same technique can be used for solutions of gases in liquids but the physical meaning of the excess free energy is now quite different since the standard state for the light component refers to the infinitely dilute solution rather than to the pure liquid as in Wohl's case. As a result, the nature of the algebraic expansion for gas-liquid solutions is also different from that for liquid-liquid solutions.

#### III C. (V) (a) Excess Gibbs Energy

The variation of activity coefficients with composition is best expressed through the auxiliary function  $G^E$ , the molar excess Gibbs energy, defined by

$$\frac{G^{E*}}{RT} = x_1 \ln \gamma_1^{(P^r)} + x_2 \ln \gamma_2^{*(P^r)} \quad (52)$$

In view of the unsymmetric normalization,  $G^{E*}$  vanishes at infinite dilution with respect to component 2 but not with respect to component 1; that is

$$\left. \begin{aligned} G^{E*} &\rightarrow 0 \quad \text{as } x_2 \rightarrow 0 \\ \text{but} & \\ G^{E*} &\neq 0 \quad \text{as } x_1 \rightarrow 0 \end{aligned} \right\} \quad (53)$$

As defined here, the ideal solution ( $G^{E*} = 0$ ) is one where, at constant temperature and pressure, the fugacity of the light component is given by Henry's law (with suitable pressure correction) and that of the heavy component by Raoult's law. In molecular terms this means that  $G^{E*}$  is zero whenever the concentration of component 2 in the liquid phase is sufficiently small to prevent molecules of component 2 from interacting with one another.

Following Wohl (113), the excess Gibbs energy can be represented by summing interactions of molecules in a power series:

$$\frac{G^{E*}}{RT (x_1 q_1 + x_2 q_2)} = -\alpha_{22(1)} \frac{\phi_2^2}{2} - \text{higher terms} \quad (54)$$

where  $\phi$  is the effective volume fraction

$$\phi_2 = \frac{x_2 q_2}{x_1 q_1 + x_2 q_2} \quad (55)$$

where  $q_i$  is the effective size of the molecule  $i$  and where  $\alpha_{22(1)}$  is the self-interaction constant of molecules 2 in the environment of molecules 1. In equation (54) only two-body interactions are considered; higher terms are neglected to keep the number of adjustable parameters to a minimum.

The activity coefficients can be found from equation (54) by using the familiar relations

$$\frac{1}{RT} \left( \frac{\partial n_T G^{E*}}{\partial n_1} \right)_{T,P,n_2} = \ln \gamma_1^{(P^r)} \quad (56)$$

$$\frac{1}{RT} \left( \frac{\partial n_T G^{E*}}{\partial n_2} \right)_{T,P,n_1} = \ln \gamma_2^{*(P^r)} \quad (57)$$

where  $n_1$  is the number of moles of component 1 and  $n_T$  is the total number of moles.

### III C. (V) (b) A Dilated Van Laar Model for Binary Liquid Mixtures

In view of the definition of ideality given earlier, deviations from ideal behavior are due not to interactions between molecules of component 1 and molecules of component 2 with each other; the ideal solution is the infinitely dilute mixture where molecules of component 2 are completely surrounded by molecules of component 1. As the mole fraction of the solute increases, molecules of solute begin to interact with each other and it is this interaction which is primarily responsible for non-ideality. Since interaction coefficients higher than those between two molecules are set equal to zero in equation (54), substitution of equations (55) and (56) yields for component 1 the familiar van Laar equation (for unsymmetric normalization)

$$\ln \gamma_1^{(P^r)} = \frac{A}{\left[ 1 + (A/B)(x_1/x_2) \right]^2} \quad (58)$$

with

$$A \equiv \alpha_{22(1)} q_1$$

$$B \equiv \alpha_{22(1)} q_2$$

For component 2, the activity coefficient takes the considerably less familiar form

$$\ln \gamma_2^{*(P^r)} = B \left\{ \frac{1}{\left[ 1 + (B/A)(x_2/x_1) \right]^2} - 1 \right\} \quad (59)$$

(If it is assumed that  $q_1 = q_2$  then  $A = B$  and equations (58) and (59) become the two-suffix Margules equations).

Prausnitz (114) has shown that equations (58) and (59), containing two adjustable parameters, are satisfactory for fitting adjusted activity coefficients for the butane-carbon dioxide system but, they have been shown to be unsatisfactory for describing the properties of some systems which are at a temperature much above the critical temperature of the light component or near the critical temperature of the heavy component (115). In addition, Prausnitz et al. found that the three-suffix Margules equations were also unsatisfactory (115).

The probable reason for the failure of the classical van Laar treatment is due to van Laar's assumption that  $q_1$  and  $q_2$  are constants independent of composition, which is another way of saying that the structure of the solution does not change much with mole fraction. The  $q$ 's are parameters which reflect the cross sections, or sizes, or spheres of influence, of the molecules; at conditions remote from critical, where the liquid molal volumes are close to a linear function of the mole fraction, it is reasonable to assume that the  $q$ 's are composition independent, but for a liquid mixture of a non-condensable component 2 with a subcritical liquid 1, the molal volume of the mixture is a highly nonlinear function of the mole fraction, especially in the vicinity of the critical composition. The liquid solution dilates as  $x_2$  rises, and van Laar's model must be modified to take this effect into account.

For practical reasons (since experimental data are usually not plentiful), it is desirable to derive equations for the adjusted (constant-pressure) activity coefficients which contain no more than two parameters. Because of this limitation, it is also desirable to assume that whereas  $q_1$  and  $q_2$  depend on composition, their ratio does not. Since the van Laar treatment is a two-body (quadratic) theory, it is assumed that  $q_1$  and  $q_2$  are given by a quadratic function of the effective volume fraction:

$$q_1 = v_{c1} \left[ 1 + \eta_{2(1)} \phi_2^2 \right] \quad (60)$$

$$q_2 = v_{c2} \left[ 1 + \eta_{2(1)} \phi_2^2 \right] \quad (61)$$

From equations (60) and (61), it follows that the volume fraction  $\phi_i$  is given by

$$\phi_i = \frac{x_i v_{ci}}{\sum_i x_i v_{ci}} \quad (62)$$

Prausnitz et al. (115) have arbitrarily used the pure-component critical volumes in equations (60) and (61) as the measure of the molecular cross sections at infinite dilution, when  $\phi_2 = 0$ . Some other constant (for example, van der Waal's  $b$  or Lennard-Jones'  $\sigma^3$ ) could just as easily be used. The dilation constant  $\eta_{2(1)}$  is a measure of how effectively the light component dilates (swells) the liquid solution.

When equations (60) and (61) are substituted into the truncated equation (54), the adjusted (pressure-independent) activity coefficients are

$$\ln \gamma_1^{(P^r)} = A \phi_2^2 + B \phi_2^4 \quad (63)$$

$$\ln \gamma_2^{*(P^r)} = A \left( \frac{v_{c2}}{v_{c1}} \right) (\phi_2^2 - 2\phi_2) + B \left( \frac{v_{c2}}{v_{c1}} \right) (\phi_2^4 - \frac{4}{3}\phi_2^3) \quad (64)$$

where

$$A \equiv \alpha_{22(1)} v_{c1} \quad (65)$$

$$B \equiv 3\eta_{2(1)} \alpha_{22(1)} v_{c1} \quad (66)$$

Equations (63) and (64) are the desired two-parameter equations. These equations provide accurate representation of the constant-pressure activity coefficients of nonpolar binary mixtures from the dilute region up to the critical composition.

### III C. (V) (c) Mixtures of Condensable Components

At temperatures sufficiently lower than the critical temperature of the light component (component 2), the dilation constant  $\eta$  obtained from data reduction becomes so small that it can be effectively equated to zero. Under these conditions, the constant-pressure activity coefficients of both components can be correlated with only one parameter,  $\alpha$ . It has been empirically found that this occurs for  $T_{R2}$  less than 0.93. Therefore, components with a reduced temperature smaller than 0.93 are treated as heavy components (solvent), and those with  $T_R$  larger than 0.93 are treated as light components (solute). Systems for which both  $T_{R1}$  and  $T_{R2}$ , are smaller than 0.93 are correlated with  $\eta = 0$  and only one parameter,  $\alpha$ . Systems for which the critical temperatures of the two components are very similar are also analyzed with only one

parameter,  $\alpha$ , even though  $T_{R2}$  is larger than 0.93; the terms "heavy" and "light" component lose their conventional meaning for such systems. In fact, it sometimes happens that the component with the higher critical temperature ("heavy") may actually have a higher vapor pressure and critical pressure than the component with the lower critical temperature ("light").

For those systems where both components can exist in the pure liquid state, it is not necessary to use the unsymmetric convention for normalization of activity coefficients. Instead, such a system can be analyzed with a one-parameter, symmetric-convention expression for the excess Gibbs energy:

$$\frac{G^E}{RT(x_1 v_{c1} + x_2 v_{c2})} = \alpha_{12} \phi_1 \phi_2 \quad (67)$$

From equations (56) and (57) it follows that

$$\ln \gamma_1^{(PR)} = v_{c1} \alpha_{12} \phi_2^2 \quad (68)$$

$$\ln \gamma_2^{(PR)} = v_{c2} \alpha_{12} \phi_1^2 \quad (69)$$

where  $\gamma_1^{(PR)}$  is given by equation (46) and  $\gamma_2^{(PR)}$  by

$$\gamma_2^{(PR)} = \frac{f_2}{x_2 f_{\text{pure } 2}^{(PR)}} \exp \int_P^{PR} \frac{-L}{v_2 RT} dP \quad (70)$$

It has been shown (116) that for the case when both components are subcritical and the excess Gibbs energy is represented by equation (67), or by equation (54) with  $q_1 = v_{c1}$ ,  $q_2 = v_{c2}$  --- i.e.,  $\eta = 0$  --- there



exist rigorous relationships between the constants in the two conventions, viz.:

$$\alpha_{22(1)} = \alpha_{12} \quad (71)$$

$$\ln H_{2(1)}^{(Pr)} = \ln f_{\text{pure}2}^{(Pr)} + v_{c2} \alpha_{12} \quad (72)$$

### III C. (VI) Effect of Pressure

When discussing the Gibbs-Duhem equation it was indicated that a useful thermodynamic analysis of high-pressure vapor-liquid equilibria requires information on the effect of pressure on liquid-phase fugacities; this information is given by partial molal volumes in the liquid mixture.

At low or moderate pressures, liquid-phase activity coefficients are only weakly dependent on pressure and, as a result, it has been customary to assume that, for all practical purposes, activity coefficients depend only on temperature and composition. In many cases this is a good assumption but for phase equilibria at high pressures, especially for those near critical conditions, it can lead to serious error.

When the standard-state fugacity is defined at a constant pressure, for any component  $i$ , the pressure dependence of the activity coefficient  $\gamma_i$  is given by equation(45). At high pressures in the critical region,  $\bar{v}_i^L$  is usually a marked function of composition, especially for heavy components where  $\bar{v}_i^L$  frequently changes sign as well as magnitude. For convenience, the superscript L on the activity coefficient has been dropped in subsequent discussion.

Experimental data for partial molal volumes are rare for binary systems and for multicomponent systems there are essentially none. Since thermodynamic analysis or prediction of multi-component high-pressure phase equilibria requires partial molal volumes, a reliable method for calculating partial molal volumes from a minimum of experimental information is required.

### III C. (VI) (a) Partial Molal Volume from an Equation of State.

The partial molal volume of component  $k$  in a mixture of  $N$  components is defined by

$$\bar{v}_k = \left( \frac{\partial V}{\partial n_k} \right)_{P, T, n_i (i \neq k)} \quad (73)$$

The partial molal volume can be evaluated from a suitable equation of state for the liquid mixture. Since most equations of state are explicit in pressure rather than in volume, it is convenient to rewrite equation (73):

$$\bar{v}_k = \frac{-\left( \frac{\partial P}{\partial n_k} \right)_{T, V, n_i (i \neq k)}}{\left( \frac{\partial P}{\partial V} \right)_{T, n_i (\text{all } i)}} = f(x_1, \dots, T, v) \quad (74)$$

With an equation of state, equation(74) gives  $\bar{v}_k$  as a function of the composition, temperature, and molal volume  $v$  of the liquid mixture. Pressure does not appear explicitly in equation (74) but is implicit in the volume, which depends on the pressure.

It is required to know partial molal volumes at saturation for practical applications to vapor-liquid equilibria; therefore, the saturated molal volume of the liquid mixture in equation (74) is

needed. The saturated molal volume of a liquid mixture can be calculated by extending to mixtures the corresponding-states correlation of Lyckman et al. (117) who slightly revised Pitzer's tables (111) for the saturated liquid volume of pure substances, for the reduced temperature region 0.56 - 1.00. Before discussing equation (74) in more detail, the method for calculating the molal volume of a saturated liquid mixture is discussed here.

### III C. (VI) (b) Saturated Molal Volume of Liquid Mixtures up to a Reduced Temperature of 0.93.

Given only the temperature and composition, it is possible, in principle, to calculate the saturated volume of a liquid mixture from an equation of state. Such a calculation, however, requires an equation of state capable of describing accurately both vapor and liquid phases of multicomponent systems. For most mixtures, no such equation of state is known. In fact, the entire problem of phase equilibria at any pressure could be completely solved if such an equation of state were available. A more realistic and fruitful approach is provided by a corresponding-states correlation specifically, developed for saturated liquids by Lyckman et al. (117) from Pitzer's tables (111). In this correlation, the reduced saturated volume is given by

$$v_R = v_R^{(0)} + \omega v_R^{(1)} + \omega^2 v_R^{(2)} \quad (75)$$

where  $\omega$  is the acentric factor (111) and  $v_R^{(0)}$ ,  $v_R^{(1)}$ , and  $v_R^{(2)}$  are functions of reduced temperature which have been tabulated for reduced temperatures from 0.560 to 0.990 (117). To facilitate calculations

with an electronic computer Chueh and Prausnitz (90) have fitted the tabulated values with the following relation:

$$v_R^{(j)} = a^{(j)} + b^{(j)}T_R + c^{(j)}T_R^2 + d^{(j)}T_R^3 + e^{(j)}/T_R + f^{(j)}\ln(1-T_R) \quad (76)$$

where  $a^{(j)}$  to  $f^{(j)}$  are coefficients for  $v_R^{(0)}$ ,  $v_R^{(1)}$  and  $v_R^{(2)}$ ; these coefficients are given in their publication (90).

The reducing parameters for the reduced volume and the reduced temperature are the critical volume and the critical temperature, respectively. For pure components, equations (75) and (76) may be used for reduced temperatures from 0.560 to 0.995. For reduced temperatures above 0.995, the reduced volume may be obtained by first calculating the reduced volumes at  $T_R$  of 0.990 and 0.995, and then interpolating to  $T_R = 1.0$ ; by definition  $v_R = 1.0$  at  $T_R = 1.0$ .

Equations (75) and (76) were obtained from pure component data. For applications to mixtures, mixing rules for the pseudocritical volume and temperature are necessary. Such rules have been proposed by several authors (90,92,109,118,119, 120). Because of the small separation between molecules, molecular size is a more important factor in the liquid phase than in the vapor phase. Therefore, use of volume fractions (equation 62) rather than mole fractions (or combinations of mole fractions and volume fractions) is desirable for pseudocritical rules. For pseudoreduced temperatures up to 0.93 the following rules proposed by Chueh et al. (90) seem better, in so far as the volume fraction has been used rather than mole fractions which were used by other authors:

$$V_{cM} = \sum_i x_i v_{ci} \quad (77)$$

$$T_{cM} = \sum_i \sum_j \phi_i \phi_j T_{cij} \quad (78)$$

$$\omega_M = \sum_i \phi_i \omega_i \quad (79)$$

where  $\phi_i$  and  $T_{cij}$  are given by equations (62) and (36) respectively.

The constant  $k_{ij}$  has an absolute value much less than unity; it represents the deviation from the geometric-mean rule for the characteristic temperature of the  $i - j$  pair. To a good approximation,  $k_{ij}$  is a constant independent of temperature, composition and density. The binary constant  $k_{ij}$  must be evaluated from some binary data (92,121), which give information on the nature of  $i - j$  interactions. Prauznitz et al. listed some values of  $k_{ij}$  obtained from liquid phase measurements (90) and from second virial coefficients (92), which are in good agreement with those reported by Pitzer (121) from compressibility factors near the critical region.

The saturated liquid volume of a multicomponent mixture may be calculated with equations (75) and (76) and equations (77) through (79). Equations (77) and (78) are good pseudocritical rules for predictions up to  $T_R \leq 0.93$ . For larger  $T_R$  (critical region) a modification of the pseudocritical rules is required in order that they may converge to the true critical constants of the mixture at the critical point. To this end, correlations for true critical temperatures and volumes of mixtures as well as an equation-of-state method for calculating the true critical pressures of mixtures, have been developed (89,122) as indicated later.

With a reliable method for calculating the volumes of saturated liquid mixtures, partial molal volumes can now be calculated with equation (74) which requires an equation of state for liquid mixtures.

### III C. (VI) (c) Equation of State for Liquid Mixtures

For nonpolar liquids, an equation of the van der Waals type provides a reasonable description of volumetric properties. Since the Redlich-Kwong equation represents a useful modification of the van der Waals equation, this can be used for liquid mixtures with certain alterations. The Redlich-Kwong equation of state is given by equation (25), and, for any pure fluid, the two constants  $a$  and  $b$  can be related to the critical properties of that fluid by equations (26) and (27). As noted in Section III B. (I), if the conditions at the critical point are imposed, the dimensionless constants  $\Omega_a$  and  $\Omega_b$  become 0.4278 and 0.0867 respectively for all fluids. Adoption of these values is equivalent to fitting the equation of state to derivatives in the critical region which, although the most sensitive, does not provide the best fit over a wide range of conditions. This is particularly true when the equation is applied to the liquid phase. If the universal values for  $\Omega_a$  and  $\Omega_b$  are accepted it is, in effect, equivalent to subscribing to a two-parameter theorem of corresponding states. Pitzer and others, (69,70, 123,124), however, have shown that the theorem of corresponding states requires a third parameter, in order to be applicable to a wide class of substances. Therefore, to evaluate the best  $\Omega_a$  and  $\Omega_b$  for each pure component, the Redlich-Kwong equation is fitted to the P-V-T data of the saturated liquid. Fortunately, such data are readily available;

results are given by Chueh et al. (90) for some common liquids. They differ slightly from the universal values and show a trend with respect to an acentric factor.

For application of equation (25) to mixtures, the same mixing rules as given by equations (28) through (36) are used, except that the cube-root average for  $v_{cij}$ , equation (34), is replaced by the arithmetic mean of  $v_{ci}$  and  $v_{cj}$ ; this is done to weight the larger molecule slightly more heavily in the liquid phase.

### III C. (VI) (d) Partial Molal Volumes

The partial molal volume can be obtained from equation (25) and the mixing rules, [equations (27) and (29)], after performing the partial differentiation indicated in equation (74):

$$\bar{v}_k = \frac{\frac{RT}{v-b} \left(1 + \frac{b_k}{v-b}\right) - \frac{2 \left(\sum_i^N x_i a_{ki}\right) - \frac{ab_k}{v+b}}{v(v+b) T^{1/2}}}{\frac{RT}{(v-b)^2} - \frac{a}{T^{1/2}} \left[ \frac{2v+b}{v^2(v+b)^2} \right]} \quad (80)$$

Using  $v$ , the saturated liquid molal volume of the mixture, calculated from a corresponding states correlation, the partial molal volume of each component in a multicomponent liquid mixture can readily be calculated from equation (80).

With partial molal volumes, the effect of pressure on liquid-phase activity coefficients can be taken into account. By separating the effect of pressure from that of composition, experimental liquid-phase activity coefficients can be subjected to rigorous thermodynamic

analysis. Such analysis permits meaningful interpretation and correlation of binary, high-pressure, vapor-liquid equilibrium data.

The simple approximation of using partial molal volumes at infinite dilution usually leads to large error near the critical region. As noted before, for mixtures, the pseudocritical rules must be modified in the critical region ( $T_R > 0.93$ ).

### III C. (VI) (e) Critical Region.

In applying previously mentioned pseudocritical rules to the critical region, it has often been found necessary to introduce an empirical exponent which depends on the proximity to critical conditions (92,109). Chueh and Prausnitz (89) have used a general proximity function which corrects the pseudocritical rules of equations (77) and (78) in the critical region.

By definition,  $T_R = 1.0$  and  $v_R = 1.0$  at the critical point when the true critical constants of the mixture are used as the reducing parameters. Therefore, if the true critical constants of a mixture can be calculated, the mixing rules, equations (77) and (78), can be modified so that they will always converge to  $T_R = 1.0$  and  $v_R = 1.0$  at the critical point. In the following, primes have been used to indicate corrected pseudocritical constants. Chueh wrote

$$T'_{cM} = T_{cM} + (T_{cT} - T_{cM}) f(T_R) \quad (81)$$

and

$$v'_{cM} = v_{cM} + (v_{cT} - v_{cM}) f(T_R) \quad (82)$$

where  $T_{cT}$  and  $v_{cT}$  referred to the true critical temperature and true critical volume of the mixture, respectively. The second terms on the



right-hand sides of equations (81) and (82) correspond to the corrections added to the simple mixing rules, equations (77) and (78). The function  $f(T_R)$  represents the proximity of the system to its critical point; it must satisfy the two boundary conditions

$$f(T_R) \rightarrow 0 \quad \text{for } T_R < 0.93 \quad (83)$$

$$f(T_R) = 1 \quad \text{at } T_R = 1.0 \quad (84)$$

The first boundary condition ensures that equations (81) and (82) reduce to the simple mixing rules, equations (77) and (78), for  $T_R \ll 0.93$ . The second boundary condition ensures that they converge to  $T_{cM}' = T_{cT}$  and  $v_{cM}' = v_{cT}$  at the critical point. Chueh et al. then suggested the following empirical function which satisfied the above boundary conditions:

$$f(T_R) = \exp \left[ (T_R - 1) \left( 2901.01 - 5738.92T_R + 2849.85T_R^2 + \frac{1.74127}{1.01 - T_R} \right) \right] \quad (85)$$

Equation (85) was found to be sufficiently general for all systems investigated by them. The reducing parameter for  $T_R$  in equation (85) is the corrected pseudocritical temperature  $T_{cM}'$  rather than the true critical temperature which is adequate at the critical point only. As a result  $T_{cM}'$  appears on both sides of equation (81) and iteration is required to solve for  $T_{cM}'$ . This is best done by rewriting equation (81):

$$\left[ \frac{(T/T_{cM}')}{T_R} - 1 \right] - \left[ \frac{(T/T_{cM}')}{(T/T_{cT})} - 1 \right] f(T_R) = 0 \quad (86)$$

Equation (86) has only one unique solution for  $T_R < 1.0$  which can readily be found by a numerical technique (for example, Reguli-falsi iteration with variable pivoting points). The method usually converges in a few iterations. From equation (82),  $v_{cM}'$  can then be obtained by direct

substitution.

Equations (81) and (82) may be considered as more general pseudocritical rules applicable over the whole temperature range up to the critical point. With the corrected pseudocritical constants, the saturated molal volumes of liquid mixtures can be calculated from equations (75) and (76) in the manner discussed before.

The true critical temperature and volume of mixtures, needed for equations (81) and (82), can be calculated from a correlation discussed in detail by Chueh et al. (122). Several other authors (82, 125 to 136) have reported correlations of the critical temperature or critical pressure of mixtures but these, by and large, have been confined to a particular chemical class of substances, viz. the paraffins. Very little work has been reported on the correlation of critical volumes of mixtures (134). Chueh et al. (122) concentrated their attention on normal fluids (as defined by Pitzer (111)); that is, on molecules which have zero (or small) dipole moments, no tendency to associate by hydrogen bonding or similar chemical forces, and which have sufficiently large mass to permit neglect of quantum corrections.

Rowlinson (24) has shown that for a binary mixture of components 1 and 2, the critical temperature of the mixture is, to a good approximation, a simple quadratic function of the mole fraction, provided components 1 and 2 consist of simple, spherically symmetric molecules of nearly the same size. Rowlinson writes

$$T_{cT} = x_1 T_{c1} + x_2 T_{c2} + 2x_1 x_2 \Delta T_{12} \quad (87)$$

where  $\Delta T_{12}$  is a known function of  $T_{c1}$ ,  $T_{c2}$ ,  $v_{c1}$  and  $v_{c2}$ , and a parameter

which depends on the two exponents used in the potential function for describing the intermolecular forces. For mixtures differing appreciably in molecular size, Rowlinson's treatment is not useful, and for such mixtures, the thermodynamic properties are quadratic functions of the mole fraction only at moderate densities (second virial coefficients); at liquid-like densities, it has been common practice to express the thermodynamic properties of such mixtures in terms of volume fractions. The critical density is intermediate between that of liquids and that where the second virial coefficient gives a sufficiently good approximation. Therefore, the true critical constants can be related to the composition by expressions using the surface fraction  $\theta$  defined by

$$\theta_i = \frac{x_i v_{ci}^{2/3}}{\sum x_i v_{ci}^{2/3}} \quad (88)$$

For a binary mixture, Chueh et al. (122) write

$$T_{cT} = \theta_1 T_{c1} + \theta_2 T_{c2} + 2\theta_1 \theta_2 \tau_{12} \quad (89)$$

$$v_{cT} = \theta_1 v_{c1} + \theta_2 v_{c2} + 2\theta_1 \theta_2 v_{12} \quad (90)$$

The correlating parameters  $\tau_{12}$  and  $v_{12}$  are measures of the (small) deviations of the mixture critical constants as given by a linear dependence on the  $\theta$  fraction; they are characteristic of the 1-2 interaction. Extensive compilations of these parameters for some systems are given by Chueh et al. (122) in their publication. The parameters are given in the reduced form as determined from experimental data of these systems.

In the critical region the calculations are strongly dependent on the accuracy of the calculated true critical temperature. Chueh et al. (90) quote an error of more than 5% in the calculated volume caused by an error of 0.5% in the calculated true critical temperature. This is obvious, since the reduced volume is a very sensitive function of reduced temperature in the critical region; for a simple fluid ( $\omega = 0$ ), the reduced volume at  $T_R = 0.99$  is 0.7327, whereas at  $T_R = 1.00$ ,  $v_R = 1.0$  by definition. Thus, near the critical point, a 1% change in reduced temperature causes a change in reduced volume of about 30%. This extreme sensitivity of volumetric properties to small changes in temperature or composition is inherent in the nature of the critical state and cannot easily be eliminated, either by experiment or by calculation.

Having correlated critical temperatures and critical volumes with quadratic functions of the surface fraction, one is tempted to try a similar correlation for the critical pressure. Attempts at such a correlation have not been fruitful. Several investigators (135) have noted that the dependence of the critical pressure on composition is much more strongly nonlinear than that of the critical temperature and the critical volume; in many systems a plot of critical pressure vs. mole fraction shows a sharp maximum and a point of inflection. The more complicated behavior of the critical pressure follows from its non-fundamental nature; subject to well-defined assumptions, both critical temperatures and critical volumes can be related directly to the intermolecular potential, but the critical pressure can be related to the intermolecular potential only indirectly through the critical temperature and critical volume.

To express the critical pressure as a function of composition, the correlations for critical temperature and critical volume can be used coupled with an equation of state, e.g., the Redlich-Kwong equation (equation 25). Thus, the experimental results can be compared with such correlations.

## CHAPTER II.

## NATURE OF THE PROBLEM AND REVIEW OF THE LITERATURE

Information on the temperature, pressure and volume at the critical point is required for the use of a number of important approximation methods for predicting pressure-volume-temperature relations for liquids and gases, heats of vaporization and other physical and thermodynamic properties. Analytical equations of state, with constants related to the composition and pure-component critical properties are used for estimating the P-V-T properties of mixtures. Experimental P-V-T data for gas mixtures are not common. To predict the properties of mixtures the critical constants of pure components are therefore required.

At the present time, no general methods are available which allow more than an approximate estimation of the density of a pure liquid under critical conditions. Values of the liquid density are available at room temperature for almost all known compounds. Although the corresponding state methods allow extrapolation with temperature and pressure when at least one liquid density datum point is available, it is desirable to measure the density directly.

The determination of the vapor-pressure of pure substances is also essential for many important practical and theoretical applications. Because only fragmentary or inconsistent experimental data are available for most substances over the complete range up to the critical region, this property is generally calculated from general relationships such as generalized charts. Therefore, investigations should continue to

obtain very precise physical property data, experimentally.

Much investigation in the field of thermodynamics of liquid solutions has been undertaken in connection with vapor-liquid equilibrium phenomena. The experimental data, specifically the measured relationship between liquid and vapor compositions, and temperature in an isobaric system or pressure in an isothermal system, as well as vapor pressures of the pure substances, are tested for thermodynamic consistency by means of the Gibbs-Duhem relationship. Such investigations are referred to as correlations.

It is often desirable to predict the vapor-liquid equilibria from a limited amount of experimental data. The more modest attempts have been aimed at predicting the most essential data, vapor composition as a function of liquid composition, from other more easily obtained experimental data. An example is the calculation of these data from experimental determinations of vapor pressures of pure components, and the boiling temperatures of mixtures at constant pressure.

The more ambitious attempts at prediction involve calculation of complete equilibria from the properties of the pure substances and a measure, independent of experimental vapor-liquid equilibrium determinations, of their behavior in mixtures. The simple example of such a method is a common Raoult's law prediction in which the vapor pressures are used and it is assumed that the behavior upon mixing is ideal. Where this assumption cannot be made, the prediction, essentially a matter of determining the liquid nonidealities, becomes much more difficult.

Several methods are presented in the literature for the

prediction of vapor-liquid equilibrium constants of mixtures from thermodynamic relationships. For many years, several different approaches, such as the convergence pressure concept, equations of state, the application of the principle of corresponding states, etc., have been tried for the correlation of such data. Although these methods are valuable, only a few can be used for the determination of vapor-liquid equilibrium constants for elevated pressure conditions. Significant deviations are found between calculated and experimental values at elevated pressures, particularly for conditions near the critical point.

The method of correlating vapor-liquid equilibrium data in this work is therefore based on the separate description of the deviations occurring in the vapor phase and liquid phase; these deviations are then correlated with thermodynamically consistent expressions. In this method, the vapor phase nonideality is calculated from the modified Redlich-Kwong equation of state (83,90); the liquid nonideality is calculated with reference to the pure liquid components and the deviations from ideal solution laws.

I chose four pure materials and one mixture for study of the physical and thermodynamic properties. The pure materials chosen for examination have different molecular sizes and shapes, and divergent properties. These materials and their extreme characteristics are as follows:

1. Acetone, a polar material having no association constant (an oxygenated solvent).
2. Chloroform, a polar material and a representative



associating compound (a halogenated hydrocarbon).

3. Benzene, a quasi-spherical polyatomic molecule, essentially non-polar (an aromatic hydrocarbon).
4. Carbon Tetrachloride, a seemingly "symmetrical" and freely rotating nearly spherical molecule, characterized by the absence of pronounced polarity.

The ternary system consisting of the first three compounds has previously been investigated in this laboratory by the author (137) in regard to its thermodynamic and physical properties. The constituent binary systems have also been investigated for vapor pressures, excess volumes on mixing, the vapor-compositions and the excess enthalpies and excess viscosities of mixing at 25°C (137). From the data obtained excess Gibbs free energies and excess entropies have been calculated (138). The pertinent review of the literature up to 1965 for the binary system investigated in this work, i.e., the acetone-benzene system is given elsewhere (137) by the author. The only work after that date is by Abbott (139) who obtained second virial coefficients from measurements made on a vapor density balance at 45°C, 60°C, 75°C, and 90°C.

In view of the interest in critical phenomena of partially miscible binary liquid systems ( $L_1 \rightleftharpoons L_2$ ) which has existed in this laboratory for several years I decided to extend the investigation to one-component gas-liquid critical points. The system acetic acid-chloroform-water is one of the classical examples of partial miscibility in a ternary system, investigated in this laboratory for the equilibrium relations at 25°C (140,141,142) and for the critical phenomena

( $L_1 - L_2$ ,  $L_1 - V$  and  $L_2 - V$ ) by Campbell and Kartzmark (143). Since the systems consisting of acetone, benzene, and chloroform have been dealt with from the thermodynamic point of view in a previous paper (138), I undertook the study of critical phenomena ( $L \rightleftharpoons V$ ) in the constituent pure components in this work.

In many critical transitions, the quantitative behavior of some thermodynamic properties and of most transport properties is unknown; further experiments are required. In recent publications from this laboratory Campbell et al. (144,145) have discussed this aspect in some detail. A rather coherent picture is now emerging as a result of a rapid increase of interest in this field. Work such as that reported by Campbell et al. (144) is of value in elucidating the nature of the irregularities in the thermodynamic functions at a liquid-liquid critical point.

Rowlinson (24) has pointed out that the critical temperature of a simple mixture ( $L \rightleftharpoons V$ ) is one of the most direct sources of information on the energy of interaction of two unlike molecules. I have therefore obtained the critical temperature versus liquid mole fraction curve for the binary system acetone-benzene in this study over the whole range of composition.

## CHAPTER III.

## EXPERIMENTAL PROCEDURE AND APPARATUS

## I. PURIFICATION OF THE MATERIALS.

Acetone, chloroform, benzene, and carbon tetrachloride, respectively, were used as the four pure liquids. Objection might be made to the choice of chloroform since it decomposes very readily in the neighborhood of the critical point. A slight yellow color was always observable in the chloroform, after an experiment. In view of the well-known effect of traces of impurity (50,146) on the critical properties, this is a serious matter but it cannot be avoided. Any determination of the critical constants of chloroform, however, carefully made, must be subject to this criticism. Errors in the measurement in the critical region due to the decomposition of chloroform are therefore larger than those in other substances.

I(a). Acetone

Spectranalyzed Acetone (A.C.S.) from the Fisher Scientific Company was dried over calcium chloride and then subjected to distillation, after adding potassium permanganate to remove any non-aqueous impurities. The distillate collected was again dried by means of calcium chloride and re-distilled. Care was taken to avoid exposure to air and the freshly distilled fraction (the distillation temperature was constant at 56.10 to 56.15°C at a pressure of 746 mm. Hg) was transferred to the deaerating apparatus. The pure liquid was contained in a flask with ground-joint and was connected to a high-

vacuum line for deaeration by distilling it back and forth from one cold trap to another. The physical properties (density and refractive index) observed for purified acetone agreed very well with the literature values.

#### I(b). Chloroform

Chloroform (A.C.S.) from the Fisher Scientific Company was purified to remove ethanol by repeated extraction with concentrated sulfuric acid and final washing with distilled water. Chloroform was dried over anhydrous calcium chloride and then finally distilled from anhydrous phosphorus pentoxide, twice. The purified reagent was stored in the dark. The sample purified in this manner could not be kept for more than 3 days. The fraction collected between 61.05 to 61.10°C at 748 mm. Hg was transferred to the vacuum-line for degassing and loading the experimental tube.

#### I(c). Benzene

Thiophene-free Benzene (A.C.S.) from the Fisher Scientific Company was frequently shaken with concentrated sulfuric acid until the yellow color in the acid layer disappeared. It was then washed twice with distilled water and then with a solution of sodium bicarbonate. After washing it again with distilled water, the product was dried with anhydrous sodium sulfate and then with sodium. The sample was cooled slowly until a certain fraction solidified, the supernatant liquid being discarded; the procedure was then repeated to ensure removal of impurities such as cyclohexane. Finally the

sample was dried over sodium wire and then fractionated twice from sodium. The constant-boiling fraction at  $80.10^{\circ}\text{C}$  (752mm. Hg) was transferred to the vacuum line. The physical properties of the purified material agreed very well with the literature values.

#### I(d). Carbon Tetrachloride

Carbon Tetrachloride (A.C.S.) from the Fisher Scientific Company was distilled through a vacuum-jacketed column with glass helix packing. The temperature was found to be constant throughout the distillation ( $76.6^{\circ}\text{C}$  at 750mm. Hg). The middle third-fraction was examined for purity by gas chromatography. A column of 6 ft. length with dimethylformamide in chromosorb-P as the supporting material for the liquid stationary phase was used. Helium was used as a carrier gas and only one main peak was observed suggesting that the sample was pure. The sample was transferred to the vacuum line for degassing, etc. Before transferring the liquids to the manifold of the vacuum line for excluding the noncondensable gases, in each case, the liquids were kept in a dry chamber. Care was taken during ordinary distillation to see that all vents communicating with atmosphere did so through drying tubes containing phosphorus pentoxide suspended on glass wool thereby excluding atmospheric moisture.

The critical temperature, critical pressure, equilibrium pressures (vapor pressures) at temperatures below the critical temperature, and orthobaric volumes of pure liquids have been determined. The literature data, even of well known liquids, such as those investigated in this research, are surprisingly limited. Table IV gives a resume of the most recent data.

TABLE IV

Most Recent Critical Data

Year	$t_c$ (°C)	$P_c$ (atm)	$d_c$ (g/cc)	Investigators
<u>A. Acetone</u>				
1902	233.7	46.78	---	Kuenan and Robson (147)
1923	235.6	---	0.252	Herz and Neukirch (148)
1943	235.8	---	---	Fischer and Reichel (149)
1951	235.5	46.6	0.273	Rosenbaum (150)
1955	236.3	47.2	---	Kobe et al. (151)
<u>B. Chloroform</u>				
1902	262.9	53.8	---	Kuenan and Robson (147)
1923	262.5	---	0.496	Herz and Neukirch (148)
1934	263.4	---	---	Harand (152)
1943	263.5	---	---	Fischer and Reichel (149)
<u>C. Benzene</u>				
1910	288.5	47.9	0.3045	Young (63)
1934	290.8	---	---	Harand (152)
1941	289.45	48.9	---	Esso Laboratories quoted in ref. 153.
1943	291.2	---	---	Fischer and Reichel (149)
1947	289.5	48.7	0.297	Gornowski, Amick and Hixson (153)
1952	288.94	48.34	0.308	Bender, Furukawa and Hyndman (154)
1962	288.84	48.28	---	Connolly and Kandalic (155)
1964	289.00	48.32	0.304	Skaates and Kay (156)
1967	288.94	48.98	---	Ambrose, Broderick, and Townsend (157)
<u>D. Carbon Tetrachloride</u>				
1910	283.15	44.97	0.5576	Young (63)
1935	282.60	---	---	Harand (152)
1943	283.2	---	---	Fischer and Reichel (149)
1964	283.15	44.97	---	Quoted by Miller (158)

## II. METHOD OF ANALYSIS

Vapor-liquid equilibrium data were determined from measurements of refractive index. Analysis by gas chromatography was attempted since this requires a very small amount of sample. Problems such as tailing, etc. coupled with relatively poor reproducibility for known samples caused me to abandon the method. Refractive index measurements required at the most 0.5 ml. of sample which was almost invariably obtained in each determination at the temperatures and pressures of study.

Generally, the analyses of the compositions of the liquid mixtures are made from physical properties. The data for refractive indices as a function of concentration were used as a calibration chart for determining the concentrations of unknown mixtures collected in the vapor-liquid equilibrium bomb.

The refractive index measurements were made using an Abbe Refractometer with the prism thermostated at  $25.00^{\circ}\text{C} \pm 0.05^{\circ}\text{C}$  and the monochromatic light of a sodium lamp ( $5893 \text{ \AA}^{\circ}$ ). The accuracy of this instrument made by Officine Galileo of Italy, is  $\pm 0.0001$  unit of refractive index. An uncertainty of  $\pm 0.0001$  in refractive index means an uncertainty of 0.001 in the values of mole-fraction.

## III. DETERMINATION OF CRITICAL PROPERTIES

### III(a). Development of Experimental Technique

The critical temperature is the easiest of the three critical constants ( $T_c$ ,  $P_c$  and  $V_c$ ) to measure and has been measured for more substances than the other constants. Kobe and Lynn (159), in an extensive review of critical properties in 1953, reported that it had

been measured for 220 substances, excluding mixtures. Most of these measurements were made by observing the temperature at which the meniscus vanished in a system maintained at an over-all density approximately equal to the critical. If a sealed tube containing liquid and vapor is heated uniformly then one of three things may happen. If the over-all density is less than the critical then the meniscus falls as the liquid evaporates. The second possibility is that the density is greater than the critical and the meniscus rises on heating until no vapor remains, i.e., the whole tube is full of liquid. If, however, the density is close to the critical then the meniscus rises slowly until it is near the center of the tube where it remains until the critical point is reached and then suddenly the flat and faint meniscus disappears, characterized by fluctuating striae. This principle has been extensively used in this work for determination of critical constants.

If the tube is not sealed but is open at its lower end to a reservoir of mercury, then the density may be altered at will and the pressure measured at the same time. This was the apparatus used in the original work of Andrews (5) and later by Young (63). The critical pressure may be measured with little more trouble than the temperature, as it is equally insensitive to small changes of density at this point. The principle of Young's apparatus has not been significantly altered since.

The measurement of the critical constants by observing the point of inflection of the critical isotherm is much more difficult and attempts to make such measurements have led to some notable



disagreements (24,160). A survey of the critical constant data measured in different ways shows not only a wide variation in the values reported by different investigators for a single liquid, but also very frequently a considerable variation in the data given by a single investigator. The chief reasons for these deviations are slow attainment of equilibrium in the critical region, large compressibility of the liquid, large spontaneous fluctuations of the density over macroscopic distances leading to the scattering of light (the critical opalescence), etc. The present experimental position is given by Heller (30) in a review article. Much of the older work is of little value now and is reviewed in great detail by Rowlinson (24). Although some of the older methods are crude, the methods are readily adaptable to refinements so that accurate determinations may be carried out.

### III(b). Orthobaric Densities

The orthobaric densities (density of vapor and liquid coexisting at the same temperature) may be determined in several ways. The method of Maass and coworkers (17,18,19,20), which utilizes the float and quartz spiral spring, is adaptable, as is the method of Traube (12), which makes use of a number of balls of different known densities. Maass determined the densities of the liquid and vapor phases by a float suspended from a quartz spiral. The volume and weight of the float and the spring constant of the quartz spiral were accurately determined; thus, the density of the fluid was calculated from the buoyancy effect.

The most used method for the determination of orthobaric

densities is that of Young (63), mainly because of the maximum return in useful data that it gives from a minimum investment in experimental effort. The method of determining the orthobaric densities in this research is based on Young's principle. The volumes of the liquid,  $v_L$ , and of the vapor,  $v_G$ , were determined for two different amounts of the substance,  $w'$  and  $w''$ , at the same temperature. The densities,  $d_L$  and  $d_G$ , are then obtained by a simultaneous solution of the two equations (Total weight of compound = volume of liquid x density of liquid + volume of gas x density of gas):

$$w' = v_L' d_L + v_G' d_G \quad (91)$$

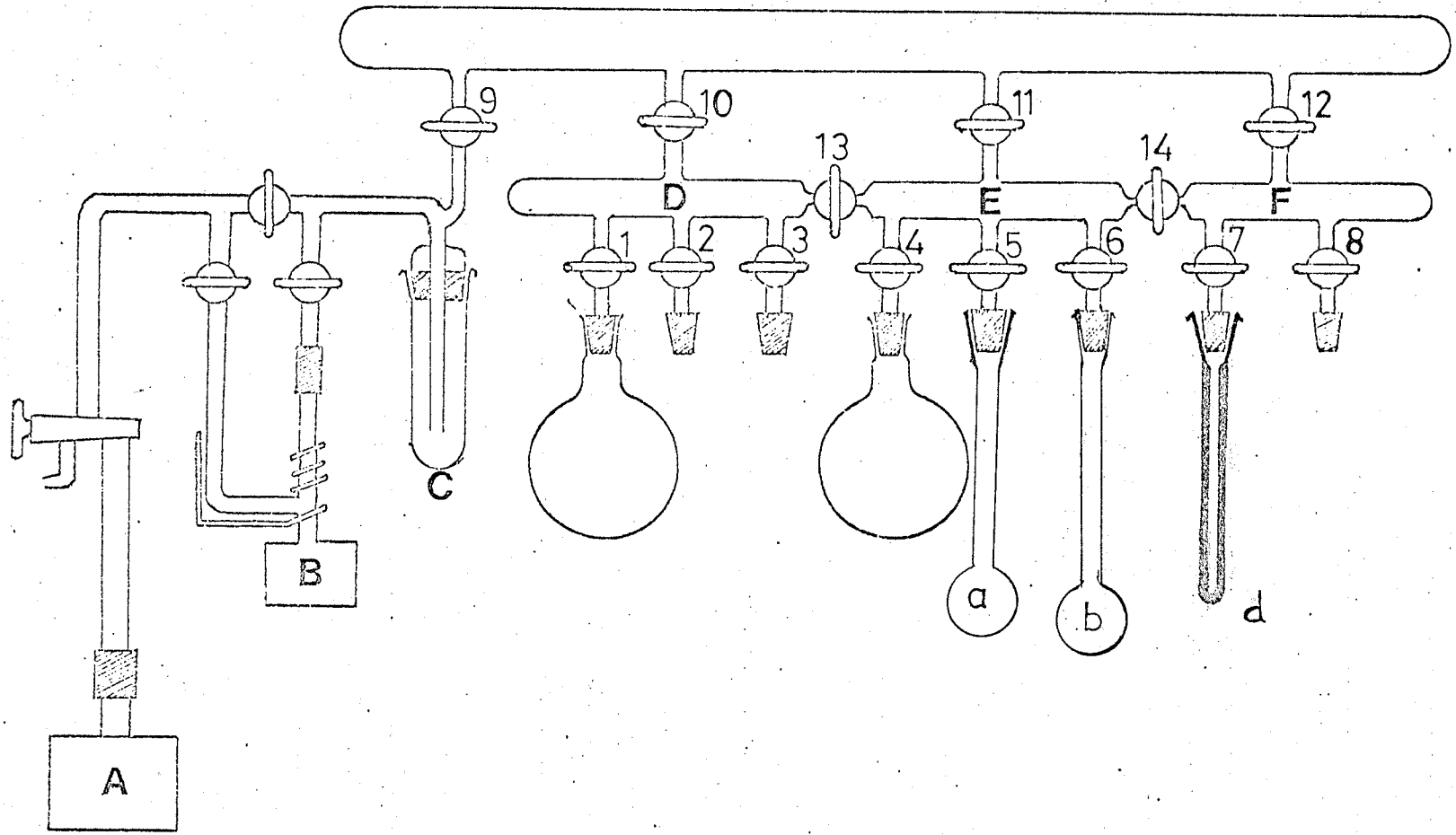
$$w'' = v_L'' d_L + v_G'' d_G \quad (92)$$

### III(b). I. Loading the Experimental Tube with a Sample

The glass apparatus for deaerating and degassing the pure liquids and for transferring a degassed sample to the experimental tube is shown in Figure 3. A mercury diffusion pump B backed by a mechanical oil pump A was used to produce a vacuum with a residual noncondensable gas pressure of less than  $10^{-5}$  mm. of mercury, as measured by a McLeod gauge. Air and other non-condensable gases were removed from the liquid samples by a series of operations which involved freezing with liquid nitrogen and pumping off the residual gas over the frozen liquid, followed by melting and distillation at low pressure.

About thirty ml. of pure liquid were contained in flask b which was then attached to the vacuum line by means of a ground joint. Upon the attainment of a fairly good vacuum, stopcock 6, connecting flask b

FIGURE 3. Apparatus for Degassing and Preparing Mixtures of Liquid Samples.



to the vacuum line was opened, momentarily, in order to remove most of the air-rich vapor over the liquid, before freezing the sample. As soon as the sample was frozen, the stopcock connecting flask b was opened and the space over the frozen liquid evacuated until the pressure was less than  $10^{-5}$  mm. Hg. For freezing the liquid, a mixture of dry ice and acetone was used at first. The stopcock connecting flask b was then closed and the sample allowed to melt, after which the stopcock was opened, cautiously, and vapor pumped off again. This procedure was repeated several times. A check showed about six times was sufficient to remove all gases. For the final few times the coolant was liquid nitrogen.

Next, the cooling flask was brought up around flask a, and cocks 4,9,10,11,12,13 and 14 were closed, cocks 5 and 6 opened, and the liquid in b was distilled and collected in flask a, except for a small residue which was pumped off into the cold trap C. After evacuating the space over the solid, cock 5 was closed, the solid melted and a small fraction of the vapor pumped off. Cocks 9 and 11 were then closed, 6 opened and the sample was distilled and collected in b, except for a small residue which was discarded as before. The distillation, back and forth between a and b, was repeated four times. The pure degassed sample was then stored in flask b in the solid state until ready to use.

The experimental tubes of heavy walled annealed glass, 15 cm. in length and 2 mm. internal diameter with ground joints were used. Two tubes were required for determination at each temperature. The capillary used in the experimental tube varied in its internal diameter from 2.05 - 2.10 mm. in different regions of its length. The volumes of each tube

were determined in the following way using pure re-distilled mercury as calibrating liquid.

Before the experimental tube was blown to its final shape, the capillary was sealed to a pyrex bulb of 10 ml. capacity. The capillary had several fine circular marks etched at about 5 mm. distance apart. These marks were made on the stem by hydrofluoric acid to facilitate accurate measurement of the liquid level inside the capillary.

The capillary with the bulb was cleaned with hot chromic acid, thoroughly rinsed with distilled water, dried and weighed. Mercury was then introduced by means of a long drawn-out capillary tube extending to the bottom of the bulb, taking care to avoid the entrapment of air bubbles. The capillary was fixed in position inside the thermostat at  $25.000 \pm 0.005^{\circ}\text{C}$  with its top protruding above the water level in the bath. The meniscus level of the mercury column inside the capillary was adjusted to coincide with one of the several marks on the stem, by using a long hypodermic needle and a syringe. The capillary with the bulb was removed from the thermostat, its outside cleaned thoroughly, dried and weighed. Using the density of mercury as given in Lange's handbook (13.5340), the volume corresponding to one of the several marks on the stem was calculated. This procedure was repeated for each of the marks and the volume per unit length in each region at  $25^{\circ}\text{C}$  was calculated. Thus, the non-uniformity of the capillary bore, if any, was taken into account. Next, the bulb was detached and the capillary sealed at the bottom. Then the volume between the sealed end and the first mark from the bottom of the tube was determined in a similar way.

The ground joint was next fused to the top of the capillary tube. The region between the top mark and the point where the experimental tube is finally sealed after transferring the experimental liquid, was not calibrated till the end of the experiment.

In the drying procedure, the first few distillations to and from b were made using solid carbon dioxide-acetone mixture, and liquid nitrogen, respectively, and care was taken never to leave the sample present as a liquid. This was necessary because high-vacuum silicone grease was used for ground joint and stop-cock lubrication, and to prevent absorption of the sample the vapor pressure must be kept as low as possible. The final distillation was made with flask b immersed in a dry ice-acetone mixture, and the system pumped out for 2 min.; the aim of this last operation was to remove carbon dioxide or gases of similar volatility from the liquids, and it was repeatedly observed that the vapor density was irreproducible unless this was done.

Before transferring the sample stored in b to the experimental tube attached to 7, the tube was flushed several times with a small amount of sample which was then discarded to trap C. By chilling the tip of the experimental tube and by manipulation of the appropriate stopcocks the liquid was distilled into d, the experimental tube. The sample was then allowed to melt and fill the end of the tube, after which it was frozen again. The process of freezing and thawing was continued to make sure that any trace of residual gas in the tube was displaced by pumping. The tube was sealed off from the line just below the female half of the ground joint in the experimental tube.

The experimental tube with the female ground joint was weighed before attaching to the vacuum line i.e., before transferring the liquid.

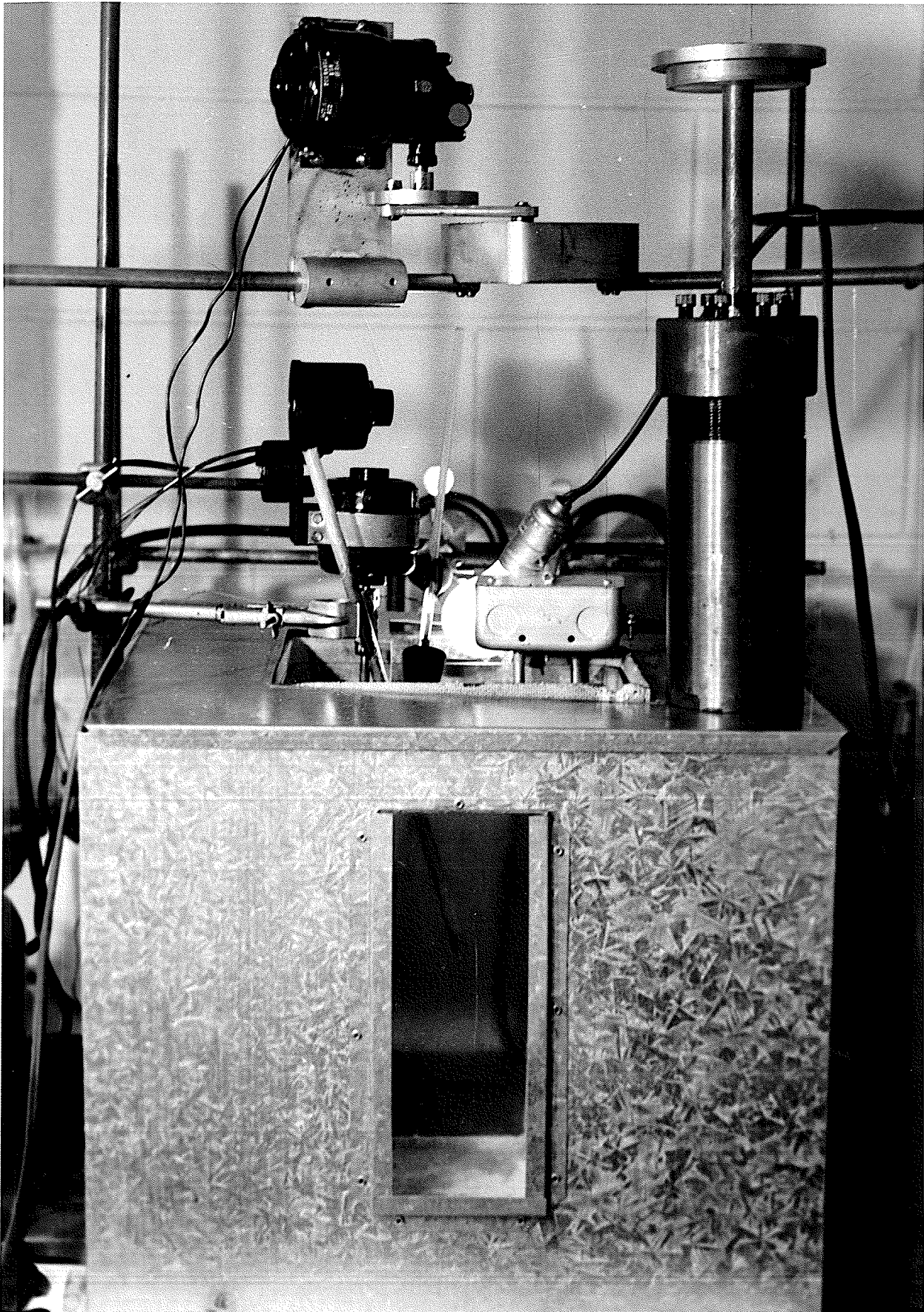
The weight of the pieces of the experimental tube after sealing off gave the total weight of substance, by difference.

### III(b). II. Thermostat

The thermostat was a glass-tank of 5 liters capacity lagged with vermiculite contained in a sheet metal rectangular cover except for a plate-glass window 3 in. wide and 9 in. high as shown in Figure 4. The thermostat was illuminated from behind by a light bulb placed in the vermiculite insulator. Up to 250<sup>o</sup>C, the thermostat liquid used was Dow-Corning Silicone fluid 550. Above 250<sup>o</sup>, the eutectic mixture of potassium, sodium, and lithium nitrates was used. This fused salt bath functioned perfectly, when the glass-bath was changed every few weeks, since the glass eventually became corroded by the salt. The thermostat liquid was stirred by a paddle rotated by a powerful motor, and the temperature control was obtained by a solid state proportional temperature controller manufactured by Athena Controls Inc., Pennsylvania. The controller provided smooth modulation of electric power in response to thermistor temperature. The continuous power supplied to the load from the power module eliminated the large fluctuations inherent in on-off or time proportioning control. A four leg null balance bridge, high gain amplifier and a feedback stabilizing network for line voltage and temperature fluctuations, gave a high degree of accuracy and stability to the controller. A power output meter showed the voltage across the load and was used to set the proportional band and also to serve as a



FIGURE 4. The Thermostat.



null indicator for bridge balance. The temperature sensor was a thermistor sheathed in stainless steel to prevent corrosion by the fused salt bath. The heating element was encased in non-corrosive "Nickel-Chrome-Iron" alloy for the same reason. Temperature measurements in this work were made with multiple-junction copper-constantan thermocouple in conjunction with a Tinsley vernier potentiometer (Type 4363A) measuring to a microvolt, for the e.m.f. measurements. The thermocouple was calibrated using the standard temperatures of the ice point, steam point, melting points of tin, bismuth, and cadmium, with the cold junction in a bath of melting ice. This calibration was compared with a certified platinum resistance thermometer supplied by National Research Council of Canada. Resistance measurements were made using a Brown recorder and a Mueller bridge. The two calibrations were identical within the experimental error of measurement. The temperature control was better than  $\pm 0.03^{\circ}\text{C}$  up to  $250^{\circ}\text{C}$ , and  $\pm 0.03^{\circ}\text{C}$  above that. The correspondence of the two calibrations was within  $\pm 0.01^{\circ}\text{C}$ .

### III(b). III. Experimental Method

Two experimental tubes were used for each temperature. In the density determination a different quantity of the pure liquids was distilled into each tube. Sample weight was determined by weighing the tubes before and after sealing, as discussed before. The tubes were then placed in the thermostat at the desired temperatures and the difference in height from the meniscus to the nearest calibration mark measured with a cathetometer reading to 0.05mm. The equilibrium vapor

and liquid volumes thus became known; correction was applied for the thermal expansion of the glass. The experimental tubes were constructed from Pyrex capillary, and the coefficient of expansion given by the manufacturer was used. The two equations obtained from the above data allowed the densities of liquid and saturated vapor to be calculated algebraically. From the orthobaric densities, the orthobaric volumes were obtained.

Because vapor densities determined in this manner are subject to error due to the small weight of the compound in the gas phase, particularly at temperatures well below the critical temperature, great care was taken in the height measurements and in degassing the samples. After the experiment was over, each tube was cut off exactly at the point where it was sealed off from the line, and the region between the top etched mark and this point calibrated using the technique previously described. The weight of mercury needed to fill this volume completed the calibration required to know the volumes of different regions of the tube as well as the total volume of the tube. The volume of any tube could not be expressed analytically in terms of the distance from the sealed end at the bottom, since precision bore capillary was not used.

The method of determining the orthobaric densities by solving simultaneous equations (91) and (92), was not applicable in the immediate neighborhood of the critical temperature because slight fluctuations of temperature caused too great fluctuations in the level. Therefore, over a temperature range of  $2^{\circ}$  below the critical temperature, I made use of the method of "total exhaustion". For this method, tubes of known total volume were charged with known weights of liquid and the

temperatures noted at which the meniscus disappeared "by exhaustion", i.e., when the meniscus either rose just to the upper extremity of the tube, when the tube was entirely filled with liquid, or sank to the bottom of the tube, when it was entirely filled with vapor. Congruent densities were therefore not obtained directly, in this region, but each determination gave a point on one side or the other of the orthobaric curve. Experience taught me how to choose the fillings so that all temperatures were within the desired narrow region of temperature.

### III(c). Critical Temperature

The classical apparatus used by Andrews (5) consisted of capillaries calibrated for capacity, and the pressure in the system was determined by the temperature-volume relations of air. Thus, the apparatus was suited for the determination of the critical constants by P-V-T relations, but Andrews noted that the disappearance of the meniscus occurred at the critical temperature, and he adopted this phenomenon as the criterion of the critical temperature; this led other investigators to use the disappearance of the meniscus as the sole criterion of the critical temperature. Young (63), for example, took the criterion as the point where the meniscus had vanished but would reappear when the volume was increased suddenly by a small amount (adiabatic cooling).

The critical temperature in this research was determined in the classical manner, using the usual sealed tube technique with different fillings. The sample purification was done as described earlier. The experimental tubes were of 2 mm. internal diameter and

15 cm. length. No calibration was necessary. Their internal volume was 0.7 - 0.8 ml. The method of loading the experimental tube with a pure air-free sample of liquid was as before.

### III(c). I. Preparation of Mixtures

In the preparation of a mixture of known composition, the second liquid component was treated in a manner exactly similar to that described earlier for the first component. Thus, the two components were stored in the solid state in bulbs a and b, respectively, until ready to use.

The experimental tube was attached to the vacuum line at 8. A small precision bore capillary (1.0 mm internal diameter) whose volume per unit length had been previously determined, was then attached to the vacuum line at 7. A quantity of liquid 1 was then transferred by distillation from the storage flask to this calibrated capillary. From the length of the tube occupied by the sample at room temperature (measured with a cathetometer reading to 0.05 mm) and the density of the liquid at this temperature, the weight of the sample was calculated. A correction was made for the weight of the vapor over the liquid, using the perfect gas law and a knowledge of the vapor pressure and the total volume of the calibrated capillary up to stopcock 7.

The measured sample was transferred to the experimental tube as usual by chilling the tip of this tube. Similarly, a measured quantity of the second liquid was transferred to the tube. The sample was allowed to melt and then frozen again. The tube was sealed off from the line under continuous suction. The weighing before and after sealing

was an independent check that a quantitative transfer of liquids from the calibrated tube to the experimental tube was obtained.

### III(c). II. Experimental Method

For pure liquids, different fillings of a sealed tube were used. In case of binary mixtures, the densities in the tubes were chosen to be within 5% of the estimated critical densities. Critical densities of the mixtures were estimated by linear interpolation of the pure component data.

Care was taken when handling tubes at high temperatures; explosions invariably occurred when they were subjected to shock. The critical temperatures were observed by allowing the tubes to warm slowly in an environment of measured uniform temperature. This environment was provided by the accurately controlled high temperature bath as described earlier. For the final few degrees rate of increase of temperature was very slow. Each tube was placed in turn in the thermostat, and was observed through the glass plate window by means of a telescope located at some distance from the set-up. As the temperature was raised, the surface tension between the two phases approached zero, the dividing meniscus became faint and hazy, and the measurement of the exact temperature of its disappearance was to some extent subjective. Nevertheless, the phenomenon was clearly distinguished as "critical" since the meniscus disappeared in the body of the tube and not "by exhaustion" at the top or bottom. No great care was needed to load the tube to exactly the critical density of the pure liquids for measurements of the precision ( $0.05^{\circ}\text{C}$ ) claimed in this research,

for a slight error in loading only caused the meniscus to vanish a little above or below the center of the tube, at a height at which the local density was equal to the critical. The tubes were not stirred in this determination. The resistance of the compounds to decomposition on prolonged heating was examined, and on the trial runs, the heating was carried out for three hours. Pure acetone, benzene and carbon tetrachloride apparently did not show any change, whereas chloroform became yellowish. The mixture of acetone and benzene also became yellowish if left in the tube for very long time at high temperature. The infra-red spectra of the decomposed chloroform samples could not identify the decomposition products, but a faint smell of HCl was always observed. This was confirmed by the production of white fumes in presence of ammonia. For this reason the tubes containing the chloroform samples were heated rapidly to within a few degrees of the desired temperature. In that way the disappearance of the meniscus was observed within 20 minutes after the tubes had been placed in the thermostat. The temperature was measured by the copper-constantan multiple junction thermocouple as mentioned earlier. The reproducibility of the observations of the critical points was  $0.03^{\circ}\text{C}$ . for pure substances and  $0.05^{\circ} - 0.10^{\circ}\text{C}$  for mixtures. It must be confessed, however, that the determination of critical temperature (temperature of the disappearance of the meniscus) by this method is the least satisfactory of the critical determinations.

#### IV. MEASUREMENT OF VAPOR-LIQUID EQUILIBRIA

The vapor-liquid equilibrium data for a given binary system over the range of temperatures and pressures of practical interest are



generally measured in two ways. The necessary P-x-y data are measured at a series of temperatures or the required T-x-y data at a series of pressures. The most obvious procedure is to equilibrate the phases in a closed bomb by vigorous shaking or stirring. The apparatus is immersed in a constant-temperature bath, the equilibrium pressure is measured, and the phases are sampled for analysis. Although this method appears to be of primitive simplicity, it is rarely used at low pressures. The primary difficulty is that the vapor phase must be sampled so extensively to obtain a sufficient sample for analysis that the equilibrium state is disturbed. This problem arises because analysis of a sample in the vapor state has always proved difficult, hence vapor samples have always been condensed for analysis, and this requires the withdrawal of a considerable amount of vapor. An additional disadvantage is that each datum point requires a separate experiment.

Because of the disadvantages of the static method just described, the dynamic equilibrium still is usually employed at low pressures. An excellent review article by Sage and Reamer (161) describes the experimental methods of measuring vapor-liquid equilibria and presents a thorough discussion of the thermodynamic data necessary to calculate vapor-liquid equilibrium compositions. Another review of the experimental techniques and their development has been given by Everett (162). Despite the disadvantages of the static method at low pressures, it is attractive for equilibration of phases at high pressures.

The measurement and maintenance of constant pressures are of fundamental importance in all methods of determining vapor pressures. High mercury columns, which in principle in no way differ from normal

manometric U-tubes, are used as an absolute standard for measuring pressures from 20 to 30 atmospheres. For routine measurements this method is of course unsuitable; the columns are very high, their construction is difficult and the reading is inconvenient. Despite this, the advantage of the mercury column is that the height of the column gives directly the absolute value of the pressure. Kamerlingh-Onnes (163) constructed a somewhat different type of mercury pressure gauge. Essentially it is a series of manometric U-tubes with compressed air in the connecting tubes, and the value of the pressure acting on one end is given by the sum of the differences of mercury levels across the entire series.

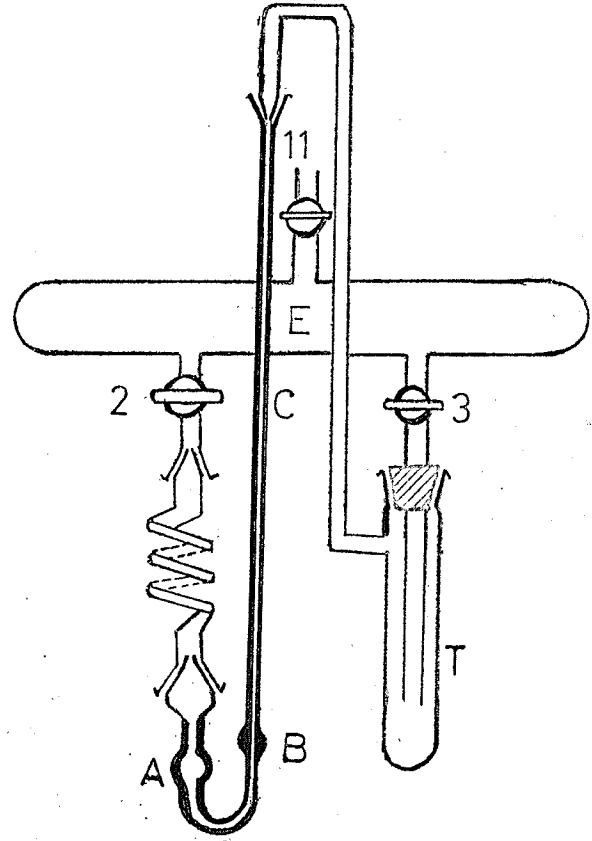
The closed mercury pressure gauge or the mercury-air manometer was used in this research. The functioning of this pressure gauge was based on the compression of a known volume of air to a measured final volume whose size was a measure of the pressure being determined.

Different kinds of pressure gauges, such as the dead-weight piston gauge and the Bourdon pressure gauge, have been used by many investigators for pressure measurements. The simplicity of the closed mercury pressure gauge as used in this research is unsurpassable.

#### IV(a). Vapor Pressure Measurements

Vapor pressures were determined in the apparatus of Figure 5, which is essentially a closed manometer containing air. The closed manometer was calibrated for volume as a function of length. The volume of the tube from each division to the sealed end was determined by the method of calibration described earlier. The region between the

FIGURE 5. Transfer of Sample to the Mercury-Air Manometer.



last etched mark and the sealed end was calibrated after the end of the experiment, as was done in case of density determinations. The total volume of the glass bulb B was approximately 1 - 1.5 ml. This was not calibrated, since the ratio of the cross-section of the tube to the volume of the bulb was chosen in such a way that the desired pressure range always remained on the exposed scale. It is best to fill the manometer with dry hydrogen whose behavior under compression deviates the least from Boyle's law. Since this was not done, the pressure was calculated, from the equilibrium volume of compressed air, using van der Waals' equation. Other equations of state gave variations within the experimental error. The manometer was filled with mercury in such a way that the bulb B and part of C was full, and was then attached to the vacuum line as shown in Figure 5. The calibrated tube of mercury-air manometer was connected by means of a ground joint to an adapter or side-arm coming out of a cold trap, T, which was connected to the vacuum line, as shown in the diagram. The other end of the manometer was also attached to the vacuum line, through a spiral tube which had ground joint and acted as a spring providing manoeuverability. The trap, T, was cooled by liquid nitrogen. This cold trap was included in the system, in addition to the one already provided as shown in Figure 3. The occluded air was boiled out from the manometer by heating gently and cautiously with a moving flame throughout the length of mercury and applying vacuum simultaneously at both A and C of the manometer. This removed any air trapped between the mercury and wall of the manometric tube. After sufficiently long pumping and tapping of the wall from outside, and when the mercury came to room temperature, the required amount of degassed liquid was distilled into the bulb A from

the calibrated precision bore capillary where it was temporarily stored. This was achieved by chilling bulb A, the U-bend of the manometer, and the bulb B with solid carbon dioxide-acetone mixture. The size of the apparatus was such that all these parts could be chilled by the freezing mixture contained in a single Dewar flask. When preparing mixtures, a measured quantity of the second liquid was also transferred to the tube in a similar manner. The method of calculating the composition has already been described under determination of critical temperatures. The process of freezing, pumping, and thawing was continued until any residual gas was expelled from the system. Great caution was exercised in the case of binary mixtures, and liquid nitrogen was used to freeze the solution. Because of the unequal volatilities of the different components, the composition is liable to change, if vacuum is applied while the sample is still liquid. The end A of the manometer, which was open to the vacuum line, was then sealed off, keeping the liquid frozen. This was difficult, since the whole manometer, along with the Dewar flask containing liquid nitrogen, had to be lowered from the vacuum line, and C disconnected from the adapter at the same time after closing stop-cock 3. Mercury and the liquid were still kept frozen till the sealed end of A cooled off. The liquid was then allowed to melt and air having entered C pushed the liquid, followed by mercury, to the end of A. The open end of C was then sealed off, under atmospheric pressure, after enclosing C in a glass mantle, through which water at 25° was circulated. Atmospheric pressure was recorded at the moment of sealing. The volume of air in C, under atmospheric pressure and at a temperature of 25°C, was then

obtained by means of a cathetometer reading.

Bulbs A and B were then immersed in a thermostat at the desired high temperature, that is, at a temperature at which the vapor pressure of the liquid was greater than 1 atm. Vapor formed in bulb A and the vapor pressure was automatically established. A time-pressure study was made with pure liquid, which showed equilibrium was achieved in 20 min. During measurement, the pressure in the liquid system drove the mercury into tube C and compressed the air. The achievement of equilibrium was evident when the mercury level in tube C came to rest. The volume of the compressed air was read off with a cathetometer reading to 0.05 mm. From the equilibrium volume of air in C, the pressure was calculated, using van der Waals' equation, the following correction being applied. The hydrostatic pressure of the mercury column was added to the calculated pressure. Taking the length of the air column in the closed limb C to be  $l_1$ , when the mercury is at the same height in both tubes, and  $l_2$  when the mercury column has risen (thereby diminishing the air column) in the closed limb C, the difference in height of the mercury columns in the two limbs is  $2(l_1 - l_2)$ . The experimental pressure which caused the mercury to rise is obviously equal to the pressure calculated from van der Waals' equation, plus that of a column of mercury of length  $2(l_1 - l_2)$ . Thus the pressure was corrected for the difference in level of the mercury in the experimental tube and manometric tube. The other recommended corrections are: 1) for the pressure of the column of unvaporized liquid, 2) for the expansion of the heated column of mercury, and 3) for capillarity of the manometric tube. The height of the unvaporized liquid column was so small that this was not necessary to take into account.

The mercury column was jacketed by thermostated liquid at 25°C, and as such this could also be neglected. Although the correction for capillarity is desirable, this was not done in this research since it was thought insignificant. No correction for the vapor-pressure of mercury was applied, because evaporation through a long column of liquid is an exceedingly slow process.

For the reason previously given, namely that, in the neighborhood of the critical temperature, slight fluctuations of temperature caused great fluctuations in level, it was not found possible to make pressure measurements by this method to temperatures higher than about 3° below the critical temperature. In this static method of pressure measurement it was necessary to keep the vapor space as small as possible so that the whole system could be kept at a uniform temperature, and so that the volume and the composition of the liquid were not changed appreciably by evaporation as the temperature was raised. Vapor space was always a tiny bubble compared to the liquid volume, which was contained in bulb A. Therefore it was reasonable to believe that the liquid composition hardly changed at high temperatures. The phase rule specifies the minimum number of independent intensive variables required to define an equilibrium system. For example, in a binary solution of acetone and benzene, if the liquid is in equilibrium with the vapor, there are two phases, and therefore the number of degrees of freedom = 2. Specifying either the temperature and pressure or temperature and one liquid composition, or any other two intensive variables, will completely define the system.

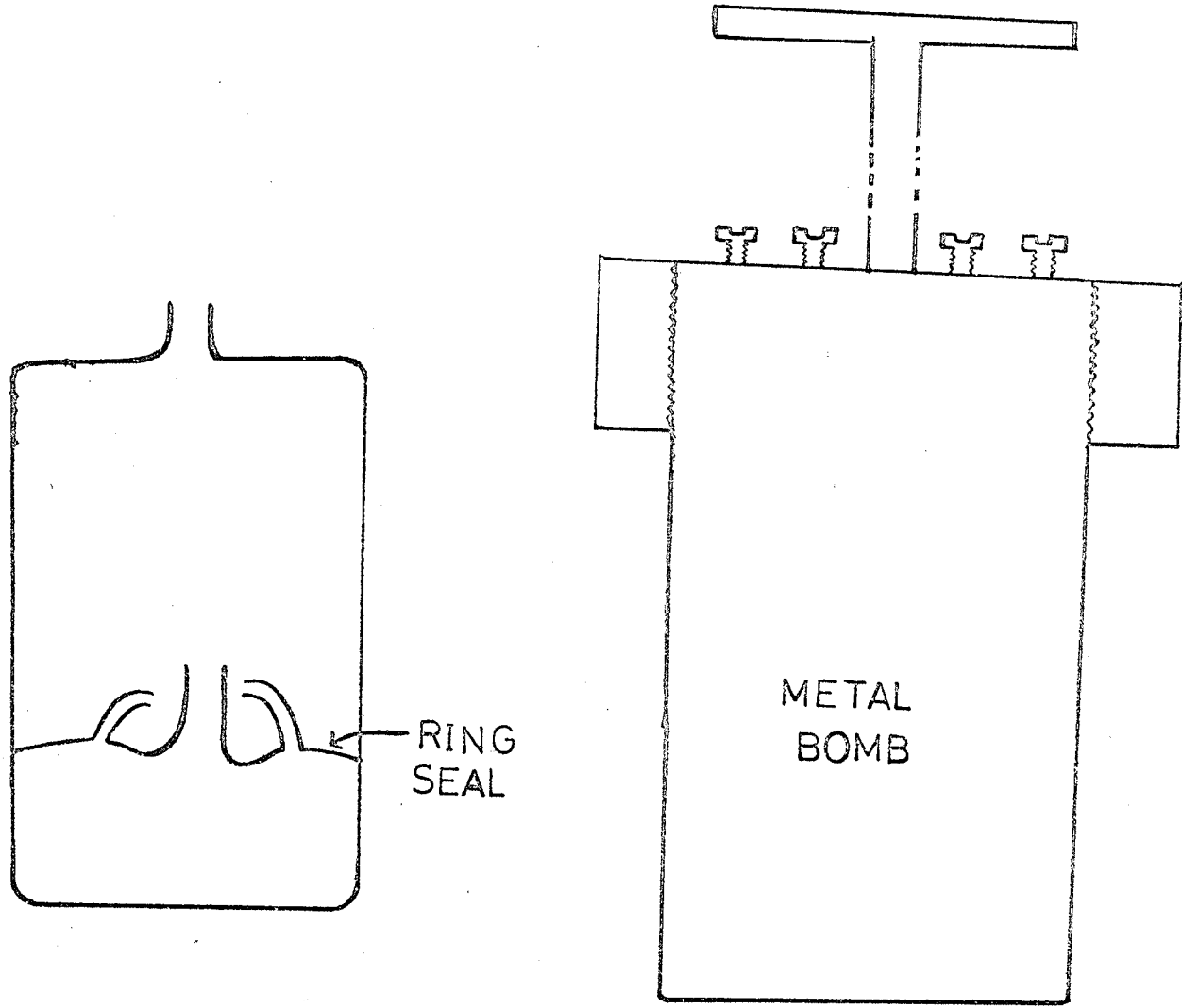


#### IV(b). Experimental Determination of Vapor-Liquid Equilibrium

The direct experimental determination of vapor-liquid equilibrium means the separation of samples of the liquid and vapor which are in true equilibrium and determination of the concentrations of both phases analytically. The methods for the direct determination of equilibrium data are classified as: 1) Distillation method, 2) Circulation method, 3) Static method, 4) Dew and Bubble point method, and 5) Flow method. The static method was used in this research, because the pressures were high enough and the temperature was in the vicinity of the critical points. A survey of the literature shows this method gives more precise results than all the other methods except the dew and bubble point method (164, 165, 166, 167) at high pressures. Verschoyle (168) used a high pressure bomb in studying the equilibrium in the system  $H_2 - N_2 - CO$  at pressures up to 225 atmospheres. This bomb was made of bronze and had a volume of 9 ml. The high-pressure bomb used in my research was made of glass, contained in a metal cylinder which was placed in a thermostat. Everything else remained the same as described earlier; the capacity of the thermostat in this case was 10 liters.

The apparatus used is shown in Figure 6. The high-pressure bomb was fabricated from 70 mm pyrex standard wall tubing and was divided into two compartments by a ring seal, such that the upper chamber was two-thirds the whole volume. The total volume of the bomb was approximately 450 ml. The liquid mixture could be charged through a 7 mm filling tube sealed to the center of the ring. Around the central tube were four vapor-escape tubes communicating with both the compartments and extending 4 mm above the ring seal. These vents were bent downwards towards the

FIGURE 6. Cross-sectional View of the Glass and Metal Bombs for Vapor-Liquid Equilibrium Determination.



central tube thereby preventing their catching the condensed vapor. The central part of the ring was lower than where the ring seal was fused to the outer wall of the bomb, in order to facilitate sampling of the condensed vapor at relatively low temperatures, since at these temperatures the volume of the collected sample was not too large. The cell could be evacuated through a pumping stem attached at the top, after freezing the charged liquid in the bottom compartment. This also served as an outlet for sampling of the equilibrium phases with a hypodermic syringe at the end of the experiment. The glass bomb was carefully annealed at  $580^{\circ}\text{C}$  for approximately eight hours to make certain that no strains were left in the body of the glass.

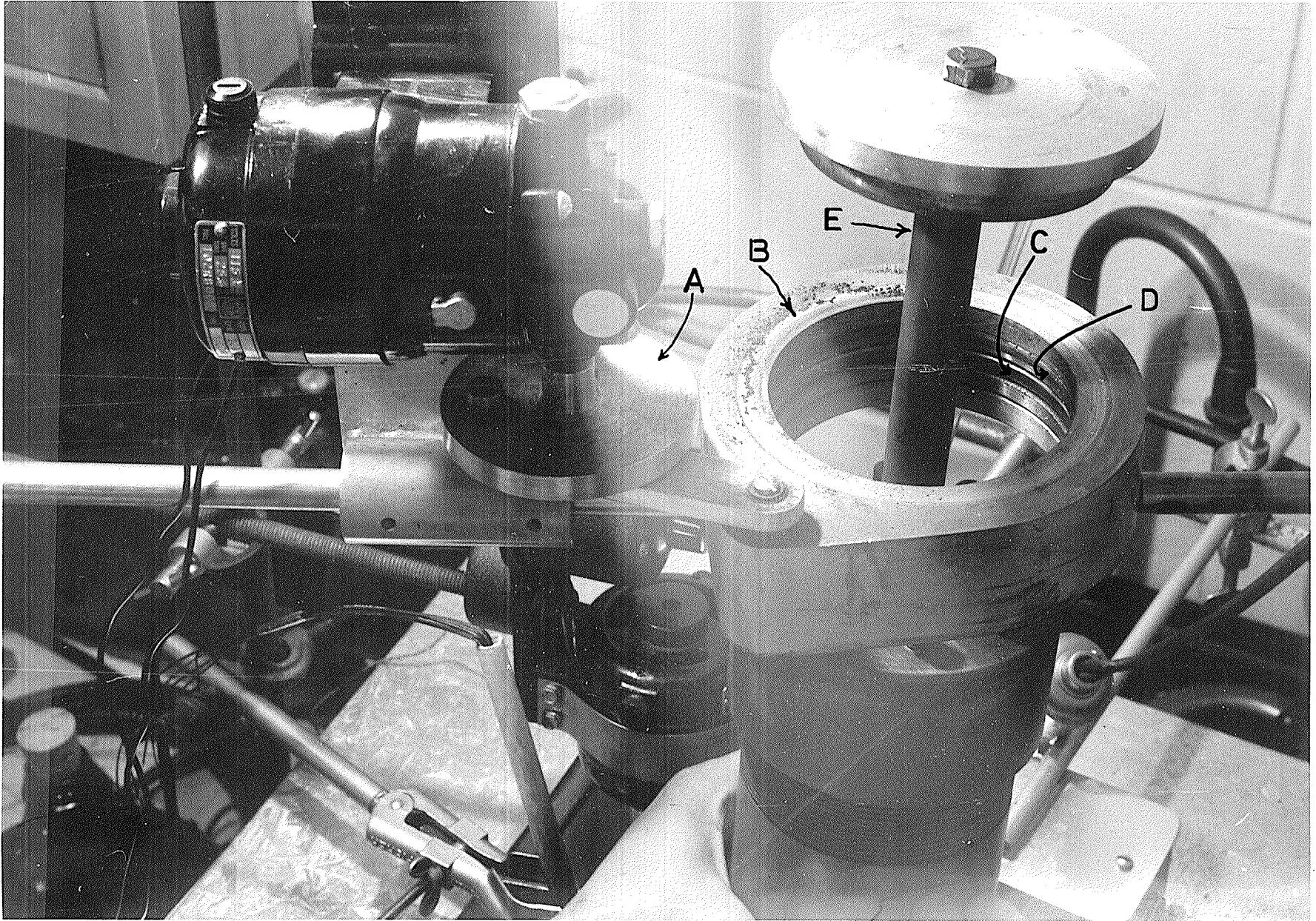
A sample of 75 ml. of mixture made up by weighing was charged in the lower compartment taking care not to spill any on the upper. The liquid was frozen and the system evacuated. After pumping for about half-an-hour the pumping stem was sealed off from the vacuum line. After the liquid came to room temperature the bomb was put inside a metal cylinder which also contained a liquid mixture of same composition. The metal cylinder had a screw-cap which fitted tightly on the cylinder. To make it perfectly pressure tight a copper O-ring was used between the screw-cap and the collar of the cylinder. After screwing the cap, the Allen-head bolts on the cap were tightened down so that the O-ring sat tightly on the groove made on the collar of the cylinder, making the system pressure-tight. The cylinder was then placed inside the thermostat and was supported from a strong horizontal metal rod attached to two retort stands on either side of the thermostat. The long metal extension of the cylinder protruding upwards helped to keep it in position inside the

thermostat and was an accessory for the shaking device. The cylinder with its contents was shaken until equilibrium was established between the liquid and its vapor. For shaking, a powerful motor was mounted in a horizontal position on the supporting rod over the thermostat as shown in Figure 7. On the shaft of the motor was mounted an eccentric cam A, which in turn was mounted on another eccentric annular disk B and thus served to change circular motion into a thrusting motion. This latter disk consisted of a thrust bearing C mounted inside an aluminum collar which had an annular aluminum cover D resting on the thrust bearing and overhanging the outside of the collar. The metal extension E of the cylinder protruding upwards was screwed on to an aluminum disk F which fitted and rested on the annular aluminum disk B of the shaker. By this arrangement, when the motor was started, the cylinder was shaken while being kept completely immersed in the bath.

After equilibration for 24 hours the cylinder was cooled rapidly by immersing in ice-water mixture, and after undoing the Allen-head bolts of the screw cap, the glass bomb was also chilled quickly by running cold water. The sealed stem of the bomb was opened, and the liquid and vapor samples were withdrawn for analysis from the lower and upper compartments respectively. The sampling was very simple since the vapor phase condensed on chilling, along the wall of the glass bomb and collected over the ring seal, and never got an opportunity to mix with the liquid phase. Vapor compositions of the systems at high pressures could thus be determined using a glass apparatus, without explosions, because the pressure inside the glass apparatus was the same as outside, due to the presence of a mixture of same composition in the metal

cylinder. Determinations could not be made without the glass bomb since the organic compounds used reacted with the metal at high temperature and pressure.

FIGURE 7. The Metal Bomb in the High-Temperature Bath with the Shaking Mechanism.





## CHAPTER IV.

## EXPERIMENTAL RESULTS

## I. ORTHOBARIC DENSITIES

I(a). Acetone

Thirty determinations of the orthobaric densities were made and the results are shown in Table V. The temperature and corresponding volumes of the saturated phases were measured while visual observation of the substance showed that both liquid and vapor were present in the tube. The experimentally measured volumes were expressed as densities in grams per cubic cm. Above  $230.2^{\circ}\text{C}$ , i.e., within five degrees of the critical temperature, only the values of the densities of either the liquid or the vapor are expressed, without the corresponding values of the densities of the equilibrium phase. These were obtained by observing the meniscus disappearing at the top or bottom of the tube respectively. The values of the total densities at which the disappearance of the meniscus (critical phenomenon) was observed within the tube, at a constant temperature of  $235.0^{\circ}\text{C}$ , are given at the end of the table. These are calculated from the total volume of the tubes and the different fillings for which critical phenomena were observed. The precision of the measurements was of the order of 0.0010 gm. per cubic cm. for the liquid and 0.0002 gm. per cubic cm. for the vapor, up to within a few degrees of the critical temperature. Saturated densities are plotted against temperature to give the coexistence curves of acetone in Figure 8.

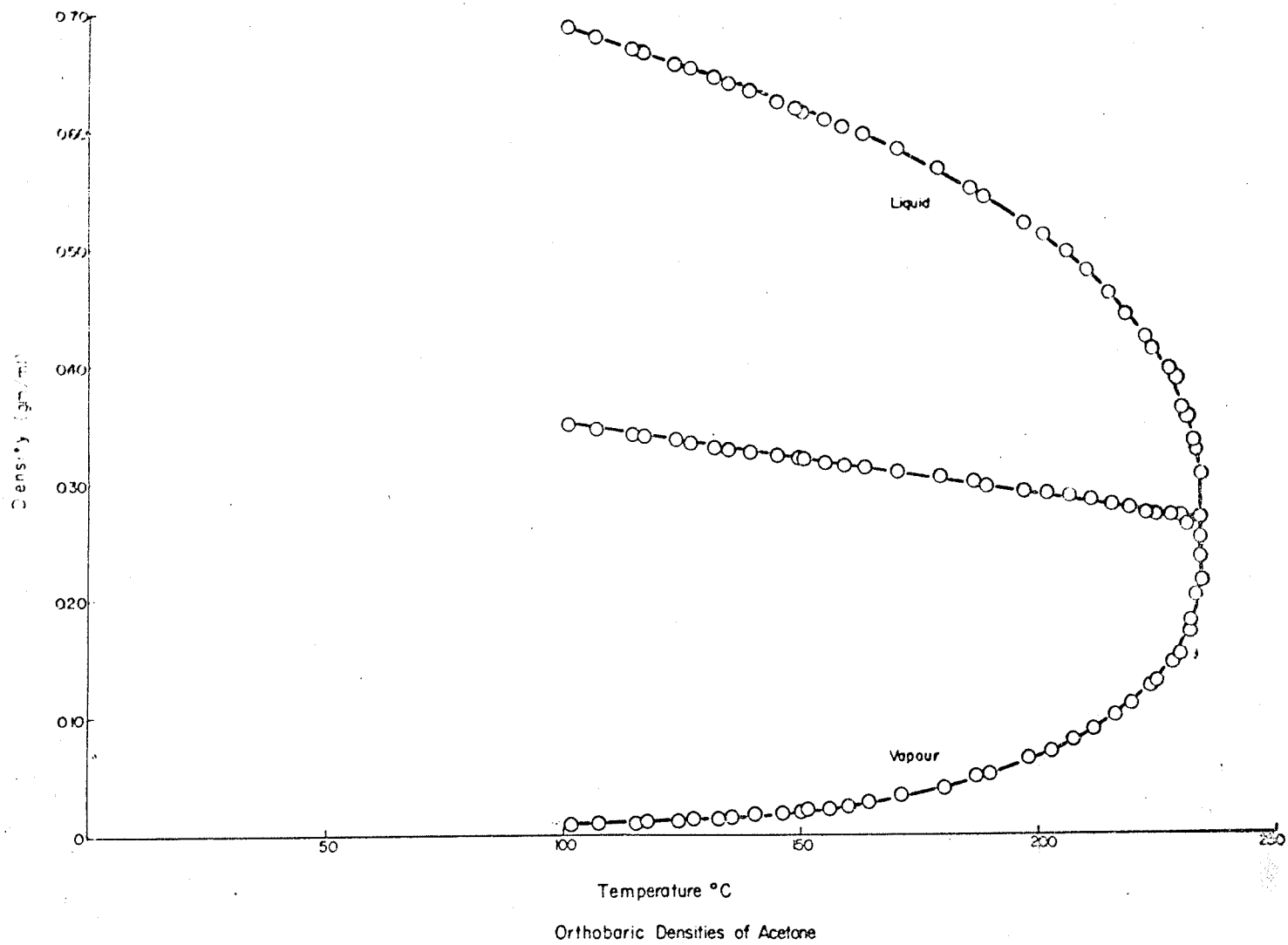
TABLE V

Orthobaric Densities of Acetone ( $t_c = 235.0^\circ\text{C}$ )

Sample	Temp. $^\circ\text{C}$ .	Experimental Density of liquid, gm/cc.	*Calculated Density of liquid, gm/cc.	Experimental Density of vapor, gm/cc.	$(t_c - t)^{1/3}$
1	101.50	0.690399	0.688542	0.0081	
2	107.40	0.681599	0.680900	0.0086	
3	115.10	0.670999	0.670699	0.0092	
4	117.50	0.667799	0.667462	0.0098	
5	124.10	0.658299	0.658400	0.0110	
6	127.40	0.653599	0.653774	0.0118	
7	132.50	0.645999	0.646486	0.0124	
8	135.40	0.641899	0.642261	0.0131	
9	140.10	0.634299	0.635275	0.0160	
10	145.80	0.625000	0.626551	0.0172	
11	149.90	0.618199	0.620084	0.0186	
12	151.20	0.616799	0.617997	0.0191	
13	155.90	0.609499	0.610290	0.0209	
14	159.90	0.603199	0.603514	0.0236	
15	164.30	0.596199	0.595802	0.0261	
16	171.20	0.583999	0.583078	0.0314	
17	180.10	0.567899	0.565268	0.0393	3.800
18	187.20	0.550799	0.549616	0.0488	3.629
19	189.70	0.542099	0.543729	0.0496	3.565
20	198.30	0.521199	0.521594	0.0632	3.323
21	202.60	0.510799	0.509179	0.0704	3.188
22	207.50	0.495199	0.493621	0.0794	3.018
23	211.70	0.480199	0.478808	0.0885	2.856
24	216.40	0.460799	0.460192	0.1002	2.651
25	219.80	0.443600	0.445045	0.1097	2.477
26	223.80	0.423799	0.424938	0.1248	2.238
27	225.30	0.413399	0.416631	0.1290	2.133
28	228.70	0.395899	0.395908	0.1450	1.847
29	230.20	0.387999	0.385793	0.1521	1.687
30	231.20	0.3627	---	---	1.563
31	232.10	0.3542	---	0.1723	1.426
32	232.50	---	---	0.1820	1.357
33	233.50	0.3356	---	---	1.145
34	233.70	---	---	0.2024	1.091
35	233.90	0.3273	---	---	1.032
36	235.00	---	---	---	---

\* Values were calculated from equation (100) and the following constants  $A=0.840081$ ,  $B=-0.961206 \times 10^{-3}$ ,  $C=-9.04112$ . The statistical analysis and the significance tests in multiple regression are reported in Table XVII. Critical phenomena were observed, at a constant temperature of  $235.0^\circ\text{C}$ , at the following total densities: 0.2160, 0.2362, 0.2372, 0.2536, 0.2693, 0.3067.

FIGURE 8. Orthobaric Densities of Acetone.



I(b). Benzene

The data for the saturated densities of benzene are presented in Table VI. These data are plotted against temperature in Figure 9. Critical phenomena were observed, at a constant temperature of  $288.95^{\circ}\text{C}$  at the following total densities: 0.3257, 0.3109, 0.2914, 0.2900. These were calculated by the method indicated for acetone.

I(c). Chloroform

In Table VII, the densities of the saturated liquid and vapor of chloroform are reported over the whole range of measurements from about  $100^{\circ}\text{C}$  to the critical temperature. These values are plotted in Figure 10 to give the coexistence curves of chloroform. Critical phenomena were observed, at a constant temperature of  $262.9^{\circ}\text{C}$ , at the following total densities: 0.4279, 0.4697, 0.4872, 0.5120, 0.5381, 0.5610. These densities were calculated from the measured volumes of the sample, as was done for acetone and benzene.

I(d). Carbon Tetrachloride

Table VIII gives the saturated densities of carbon tetrachloride at approximately 40 temperatures ranging from near the standard boiling point to the critical point. The experimental measurements permitted the construction of the saturation density envelope as shown in Figure 11. This is a plot of coexistence curves against temperature. Critical phenomena were observed, at a constant temperature of  $283.15^{\circ}\text{C}$ , at the following total densities: 0.4953, 0.5095, 0.5424, 0.5578, 0.5829, 0.6047. These were derived by the method given for acetone. The precision of the measurements was the same as that for acetone.

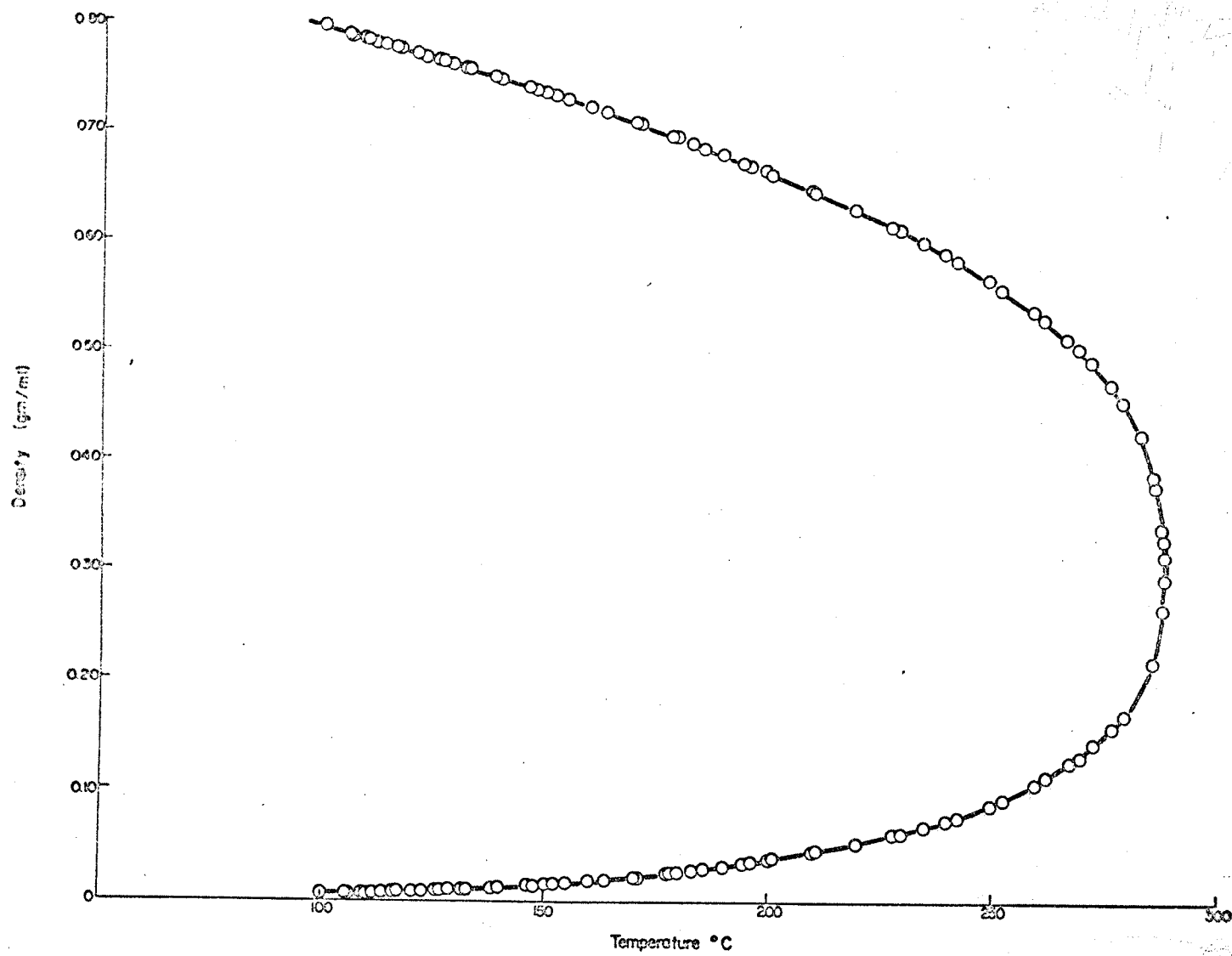
TABLE VI

Orthobaric Densities of Benzene ( $t_c = 288.95^\circ\text{C}$ )

Sample	Temp. $^\circ\text{C}$ .	Experimental Density of liquid, gm/cc.	*Calculated Density of liquid, gm/cc.	Experimental Density of vapor, gm/cc.	$(t_c - t)^{1/3}$
1	106.25	0.7858	0.7860	0.0060	
2	109.40	0.7831	0.7822	0.0057	
3	113.75	0.7764	0.7769	0.0072	
4	117.05	0.7726	0.7729	0.0079	
5	120.85	0.7679	0.7682	0.0080	
6	122.80	0.7657	0.7658	0.0083	
7	125.80	0.7618	0.7620	0.0088	
8	131.80	0.7550	0.7546	0.0106	
9	138.15	0.7464	0.7465	0.0110	
10	139.85	0.7441	0.7443	0.0118	
11	146.25	0.7371	0.7361	0.0121	
12	147.60	0.7350	0.7343	0.0123	
13	152.25	0.7290	0.7282	0.0140	
14	154.90	0.7248	0.7247	0.0144	
15	160.35	0.7181	0.7174	0.0163	
16	163.60	0.7136	0.7130	0.0179	
17	170.45	0.7041	0.7036	0.0203	
18	171.50	0.7020	0.7021	0.0208	
19	177.55	0.6932	0.6936	0.0237	
20	178.50	0.6919	0.6922	0.0240	
21	183.20	0.6850	0.6854	0.0261	
22	185.70	0.6812	0.6818	0.0278	
23	190.00	0.6746	0.6753	0.0300	
24	194.50	0.6670	0.6685	0.0326	
25	196.40	0.6647	0.6655	0.0338	
26	204.15	0.6571	0.6532	0.0372	4.393
27	210.95	0.6408	0.6419	0.0438	4.273
28	219.95	0.6257	0.6260	0.0508	4.101
29	228.05	0.6100	0.6106	0.0581	3.934
30	232.25	0.5960	0.5959	0.0658	3.773
31	242.65	0.5790	0.5793	0.0739	3.591
32	252.85	0.5521	0.5535	0.0900	3.306
33	262.25	0.5244	0.5250	0.1101	2.989
34	267.75	0.5070	0.5055	0.1239	2.768
35	272.80	0.4868	0.4848	0.1400	2.528
36	277.20	0.4660	0.4639	0.1556	2.273
37	280.00	0.4508	0.4489	0.1661	2.077
38	284.05	0.4199	0.4241	--	1.698
39	286.30	--	--	0.2144	--
40	286.65	0.3844	--	--	1.320
41	287.15	0.3737	--	--	1.216
42	288.40	0.3360	--	--	--
43	288.50	0.2625	--	--	--

\*Values were calculated from equation (100) using the constants given in Table XVII.

FIGURE 9. Orthobaric Densities of Benzene.



Orthobaric Densities of Benzene



TABLE VII

Orthobaric Densities of Chloroform ( $t_c = 262.9^\circ\text{C}$ )

Sample	Temp. $^\circ\text{C}$ .	Experimental Density of liquid, gm/cc.	*Calculated Density of liquid, gm/cc.	Experimental Density of vapor, gm/cc.	$(t_c - t)^{1/3}$
1	101.40	1.4884	1.4855	0.0136	
2	111.70	1.4510	1.4485	0.0182	
3	119.20	1.4230	1.4213	0.0224	
4	127.50	1.3914	1.3909	0.0278	
5	135.70	1.3612	1.3605	0.0320	
6	144.70	1.3259	1.3267	0.0389	
7	151.30	1.3000	1.3015	0.0440	
8	160.00	1.2652	1.2678	0.0512	
9	167.60	1.2346	1.2377	0.0578	
10	173.20	1.2127	1.2151	0.0621	
11	180.50	1.1832	1.1850	0.0684	
12	187.10	1.1552	1.1571	0.0756	
13	196.30	1.1149	1.1168	0.0871	
14	207.40	1.0628	1.0653	0.1038	3.814
15	213.70	1.0336	1.0342	0.1132	3.664
16	219.60	1.0044	1.0036	0.1236	3.512
17	225.30	0.9740	0.9722	0.1360	3.350
18	231.20	0.9410	0.9373	0.1504	3.164
19	237.50	0.9024	0.8966	0.1690	2.940
20	244.90	0.8482	0.8425	0.1998	2.523
21	252.70	0.7788	0.7747	0.2446	2.169
22	258.30	0.7052	0.7154	0.3008	1.663
23	260.20	0.6699	--	0.3301	1.393
24	261.50	0.6314	--	0.3642	1.119
25	262.50	0.5786	--	0.4138	0.737
26	262.80	--	--	0.4201	0.464
27	262.80	0.5662	--	--	0.464

\*Values were calculated from equation (100) using the constants given in Table XVII.

FIGURE 10. Orthobaric Densities of Chloroform.

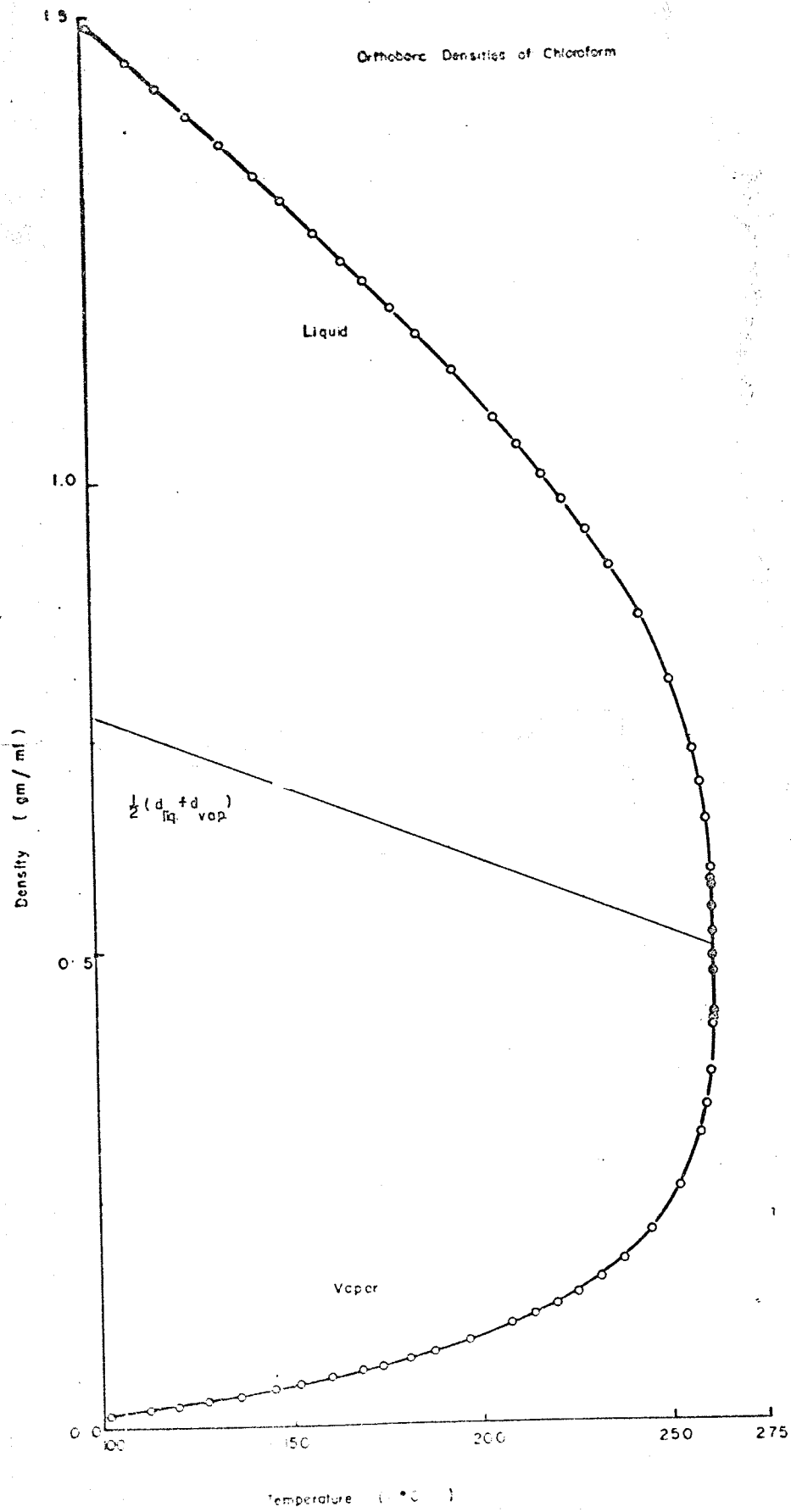


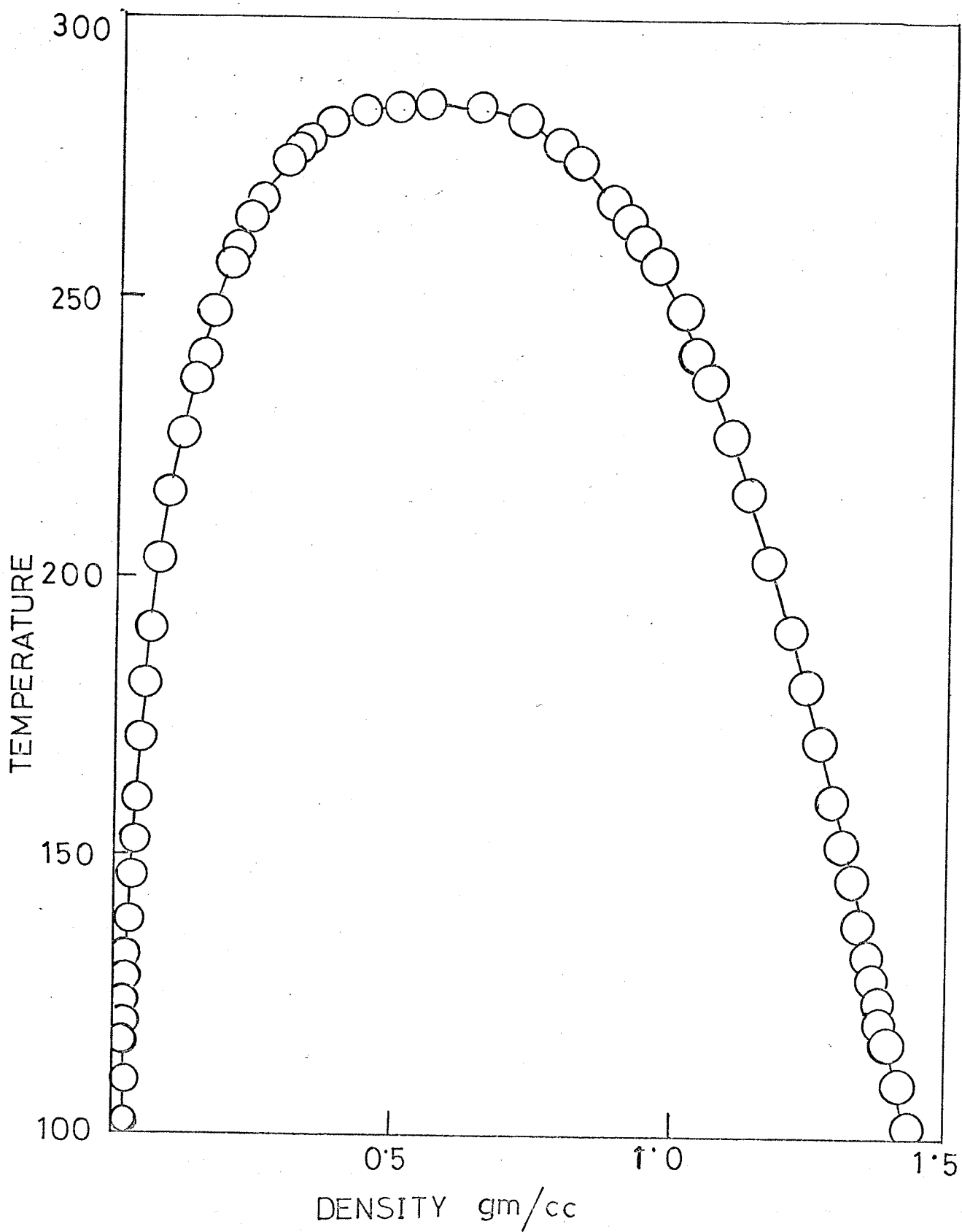
TABLE VIII

Orthobaric Densities of Carbon Tetrachloride ( $t_c=283.15$ )

Sample	Temp. °C.	Experimental Density of liquid, gm/cc.	*Calculated Density of liquid, gm/cc.	Experimental Density of vapor, gm/cc.	$(t_c - t)^{1/3}$
1	101.50	1.4315	1.4332	0.0118	
2	109.85	1.4131	1.4145	0.0141	
3	116.35	1.3984	1.3998	0.0162	
4	120.85	1.3880	1.3895	0.0179	
5	124.10	1.3808	1.3820	0.0190	
6	128.35	1.3716	1.3721	0.0202	
7	132.55	1.3621	1.3623	0.0220	
8	138.15	1.3486	1.3491	0.0239	
9	142.50	1.3390	1.3388	0.0259	
10	145.80	1.3311	1.3308	0.0276	
11	147.65	1.3263	1.3264	0.0284	
12	152.35	1.3151	1.3149	0.0316	
13	159.90	1.2973	1.2962	0.0362	
14	163.60	1.2880	1.2869	0.0389	
15	170.85	1.2700	1.2682	0.0447	
16	174.90	1.2597	1.2576	0.0481	
17	180.15	1.2458	1.2437	0.0529	
18	185.70	1.2312	1.2285	0.0579	
19	190.55	1.2181	1.2150	0.0626	
20	196.40	1.2009	1.1982	0.0694	
21	202.60	1.1808	1.1798	0.0778	4.316
22	208.75	1.1598	1.1607	0.0862	4.206
23	214.40	1.1412	1.1425	0.0952	4.097
24	219.95	1.1337	1.1238	0.1042	3.983
25	225.30	1.1028	1.1048	0.1143	3.867
26	231.05	1.0810	1.0832	0.1253	3.734
27	235.25	1.0640	1.0665	0.1340	3.632
28	240.00	1.0441	1.0464	0.1462	3.507
29	243.10	1.0269	1.0325	0.1566	3.422
30	247.55	1.0110	1.0114	0.1670	3.291
31	251.45	0.9910	0.9915	0.1797	3.164
32	256.05	0.9641	0.9659	0.1960	3.004
33	259.60	0.9419	0.9444	0.2122	2.866
34	264.15	0.9120	0.9139	0.2351	2.668
35	267.75	0.8838	0.8869	0.2568	2.488
36	271.35	0.8560	0.8567	0.2792	2.277
37	274.80	0.8261	0.8241	0.3076	2.029
38	276.95	0.8059	0.8015	0.3258	1.837
39	278.10	0.7910	0.7886	0.3386	1.716
40	280.10	0.7612	--	--	1.450
41	281.20	--	--	0.3788	1.249
42	281.55	0.7284	--	--	1.169

\*Values were calculated using equation (100) and the constants given in Table XVII.

FIGURE 11. Orthobaric Densities of Carbon Tetrachloride.



## II. VAPOR PRESSURE

II(a). Acetone

The vapor pressures of acetone determined at 5-10° intervals from 100°C to the critical point are reported in Table IX. The variation in pressure in separate determinations on the same sample amounted to 0.02 atm., on the average. This was arrived at from the results of a series of vapor pressure measurements at a few trial temperatures. The standard deviation for an individual measurement,  $\sigma$  was calculated from  $\sigma = \left[ \frac{\sum (\bar{p} - p)^2}{(n - 1)} \right]^{1/2}$ , where  $\bar{p}$  is the mean value at each temperature,  $p$  the experimental value at the same temperature, and  $n$  the no. of vapor pressure measurements at that temperature. The standard error of the mean,  $\sigma_s = \sigma/n^{1/2}$  was 0.01. The  $\sigma$  values are consistent with the estimated experimental uncertainty arising in the measurements of temperature and pressure, which increase from  $\pm 0.02$  atm. at 100°C to  $\pm 0.03$  atm. near the critical point. During the trial measurements the quantity of liquid in the manometer was varied so that these data actually represented conditions of dew-point, bubble-point, and a variety of liquid levels in the tube. It was observed that the pressure at large values of the vapor-liquid ratio (volume of vapor to the volume of liquid) more nearly represented the true vapor pressure. Vapor pressure versus temperature has been plotted in Figure 12.

II(b). Benzene

The results of vapor pressure measurements over a temperature range from 100°C to the critical temperature are set out in Table X. The last measured point is 0.45°C below the critical temperature of

TABLE IX

Vapor Pressure of Acetone

Sample	Temp. (°K)	Pressure (Cm of Hg at 0°C)	Pressure(atm)	*Calculated Pressure(atm)	Delta P atm = (P <sub>obs</sub> - P <sub>calc.</sub> )
1	374.65	284.2	3.739	3.755	-0.016
2	380.55	331.8	4.366	4.374	-0.008
3	388.25	403.5	5.309	5.299	+0.010
4	390.65	428.0	5.632	5.615	+0.017
5	397.25	500.2	6.582	6.557	+0.025
6	400.55	532.4	7.005	7.060	-0.055
7	405.65	604.3	7.951	7.921	+0.030
8	408.55	646.7	8.509	8.442	+0.067
9	413.25	712.3	9.372	9.328	+0.044
10	418.95	805.6	10.60	10.51	+0.09
11	423.05	872.3	11.48	11.41	+0.07
12	424.35	896.7	11.80	11.71	+0.09
13	429.05	939.5	12.36	12.76	-0.40
14	433.05	1052.1	13.84	13.85	-0.01
15	437.45	1140.9	15.01	15.04	-0.03
16	444.35	1292.3	17.00	17.06	-0.06
17	453.25	1518.6	19.97	19.98	-0.01
18	460.35	1716.0	22.58	22.56	+0.02
19	462.85	1799.3	23.67	23.56	+0.11
20	471.45	2051.1	26.99	27.05	-0.06
21	475.75	2201.6	28.97	28.98	-0.01
22	480.65	2392.5	31.49	31.36	+0.13
23	484.85	2541.0	33.43	33.41	+0.02
24	489.55	2738.8	36.04	35.92	+0.12
25	492.95	2877.1	37.86	37.79	+0.07
26	496.95	3053.3	40.17	40.11	+0.06
27	498.45	3118.7	41.03	40.99	+0.04
28	501.85	3271.1	43.04	43.04	0.0
29	503.35	3330.8	43.82	43.92	-0.10
30	505.25	3432.1	45.16	45.20	-0.04

Standard Deviation = 0.039 atm.

\*Values were calculated from equation (105) using the constants given in Table XVIII.



FIGURE 12. Vapor Pressure of Acetone from 100°C to  $T_c$ .

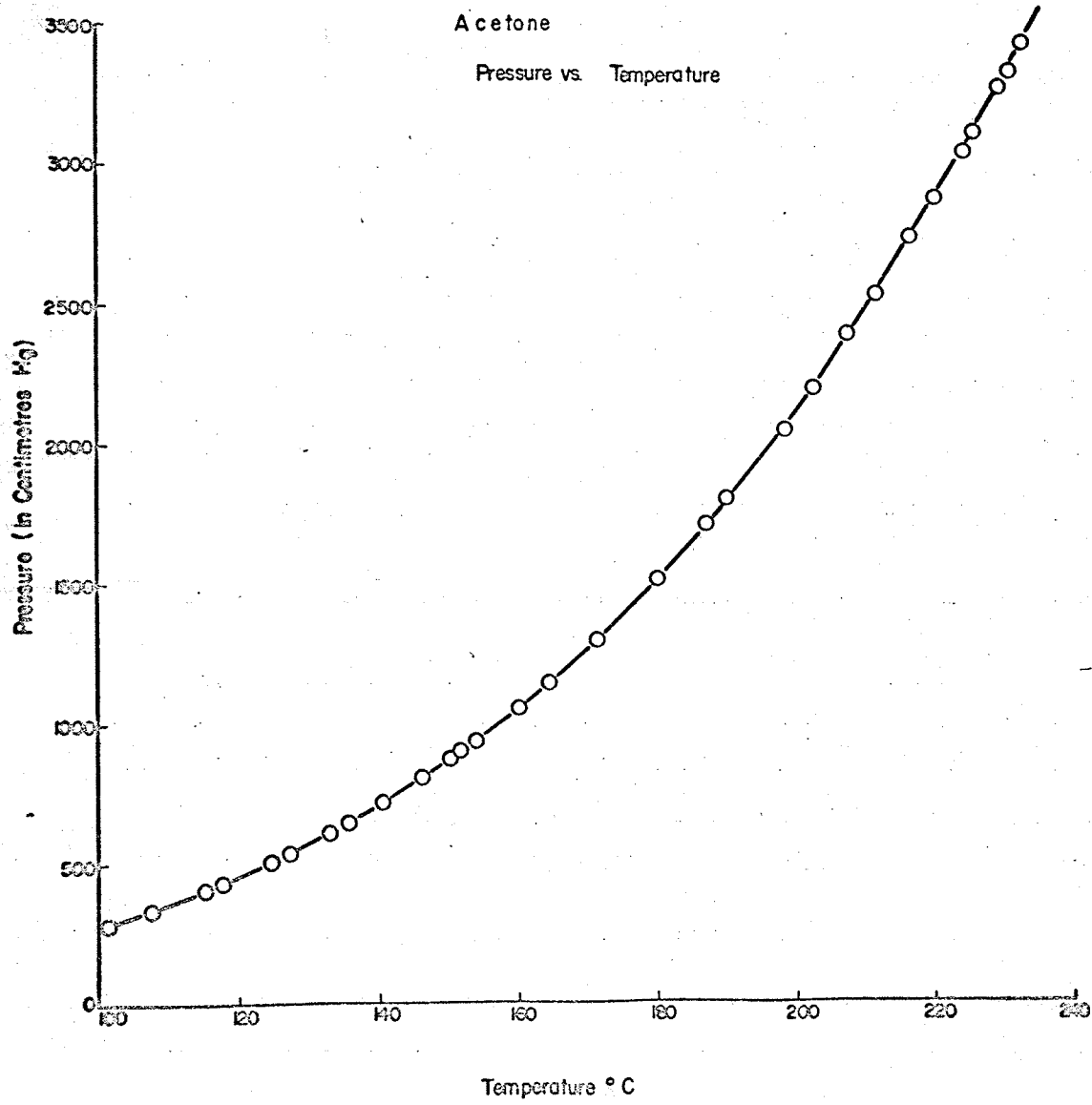


TABLE X

Vapor Pressure of Benzene

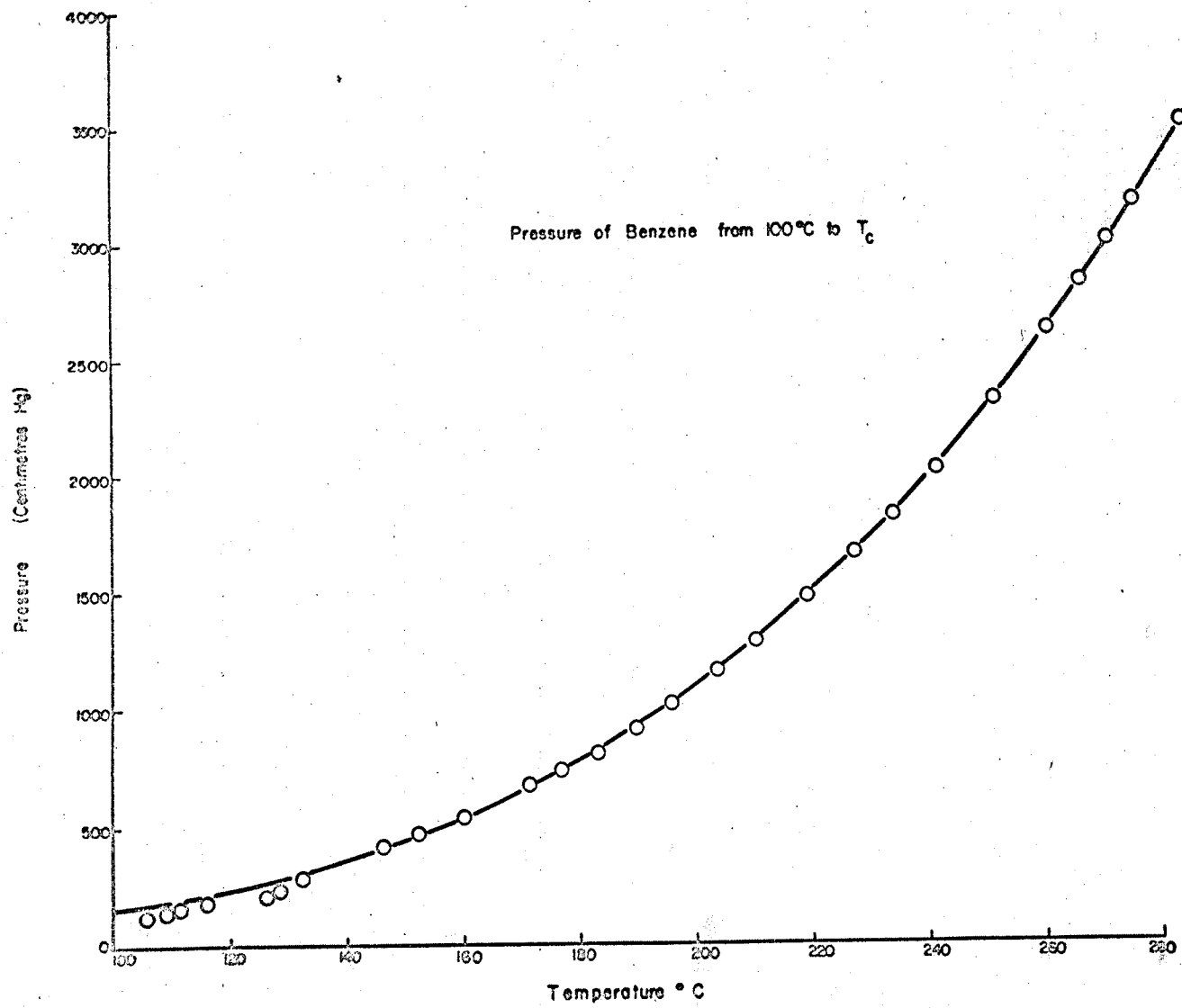
Sample	Temp. (°K)	Pressure (Cm of Hg at 0°C)	Pressure(atm)	*Calculated Pressure(atm)	Delta P atm = (P <sub>obs</sub> - P <sub>calc.</sub> )
1	379.40	173.7	2.286	2.263	+0.023
2	382.55	189.5	2.493	2.443	+0.050
3	386.90	206.7	2.720	2.705	+0.015
4	390.20	222.5	2.928	2.920	+0.008
5	394.00	241.2	3.174	3.181	-0.007
6	395.95	255.5	3.362	3.326	+0.036
7	398.95	270.5	3.559	3.552	+0.007
8	404.95	298.7	3.930	4.033	-0.103
9	411.30	343.6	4.521	4.608	-0.087
10	413.00	354.6	4.666	4.771	-0.105
11	419.40	410.8	5.405	5.433	-0.028
12	420.75	421.7	5.549	5.580	-0.031
13	425.40	461.6	6.074	6.108	-0.034
14	428.05	487.8	6.418	6.429	-0.011
15	433.50	537.7	7.075	7.119	-0.044
16	436.75	573.8	7.550	7.562	-0.012
17	443.60	651.7	8.595	8.564	+0.031
18	444.65	662.6	8.718	8.720	-0.002
19	450.70	739.1	9.725	9.699	+0.026
20	451.65	748.0	9.842	9.852	-0.010
21	456.35	810.1	10.66	10.67	-0.01
22	458.85	844.3	11.11	11.13	-0.02
23	463.15	909.9	11.97	11.96	+0.01
24	467.65	987.2	12.99	12.89	+0.10
25	469.55	1015.8	13.37	13.29	+0.08
26	477.30	1151.5	15.16	15.03	+0.13
27	484.10	1279.9	16.84	16.70	+0.14
28	493.10	1472.8	19.38	19.15	+0.23
29	501.20	1652.3	21.74	21.54	+0.20
30	508.40	1829.6	24.08	23.89	+0.19
31	515.80	2021.4	26.59	26.47	+0.12
32	526.00	2320.5	30.54	30.45	+0.09
33	535.40	2624.7	34.54	34.52	+0.02
34	540.90	2827.6	37.21	37.16	+0.05
35	545.95	3006.8	39.57	39.63	-0.06
36	550.35	3175.5	41.79	41.94	-0.15
37	553.15	3282.4	43.18	43.43	-0.25
38	558.45	3521.5	46.34	46.56	-0.22
39	561.65	3636.7	47.86	48.35	-0.49

---

Standard Deviation = 0.061 atm.

\*Values calculated from equation (105) using the constants given in Table XVIII.

FIGURE 13. Vapor Pressure of Benzene from 100°C to  $T_c$ .



benzene ( $288.95^{\circ}\text{C}$ ). The data have been plotted in Figure 13 which shows the variation of saturation vapor pressure of benzene with temperature. The uncertainty of the measurements is as indicated for acetone.

#### II(c). Chloroform

The vapor pressures of chloroform measured at approximately 25 temperatures from  $100^{\circ}\text{C}$  to within a few degrees of the critical temperature are presented in Table XI. These are plotted as a function of temperature in Figure 14.

#### II(d). Carbon Tetrachloride

The vapor pressure measurements of carbon tetrachloride were made at 40 different temperatures ranging from  $100^{\circ}\text{C}$  to within a few degrees of the critical temperature and are shown in Table XII. The data have been plotted in Figure 15.

### III. CRITICAL TEMPERATURE

#### III(a). Pure Liquids

The critical points of the pure liquids were observed visually and this gave critical temperatures of  $235.0^{\circ}\text{C}$  for acetone,  $288.95^{\circ}\text{C}$  for benzene,  $262.9^{\circ}\text{C}$  for chloroform and  $283.15^{\circ}\text{C}$  for carbon tetrachloride.

#### III(b). The System Acetone-Benzene

The gas-liquid critical temperatures have been measured for this binary mixture over the whole concentration range. The data are represented in Table XIII. The concentrations are given in mole-

TABLE XI

Vapor Pressure of Chloroform

Sample	Temp. (°K)	Pressure (Cm of Hg at 0°C)	Pressure (atm)	*Calculated Pressure (atm)	Delta P atm = (P <sub>obs</sub> - P <sub>calc.</sub> )
1	374.55	245.7	3.233	3.180	+0.053
2	384.85	313.2	4.121	4.113	+0.008
3	392.35	371.4	4.887	4.912	-0.025
4	400.65	450.8	5.932	5.933	-0.001
5	408.85	537.6	7.074	7.086	-0.012
6	417.85	642.5	8.454	8.529	-0.075
7	424.45	739.8	9.734	9.734	0.0
8	433.15	865.4	11.39	11.72	-0.33
9	440.75	989.6	13.02	13.18	-0.16
10	446.35	1093.5	14.39	14.56	-0.17
11	453.65	1250.1	16.45	16.54	-0.09
12	460.25	1401.3	18.44	18.49	-0.05
13	469.45	1628.6	21.43	21.46	-0.03
14	480.55	1963.2	25.83	25.60	+0.23
15	486.85	2177.3	28.65	28.20	+0.45
16	492.75	2388.5	31.43	30.82	+0.61
17	498.45	2592.7	34.11	33.47	+0.64
18	504.35	2815.1	37.04	36.39	+0.65
19	510.65	3040.3	40.00	39.58	+0.42
20	518.05	3313.6	43.60	43.53	+0.07
21	525.85	3609.7	47.50	47.94	-0.44
22	531.45	3818.9	50.25	51.21	-0.96
23	533.35	3890.8	51.19	52.32	-1.13

Standard Deviation = 0.064 atm.

\*Values were calculated from equation (105) using the constants given in Table XVIII.

FIGURE 14. Vapor Pressure of Chloroform from 100°C to  $T_c$ .



## Vapor Pressure of Pure Chloroform

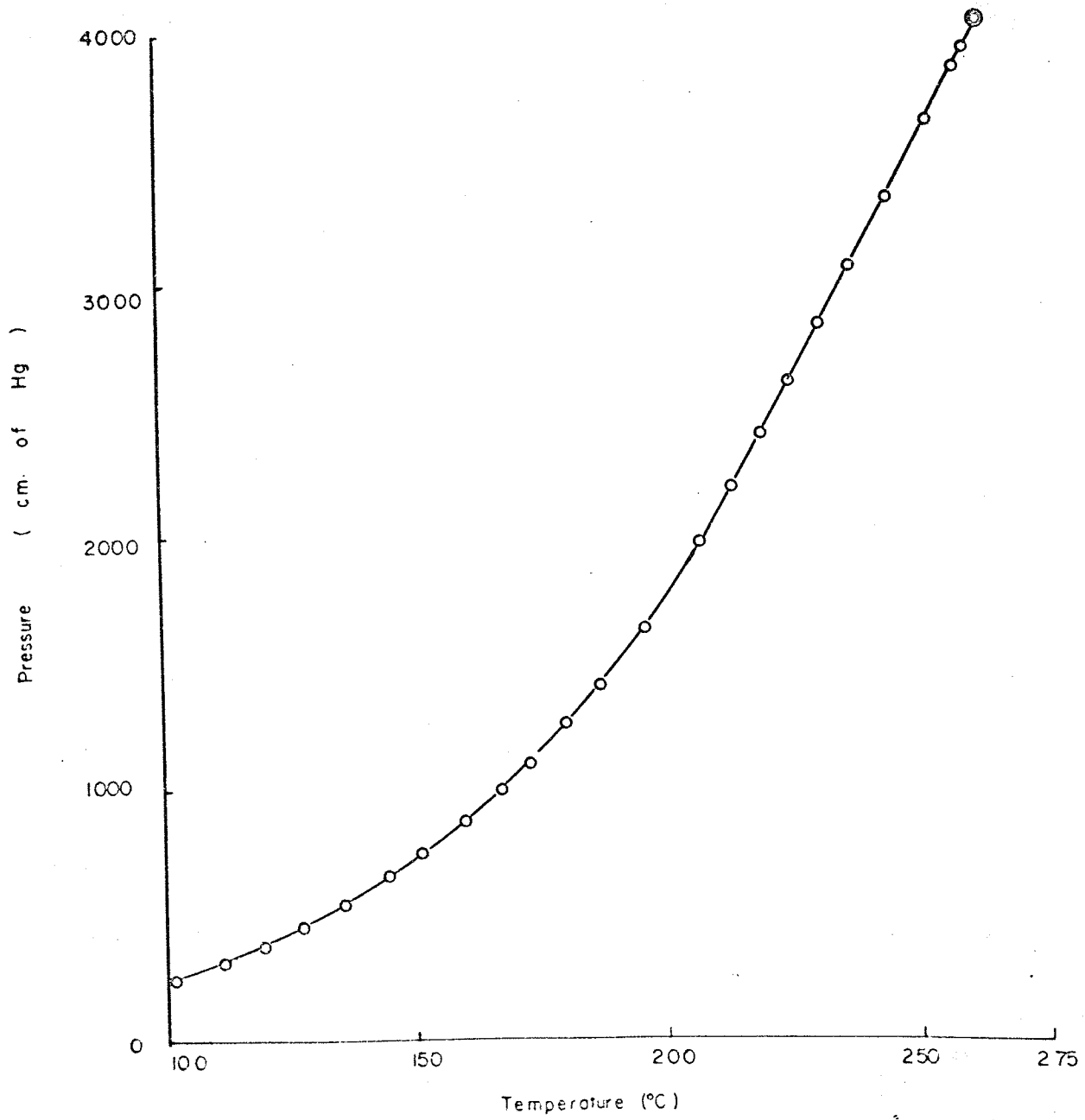
from 100°C to  $T_c$ 

TABLE XII

## Vapor Pressure of Carbon Tetrachloride

Sample	Temp. (°K)	Pressure (Cm of Hg at 0°C)	Pressure(atm)	*Calculated Pressure(atm)	Delta P atm = (P <sub>obs</sub> - P <sub>calc.</sub> )
1	374.65	153.1	2.014	2.008	+0.006
2	383.00	187.3	2.464	2.473	-0.009
3	389.50	219.8	2.892	2.891	+0.001
4	394.00	244.5	3.217	3.210	+0.007
5	397.25	262.4	3.453	3.457	-0.004
6	401.50	287.9	3.788	3.801	-0.013
7	405.70	316.7	4.167	4.167	0.0
8	411.30	357.3	4.701	4.695	+0.006
9	415.65	382.8	5.037	5.129	-0.092
10	418.95	417.4	5.492	5.493	-0.001
11	420.80	438.6	5.771	5.707	+0.064
12	425.50	475.2	6.253	6.253	0.0
13	433.05	554.1	7.291	7.233	+0.058
14	436.75	587.2	7.726	7.739	-0.013
15	444.00	668.8	8.800	8.824	-0.024
16	448.05	719.8	9.471	9.482	-0.011
17	453.30	792.5	10.43	10.40	+0.03
18	458.85	869.9	11.45	11.41	+0.04
19	463.70	941.2	12.38	12.36	+0.02
20	469.55	1034.4	13.61	13.58	+0.03
21	475.75	1136.5	14.95	14.98	-0.03
22	481.90	1248.4	16.43	16.45	-0.02
23	487.55	1357.7	17.86	17.91	-0.05
24	493.10	1473.4	19.39	19.43	-0.04
25	498.45	1597.5	21.02	21.01	+0.01
26	504.20	1735.6	22.84	22.80	+0.04
27	508.40	1837.5	24.18	24.16	+0.02
28	513.15	1962.3	25.82	25.79	+0.03
29	516.25	2047.1	26.94	26.90	+0.04
30	520.70	2174.8	28.62	28.56	+0.06
31	524.60	2284.3	30.06	30.04	+0.02
32	529.20	2428.0	31.95	31.92	+0.03
33	532.75	2544.7	33.48	33.42	+0.06
34	537.30	2684.3	35.32	35.37	-0.05
35	540.90	2815.5	37.05	37.05	0.0
36	544.50	2943.0	38.72	38.75	-0.03
37	547.95	3071.2	40.41	40.43	-0.02
38	550.10	3155.4	41.52	41.54	-0.02
39	553.25	3283.7	43.21	43.19	+0.02
40	554.70	3348.2	44.06	43.99	+0.07

Standard Deviation = 0.038 atm.

\*Values were calculated from equation (105) using the constants given in Table XVIII.

FIGURE 15. Vapor Pressure of Carbon Tetrachloride from 100°C to  $T_c$ .

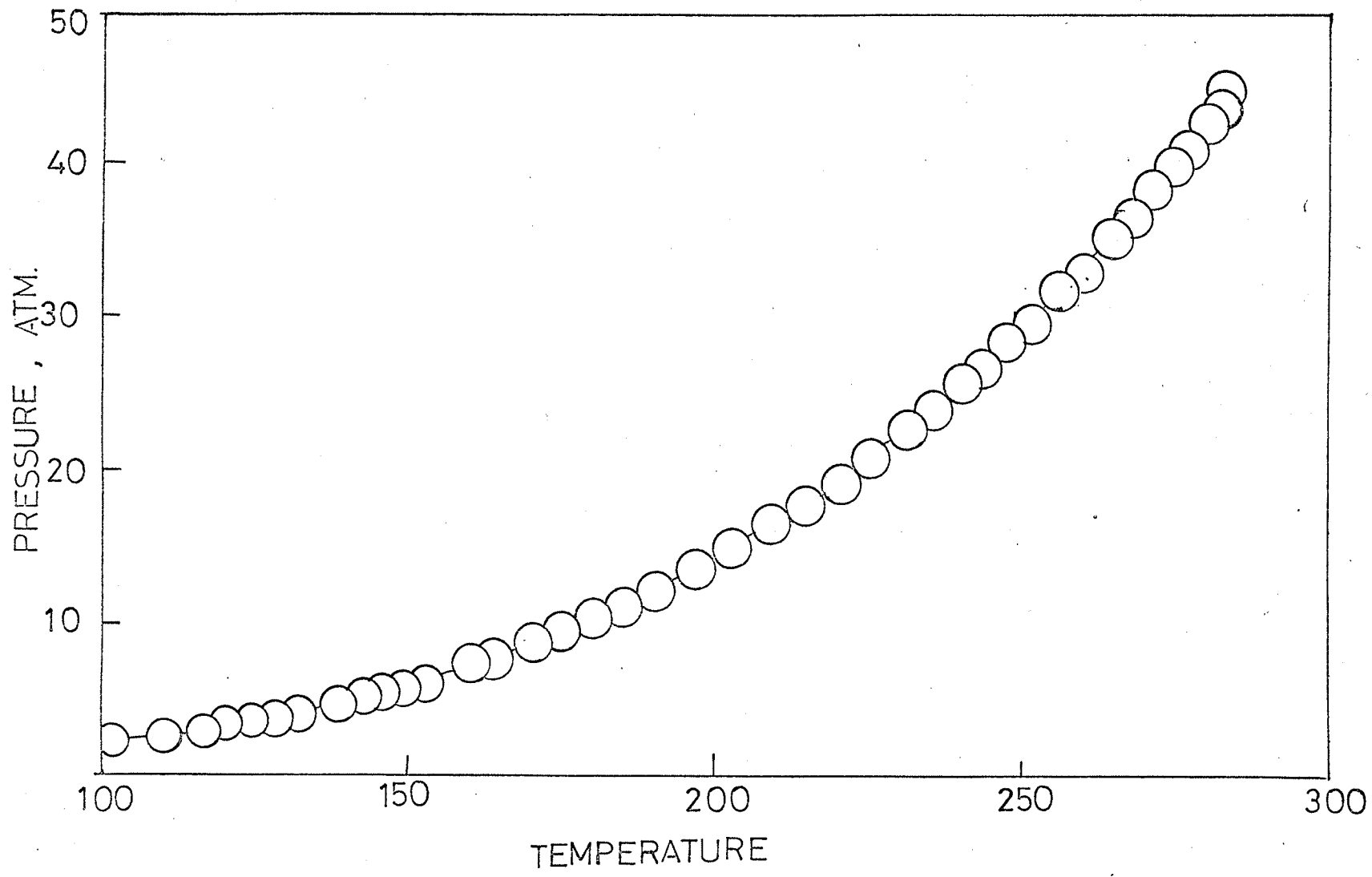


TABLE XIII

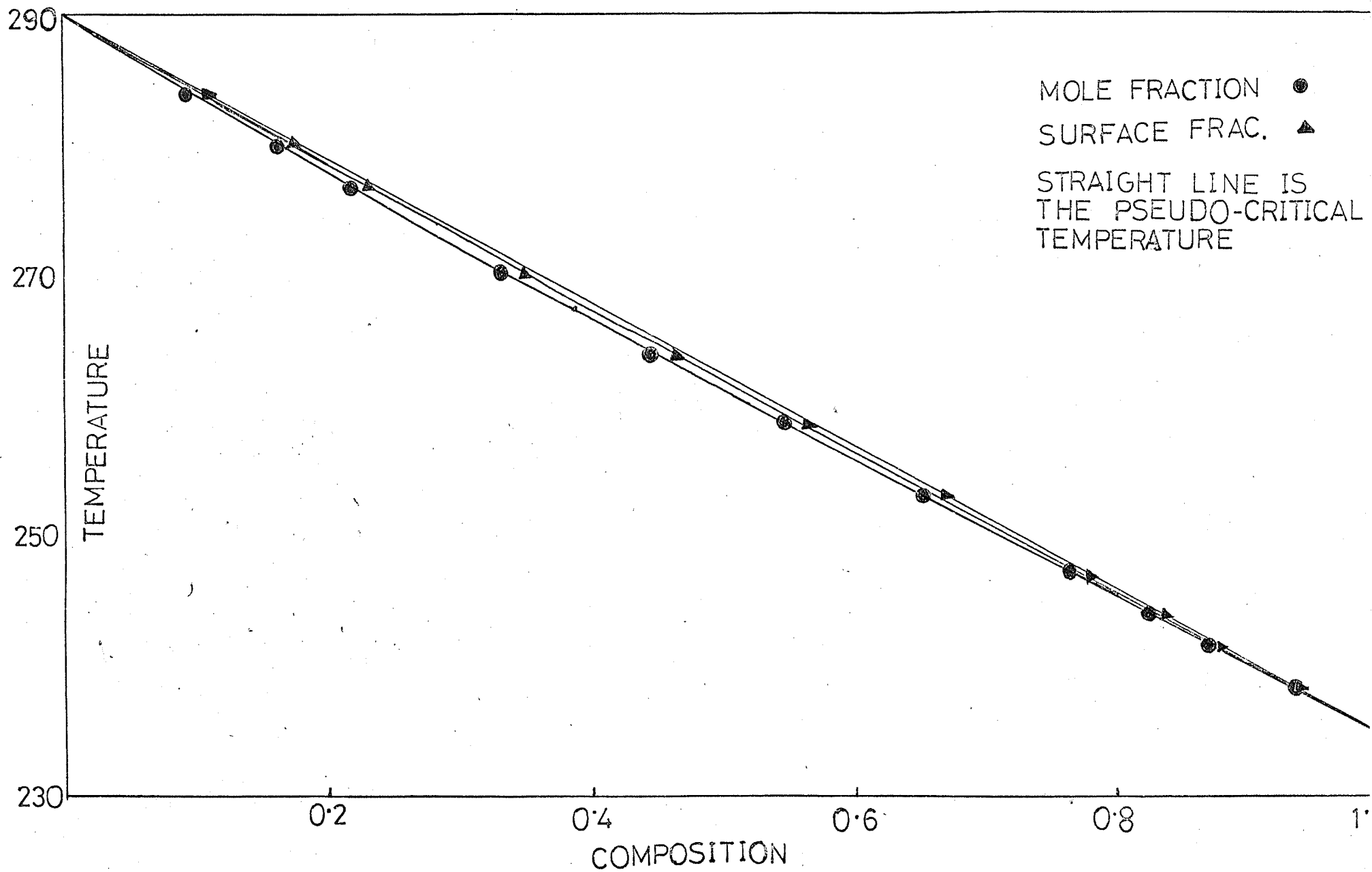
Gas-liquid Critical Temperatures of the System Acetone-Benzene

No.	Composition of the Mixture		Experimental Critical Temp. (°C)	$\frac{2\tau_{12}}{T_{c1} + T_{c2}}$
	Mole Fraction Acetone	Surface Fraction Acetone		
1	0.0925	0.0997	283.95	-0.004
2	0.1580	0.1690	279.70	-0.011
3	0.2160	0.2300	276.75	-0.009
4	0.3290	0.3480	270.20	-0.010
5	0.4410	0.4620	264.00	-0.010
6	0.5440	0.5640	258.90	-0.009
7	0.6530	0.6720	252.95	-0.009
8	0.7640	0.7790	247.35	-0.008
9	0.8250	0.8366	244.10	-0.008
10	0.8690	0.8781	241.55	-0.010
11	0.9370	0.9410	238.20	-0.009

Value of the correlating parameter  $\tau_{12}$  selected = -0.0096.

See Appendix.

FIGURE 16. Gas-Liquid Critical Temperatures of the Benzene-Acetone System as a Function of Mole Fraction and Surface Fraction.



fraction as well as surface-fraction (equation 88). These data are plotted in Figure 16, which depicts the variation of the critical point with mole-fraction, and surface-fraction of the mixture. The uncertainty of the measurements was  $\pm 0.1^{\circ}\text{C}$ .

#### IV. VAPOR-LIQUID EQUILIBRIUM

The experimental data obtained for saturation vapor pressure measurements of seven mixtures of the system acetone-benzene covering the whole range of composition from a temperature of  $100^{\circ}\text{C}$  and a pressure of about 2 atmospheres to the highest temperature and pressure at which liquid and vapor coexist are summarized in Table XIV. Figure 17 shows the constant composition plots of the relation between pressure and temperature at the bubble-points of the acetone-benzene system. From a large-scale plot of this nature the isothermal experimental data required for the correlation and thermodynamic treatment were read as indicated in a later chapter.

The results obtained in the static method of determination of vapor-phase compositions in equilibrium with liquid-phase are presented in Table XV. The isothermal liquid-vapor equilibrium data are plotted in Figure 18. The calibration curve of refractive index vs. composition of acetone-benzene system was plotted in a large-scale graph from the data listed in Table XVI. This plot was not far from a straight line when the composition was expressed as weight fraction.



TABLE XIV

## Experimental Saturation Pressure of the System Acetone-Benzene

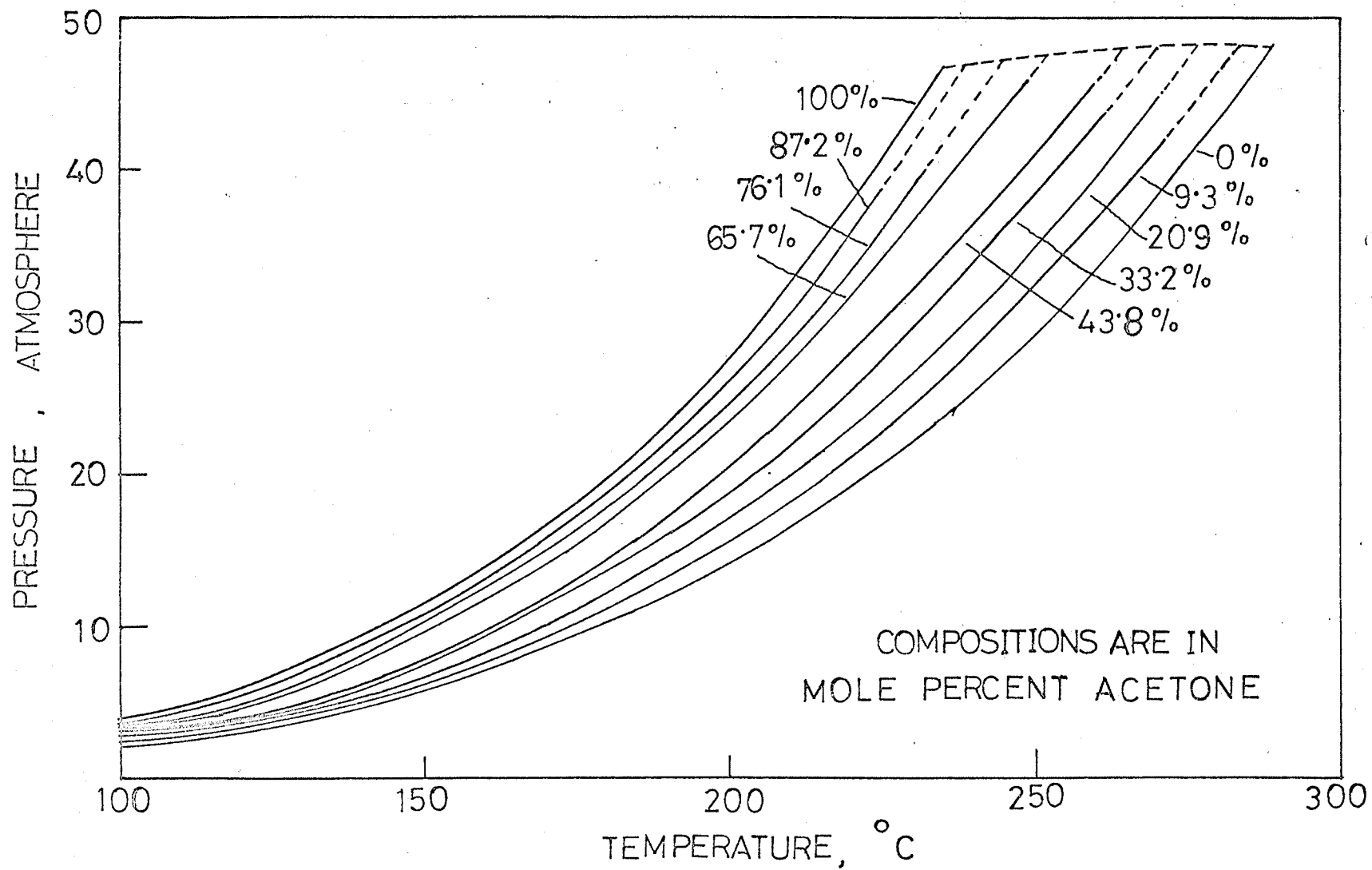
Temp. °C	Saturated Pressure, atm.	Temp. °C	Saturated Pressure, atm.	Temp. °C	Saturated Pressure, atm.
<u>Composition of the mixture = 0.093 mole fraction acetone.</u>		233.85	28.49	132.65	5.886
		241.90	31.76	140.10	6.823
		248.45	34.54	149.90	8.250
		255.60	37.78	157.55	9.621
99.85	2.083	259.55	39.69	165.40	11.22
110.05	2.808	265.30	42.39	173.95	13.08
117.45	3.243	268.35	43.81	178.50	14.19
127.35	3.983	270.10	44.79	187.05	16.26
134.60	4.610			193.60	18.14
143.35	5.427	<u>Composition of the mixture = 0.332 mole fraction acetone.</u>		199.75	20.11
152.70	6.634			207.35	22.74
161.55	7.842			216.00	25.99
173.30	9.780	100.05	2.481	222.95	28.90
185.75	12.30	108.55	3.170	230.50	32.18
194.05	14.18	114.60	3.625	238.55	35.88
207.30	17.36	123.50	4.395	244.70	38.67
216.65	20.08	132.35	5.390	249.85	41.18
223.50	22.39	140.65	6.402	257.60	44.71
231.65	25.18	149.85	7.635	260.10	45.95
243.30	29.70	157.65	8.946		
251.55	33.08	168.50	10.98	<u>Composition of the mixture = 0.657 mole fraction acetone.</u>	
258.10	35.92	175.95	12.44	99.85	2.996
263.15	38.19	183.50	14.18	107.50	3.605
269.25	40.92	190.45	15.92	115.30	4.421
271.50	41.89	196.70	17.80	122.55	5.220
		204.50	20.24	127.65	5.923
<u>Composition of the mixture = 0.209 mole fraction acetone.</u>		211.35	22.48	134.70	6.907
99.95	2.275	218.60	25.17	143.15	8.285
108.50	2.846	224.75	27.43	149.60	9.496
116.25	3.368	231.55	30.34	157.55	11.19
125.30	4.052	238.30	33.19	165.85	12.96
135.55	5.246	246.65	36.89	174.80	15.20
145.50	6.368	254.85	40.70	179.50	16.41
154.45	7.645	259.05	42.64	186.30	18.44
161.05	8.683	261.40	43.78	194.70	21.39
170.50	10.42	<u>Composition of the mixture = 0.438 mole fraction acetone.</u>		199.65	23.16
182.35	12.79			207.50	26.37
192.55	15.26	99.90	2.645	214.05	29.13
203.70	18.04	105.60	3.096	221.35	32.47
210.50	20.26	112.45	3.763	227.50	35.31
217.65	22.60	119.85	4.398	235.95	39.26
225.50	25.28	125.60	4.947	242.35	42.24

TABLE XIV(Cont'd)

Experimental Saturation Pressure of the System Acetone-Benzene

<u>Temp. °C</u>	<u>Saturated Pressure, atm.</u>	<u>Temp. °C</u>	<u>Saturated Pressure, atm.</u>
247.60	44.76	189.50	22.06
250.05	45.99	198.95	25.62
<u>Composition of the mixture = 0.761 mole fraction acetone.</u>		208.40	29.96
99.95	3.166	215.35	33.39
109.55	4.089	221.45	36.50
117.35	4.888	225.15	38.49
124.60	5.820	<u>Composition of the mixture = 0.151 mole fraction acetone.</u>	
132.50	6.995	261.70	39.11
139.95	8.226	263.35	39.84
147.50	9.689	265.80	40.88
156.70	11.62	267.65	41.77
164.85	13.63	269.30	42.50
172.55	15.59	270.80	43.29
179.90	17.50	271.55	43.63
188.65	20.39		
196.30	23.20		
202.55	25.80		
210.10	29.08		
216.80	32.16		
222.55	35.01		
224.65	36.02		
225.40	36.32		
232.50	39.83		
<u>Composition of the mixture = 0.872 mole fraction acetone.</u>			
99.85	3.340		
107.70	4.163		
116.40	5.196		
123.85	6.193		
129.90	7.089		
139.65	8.786		
144.35	9.608		
149.95	10.69		
157.85	12.57		
164.05	14.12		
174.80	17.09		
181.95	19.39		

FIGURE 17. Lines of Constant Composition on a Pressure-Temperature Diagram.



## EXPERIMENTAL VAPOR-LIQUID EQUILIBRIA OF THE SYSTEM

## ACETONE-BENZENE AT DIFFERENT ISOTHERMS

<u>Compositions</u> Mole Fraction Acetone in Liquid	<u>Compositions</u> Mole Fraction Acetone in Vapor	<u>Compositions</u> Mole Fraction Acetone in Liquid	<u>Compositions</u> Mole Fraction Acetone in Vapor
	<u>T = 100°C</u>	0.842	0.885
0.085	0.207	0.885	0.913
0.149	0.285		<u>T = 200°C</u>
0.177	0.325	0.105	0.154
0.222	0.387	0.236	0.312
0.284	0.421	0.348	0.445
0.371	0.543	0.413	0.507
0.378	0.558	0.540	0.635
0.439	0.609	0.638	0.723
0.510	0.667	0.735	0.802
0.548	0.699	0.796	0.848
0.611	0.742	0.892	0.918
0.635	0.764		<u>T = 225°C</u>
0.758	0.843	0.116	0.155
0.784	0.865	0.208	0.308
0.862	0.913	0.260	0.360
	<u>T = 125°C</u>	0.320	0.403
0.100	0.186	0.432	0.513
0.168	0.293	0.576	0.661
0.247	0.393	0.700	0.764
0.364	0.518	0.822	0.860
0.456	0.611	0.899	0.920
0.575	0.707		<u>T = 250°C</u>
0.704	0.799	0.096	0.113
0.816	0.875	0.194	0.225
0.880	0.917	0.280	0.328
	<u>T = 150°C</u>	0.400	0.451
0.070	0.126	0.499	0.539
0.127	0.221	0.597	0.622
0.188	0.301	0.656	0.669
0.237	0.356		<u>T = 260°C</u>
0.321	0.450	0.066	0.073
0.429	0.559	0.162	0.184
0.534	0.655	0.261	0.289
0.622	0.729	0.360	0.385
0.732	0.810	0.427	0.442
0.789	0.850		<u>T = 270°C</u>
0.860	0.903	0.101	0.108
	<u>T = 175°C</u>	0.141	0.149
0.086	0.144	0.186	0.196
0.146	0.220	0.226	0.233
0.218	0.311		
0.305	0.411		
0.401	0.517		
0.510	0.621		
0.625	0.720		
0.741	0.812		

FIGURE 18. Liquid-Vapor Composition Equilibrium Curves for the System Benzene-Acetone at 100°, 125°, 150°, 175°, 200°, 225°, 250°, 260°, and 270°C.

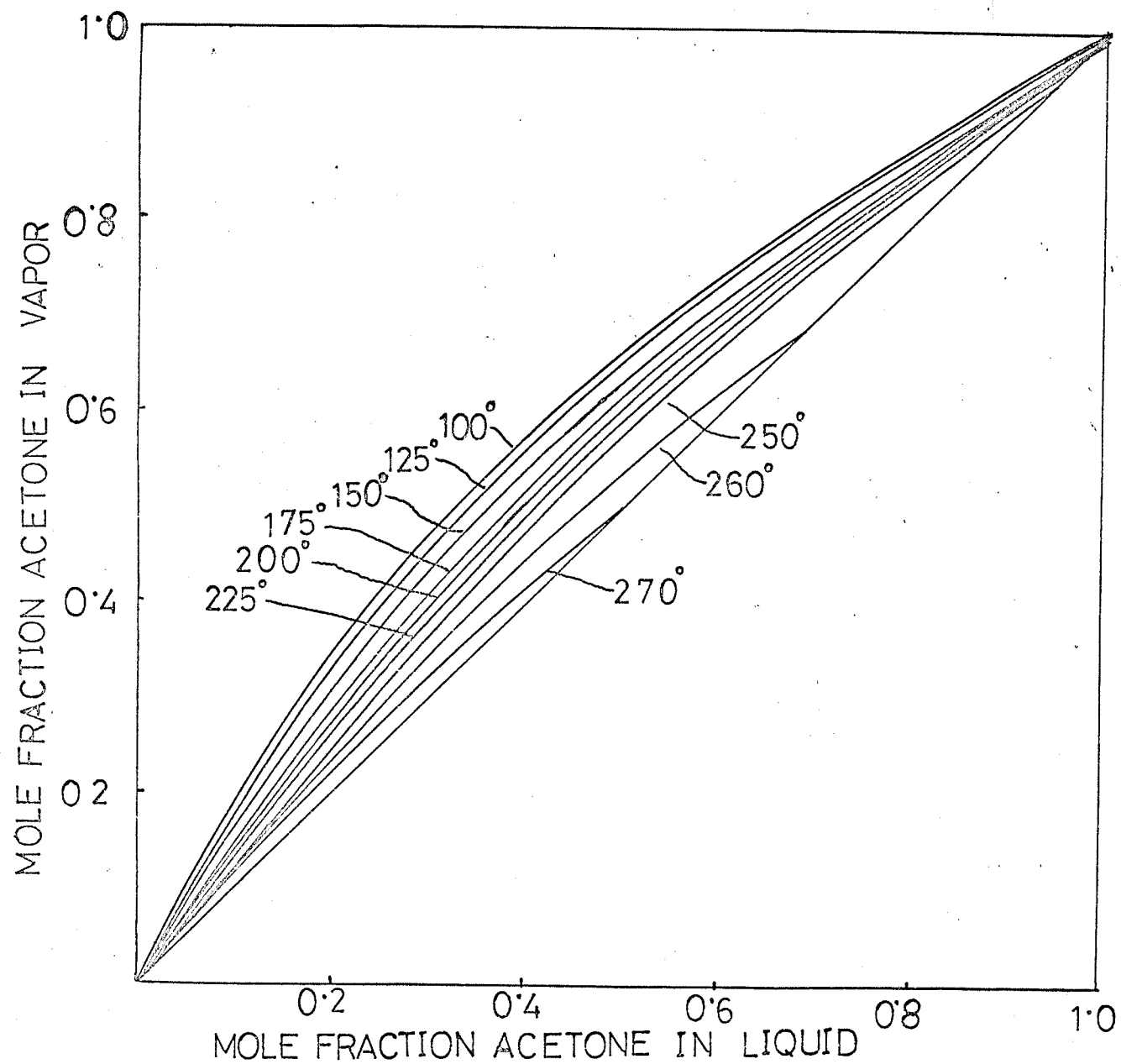


TABLE XVIDENSITY AND REFRACTIVE INDEX DATA FOR THE  
SYSTEM ACETONE-BENZENE

<u>Sample</u>	<u>Mole Fraction Acetone</u>	<u>Density, <math>d_4^{25}</math></u>	<u>Refractive Index <math>n_D^{25}</math></u>
1	0.0000	0.8734	1.4979
2	0.0920	0.8663	1.4879
3	0.1895	0.8592	1.4764
4	0.2364	0.8557	1.4704
5	0.2986	0.8506	1.4624
6	0.3321	0.8481	1.4584
7	0.4076	0.8417	1.4484
8	0.4692	0.8365	1.4397
9	0.4900	0.8346	1.4364
10	0.5552	0.8288	1.4279
11	0.5608	0.8283	1.4264
12	0.6629	0.8188	1.4105
13	0.7262	0.8127	1.4014
14	0.7691	0.8084	1.3954
15	0.8080	0.8046	1.3883
16	0.8946	0.7956	1.3745
17	1.0000	0.7842	1.3563



## CHAPTER V

## DISCUSSION

## I. CORRELATION OF DATA

I(a). Critical Constants

Several empirical methods for estimating the critical constants of a pure compound have been suggested in the literature. In a thorough study of the literature Reid and Sherwood (169,170) have recommended certain methods on the basis of the degree of agreement between the calculated and the experimental values. Kobe and Lynn (159) have also reviewed many of the estimation methods. Later, Moritz (171) suggested an empirical equation to calculate the logarithmic values of critical temperatures of different types of compounds. He wrote

$$\log T_c = b \log (n + c) + d \quad (93)$$

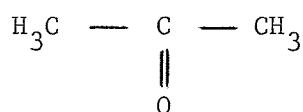
where  $b$ ,  $c$  and  $d$  are constants characteristic of each homologous series. Thodos (172) has developed a method for the calculation of critical constants through the use of group contributions specific to various types of carbon atoms. These group contributions are added to produce the van der Waals' constants, from a consideration of the molecular structure of the hydrocarbons only, including the aliphatic, naphthenic, and aromatic types, and this in turn permits the calculation of the critical temperature, pressure, and volume. For a pure substance the critical temperature and pressure are related to the van der Waals' constants  $a$  and  $b$  by the relationships

$$T_c = \frac{8a}{27Rb} \quad \text{and} \quad P_c = \frac{a}{27b^2} \quad (94)$$

conversely, equation (94) permits the calculation of the van der Waals' constants from available critical temperatures and pressures:

$$a = \frac{27R^2T_c^2}{64P_c} \quad \text{and} \quad b = \frac{RT_c}{8P_c} \quad (95)$$

By means of equation (95) Thodos evaluated both van der Waals' constants (a and b) from the literature data on seventy-five saturated and unsaturated aliphatic, naphthenic, and aromatic hydrocarbons and tabulated them (172). I have calculated the critical temperature and pressure of acetone by the method suggested by Thodos, and compared them with the results obtained in this study. The structure of acetone



shows that it contains two type-1 (methyl group) carbons (Table I in both reference 172(e) and 172(f)), and one carbonyl (  $\text{-}\overset{\text{O}}{\underset{\text{O}}{\text{C}}}\text{-}$  ) functional group. The number of functional atoms is 4. From the group contributions presented in Thodos' articles,  $a^{2/3}$  and  $b^{3/4}$  are calculated as follows:

2 carbon atoms (type - 1)	2(15,035)	2(11.435)
1 carbonyl group	32,400	11.35
	62,470	34.26
	$a^{2/3} = 62,470$	$b^{3/4} = 34.26$

These values yield the following calculated van der Waals' constants:

$$a = 15.614 \times 10^6 \text{ (cc./gm. - mole)}^2 \text{ atm.}$$

$$b = 111.26 \text{ cc./gm. - mole}$$

Equation (94), then yields

$$T_c = \frac{8(15.614 \times 10^6)}{27(82.055)(111.26)} = 506.8^\circ\text{K}$$

$$P_c = \frac{15.614 \times 10^6}{27(111.26)^2} = 46.7 \text{ atm.}$$

The values calculated by Thodos' method for acetone agreed well with the critical temperature (508.15°K) and critical pressure (46.96 atm.) obtained experimentally in this research. Nevertheless, it should be emphasized that Thodos' method is only empirical and equations (94) and (95) are valid to the extent van der Waals' development is correct. It has long been recognized (74) that the selection of any particular pair of independent quantities from  $P_c$ ,  $V_c$ , and  $T_c$  permits different expressions for  $a$  and  $b$  by elimination of the dependent quantity through  $Z_c = \frac{P_c V_c}{RT_c} = 0.375$ , which is based on van der Waals' development. Martin (74) further says that this inconsistency is partially resolved if  $a$  and  $b$  are computed simultaneously from the same pair of independent quantities. Thodos et al. (75) have indicated that the gaseous state behavior based on van der Waals' treatment is acceptable for subcritical temperatures.

The critical temperature of a substance is a reproducible and directly observable property, and so is the critical pressure. However, because of the difficulties discussed by Campbell and Chatterjee (173), the critical pressures in this research were obtained by an extension of the  $\log p$  versus  $1/T$  line to critical temperature: the agreement with the latest figures is good as is evident from a comparison of Table IV (p.82) with the following experimental values obtained in this study

Acetone,  $P_c = 46.96 \text{ atm.}$

Benzene,  $P_c = 48.22 \text{ atm.}$

Chloroform,  $P_c = 52.59 \text{ atm.}$

Carbon Tetrachloride,  $P_c = 44.98 \text{ atm.}$

On the other hand, the critical density can only be obtained by extrapolation from results obtained at lower temperatures and this is the most difficult of the three constants to measure accurately. The method which is probably the best, and is certainly the most commonly used, is to extrapolate the mean of the orthobaric liquid and vapor densities up to the critical temperature. It can be shown (24) that the classical description of the critical region requires that the critical density should be equal to the arithmetic mean of the orthobaric densities at temperatures just below the critical.

In a very interesting paper Mathias (174) discussed the law of rectilinear diameters, discovered in 1886, by Cailletet and himself (175), and the law of the corresponding states of matter. The law of Cailletet and Mathias may be stated simply in this way -- "The means of the densities of liquid and saturated vapor for any stable substance are a rectilinear function of the temperature". This was shown to be experimentally true by Cailletet and Mathias (175) for a considerable number of substances, though it was not strictly applicable in all cases. It was pointed out by Guye (176) that the law did not, as a rule, apply at all for substances the molecules of which differed in complexity in the gaseous and liquid states. For example, acetic acid vapor is known to dimerize and therefore this law does not apply for such associating molecules. This is understandable, since the thermodynamic properties of associating vapors do not follow the general trend of normal vapors as was shown by Campbell, Kartzmark and Gieskes (141). Cailletet and Mathias thought at first that the mean density line was parallel to the temperature axis but it is now known that it has a slight negative slope and a very small but usually

negligible curvature as was first shown by Young (65). This line may be represented, by

$$\frac{1}{2} (\rho_l + \rho_v) = a - bt \quad (96)$$

This line intersects the coexistence curve at the critical point.

Therefore,

$$\frac{1}{2} (\rho_l + \rho_v) = \rho_c + b (t_c - t) \quad (97)$$

The parameters  $a$  and  $b$  are positive. This empirical equation holds over the whole liquid range, but is most commonly used to fit measurements of  $\rho_l$  and  $\rho_v$  from about  $50^\circ$  to  $3^\circ\text{C}$  below  $T_c$ , so as to obtain  $\rho_c$  by extrapolation. If, however, the critical density be calculated from the mean densities at low temperatures (say below the boiling-point) only, the error may be considerable. The critical densities for the following substances were therefore obtained by application of the law of rectilinear diameters to the data in the temperature range of  $50^\circ\text{C}$  below the critical temperature:

Acetone,  $\rho_c = 0.269$  gm/cc.

Benzene,  $\rho_c = 0.306$  gm/cc.

Chloroform,  $\rho_c = 0.491$  gm/cc.

Carbon Tetrachloride,  $\rho_c = 0.557$  gm/cc.

It was thought for a time that the critical volume could be directly determined by causing the disappearance of the meniscus to take place just at the top of the tube. It was, however, pointed out by Gouy (177) that, owing to the extreme compressibility of a substance at its critical point, the density of the column of fluid varies very considerably at different levels. The small hydrostatic pressure of the fluid above a

given level is quite sufficient to cause a considerable compression of the fluid below that level. The true critical density is the density of the fluid at the level where the meniscus has disappeared. Above that level the density is lower; below, it is higher. The mean density is equal to the true critical density when the meniscus disappears at about the centre of the column. This is a subjective observation. The matter is further complicated by the occurrence of opalescence phenomena in the neighborhood of the critical point. The method of the rectilinear diameter, whatever may be its theoretical basis, or lack of it, does in fact work rather well, if the true values of the orthobaric densities are known. Guggenheim (178) has shown that the coefficient  $b$  in equations (96) and (97) is close to  $(3\rho_c/4T_c)$  for the inert gases, neon, argon, krypton and xenon. The numerical factor is smaller than  $3/4$  for hydrogen and helium and a little larger for other gases.

According to the classical theory the co-existence curve has a rounded top which is quadratic in volume (24). The order of the curve depends on the order of the first non-vanishing derivative of  $P$  with respect to volume. The conditions which characterize the liquid-vapor critical point on the  $P$ - $V$ - $T$  surface for a pure substance are:

$$\left(\frac{\partial P}{\partial V}\right)_{T_c} = 0, \left(\frac{\partial^2 P}{\partial V^2}\right)_{T_c} = 0, \dots\dots\dots, \left(\frac{\partial^n P}{\partial V^n}\right)_{T_c} < 0. \text{ If the critical}$$

isotherm is to be a continuously differentiable function, thermodynamic stability requires  $n$  to be an odd integer in the first nonzero derivative (24). For a classical or van der Waals' fluid, the familiar value of  $n$  is 3. The thermodynamic similarities of single- and two-component systems have been discussed by Rice (25). The corresponding conditions for a critical-solution point in a two-component system may be expressed

as derivatives of the chemical potential with respect to mole-fraction.

There have been several experimental and theoretical investigations to find the order of the first nonvanishing derivative (25,51,58,59,61,179, to 187) which has been used as the criterion for determining the shape of the coexistence curve. From their measurements of the compressibility of xenon in the critical region, Habgood and Schneider (180) found the critical isotherm considerably flatter than that corresponding to a van der Waals' fluid. The function  $\left(\frac{\partial^2 P}{\partial V^2}\right)_{T_c}$  versus density has an inflection at or very near the critical density indicating that  $\left(\frac{\partial^4 P}{\partial V^4}\right)_{T_c}$  must vanish if the isotherm is continuous. The third derivative was shown to be small, and they suggested that it may also vanish. Zimm (51,179) from an analysis of his light-scattering data in the critical-solution region of the system perfluoromethylcyclohexane-carbon tetrachloride, found evidence that the third derivative of the chemical potential tends toward zero. When Edwards and Woodbury (182) first published and treated their data on the coexistent curves of helium near its critical temperature, they used the variables of reduced volume and reduced temperature. Recently Tisza and Chase (186) have re-examined the data of Edwards and Woodbury, using the variables of reduced density and reduced temperature. Tisza and Chase show that the use of the reduced density and reduced temperature leads to functions that are more linear and more coincident than when the reduced volume and reduced temperature variables are used. The same is true for a van der Waals' gas. From an analysis of their data Edwards and Woodbury found it necessary to modify slightly and extend the Landau-Lifshitz theory (181) of the properties of

a substance "near" the critical point to force agreement with their experimental data. This modified theory gave excellent agreement with their experimental values of the molar volumes of saturated helium-4 within about 0.001 degree of the critical temperature. This agreement is taken as evidence that  $\left(\frac{\partial^3 P}{\partial V^3}\right)_{T_c}$  is negative at the critical point -- in clear contradiction of theories which suggest that this derivative is zero at  $T_c$ . According to Landau and Lifshitz (181) the conditions  $\left(\frac{\partial P}{\partial V}\right)_T = 0$ ,  $\left(\frac{\partial^2 P}{\partial V^2}\right)_T = 0$  and  $\left(\frac{\partial^3 P}{\partial V^3}\right)_T < 0$  hold at the critical point. The fact that the third derivative is negative has never been shown experimentally except for Edwards and Woodbury's work which might be a particular quantum effect. Rowlinson (22) has suggested that the second derivatives  $\left(\frac{\partial^2 V}{\partial x^2}\right)$  and  $\left(\frac{\partial^2 H}{\partial x^2}\right)$  should both vanish at the critical-solution point. Scott (188) quotes calorimetric measurements on the system  $n - C_6H_{14} + n - C_6F_{14}$  to support this conclusion. Dunlap and Furrow (61) report that their data show this tendency but the condition is not firmly resolved. They further say that the third derivatives, however, clearly vanish. By analogy with the vanishing of the third derivatives for the volume and enthalpy of mixing at or near the critical-solution point, they conclude that  $\left(\frac{\partial^3 P}{\partial V^3}\right)_{T_c}$  for a single component system also vanishes. Therefore, it cannot be definitely concluded whether the first four derivatives of pressure with respect to volume (at constant temperature) vanish at the critical point or not, but it seems reasonable to assume that the first two derivatives actually do vanish whereas the vanishing of the third and fourth is probable. The measurement of the critical constants by finding the point of zero slope and of inflection on the



critical isotherm is therefore difficult, as was discussed in detail in Chapter I.

It has been shown repeatedly (21,145,178 and 189 to 192) that the variations of both orthobaric densities with temperature are represented by a leading term proportional to  $(T_c - T)^{1/3}$ , not  $(T_c - T)^{1/2}$ . A coexistence curve of this type was first proposed by Goldhammer (189) in 1910 and has more recently been used to good advantage by others (21,145,178,192). Experimentally it has been found by these investigators that the difference  $(\rho_v - \rho_l)$  varies as the cube-root of  $(T_c - T)$  in the neighborhood of the critical point, so that neither the square nor the fourth-root corresponds to the facts. In order to show that the principle of corresponding states applied to two-phase equilibrium between liquid and vapor, Guggenheim (193) plotted the reduced temperature versus the ratio  $\frac{\rho}{\rho_c}$  of the density  $\rho$  of either coexisting phase to the critical density,  $\rho_c$ . The curve drawn had the remarkably simple formula

$$\frac{\rho}{\rho_c} = 1 + \frac{3}{4} \left(1 - \frac{T}{T_c}\right) \pm \frac{7}{4} \left(1 - \frac{T}{T_c}\right)^{1/3} \quad (98)$$

where the plus sign referred to the liquid and the minus sign to the vapor. A large amount of experimental evidence has shown that, for binary liquid mixtures close to the critical solution region, the coexistence curves are cubic, i.e.,

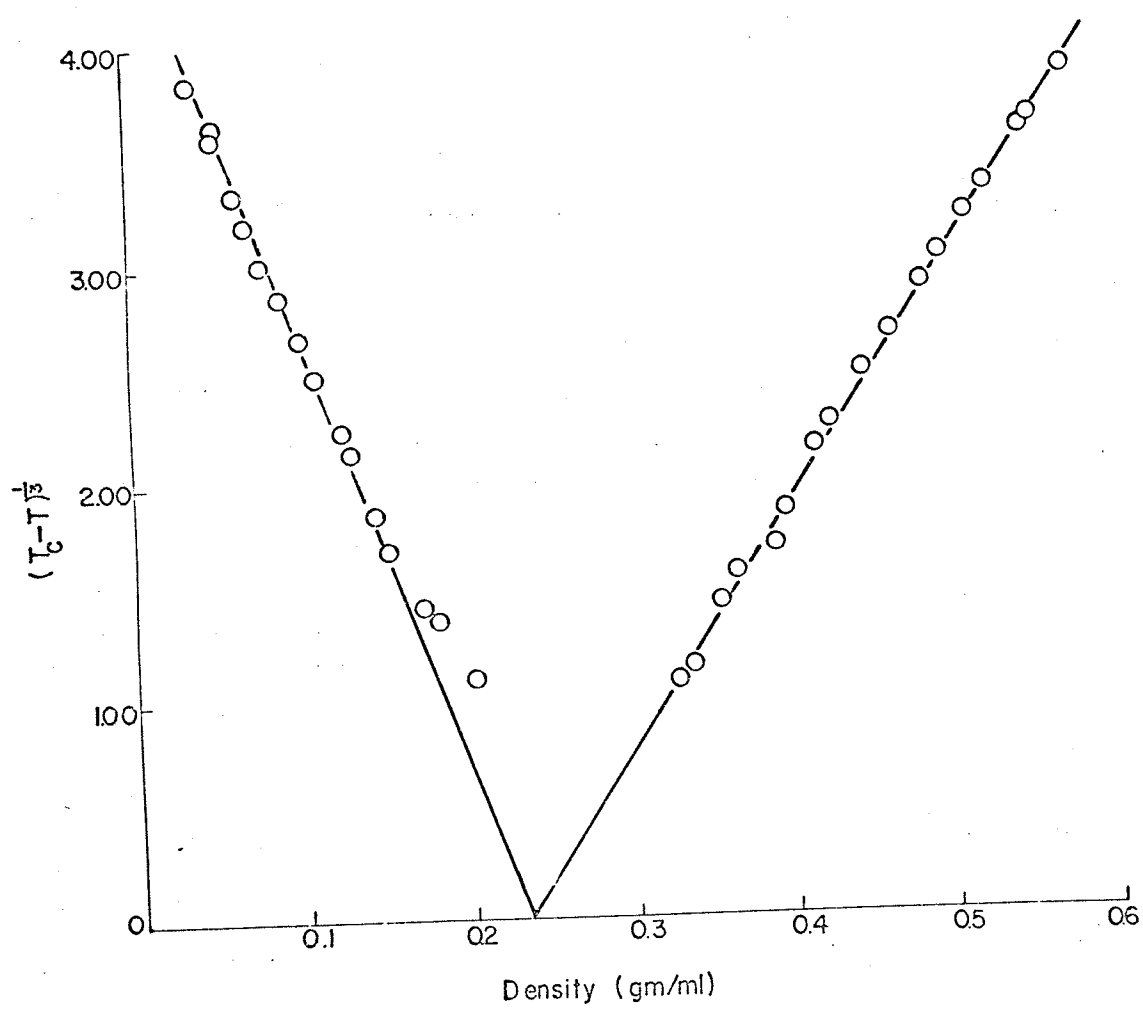
$$(x' - x'') = k (T_c - T)^{1/3} \quad (99)$$

where  $(x' - x'')$  is a measure of the difference between coexisting phases. Campbell and Kartzmark (145) carried out investigation of several systems across the complete range of composition and obtained two straight lines,

presumably intersecting at  $(T_c - T) = 0$  and at the critical composition. Work on some systems (53), for example, suggests that this relation does not hold at temperatures very close to the critical solution temperature, and in this region, the coexistence curve has a flat top. For some other systems Kreglewski (194) found a fractional power other than  $1/3$  as the temperature approached the critical solution temperature. He suggests that the coexistence curve will always appear to be very flat, but whether it is truly horizontal is doubtful. The outstanding experimental work of Thompson and Rice (49) referred to in Chapter I, demonstrates that the coexistence curve follows a cubic relation to within  $0.0001^\circ\text{C}$  of the critical solution temperature with no evidence of an apparent flat region. This means that the nose of the curve representing, say, congruent concentrations in  $L_1 \rightleftharpoons L_2$  critical phenomenon, or orthobaric densities in  $L \rightleftharpoons V$  equilibrium, is probably rounded but appears flat due to the limitation of experimental conditions and the question reduces to whether or not the curve is flatter than the cubic relation requires (173). Recent work of Campbell and Kartzmark (145) might be taken to demonstrate that some systems yield two straight lines intersecting at the critical solution temperature, while others, which also present two straight lines, show a gap at the critical solution temperature, when the two congruent concentrations are plotted against  $(T_c - T)^{1/3}$ . On this basis, the systems showing a gap on the  $(T_c - T)^{1/3}$  plot should represent those systems having a horizontal nose on the usual composition versus temperature plot. I share their suspicion and quote from their publication, "We are doubtful, however, whether this conclusion is justified".

Lorentzen (44) confirmed the  $(T_c - T)^{1/3}$  law to within  $0.014^\circ\text{C}$  of the critical temperature of carbon dioxide in a vertical tube, that is, under conditions where Schneider (21) found a flatter, but still rounded, curve. To be exact, he used an exponent of 0.357 and not  $1/3$ , as this was the value suggested earlier by Michels et al. (195) for carbon dioxide. The difference between these exponents would be within experimental error, at a temperature so close to the critical point. The straight lines obtained in the cube-root plot for acetone, benzene, chloroform and carbon tetrachloride are shown in Figures 19 to 22 with the corresponding data reported in Tables V to VIII. One would expect these straight lines to intersect at the critical volume, at the critical temperature. Work by Campbell and Kartzmark (145) on the analogous critical phenomenon,  $L_1 \rightleftharpoons L_2$ , indicates that this is not always the case. When, however, the  $(T_c - T)^{1/3}$  relation is obeyed, the slope of the P versus V curve, in the neighborhood of  $T_c$ , will be very slight. The crux of the problem therefore is: is the slope of the curve, near  $T_c$ , less than that predicted by the  $(T_c - T)^{1/3}$  relation? If it is, the existence of a horizontal might be conceded. To settle the point experimentally, materials of the highest purity must be used and the temperature controlled with great accuracy, say to  $\pm 0.001^\circ$ . My temperature control was only good to  $\pm 0.03^\circ$  and therefore my conclusions are only valid to this extent. Thus, for example, while I am in a position to say that, although at a temperature of  $(T_c - 0.03^\circ)$  two different phases of distinctly different orthobaric volumes are detectable, at a temperature  $0.03^\circ$  higher no meniscus is detectable in an ordinary telescope: an interferometer technique might, and probably

FIGURE 19. Plot of  $d_\ell$  and  $d_v$  versus  $(T_c - T)^{1/3}$  for Acetone.



Plot of  $d_l$  and  $d_v$  vs.  $(T_c - T)^{1/3}$  for Acetone

FIGURE 20. Plot of  $d_l$  and  $d_v$  versus  $(T_c - T)^{1/3}$  for Benzene.

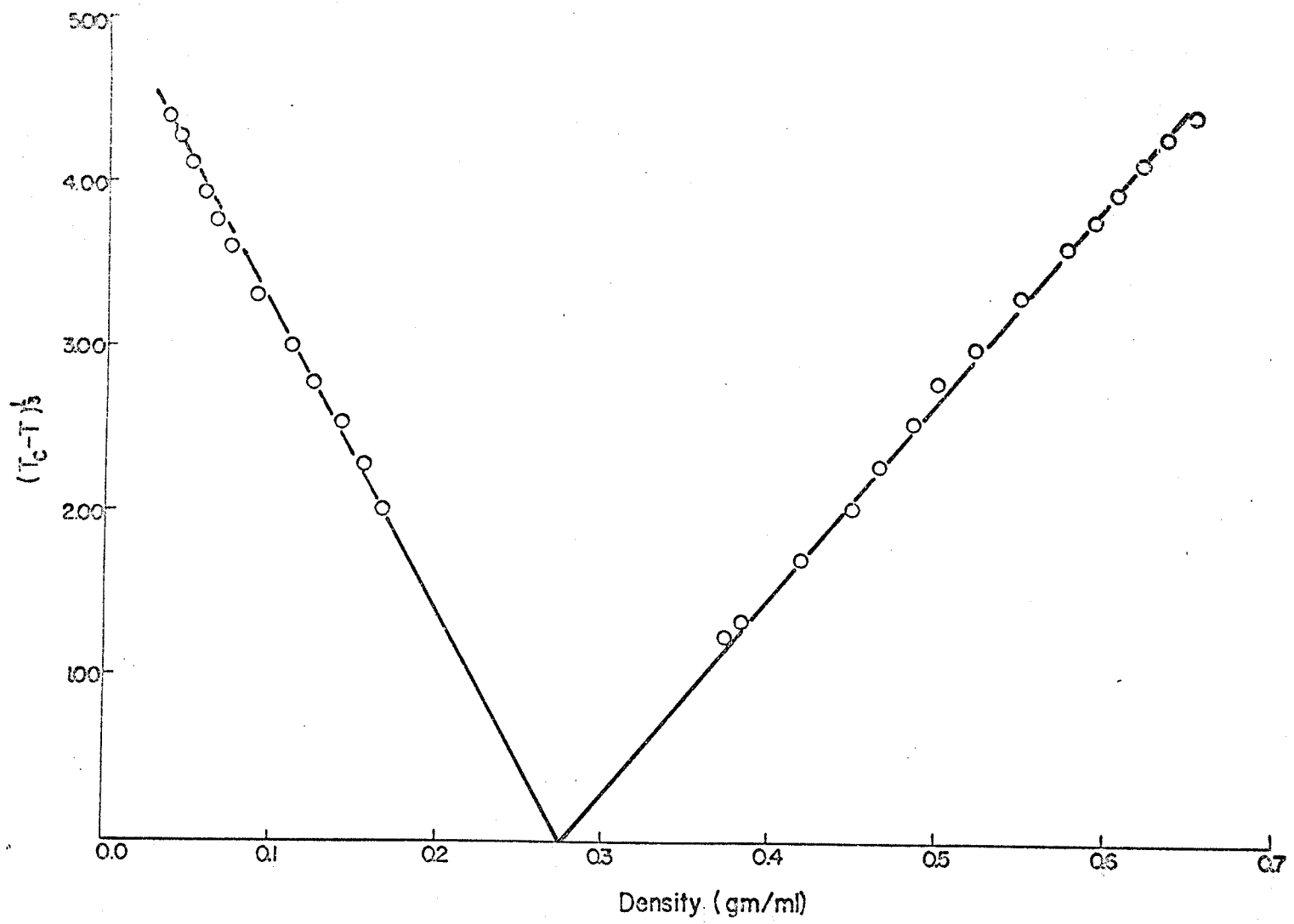
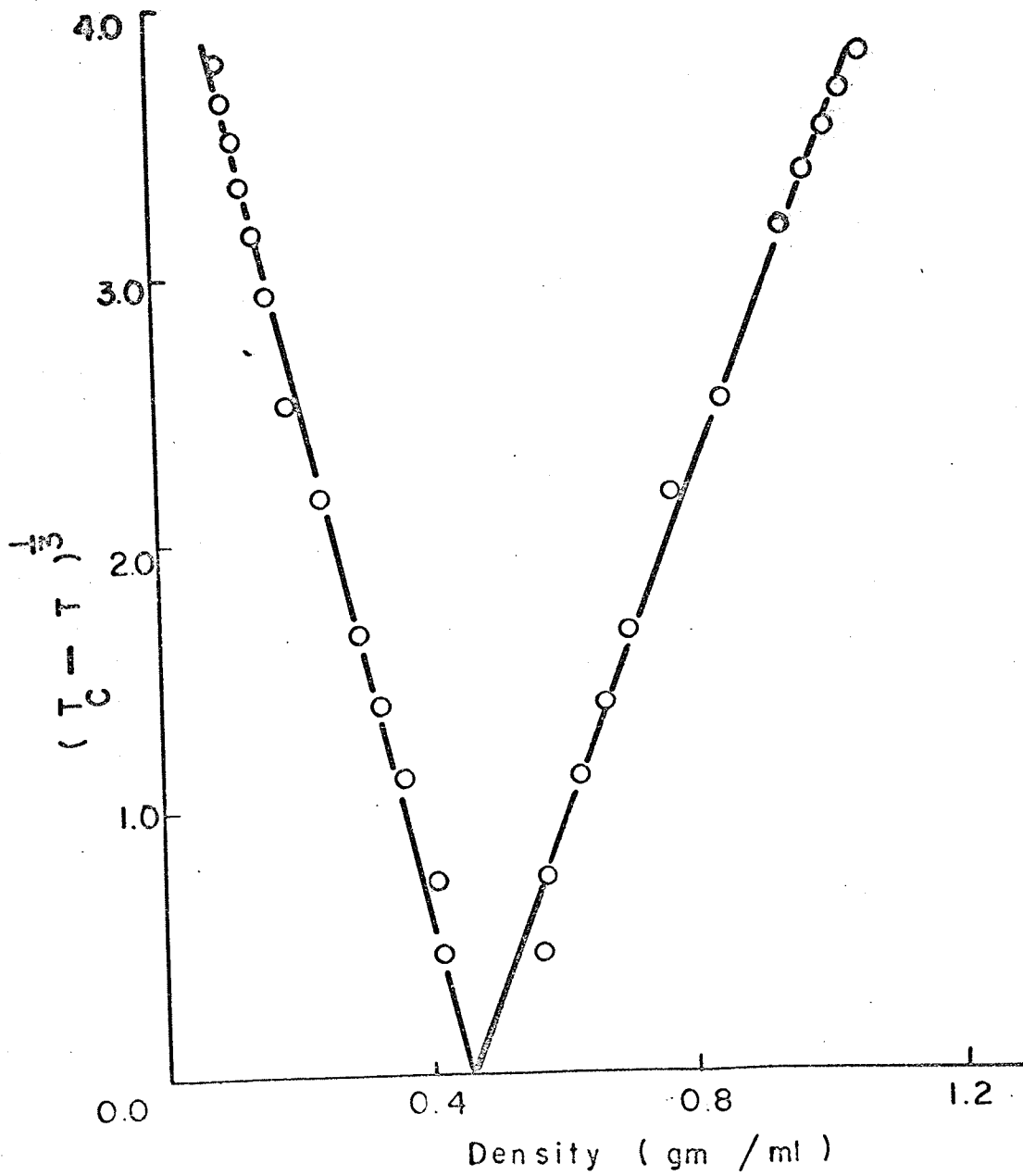


Fig. Plot of  $d_l$  and  $d_v$  vs.  $(T_c - T)^{1/3}$  for Benzene.

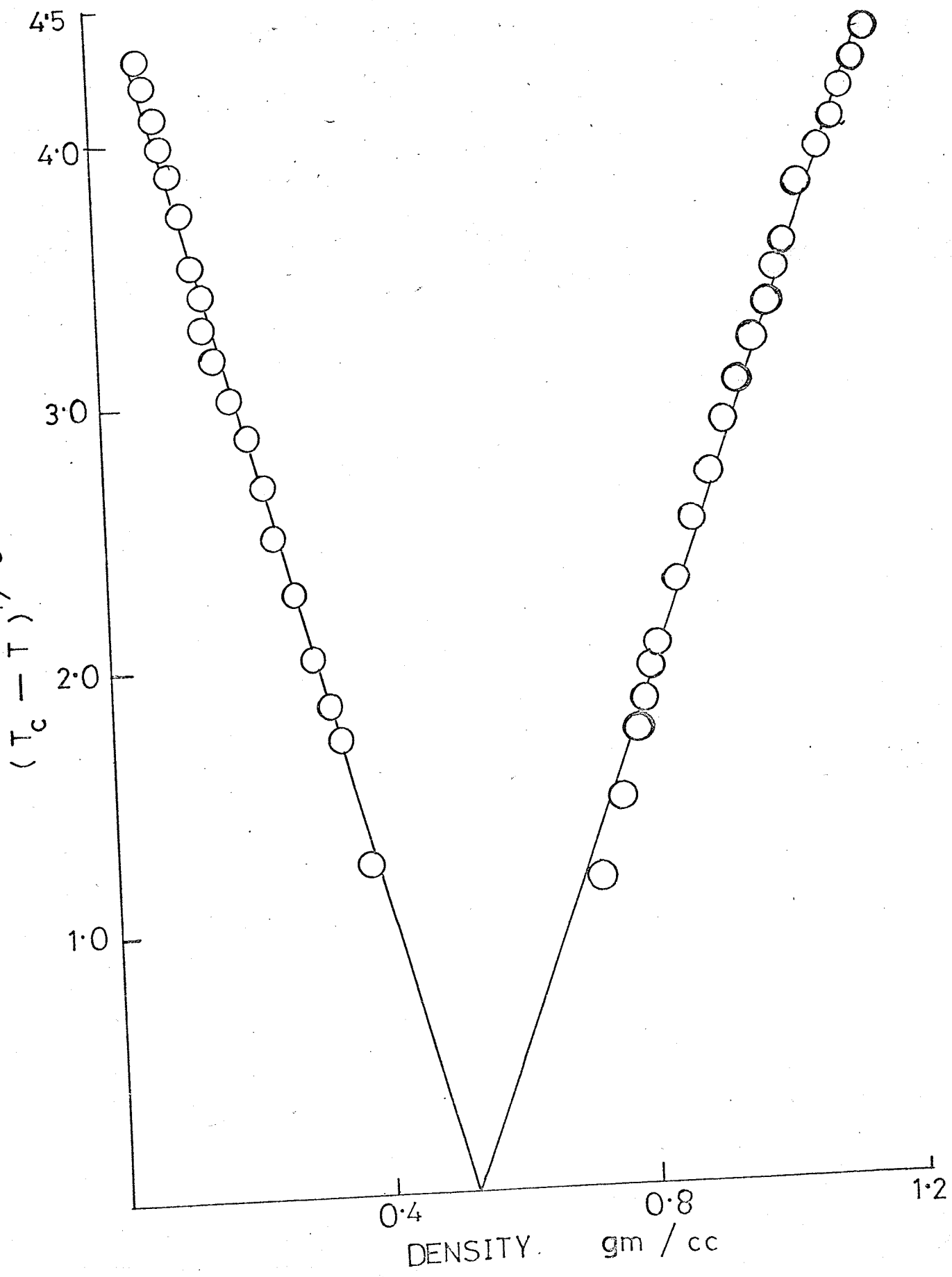
FIGURE 21. Plot of  $d_\ell$  and  $d_v$  versus  $(T_c - T)^{1/3}$  for Chloroform.





Plot of  $d_l$  and  $d_v$  vs  $(T_C - T)^{\frac{1}{3}}$  for  $\text{CHCl}_3$

FIGURE 22. Plot of  $d_\ell$  and  $d_v$  versus  $(T_c - T)^{1/3}$  for Carbon Tetrachloride.



would, reveal differences in refractive index with differences in height which however will not prove anything. In the case of the  $L \rightleftharpoons V$  critical point, certain characteristic phenomena, such as the occurrence of fluctuating striae, are usually considered peculiar to the critical volume. This has never been proved, however, and even if it is found that such phenomena can be observed over a range of volume, their occurrence proves nothing. The point in which I am interested is whether or not a horizontal really exists at the temperature of disappearance of the meniscus. It would mean experimentally that, at the temperature of disappearance of the meniscus, there is a demonstrable difference in orthobaric volumes of liquid and vapor. It has been pointed out in Chapter I that Rice (25) arrived at the conclusion that the area of heterogeneity is bounded at the top by a horizontal straight line at  $T_c$  (identified by him with  $T_m$ ), i.e. there is no such thing as a critical volume but discrete orthobaric volumes of liquid and vapor exist, even at the critical temperature. This means that critical phenomena (fluctuating striae, sharp disappearance of the meniscus, etc.) will be observed over a range of total volume of the system. It is notorious among workers (20,50,173,196,197) in this field that this is so, although this does not necessarily establish Rice's point of view of associating molecules in the process of condensation of vapor to liquid. Though I have observed critical phenomena over a finite density range for all the pure substances I have investigated, it cannot be concluded that the top of the observable coexistence curve is horizontal over a finite density range. I believe that if hydrostatic and gravitational effects are taken into account, the classical van der

Waals isotherm can account for a large portion of the flat-top co-existence curves observed in this work (vertical sealed-tube technique). In any case, at the present time it is not possible to resolve the problem since, even if the temperature is controlled to the extent that Thompson and Rice (49) did for their measurements, it can always be argued that a better temperature control will yield better "roundness" of the curve. This problem cannot be solved unambiguously by direct experimental study since in practice it is impossible to distinguish between a straight line and a curve of high degree or even a parabola with a high parameter.

No attempt has been made in this work to recheck the power  $1/3$ . The validity of the cubical relation has frequently been confirmed (21, 145, 178, 189 to 192), despite the lack of rigidity in its deduction. Others have proposed a power other than  $1/3$  on the basis of theoretical and sometimes experimental considerations, for example, Fisher (39) has suggested a power of  $5/16$  (or  $0.31250$ ). I have found no need in this work for such a relationship since the difference between these exponents would be within my experimental error, and in any case my arguments do not depend to any extent on the validity of the cube-root law.

It is interesting to note that in an attempt to deduce the exponent of the critical isotherm,  $\delta$  in Table I, Scott (page 25, reference 22) plotted data on mixtures of  $\text{CF}_4 + \text{C}_2\text{H}_6$ , at about  $0.5^\circ$  above the critical solution temperature and obtained a very flat vapor pressure curve consistent with an exponent  $\delta = 4$ . He further suggested that it would not be difficult to make the data consistent with the exponent  $\delta = 5$ .

The different values of the critical exponents which fit well the measurements of the phase boundaries suggest that the behavior close to a critical point is insensitive to the detailed nature of the intermolecular forces. It may however be observed that any value of the exponent  $\beta$  between  $\frac{1}{2}$  and  $\frac{1}{4}$  is inconsistent with the assumption that the critical point is a nonsingular point of the free energy in the sense discussed in the introduction (Chapter I).

Be that as it may, the observed fact remains that, at the critical temperature, the meniscus disappears sharply in the body of the liquid, with accompanying phenomena usually described as "critical", over a rather extensive range of total density (or volume) for all the four pure compounds. It is an old observation, however, which has recently been reaffirmed by Lorentzen (44) that the disappearance of the meniscus in the body of the tube (and not by "moving out", as Lorentzen calls it) is not confined to the critical volume. Therefore, in conclusion, it may be said that this observation does not necessarily prove that the nose of the curve of orthobaric densities versus temperature is horizontal, as explained earlier.

A point which needs further clarification is the way in which I obtained critical densities for the pure substances in a recent publication (173). The critical density was obtained by extrapolation of plots of  $\rho_l$  and  $\rho_v$  against the cube root of  $(T_c - T)$ , with the result that my values are much lower for the three compounds I have reported, than those reported by other workers (Table IV). The methods of obtaining critical densities by extrapolation are empirical, so that it could be argued that other methods than those currently in use are equally valid.

The cube-root plot of the orthobaric densities should identically converge at the critical volume, at the critical temperature. That this is not generally true is evident from the difference in values of critical densities obtained by application of rectilinear diameter. Benson and Copeland (198) have reported that a virial expansion of the equation of state around the critical point could be used to derive an equation of the form  $\frac{\rho_v}{\rho_c} + \frac{\rho_l}{\rho_c} - 2 = k \left(1 - \frac{T}{T_c}\right)$ . A less detailed derivation has been shown (181,199) to lead to a similar relation with  $k = 0$ . Interestingly enough, if the sums of the experimentally observed specific volumes of coexistent liquid and vapor are plotted against temperature, the points fall on an excellent straight line for data within about 15-30°C of the critical temperature. Below a reduced temperature of 0.95, this sum of coexistent volumes begins to show deviations from the straight line relation. The law of rectilinear densities, which seems to be obeyed experimentally over a much greater range of temperatures, is of course inconsistent with the law of rectilinear volumes presented in their publication. The two laws appear to coincide within the accuracy of the data only if the temperature coefficient  $k$  is zero or very small.

A much more disturbing feature of the two laws however is that if the coexistent volumes are extrapolated to the critical temperature, the reciprocal of the intercept is not the same as that obtained from the intercept given by the law of rectilinear densities. It has been observed that the density predicted by the law of rectilinear densities is about four percent higher for most substances than that given by the law of rectilinear volumes. This is beyond the experimental errors

in the determinations. There are no convincing theoretical or experimental arguments available by which this anomaly can be resolved in favor of one or the other extrapolation methods. There is a possibility that one or both of these extrapolation methods is incorrect. The method used by Campbell and myself (173) has never been attempted by any other investigator. However, since I have chosen a different method of extrapolation in the publication (173), I think I should make it clear that it is the method, and not the values on which it is based, that leads to an answer different from those to be found in the literature (Table IV). In any case, I have now revised the values of critical densities for those three pure compounds by applying the law of rectilinear densities as tabulated earlier. The revised values agree very well with the literature values. My orthobaric volume data for benzene have been processed by Ambrose (200) and I quote from his letter, "We have processed your values for benzene by our standard programme to obtain the critical density from the law of rectilinear diameters, and to fit equations for the variation in  $(\rho_l + \rho_v)$  and  $(\rho_l - \rho_v)$  as power series in  $(T_c - T)$  and  $(T_c - T)^{1/3}$  respectively. From this we find your results give us a critical volume of 0.306 g./cc, in very close agreement with the values of Young and of Bender, Furukawa and Hyndman. In fact, the agreement throughout the whole range of your experimnts with those of Young is very good".

Recently, Davis and Rice (60) have proposed a method to determine the critical constants  $\rho_c$ ,  $T_c$  and  $P_c$  based on a set of assumptions which are subject to further verification. They suggest that two different Taylor series for pressure are required to account for a cubic-coexistence



curve and for behavior in the "Vapor" and "Liquid" single-phase regions (see Page 22, Chapter I, this thesis). In spite of the apparent agreement of their treatment with the experimental facts, it is still entirely possible that no ordinary Taylor series is valid anywhere near the critical point. They have suggested a method of determining the critical density by means of saturation densities alone, avoiding the data or observations of the critical temperature made by watching the meniscus disappear in the critical region. They found that plots of  $(\rho_l + \rho_v)$  versus  $(\rho_l - \rho_v)^3$  were straight lines over a substantial range and the intercept of such a straight line was taken as twice the critical density. This method was first dealt with by Goldhammer (189) in 1910, but it seems to have escaped the attention of the modern investigators. It has the advantage of allowing computation of the critical density without regard to a temperature scale or the choice of a critical temperature. Once critical densities are obtained in this way, critical temperatures can be ascertained by the law of rectilinear diameters. Since the method used by Rice and Davis is not based on exact relationships, the critical constants derived from them cannot be expected to be exact, even if the experimental error in orthobaric densities were vanishingly small. In view of this argument, I have not attempted plotting my data by their method.

#### I(b). Density

Density curves of coexisting liquid and vapor phases of pure substances are generally of the form shown in Figures 8 to 11. To increase the accuracy of the rectilinear diameters, quadratic equations have been used by Young (65). The relation serves to detect discrepancies in observed data. The curvatures of the density curves increase rapidly

in the region approaching the critical temperature. Francis (201, 202), in a comprehensive study of the density-temperature relationship of a pure compound, showed that the saturated density of the liquid phase, ( $\rho_l$  i.e. under its own vapor pressure), as a function of temperature in degrees centigrade,  $t$ , can be expressed by the four-constant empirical equation

$$\rho_l = A + Bt + \frac{C}{E - t} \quad (100)$$

In this equation  $A$  is a constant, generally about 0.06 higher than the density at 20°C;  $B$  is the slope coefficient, a little lower than the expansion coefficient at ordinary temperature;  $C$  is an integer, generally from 6 to 10; and  $E$  is a number generally 34°C above the critical temperature. In a test of its applicability to hydrocarbons, Francis (201) and Kay (203) found a reasonably good fit of the experimental data.

There are two distinct and not necessarily compatible reasons for fitting an equation to data. One is simply to reduce the space required for presenting the information; in this case the best fit possible with the equation is desired. The other reason is to permit extrapolation from the data. In this case a best fit to the experimental data does not necessarily yield the best coefficients unless all the data are of equally excellent quality and the equation is an accurate model of the phenomenon. In correlating the density data I have omitted the observations which are within 5°C of the critical temperature. The four constants in the equation were evaluated for all four pure compounds with the aid of an IBM 360/65 electronic computer, using a multiple regression method of analysis. The values of the constants and of the calculated densities are given in Tables V through VIII and XVII.

It will be noted that in most instances the calculated liquid densities are within 0.0010 gm/cc of the experimental values listed in the tables, which correspond with the experimental uncertainty of the data. According to Francis, the constant C is an integer but it will be noted that my values of constant C are not necessarily integral. Kay's analysis (203) of liquid densities of the isomeric heptanes and isomeric octanes yielded real values for C consistent with the results obtained in this work.

The statistical analysis of the liquid density correlation is given in the following table (Table XVII). The coefficients were determined by the matrix inversion method of least squaring. The low values of standard deviations for the coefficients suggest that the coefficients are highly significant (204). The multiple correlation coefficient in each case is overwhelmingly significant. All the datum points were given equal weight of 1.

TABLE XVII

STATISTICAL ANALYSIS OF EQUATION (100)

Acetone

<u>COEFFICIENTS</u>	<u>STANDARD DEVIATION</u>
A = 0.840081	0.0
B = $-0.961206 \times 10^{-3}$	$0.186739 \times 10^{-4}$
C = -9.04112	0.124244
E = 269.0	0.0
Multiple Correlation Coefficient = 0.999894	
Standard Error of Estimate = $0.141144 \times 10^{-2}$	

TABLE XVII (Cont'd.)

STATISTICAL ANALYSIS OF EQUATION (100)Benzene

<u>COEFFICIENTS</u>	<u>STANDARD DEVIATION</u>
A = 0.934348	0.0
B = $-0.102571 \times 10^{-2}$	$0.958163 \times 10^{-5}$
C = -8.52229	$0.914741 \times 10^{-1}$
E = 323.0	0.0
Multiple Correlation Coefficient = 0.999920	
Standard Error of Estimate = $0.132441 \times 10^{-2}$	

Chloroform

<u>COEFFICIENTS</u>	<u>STANDARD DEVIATION</u>
A = 1.87908	0.0
B = $-0.324651 \times 10^{-2}$	$0.406807 \times 10^{-4}$
C = $-0.125809 \times 10^2$	0.337744
E = 297.0	0.0
Multiple Correlation Coefficient = 0.999875	
Standard Error of Estimate = $0.374888 \times 10^{-2}$	

Carbon Tetrachloride

<u>COEFFICIENTS</u>	<u>STANDARD DEVIATION</u>
A = 1.69534	0.0
B = $-0.191825 \times 10^{-2}$	$0.189715 \times 10^{-4}$
C = $-0.145197 \times 10^2$	0.169265
E = 317.0	0.0
Multiple Correlation Coefficient = 0.999907	
Standard Error of Estimate = $0.267937 \times 10^{-2}$	

I(c). Vapor Pressure

The purpose of fitting vapor pressure data to an analytical equation over the complete range between boiling and critical points is obvious. The thermodynamically exact Clapeyron equation (equation 16, Chapter I) yields with certain assumptions the simplest theoretical relation

$$\log P = A - \frac{B}{T} \quad (101)$$

where A and B are empirical constants. This is the Clausius-Clapeyron equation which predicts that a plot of  $\log P$  versus  $\frac{1}{T}$  is a straight-line. It is well-known that this is not so because (i)  $\Delta H$  is not independent of T, (ii) liquid volume cannot be neglected, and (iii) the vapor is not an ideal gas, at conditions even slightly removed from ordinary temperatures.

In an extensive survey of experimental vapor pressure data for the saturated hydrocarbons, Thodos (205) has pointed out that the plot of  $\log P$  versus  $\frac{1}{T}$  is not quite linear but really S shaped with a reversal of curvature at an inflection point which for most substances occurs at a reduced temperature of about 0.80 or 0.85. The effective reversal of the logarithmic vapor pressure curves becomes conspicuous when a graphical residual method is applied. The deviation of the logarithm of the experimental vapor pressure from the calculated value, at a given temperature, is defined as the graphical residual. The calculated value may be obtained from a simple vapor pressure equation such as that represented in equation (101) and a straight line may be drawn between two reference points such as the boiling and critical points. This

serves the purpose of checking the self-consistency of the results. Although the vapor pressure relationship is well defined by this method near the critical point, it fails considerably in accuracy at lower vapor pressures. I have, therefore, not attempted any representation of my data by this method. Waring (206) has suggested a criterion for a qualitative test for the suitability of various vapor pressure equations. From the Clapeyron equation he has derived a thermodynamically exact equation

$$\frac{\Delta H}{\Delta Z} = -R \frac{d \ln P}{d(1/T)} \quad (102)$$

where  $Z$ , the compressibility factor is defined as usual by  $\frac{PV}{RT}$ . Then the reproducibility of the curvature of  $\log P$  versus  $1/T$  is provided by the form of the curve for  $\Delta H/\Delta Z$  as a function of temperature. In the region below a reduced temperature of 0.80 or 0.85 (which is the temperature of minimum  $\Delta H/\Delta Z$ ), the first temperature derivative of  $\Delta H/\Delta Z$  must be negative and the second derivative positive. Equations which do not lead to this should in general not be used for extrapolation, although they may be used satisfactorily for interpolation of experimental data. At temperatures above  $T_R = 0.85$ , the first and second derivatives must both be positive. Approaching the critical point  $\Delta H/\Delta Z$  remains finite although  $\Delta H$  and  $\Delta Z$  separately tend to go to zero. In view of this analysis by Waring, vapor pressure equations should be very carefully selected to fit the experimental data. Recently Ambrose et al. (207) have chosen the following equations for their study

$$\text{Cox (208), } \log_{10} P = A \left[ 1 - (T_b/T) \right] \quad (103)$$

$$\text{where } \log_{10} A = \log_{10} A_c + E(1 - T_R)(0.85 - T_R)$$

$$\text{Cragoe (209), } \log_{10} P = A + B/T + CT + DT^2 \quad (104)$$

$$\text{Frost-Kalkwarf (210), } \log_{10} P = A + B/T + C \log_{10} T + DP/T^2 \quad (105)$$

In the above equations A, B, C, D, and E are constants, T is the temperature in ( $^{\circ}\text{K}$ ),  $T_R$  the reduced temperature,  $T_b$  the temperature of the normal boiling point, and  $A_c$  the value of A at the critical point for equation (103). In addition to these three four-constant equations Ambrose et al. (207) have also used a seven-constant equation for representing their vapor pressure data. For very few substances are data of sufficient precision available over a wide enough pressure range to require more than four parameters. This is confirmed from their conclusion that their seven-constant equation was only slightly better than the Frost-Kalkwarf equation over the whole temperature range, except for the range  $T_R$  0.95 - 1.00, where the seven-constant equation gave a markedly better fit than equation (105). I have preferred to fit my data for four pure compounds to the Frost-Kalkwarf equation which is a semi-theoretical equation. This vapor pressure equation has received considerable attention because of its ability to account for the vapor pressure between the boiling point and the critical point, the range in which I am interested in this work. In this semi-theoretical equation, the slight reverse curvature in the plot of  $\log P$  versus  $\frac{1}{T}$  is explained on the basis of the nonideal behavior of the vapor, together with the change in heat of vaporization with temperature. If it is assumed that  $\Delta H$  is linear with T and that the van der Waals  $a/V^2$  term is a first approximation to the deviation from the ideality, equation (105) is obtained by integration of the Clapeyron equation (equation 16, Chapter I). In equation (105), A, B,

and C are empirical constants, B and C being negative, and D is related to van der Waals a by

$$D = \frac{a}{2.303R^2} \quad (106)$$

Thodos has shown that the van der Waals constant "a" is given by equation (95). Thus, for the general case applicable to equation (105),  $D = \frac{27}{64 \times 2.303} \times \frac{T_c^2}{P_c} = 0.18318 T_c^2/P_c$ . The evaluation of constants A, B, and C has been carried out by multiple regression analysis. The statistical analysis of the coefficients is given in Table XVIII, which lists the values of the coefficients, the standard deviations in their estimation, and the values of the multiple correlation coefficient, etc. The regression coefficients are highly significant and the correlation coefficient in each case is overwhelmingly significant. The calculated values of the vapor pressure for each substance from equation (105), and using constants given in Table XVIII, are tabulated along with the experimentally observed values in Tables IX through XII. The agreement with the observed values is fairly good for benzene, acetone and carbon tetrachloride. Chloroform data seem to scatter, specially at high temperatures, as evidenced by the large values of  $\Delta P = P(\text{obs.}) - P(\text{calc.})$ , which are tabulated in the sixth column of these tables. This is probably due to the decomposition of this compound near the critical temperature (see p. 79, Chapter III). For this reason, no attempt was made to fit the vapor pressure data of chloroform to either Cox or Cragoe equations. The analysis of data for benzene and carbon tetrachloride with Cox and Cragoe equations has been done by Dr. J. F. Counsell (211) of the National Physical Laboratory, England with the aid of a digital computer (KDF9). The results are shown in Tables XIX and XX.



In columns 5 and 7 of these tables are tabulated the values of  $\Delta P$ .

TABLE XVIII

STATISTICAL ANALYSIS OF THE COEFFICIENTS OF EQUATION (105)

Acetone

<u>COEFFICIENTS</u>	<u>STANDARD DEVIATION</u>
A = $0.261062 \times 10^2$	0.0
B = $-0.269100 \times 10^4$	$0.948664 \times 10^2$
C = -7.14004	0.497585
D = 1007.0	0.0
Multiple Correlation Coefficient = 0.999897	
Standard Error of Estimate = $0.427330 \times 10^{-2}$	

Benzene

<u>COEFFICIENTS</u>	<u>STANDARD DEVIATION</u>
A = $0.131489 \times 10^2$	0.0
B = $-0.195618 \times 10^4$	$0.494399 \times 10^2$
C = -2.96899	0.248025
D = 1200.0	0.0
Multiple Correlation Coefficient = 0.999933	
Standard Error of Estimate = $0.416288 \times 10^{-2}$	

Chloroform

<u>COEFFICIENTS</u>	<u>STANDARD DEVIATION</u>
A = $0.220199 \times 10^2$	0.0
B = $-0.24567 \times 10^4$	$0.137857 \times 10^2$
C = -5.82143	$0.706142 \times 10^{-1}$
D = 1001.0	0.0
Multiple Correlation Coefficient = 0.999997	
Standard Error of Estimate = $0.756441 \times 10^{-3}$	

TABLE XVIII (Cont'd)

STATISTICAL ANALYSIS OF THE COEFFICIENTS OF EQUATION (105)Carbon Tetrachloride

<u>COEFFICIENTS</u>	<u>STANDARD DEVIATION</u>
A = 0.182145 x 10 <sup>2</sup>	0.0
B = -0.226846 x 10 <sup>4</sup>	0.794815 x 10 <sup>2</sup>
C = -4.61431	0.397608
D = 1260.0	0.0
Multiple Correlation Coefficient = 0.999842	
Standard Error of Estimate = 0.646184 x 10 <sup>-2</sup>	

The sum of residuals squared is also given at the end of Tables XIX and XX. The values of the standard error of estimate, are reported at the end of Tables IX through XII, which is defined in the usual way:

$$\text{Standard deviation} = \left[ \frac{1}{N-1} \sum_1^N (P_{\text{obs.}} - P_{\text{calc.}})^2 \right]^{\frac{1}{2}}$$

where N is the number of measurements. The units of pressure and temperature are given at the top of the individual column (1 atm. = 760 mm. Hg and (°K) = (°C) x 273.15). As has been discussed in Chapter III, the observed pressure in the static method was calculated from the equilibrium volume of air in the manometer by using van der Waals' equation. Other equations of state gave variations within the experimental error. Thus, using the Beattie-Bridgman equation, at 288.50°, i.e. 0.45° below the critical temperature of benzene, the pressure calculated by van der Waals was 3636.7 cm Hg, by Beattie-Bridgman 3651.2 cm Hg, while the experimental figure of Bender, Furukawa, and Hyndman (much the best figure) is 3641.0. The maximum error of

TABLE XIX

TREATMENT OF VAPOR PRESSURE DATA FOR BENZENE BY  
COX AND CRAGOE EQUATIONS

Constants for the Cox Equation (103)      Constants for the Cragoe Equation (104)

log  $A_c$  = 0.6408  
 E = -0.2445  
 $T_b$  = 346.10  
 $T_c$  = 657.60

A = +2.217305<sub>10</sub> +0  
 B = -7.035734<sub>10</sub> +2  
 C = +1.005633<sub>10</sub> -2  
 D = -6.508827<sub>10</sub> -6

Sample	T OBS (°K)	P OBS (mm Hg at 0°C)	P COX	DELTA P	P CRAGOE	DELTA P
1	379.400	1737.00	1739.75	-2.75	1743.16	-6.16
2	382.550	1895.00	1870.68	+24.32	1873.54	+21.46
3	386.900	2067.00	2064.73	+2.27	2066.81	+0.19
4	390.200	2225.00	2222.72	+2.28	2224.20	+0.80
5	394.000	2412.00	2416.79	-4.79	2417.59	-5.59
6	395.950	2555.00	2521.64	+33.36	2522.09	+32.91
7	398.950	2705.00	2690.18	+14.82	2690.11	+14.89
8	404.950	2987.00	3054.89	-67.89	3053.82	-66.82
9	411.300	3436.00	3483.71	-47.71	3481.68	-45.68
10	413.000	3546.00	3606.43	-60.43	3604.17	-58.17
11	419.400	4108.00	4100.23	+7.77	4097.20	+10.80
12	420.750	4217.00	4211.05	+5.95	4207.88	+9.12
13	425.400	4616.00	4611.37	+4.63	4607.80	+8.20
14	428.050	4878.00	4852.85	+25.15	4849.11	+28.89
15	433.500	5377.00	5381.32	-4.32	5377.39	-0.39
16	436.750	5738.00	5717.73	+20.27	5713.77	+24.23
17	443.600	6517.00	6481.61	+35.39	6477.89	+39.11
18	444.650	6626.00	6605.53	+20.47	6601.88	+24.12
19	450.700	7391.00	7356.52	+34.48	7353.45	+37.55
20	451.650	7480.00	7480.32	-0.32	7477.37	+2.63
21	456.350	8101.00	8117.08	-16.08	8114.85	-13.85
22	458.850	8443.00	8472.67	-29.67	8470.89	-27.89
23	463.150	9099.00	9112.63	-13.63	9111.76	-12.76
24	467.650	9872.00	9822.00	+50.00	9822.24	+49.76
25	469.550	10158.00	10134.04	+23.96	10134.81	+23.19
26	477.300	11515.00	11486.85	+28.15	11489.99	+25.01
27	484.100	12799.00	12784.11	+14.89	12789.60	+9.40
28	493.100	14728.00	14668.56	+59.44	14677.32	+50.68
29	501.200	16523.00	16536.27	-13.27	16547.85	-24.85
30	508.400	18296.00	18339.64	-43.64	18353.30	-57.30
31	515.400	20214.00	20227.25	-13.25	20242.21	-28.21
32	526.000	23205.00	23347.54	-142.53	23362.26	-157.26
33	535.400	26247.00	26387.99	-140.99	26399.09	-152.09
34	540.900	28276.00	28289.48	-13.48	28296.39	-20.39
35	545.950	30068.00	30116.42	-48.42	30117.79	-49.79
36	550.350	31755.00	31772.08	-17.08	31767.08	-12.08
37	553.150	32824.00	32856.87	-32.87	32846.97	-22.97
38	558.450	35215.00	34976.94	+238.05	34955.76	+259.24
39	561.650	36367.00	36299.40	+67.60	36269.99	+97.01

Sum of residuals  
 squared =  
 +1.330790<sub>10</sub> +5

Sum of residuals  
 squared =  
 +1.571630<sub>10</sub> +5

TREATMENT OF VAPOR PRESSURE DATA FOR CARBON TETRACHLORIDE  
BY COX AND CRAGOE EQUATIONS

Constants for the Cox Equation (103)      Constants for the Cragoe Equation (104)

$\log A_c = 0.6475$   
 $E = 0.1719$   
 $T_b = 349.71$   
 $T_c = 547.28$

$A = +1.062382_{10} +1$   
 $B = -2.033738_{10} +3$   
 $C = -7.418258_{10} -3$   
 $D = +5.463349_{10} -6$

Sample	T OBS (°K)	P OBS (mm Hg)	P COX	DELTA P	P CRAGOE	DELTA P
1	374.650	1531.00	1522.61	+8.39	1524.27	+6.73
2	383.000	1873.00	1878.29	-5.29	1879.45	-6.45
3	389.500	2198.00	2196.42	+1.58	2197.14	+0.86
4	394.000	2445.00	2439.50	+5.50	2439.91	+5.09
5	397.250	2624.00	2627.32	-3.32	2627.51	-3.51
6	401.500	2879.00	2889.15	-10.15	2889.05	-10.05
7	405.700	3167.00	3166.74	+0.26	3166.35	+0.65
8	411.300	3573.00	3567.43	+5.57	3566.69	+6.31
9	415.650	3828.00	3903.99	-75.99	3902.99	-74.99
10	418.950	4174.00	4174.72	-0.72	4173.54	+0.46
11	420.800	4386.00	4332.49	+53.51	4331.22	+54.78
12	425.500	4752.00	4753.30	-1.30	4751.83	+0.17
13	433.050	5541.00	5492.02	+48.98	5490.31	+50.69
14	436.750	5872.00	5883.67	-11.67	5881.90	-9.90
15	444.000	6688.00	6710.77	-22.77	6708.99	-20.99
16	448.050	7198.00	7208.74	-10.74	7207.01	-9.01
17	453.300	7925.00	7894.41	+30.59	7892.83	+32.17
18	458.850	8699.00	8670.66	+28.34	8669.33	+29.67
19	463.700	9412.00	9394.17	+17.83	9393.14	+18.86
20	469.550	10344.00	10325.42	+18.58	10324.85	+19.15
21	475.750	11365.00	11385.58	-20.58	11385.59	-20.59
22	481.900	12484.00	12515.30	-31.30	12515.99	-31.99
23	487.550	13577.00	13625.12	-48.12	13626.48	-49.48
24	493.100	14734.00	14785.54	-51.54	14787.57	-53.57
25	498.450	15975.00	15973.01	+1.99	15975.68	-0.68
26	504.200	17356.00	17328.06	+27.94	17331.36	+24.64
27	508.400	18375.00	18371.59	+3.41	18375.26	-0.26
28	513.150	19623.00	19608.65	+14.35	19612.63	+10.37
29	516.250	20471.00	20449.62	+21.38	20453.71	+17.29
30	520.700	21748.00	21704.84	+43.16	21708.93	+39.07
31	524.600	22843.00	22852.94	-9.94	22856.83	-13.83
32	529.200	24280.00	24266.84	+13.16	24270.21	+9.79
33	532.750	25447.00	25403.71	+43.29	25406.42	+40.58
34	537.300	26843.00	26921.14	-78.14	26922.60	-79.60
35	540.900	28155.00	28171.36	-16.36	28171.47	-16.47
36	544.500	29430.00	29466.90	-36.90	29465.27	-35.27
37	547.950	30712.00	30752.30	-40.30	30748.59	-36.59
38	550.100	31554.00	31575.62	-21.62	31570.40	-16.40
39	553.250	32837.00	32813.58	+23.42	32805.77	+31.23
40	554.700	33482.00	33396.34	+85.66	33387.20	+94.80

Sum of residuals  
squared =  
+4.404287<sub>10</sub> +4

Sum of residuals  
squared =  
+4.538068<sub>10</sub> +4

0.3% is about that of my experimental work.

Often, interpolations of vapor pressure data are necessary, for example, in the calculation of derived thermodynamic properties. It is best to relate  $\log P$  and  $T$  by polynomial expressions which can then be differentiated to give heat of vaporization, if the volumetric data are also available. Chebyshev (212) discussed polynomials of an orthogonal system to solve the problem of the best approximation of continuous functions. Thus,  $T \log_{10} P$  (mm) can be fitted to an orthogonal series in  $T$  and the constants rearranged so that  $T \log_{10} P$  is expressed as a Chebyshev series. It is then possible to write  $T \log_{10} P$  as

$$T \log_{10} P = \frac{1}{2} a_0 + a_1 C_1(x) + a_2 C_2(x) + \dots \quad (107)$$

where  $a_0, a_1, a_2, \dots$  are constants and  $C_1(x), C_2(x), \dots$  are Chebyshev polynomials. Truncation may occur wherever desired by the size of residuals and smoothness of fit, and  $x$  is defined by

$$x = \frac{2T - (T_{\max} + T_{\min})}{T_{\max} - T_{\min}} \quad (108)$$

Again, Dr. Counsell (211) has carried out the fits for me for the four compounds. The program used by him gave fittings for each order of 1 to 6, and the values of residuals in  $T \log_{10} P$ . From the lowest values of residuals and smoothness of fit the orders of polynomials were selected and these are tabulated in Tables XXI through XXIV. The values of residuals squared are also given in these tables. The constants of the fit are tabulated at the end. Dr. Counsell has indicated the method of summation of the Chebyshev series by the

TABLE XXI

## POLYNOMIAL EXPRESSIONS FOR VAPOR PRESSURE OF ACETONE

<u>Temp. °K</u>	<u>T log<sub>10</sub> P (mm)</u>	<u>Residuals</u>
+3.7465000000 <sub>10</sub> 02	+1.2938974999 <sub>10</sub> 03	+2.4668750427 <sub>10</sub> 00;
+3.8055000000 <sub>10</sub> 02	+1.3398666499 <sub>10</sub> 03	+1.4601133354 <sub>10</sub> 00;
+3.8825000000 <sub>10</sub> 02	+1.3999657700 <sub>10</sub> 03	+4.0720440447 <sub>10</sub> -02;
+3.9064999999 <sub>10</sub> 02	+1.4186204900 <sub>10</sub> 03	-3.2421448826 <sub>10</sub> -01;
+3.9725000000 <sub>10</sub> 02	+1.4694816999 <sub>10</sub> 03	-8.8851554691 <sub>10</sub> -01;
+4.0054999999 <sub>10</sub> 02	+1.4925414699 <sub>10</sub> 03	+1.2001689225 <sub>10</sub> 00;
+4.0565000000 <sub>10</sub> 02	+1.5338618499 <sub>10</sub> 03	-1.2544177994 <sub>10</sub> 00;
+4.0855000000 <sub>10</sub> 02	+1.5568593399 <sub>10</sub> 03	-2.1517508439 <sub>10</sub> 00;
+4.1325000000 <sub>10</sub> 02	+1.5921095700 <sub>10</sub> 03	-1.5844850800 <sub>10</sub> 00;
+4.1895000000 <sub>10</sub> 02	+1.6364652600 <sub>10</sub> 03	-2.5019355379 <sub>10</sub> 00;
+4.2305000000 <sub>10</sub> 02	+1.6670951400 <sub>10</sub> 03	-1.8867660425 <sub>10</sub> 00;
+4.2434999999 <sub>10</sub> 02	+1.6773022499 <sub>10</sub> 03	-2.1869091354 <sub>10</sub> 00;
+4.2905000000 <sub>10</sub> 02	+1.7045677300 <sub>10</sub> 03	+6.3651066310 <sub>10</sub> 00;
+4.3304999999 <sub>10</sub> 02	+1.7417480800 <sub>10</sub> 03	-3.3226825296 <sub>10</sub> -01;
+4.3745000000 <sub>10</sub> 02	+1.7748391700 <sub>10</sub> 03	+1.0791437700 <sub>10</sub> -01;
+4.4434999999 <sub>10</sub> 02	+1.8268804099 <sub>10</sub> 03	+6.4980645105 <sub>10</sub> -01;
+4.5325000000 <sub>10</sub> 02	+1.8952351799 <sub>10</sub> 03	+1.1965603969 <sub>10</sub> -01;
+4.6034999999 <sub>10</sub> 02	+1.9493558800 <sub>10</sub> 03	+1.0623591976 <sub>10</sub> -01;
+4.6284999999 <sub>10</sub> 02	+1.9694704900 <sub>10</sub> 03	-9.5651363208 <sub>10</sub> -01;
+4.7145000000 <sub>10</sub> 02	+2.0328818599 <sub>10</sub> 03	+1.1705128736 <sub>10</sub> 00;
+4.7575000000 <sub>10</sub> 02	+2.0660534000 <sub>10</sub> 03	+7.6817112416 <sub>10</sub> -01;
+4.8065000000 <sub>10</sub> 02	+2.1046906999 <sub>10</sub> 03	-5.2748435735 <sub>10</sub> -01;
+4.8484999999 <sub>10</sub> 02	+2.1357619600 <sub>10</sub> 03	+4.0837951004 <sub>10</sub> -01;
+4.8954999999 <sub>10</sub> 02	+2.1724030199 <sub>10</sub> 03	-4.1518472880 <sub>10</sub> -01;
+4.9294999999 <sub>10</sub> 02	+2.1980371600 <sub>10</sub> 03	-1.3879587501 <sub>10</sub> -01;
+4.9695000000 <sub>10</sub> 02	+2.2287014400 <sub>10</sub> 03	-3.2010075449 <sub>10</sub> -01;
+4.9845000000 <sub>10</sub> 02	+2.2400163699 <sub>10</sub> 03	-2.0391508191 <sub>10</sub> -01;
+5.0184999999 <sub>10</sub> 02	+2.2656942699 <sub>10</sub> 03	+2.8713762760 <sub>10</sub> -02;
+5.0334999999 <sub>10</sub> 02	+2.2764199600 <sub>10</sub> 03	+7.3413942754 <sub>10</sub> -01;
+5.0525000000 <sub>10</sub> 02	+2.2915867699 <sub>10</sub> 03	+4.6742610633 <sub>10</sub> -02;

Order 1

Sum Squares +7.9152629856 x 10

Delta Squared +1.3082342868 x 10<sup>-3</sup>

Max Residuals -2.5019355379

and +6.3651066310

+5.8532248003 x 10<sup>3</sup>at +4.1895000000 x 10<sup>2</sup>at +4.2905000000 x 10<sup>2</sup>+1.1637344964 x 10 +6.3120667981 x 10<sup>-1</sup>Acetone T<sub>max</sub> = +5.0599 x 10<sup>2</sup>T<sub>min</sub> = +3.7400 x 10<sup>2</sup>

Order 1

+3.5887599620 x 10<sup>3</sup>+5.0296908943 x 10<sup>2</sup>

TABLE XXII

## POLYNOMIAL EXPRESSIONS FOR VAPOR PRESSURE OF BENZENE

Temp. °K	T log <sub>10</sub> P (mm)	Residuals
+3.7940000000 <sub>10</sub> 02	+1.2291774299 <sub>10</sub> 03	+3.7720509991 <sub>10</sub> -01;
+3.8254999999 <sub>10</sub> 02	+1.2538467300 <sub>10</sub> 03	-2.0502552017 <sub>10</sub> 00;
+3.8690000000 <sub>10</sub> 02	+1.2827025000 <sub>10</sub> 03	-1.1444202437 <sub>10</sub> -01;
+3.9020000000 <sub>10</sub> 02	+1.3061253899 <sub>10</sub> 03	-1.2040960738 <sub>10</sub> -01;
+3.9400000000 <sub>10</sub> 02	+1.3326538200 <sub>10</sub> 03	+3.7612996250 <sub>10</sub> -01;
+3.9594999999 <sub>10</sub> 02	+1.3491535499 <sub>10</sub> 03	-2.2311459183 <sub>10</sub> 00;
+3.9894999999 <sub>10</sub> 02	+1.36922602100 <sub>10</sub> 03	-9.3324264511 <sub>10</sub> -01;
+4.0495000000 <sub>10</sub> 02	+1.4072935000 <sub>10</sub> 03	+3.9540234276 <sub>10</sub> 00;
+4.1129999999 <sub>10</sub> 02	+1.4543755600 <sub>10</sub> 03	+2.4513068348 <sub>10</sub> 00;
+4.1300000000 <sub>10</sub> 02	+1.4660389700 <sub>10</sub> 03	+3.0162221156 <sub>10</sub> 00;
+4.1940000000 <sub>10</sub> 02	+1.5155533700 <sub>10</sub> 03	-3.6790834739 <sub>10</sub> -01;
+4.2075000000 <sub>10</sub> 02	+1.5252170099 <sub>10</sub> 03	-2.8248338401 <sub>10</sub> -01;
+4.2540000000 <sub>10</sub> 02	+1.5587753500 <sub>10</sub> 03	-2.1342206001 <sub>10</sub> -01;
+4.2804999999 <sub>10</sub> 02	+1.5787485399 <sub>10</sub> 03	-9.9075964093 <sub>10</sub> -01;
+4.3350000000 <sub>10</sub> 02	+1.6171856599 <sub>10</sub> 03	+1.1990463361 <sub>10</sub> -01;
+4.3675000000 <sub>10</sub> 02	+1.6416351700 <sub>10</sub> 03	-7.0333621650 <sub>10</sub> -01;
+4.4360000000 <sub>10</sub> 02	+1.6919079600 <sub>10</sub> 03	-1.0807077065 <sub>10</sub> 00;
+4.4465000000 <sub>10</sub> 02	+1.6991158299 <sub>10</sub> 03	-6.2908257544 <sub>10</sub> -01;
+4.5069999999 <sub>10</sub> 02	+1.7436208199 <sub>10</sub> 03	-9.4567741081 <sub>10</sub> -01;
+4.5164999999 <sub>10</sub> 02	+1.7496439300 <sub>10</sub> 03	-2.1881848573 <sub>10</sub> -02;
+4.5635000000 <sub>10</sub> 02	+1.7836577999 <sub>10</sub> 03	+3.6427798494 <sub>10</sub> -01;
+4.5884999999 <sub>10</sub> 02	+1.8016692100 <sub>10</sub> 03	+6.7103318870 <sub>10</sub> -01;
+4.6315000000 <sub>10</sub> 02	+1.8336040099 <sub>10</sub> 03	+2.7452931180 <sub>10</sub> -01;
+4.6765000000 <sub>10</sub> 02	+1.8679795899 <sub>10</sub> 03	-1.0563140995 <sub>10</sub> 00;
+4.6955000000 <sub>10</sub> 02	+1.8813927799 <sub>10</sub> 03	-5.0586960837 <sub>10</sub> -01;
+4.7730000000 <sub>10</sub> 02	+1.9384371500 <sub>10</sub> 03	-5.2905823662 <sub>10</sub> -01;
+4.8410000000 <sub>10</sub> 02	+1.9882796799 <sub>10</sub> 03	-2.6423193886 <sub>10</sub> -01;
+4.9309999999 <sub>10</sub> 02	+2.0553073199 <sub>10</sub> 03	-8.8306331634 <sub>10</sub> -01;
+5.0120000000 <sub>10</sub> 02	+2.1141016500 <sub>10</sub> 03	+1.5986546128 <sub>10</sub> -01;
+5.0840000000 <sub>10</sub> 02	+2.1669772500 <sub>10</sub> 03	+5.1305931806 <sub>10</sub> -01;
+5.1540000000 <sub>10</sub> 02	+2.2191284500 <sub>10</sub> 03	+1.3583793491 <sub>10</sub> -01;
+5.2599999999 <sub>10</sub> 02	+2.2962910100 <sub>10</sub> 03	+1.3925106003 <sub>10</sub> 00;
+5.3540000000 <sub>10</sub> 02	+2.3659702099 <sub>10</sub> 03	+1.2451912015 <sub>10</sub> 00;
+5.4089999999 <sub>10</sub> 02	+2.4077668499 <sub>10</sub> 03	+1.1614246666 <sub>10</sub> -01;
+5.4594999999 <sub>10</sub> 02	+2.4448159599 <sub>10</sub> 03	+3.9093781262 <sub>10</sub> -01;
+5.5034999999 <sub>10</sub> 02	+2.4775670200 <sub>10</sub> 03	+1.4347746968 <sub>10</sub> -01;
+5.5314999999 <sub>10</sub> 02	+2.4981260100 <sub>10</sub> 03	+2.5933726131 <sub>10</sub> -01;
+5.5844999999 <sub>10</sub> 02	+2.5391146699 <sub>10</sub> 03	-1.6175137460 <sub>10</sub> 00;
+5.6165000000 <sub>10</sub> 02	+2.5615159000 <sub>10</sub> 03	-4.2019160836 <sub>10</sub> -01;

Order 3

Sum Squares +5.5317995956 x 10

Delta Squared -3.5662922487 x 10<sup>-4</sup>

Max residuals -2.2311459183

and +3.9540284276

-1.6562435425 x 10

at +3.9594999999 x 10<sup>2</sup>at +4.0495000000 x 10<sup>2</sup>

+1.5411689155 x 10

+2.4568716904 x 10<sup>-1</sup>Benzene T<sub>Max</sub> = +5.6199 x 10<sup>2</sup>T<sub>min</sub> = +3.7899 x 10<sup>2</sup>Order 3. +3.7830759949 x 10<sup>3</sup>+6.6954583090 x 10<sup>2</sup>

+3.6668404642

-1.0746671087

TABLE XXIII

## POLYNOMIAL EXPRESSIONS FOR VAPOR PRESSURE OF CHLOROFORM

Temp. °K	T log <sub>10</sub> P (mm)	Residuals
+3.7455000000 <sub>10</sub> 02	+1.2698735500 <sub>10</sub> 03	+2.2332765273 <sub>10</sub> 00;
+3.8484999999 <sub>10</sub> 02	+1.3453641300 <sub>10</sub> 03	+6.3975945860 <sub>10</sub> -01;
+3.9234999999 <sub>10</sub> 02	+1.4006244799 <sub>10</sub> 03	-5.9240270406 <sub>10</sub> -02;
+4.0065000000 <sub>10</sub> 02	+1.4639655299 <sub>10</sub> 03	-2.3773888088 <sub>10</sub> 00;
+4.0884999999 <sub>10</sub> 02	+1.5251950200 <sub>10</sub> 03	-2.7499739602 <sub>10</sub> 00;
+4.1784999999 <sub>10</sub> 02	+1.5911163999 <sub>10</sub> 03	-1.3387553319 <sub>10</sub> 00;
+4.2445000000 <sub>10</sub> 02	+1.6422420799 <sub>10</sub> 03	-2.7991120554 <sub>10</sub> 00;
+4.3315000000 <sub>10</sub> 02	+1.7054018600 <sub>10</sub> 03	-2.1097020059 <sub>10</sub> -01;
+4.4075000000 <sub>10</sub> 02	+1.7609951000 <sub>10</sub> 03	+1.8102550618 <sub>10</sub> 00;
+4.4634999999 <sub>10</sub> 02	+1.8027229199 <sub>10</sub> 03	+2.5960381105 <sub>10</sub> 00;
+4.5365000000 <sub>10</sub> 02	+1.8585750299 <sub>10</sub> 03	+2.1857759989 <sub>10</sub> 00;
+4.6024999999 <sub>10</sub> 02	+1.9084368799 <sub>10</sub> 03	+2.4200554378 <sub>10</sub> 00;
+4.6944999999 <sub>10</sub> 02	+1.9772320699 <sub>10</sub> 03	+3.3133153915 <sub>10</sub> 00;
+4.8055000000 <sub>10</sub> 02	+2.0629797199 <sub>10</sub> 03	+1.2521270439 <sub>10</sub> 00;
+4.8684999999 <sub>10</sub> 02	+2.1119110099 <sub>10</sub> 03	-4.5653948932 <sub>10</sub> -01;
+4.9275000000 <sub>10</sub> 02	+2.1573166199 <sub>10</sub> 03	-1.8663609847 <sub>10</sub> 00;
+4.9845000000 <sub>10</sub> 02	+2.2000301299 <sub>10</sub> 03	-2.3192573487 <sub>10</sub> 00;
+5.0434999999 <sub>10</sub> 02	+2.2440974299 <sub>10</sub> 03	-2.9296935498 <sub>10</sub> 00;
+5.1065000000 <sub>10</sub> 02	+2.2891964000 <sub>10</sub> 03	-1.9867293164 <sub>10</sub> 00;
+5.1805000000 <sub>10</sub> 02	+2.3417364699 <sub>10</sub> 03	-9.7896469384 <sub>10</sub> -01;
+5.2584999999 <sub>10</sub> 02	+2.3965410800 <sub>10</sub> 03	-3.7636697292 <sub>10</sub> -02;
+5.3144999999 <sub>10</sub> 02	+2.4350711000 <sub>10</sub> 03	+9.6970208734 <sub>10</sub> -01;
+5.3334999999 <sub>10</sub> 02	+2.4480972500 <sub>10</sub> 03	+1.2596112489 <sub>10</sub> 00;
+5.3605000000 <sub>10</sub> 02	+2.4667595899 <sub>10</sub> 03	+1.4307063817 <sub>10</sub> 00;

Order 3

Sum Squares +8.8617601567 x 10

Delta Squared +2.3512013137 x 10<sup>-4</sup>Max residuals -2.9296935498 at +5.0434999999 x 10<sup>2</sup>and +3.3133153915 at +4.6944999999 x 10<sup>2</sup>-4.3381140910 x 10 +1.1318947831 x 10 -9.0055969547 x 10<sup>-2</sup>Chloroform T<sub>max</sub> = +5.3650 x 10<sup>2</sup> Order 3T<sub>min</sub> = +3.7400 x 10<sup>2</sup> +3.7426681407 x 10<sup>3</sup>+6.0539318674 x 10<sup>2</sup>

-1.5758486165

-3.8326124969



## TABLE XXIV

## POLYNOMIAL EXPRESSIONS FOR VAPOR PRESSURE OF CARBON TETRACHLORIDE

Temp. °K	T log <sub>10</sub> P (mm)	Residuals
+3.7465000000 02	+1.1932484099 03	-7.8943194076 01
+3.8300000000 02	+1.2533793000 03	+5.3376861289 01
+3.8950000000 02	+1.3017170099 03	-8.2189772278 02
+3.9400000000 02	+1.3349790299 03	-3.6049696803 01
+3.9725000000 02	+1.3581604900 03	+2.3396504670 01
+4.0149999999 02	+1.3888825699 03	+6.1934944987 01
+4.0570000000 02	+1.4202098899 03	-1.7590045928 02
+4.1129999999 02	+1.4613593700 03	-2.9064792767 01
+4.1564999999 02	+1.4892591100 03	+3.5305519215 00
+4.1895000000 02	+1.5168272099 03	+1.0273274034 02
+4.2079999999 02	+1.5325792100 03	-2.2660235539 00
+4.2550000000 02	+1.5645075899 03	+2.4633549153 02
+4.3304999999 02	+1.6211573899 03	-1.6985312290 00
+4.3675000000 02	+1.6460137999 03	+3.4751655906 01
+4.4400000000 02	+1.6984279199 03	+6.2693766589 01
+4.4805000000 02	+1.7282200799 03	+2.6254348829 01
+4.5329999999 02	+1.7674126000 03	-7.8688568621 01
+4.5884999999 02	+1.8076216500 03	-6.7301733419 01
+4.6370000000 02	+1.8425923799 03	-4.0191964432 01
+4.6955000000 02	+1.8850929699 03	-3.8272145763 01
+4.7575000000 02	+1.9294330499 03	+3.6194668710 01
+4.8190000000 02	+1.9740286699 03	+5.1675178110 01
+4.8754999999 02	+2.0149442099 03	+7.4591271206 01
+4.9309999999 02	+2.0553945400 03	+7.4852279573 01
+4.9845000000 02	+2.0952006400 03	-2.2695787250 02
+5.0420000000 02	+2.1375259500 03	-3.4511981159 01
+5.0840000000 02	+2.1679285599 03	-3.1303182244 02
+5.1315000000 02	+2.2028278700 03	-1.5155705809 01
+5.1625000000 02	+2.2256208000 03	-2.2187233186 01
+5.2069999999 02	+2.2584894300 03	-4.3609447777 01
+5.2459999999 02	+2.2865970200 03	+1.1224946379 01
+5.2919999999 02	+2.3206686600 03	-1.1221788823 01
+5.3274999999 02	+2.3470978900 03	-3.8285575807 01
+5.3730000000 02	+2.3796058500 03	+6.8670645356 01
+5.4089999999 02	+2.4067594600 03	+1.4193574339 01
+5.4450000000 02	+2.4332511100 03	+2.9797139763 01
+5.4794999999 02	+2.4588152299 03	+3.0914426594 01
+5.5010000000 02	+2.4749245599 03	+1.5744575858 01
+5.5325000000 02	+2.4986727700 03	-1.8323839455 01
+5.5469999999 02	+2.5099075300 03	-6.3176637142 01

Sum squares +2.7219313277 x 10

Delta Squared -5.0769518845 x 10<sup>-5</sup>Max residuals -2.2660235539 at +4.2079999999 x 10<sup>2</sup>and +3.5305519215 at +4.1564999999 x 10<sup>2</sup>+1.7626166924 x 10 +1.6701761089 x 10 -3.8017599369 x 10<sup>-1</sup>Carbon Tetrachloride T<sub>max</sub> = +5.5500 x 10<sup>2</sup> Order 3T<sub>min</sub> = +3.7400 x 10<sup>2</sup>+3.6975921726 x 10<sup>3</sup>+6.6086503780 x 10<sup>2</sup>+7.9183306286 x 10<sup>-1</sup>

+1.0553478061

iterative relationship:

$$b_r = 2x b_{r+1} - b_{r+2} + a_r, \quad b_{r+1} = b_{r+2} = 0$$

$$T \log P = \frac{1}{2}(b_0 - b_2) \quad (109)$$

Van Ness (213) has recently advocated the use of orthogonal polynomials for representing thermodynamic excess functions and in view of this work, I thought it may be worthwhile to represent vapor pressure data as suggested by Dr. Counsell, since this is a property of pure liquids which is very often used to give other thermodynamic functions.

## II. THERMODYNAMIC ANALYSIS

### II(a). Vapor-liquid Equilibrium Data

In order to understand and interpret the phase behavior of mixtures the experimental data are usually subjected to thermodynamic analysis. The equilibrium properties of fluids are related to intermolecular forces. The statistical description of fluids is as yet incomplete and therefore until a satisfactory theoretical model of general validity is devised to relate the properties of solutions to theoretically derived properties of the pure components, experimental data will continue to be represented by well-behaved mathematical functions arbitrarily chosen by the individual investigator. In this work I have chosen the method suggested by Chueh and Prausnitz (116) as described in detail in Chapter I. Vapor-phase non-idealities are expressed as fugacity coefficients (equation 21) and the liquid-phase nonidealities are given by activity coefficients. The composition dependence of the activity coefficients is represented by the van Laar equation, which is an integrated form of isothermal, isobaric Gibbs-

Duhem equation. The parameters required for this representation are: the Henry's constant,  $H_{2(1)}^{(PO)}$ , the binary interaction constant  $\alpha_{22(1)}$  (or  $\alpha_{12}$ ), and the dilation constant  $\eta_{2(1)}$ . Since these parameters depend only on temperature, isothermal experimental data are required for thermodynamic analysis. Therefore, for each isotherm, P - x - y data were read from large-scale plots of vapor-liquid equilibrium compositions (Table XV) and of lines of constant composition on the pressure-temperature diagram (Table XIV). Calculations were done with IBM 360/65 electronic computer using the programs written by Chueh and Prausnitz (116).

The analysis of binary mixtures of condensable components (both  $T_{R1}$  and  $T_{R2} < 0.93$ ) is performed using the symmetric convention of normalization for activity coefficients. For such mixtures a one-parameter model for the excess Gibbs energy with  $\eta_{2(1)} = 0$  is used. On the other hand, for the binary mixtures at a reduced temperature  $T_{R2} \geq 0.93$ , a two-parameter model for the excess Gibbs energy and the unsymmetric convention for normalization of activity coefficients are used.

#### II(a).(I) Analysis of the Binary System where $T_{R1}$ and $T_{R2} < 0.93$

As explained in Chapter I (Section III. C. (V). (c), page 59), the constant-pressure activity coefficients for binary systems for which both  $T_{R1}$  and  $T_{R2}$  fall below 0.93 are analyzed with a one-parameter model ( $\eta_{2(1)} = 0$ ). The expressions for activity coefficients are given by equations (68) and (69). Data reduction is performed by a computer program which contains a main program, SYMFIT, and three subroutines,

VOLPAR, PHIMIX and CUBEQN. The subroutine VOLPAR, calculates partial molal volume of each component in the liquid mixture, using the method described in Chapter I (see equation (80)). This quantity is required in the Poynting correction of the liquid-phase activity coefficient. The subroutine PHIMIX calculates the vapor-phase fugacity coefficient  $\phi_i$ , using the revised Redlich-Kwong equation discussed in Chapter I (see equations (25) and (40)). Since the calculation of  $\phi_i$  from equation (40) requires a knowledge of the molal volume,  $v$ , of the mixture, and since I have not obtained the volumetric properties of the mixture in the gaseous phase experimentally, I calculated this quantity (molal volume) from equation (25). The subroutine CUBEQN was used for this purpose which solved the cubic equation in  $v$  (the Redlich-Kwong equation).

The input data for the program, SYMFIT are the following:

(1) the pure-component data  $T_c$ ,  $P_c$ ,  $v_c$ ,  $\omega$ ,  $\Omega_a^V$ ,  $\Omega_b^V$ ,  $\Omega_a^L$ ,  $\Omega_b^L$ , molecular weight,  $f_{\text{pure}}^{(PO)}$ , (2) vapor-phase and critical binary constants ( $k_{12}$ ,  $\tau_{12}$ ,  $v_{12}$ ), and (3) the experimental data -- temperature  $T$ , total pressure  $P$ , liquid-phase composition  $x$ , and vapor-phase composition  $y$  (see appendix). The binary system is actually overspecified when all these experimental data are supplied; theoretically, it suffices to specify  $T$ ,  $P$ , and  $x$  for data reduction of a binary, two-phase system. Fitting to  $T$ ,  $P$ , and  $x$  data alone, however, requires a lengthy iterative procedure of trial and error. Use of experimental  $y$  facilitates calculation of activity coefficients and provides direct and analytical fitting to the solution model by the method of least squares. Moreover, utilizing  $y$  data in the fitting program in addition to  $T$ ,  $P$ ,  $x$  data also

gives information on the consistency of the experimental data.

For each datum point, Poynting corrections are calculated for both components and the constant-pressure activity coefficients are then calculated by equations (46) and (70), assuming the liquid partial molal volumes to be incompressible. The logarithms of activity coefficients are fitted by a least-squares technique to equations (68) and (69) to evaluate the binary interaction constant,  $\alpha_{12}$ . Both  $\gamma_1$  and  $\gamma_2$  are weighted equally in the first round of fitting; but zero weight is given to those  $\gamma_i$  where either  $x_i$  or  $y_i$  falls below a specified minimum value (0.005 was chosen as the minimum value). Using  $\alpha_{12}$ , calculated  $\gamma$ 's are then produced and percent deviations of  $\gamma$ 's are computed for each datum point ( $\Delta\gamma_i = \gamma_i^{(PO)} \text{ experim.} - \gamma_i^{(PO)} \text{ calc.}$ ). The average percent deviations of  $\gamma_1$  and  $\gamma_2$  are then calculated respectively. These average percent deviations in  $\gamma_1$  and  $\gamma_2$  are used in the second round of fitting to test the thermodynamic consistency of the experimental data. If the data are thermodynamically consistent, both  $\gamma_1$  and  $\gamma_2$  are utilized in the second round of fitting. If the data are thermodynamically inconsistent, the less reliable set of  $\gamma$  is discarded in the second round of fitting. In any case, the percent deviation of  $\gamma$  for each component and for each individual point is used to screen out bad datum points (see the following section on thermodynamic consistency test).

Thus, for each round of fitting, the following information is obtained as shown in Table XXV: the parameter  $\alpha_{12}$ , the number of experimental points used for  $\gamma_1$  and  $\gamma_2$ , the calculated and experimental activity coefficients for each point, and the average percent deviation in  $\gamma_1$  and  $\gamma_2$ . The standard state fugacities, liquid-phase partial molal volumes, the Poynting corrections and vapor-phase fugacity coefficients

TABLE XXV

THERMODYNAMIC ANALYSIS OF THE SYSTEM BENZENE (1) - ACETONE (2) UP TO  $T_{R2} = 0.93$

Correction to Geometric-mean  $T_{c12} = 0.01$ ,  $2\tau_{12}/(T_{c1} + T_{c2}) = -0.0096$ ,  $2v_{12}/(v_{c1} + v_{c2}) = -0.0165$

Temperature = 100°C, Reference Fugacity (1) = 1.685 atm., Reference Fugacity (2) = 3.492 atm.

$x_2$	$y_2$	$\phi_2$	P, atm.	$\bar{V}_1^L$ , cc/mole	$\bar{V}_2^L$ , cc/mole	Poynting Correction for $\gamma_1$	Poynting Correction for $\gamma_2$	$\gamma_1^{(PO)}$	$\gamma_2^{(PO)}$	$\phi_1$	$\phi_2$
0.093	0.181	0.0786	2.085	99.34	96.49	1.0068	1.0066	1.0571	1.1148	0.9527	0.9658
0.209	0.368	0.1802	2.277	98.38	94.41	1.0073	1.0070	1.0170	1.0952	0.9490	0.9608
0.332	0.500	0.2925	2.475	97.63	92.52	1.0079	1.0075	1.0311	1.0130	0.9454	0.9563
0.438	0.607	0.3933	2.648	97.19	91.14	1.0084	1.0079	1.0271	0.9931	0.9425	0.9525
0.657	0.783	0.6144	3.001	96.85	88.90	1.0095	1.0088	1.0457	0.9596	0.9371	0.9452
0.761	0.847	0.7259	3.169	96.94	88.12	1.0101	1.0092	1.1138	0.9427	0.9346	0.9420
0.872	0.921	0.8500	3.346	97.19	87.47	1.0107	1.0096	1.1302	0.9407	0.9322	0.9386

$\alpha_{12}$ , interaction constant of molecules (1) and (2) = 0.00054 mole/cc.

$x_2$	$\ln \gamma_1^{(PO)}$	Calc. $\ln \gamma_1^{(PO)}$	# $\Delta \ln \gamma_1^{(PO)}$	$\ln \gamma_2^{(PO)}$	Calc. $\ln \gamma_2^{(PO)}$	# $\Delta \ln \gamma_2^{(PO)}$	Calc. $\gamma_1^{(PO)}$	# $\Delta \gamma_1^{(PO)}$	Calc. $\gamma_2^{(PO)}$	# $\Delta \gamma_2^{(PO)}$
0.093	0.0555	0.0009	0.0547	0.1087	0.0990	0.0096	1.0009	0.0562	1.1041	0.0107
0.209	0.0168	0.0046	0.0123	0.0909	0.0784	0.0125	1.0046	0.0124	1.0816	0.0136
0.332	0.0306	0.0120	0.0186	0.0129	0.0584	-0.0455	1.0121	0.0190	1.0601	-0.0472
0.438	0.0268	0.0217	0.0051	-0.0069	0.0429	-0.0498	1.0219	0.0052	1.0439	-0.0508
0.657	0.0447	0.0529	-0.0082	-0.0413	0.0173	-0.0586	1.0544	-0.0086	1.0175	-0.0579
0.761	0.1078	0.0739	0.0338	-0.0591	0.0088	-0.0678	1.0767	0.0371	1.0088	-0.0661
0.872	0.1224	0.1013	0.0211	-0.0612	0.0026	-0.0638	1.1067	0.0236	1.0026	-0.0620

Average deviation in  $\gamma_1^{(PO)} = 0.02316$       Average deviation in  $\gamma_2^{(PO)} = 0.04404$

Average deviation in  $\ln \gamma_1^{(PO)} = 0.02197$       Average deviation in  $\ln \gamma_2^{(PO)} = 0.04397$

No. of  $\gamma_1$  data = 7.0

No. of  $\gamma_2$  data = 7.0

TABLE XXV (Cont'd)

Temperature = 125°C, Reference fugacity (1) = 3.062 atm, Reference fugacity (2) = 6.025 atm.

$x_2$	$y_2$	$\phi_2$	P, atm.	$\bar{V}_1^L$ , cc/mole	$\bar{V}_2^L$ , cc/mole	Poynting Correction for $\gamma_1$	Poynting Correction for $\gamma_2$	$\gamma_1^{(PO)}$	$\gamma_2^{(PO)}$	$\phi_1$	$\phi_2$
0.093	0.176	0.0786	3.657	103.33	102.45	1.0116	1.0115	0.9978	1.0789	0.9304	0.9501
0.209	0.348	0.1802	4.045	102.27	100.03	1.0127	1.0125	0.9933	1.0403	0.9240	0.9422
0.332	0.493	0.2925	4.459	101.47	97.84	1.0139	1.0134	1.0000	1.0131	0.9176	0.9344
0.438	0.600	0.3933	4.817	101.05	96.23	1.0150	1.0143	1.0064	1.0019	0.9124	0.9279
0.657	0.762	0.6144	5.554	100.94	93.69	1.0173	1.0161	1.1160	0.9633	0.9022	0.9155
0.761	0.833	0.7259	5.905	101.23	92.83	1.0185	1.0169	1.1876	0.9597	0.8977	0.9098
0.872	0.919	0.8500	6.279	101.79	92.17	1.0198	1.0179	1.1370	0.9751	0.8936	0.9037

$\alpha_{12}$ , interaction constant of molecules (1) and (2) = 0.00056 mole/cc.

$x_2$	$\ln \gamma_1^{(PO)}$	Calc. $\ln \gamma_1^{(PO)}$	# $\Delta \ln \gamma_1^{(PO)}$	$\ln \gamma_2^{(PO)}$	Calc. $\ln \gamma_2^{(PO)}$	# $\Delta \ln \gamma_2^{(PO)}$	Calc. $\gamma_1^{(PO)}$	# $\Delta \gamma_1^{(PO)}$	Calc. $\gamma_2^{(PO)}$	# $\Delta \gamma_2^{(PO)}$
0.093	-0.0022	0.0009	-0.0031	0.0759	0.1021	-0.0261	1.0009	-0.0031	1.1075	-0.0286
0.209	-0.0067	0.0047	-0.0114	0.0395	0.0808	-0.0414	1.0047	-0.0114	1.0842	-0.0439
0.332	-0.0000	0.0124	-0.0124	0.0130	0.0602	-0.0472	1.0124	-0.0125	1.0620	-0.0490
0.438	0.0064	0.0224	-0.0160	0.0019	0.0443	-0.0423	1.0226	-0.0162	1.0453	-0.0433
0.657	0.1098	0.0546	0.0552	-0.0374	0.0179	-0.0552	1.0561	0.0599	0.0180	-0.0547
0.761	0.1719	0.0762	0.0957	-0.0411	0.0090	-0.0501	1.0792	0.1084	1.0091	-0.0493
0.872	0.1284	0.1044	0.0240	-0.0252	0.0027	-0.0279	1.1101	0.0269	1.0027	-0.0276

Average deviation in  $\ln \gamma_1^{(PO)}$  = 0.03407      Average deviation in  $\ln \gamma_2^{(PO)}$  = 0.04234

Average deviation in  $\ln \gamma_1^{(PO)}$  = 0.03112      Average deviation in  $\ln \gamma_2^{(PO)}$  = 0.04147

No. of  $\gamma_1$  data = 7.0

No. of  $\gamma_2$  data = 7.0

TABLE XXV (Cont'd)

Temperature = 150°C, Reference Fugacity (1) = 5.062 atm., Reference Fugacity (2) = 9.472 atm.

$x_2$	$y_2$	$\phi_2$	P, atm.	$\bar{V}_1^L$ , cc/mole	$\bar{V}_2^L$ , cc/mole	Poynting Correction for $\gamma_1$	Poynting Correction for $\gamma_2$	$\gamma_1^{(PO)}$	$\gamma_2^{(PO)}$	$\phi_1$	$\phi_2$
0.093	0.170	0.0786	6.284	107.98	109.82	1.0197	1.0201	1.0014	1.1035	0.8989	0.9283
0.209	0.320	0.1802	6.944	106.76	106.95	1.0216	1.0216	1.0268	1.0077	0.8894	0.9172
0.332	0.458	0.2925	7.649	105.89	104.35	1.0236	1.0233	1.0542	0.9863	0.8800	0.9060
0.438	0.572	0.3933	8.255	105.48	102.46	1.0254	1.0247	1.0571	0.9958	0.8727	0.8965
0.657	0.754	0.6144	9.507	105.65	99.52	1.0294	1.0276	1.1235	0.9846	0.8585	0.8783
0.761	0.836	0.7259	10.10	106.24	98.58	1.0314	1.0291	1.1319	0.9905	0.8525	0.8700
0.872	0.918	0.8500	10.74	107.25	97.91	1.0337	1.0307	1.1130	0.9973	0.8466	0.8614

 $\alpha_{12}$ , interaction constant of molecules (1) and (2) = 0.00049 mole/cc.

$x_2$	$\ln \gamma_1^{(PO)}$	Calc. $\ln \gamma_1^{(PO)}$	# $\Delta \ln \gamma_1^{(PO)}$	$\ln \gamma_2^{(PO)}$	Calc. $\ln \gamma_2^{(PO)}$	# $\Delta \ln \gamma_2^{(PO)}$	Calc. $\gamma_1^{(PO)}$	# $\Delta \gamma_1^{(PO)}$	Calc. $\gamma_2^{(PO)}$	# $\Delta \gamma_2^{(PO)}$
0.093	0.0014	0.0008	0.0006	0.0985	0.0902	0.0083	1.0008	0.0006	1.0944	0.0091
0.209	0.0264	0.0041	0.0223	0.0077	0.0714	-0.0637	1.0042	0.0226	1.0740	-0.0663
0.332	0.0528	0.0109	0.0418	-0.0138	0.0532	-0.0670	1.0110	0.0432	1.0546	-0.0684
0.438	0.0555	0.0198	0.0358	-0.0042	0.0391	-0.0433	1.0200	0.0372	1.0399	-0.0441
0.657	0.1164	0.0482	0.0682	-0.0156	0.0158	-0.0314	1.0494	0.0741	1.0159	-0.0314
0.761	0.1239	0.0673	0.0566	-0.0095	0.0080	-0.0175	1.0697	0.0623	1.0080	-0.0175
0.872	0.1070	0.0923	0.0147	-0.0027	0.0024	-0.0051	1.0967	0.0162	1.0024	-0.0051

Average deviation in  $\gamma_1^{(PO)}$  = 0.03660Average deviation in  $\ln \gamma_1^{(PO)}$  = 0.03429No. of  $\gamma_1$  data = 7.0Average deviation in  $\gamma_2^{(PO)}$  = 0.03455Average deviation in  $\ln \gamma_2^{(PO)}$  = 0.03376No. of  $\gamma_2$  data = 7.0



TABLE XXV (Cont'd)

Temperature = 175°C, Reference Fugacity (1) = 7.745 atm., Reference fugacity (2) = 13.80 atm.

$x_2$	$y_2$	$\phi_2$	P, atm.	$\bar{V}_1^L$ , cc/mole	$\bar{V}_2^L$ , cc/mole	Poynting Correction for $\gamma_1$	Poynting Correction for $\gamma_2$	$\gamma_1^{(PO)}$	$\gamma_2^{(PO)}$	$\phi_1$	$\phi_2$
0.093	0.154	0.0786	10.18	113.41	119.10	1.0319	1.0335	1.0221	1.0665	0.8603	0.9027
0.209	0.300	0.1802	11.21	111.97	115.65	1.0347	1.0359	1.0493	0.9990	0.8477	0.8878
0.332	0.442	0.2925	12.31	110.99	112.54	1.0379	1.0384	1.0688	0.9977	0.8353	0.8724
0.438	0.556	0.3933	13.26	110.58	110.28	1.0407	1.0406	1.0730	1.0075	0.8255	0.8597
0.657	0.750	0.6144	15.22	111.15	106.86	1.0471	1.0452	1.1040	1.0056	0.8071	0.8350
0.761	0.834	0.7259	16.15	112.16	105.84	1.0505	1.0476	1.1021	1.0085	0.7993	0.8239
0.872	0.916	0.8500	17.15	113.85	105.22	1.0545	1.0503	1.0905	1.0092	0.7916	0.8124

$\alpha_{12}$ , interaction constant of molecules (1) and (2) = 0.00040 mole/cc.

$x_2$	$\ln \gamma_1^{(PO)}$	Calc. $\ln \gamma_1^{(PO)}$	# $\Delta \ln \gamma_1^{(PO)}$	$\ln \gamma_2^{(PO)}$	Calc. $\ln \gamma_2^{(PO)}$	# $\Delta \ln \gamma_2^{(PO)}$	Calc. $\gamma_1^{(PO)}$	# $\Delta \gamma_1^{(PO)}$	Calc. $\gamma_2^{(PO)}$	# $\Delta \gamma_2^{(PO)}$
0.093	0.0218	0.0006	0.0212	0.0644	0.0740	-0.0096	1.0006	0.0214	1.0768	-0.0103
0.209	0.0482	0.0034	0.0447	-0.0010	0.0586	-0.0596	1.0034	0.0459	1.0603	-0.0613
0.332	0.0665	0.0090	0.0575	-0.0023	0.0436	-0.0459	1.0090	0.0598	1.0446	-0.0469
0.438	0.0705	0.0162	0.0543	0.0075	0.0321	-0.0246	1.0163	0.0567	1.0326	-0.0251
0.657	0.0990	0.0396	0.0594	0.0056	0.0130	-0.0073	1.0403	0.0637	1.0130	-0.0074
0.761	0.0972	0.0552	0.0420	0.0085	0.0065	0.0020	1.0568	0.0454	1.0066	0.0020
0.872	0.0867	0.0757	0.0109	0.0092	0.0020	0.0072	1.0787	0.0119	1.0020	0.0073

Average deviation in  $\gamma_1^{(PO)}$  = 0.04353

Average deviation in  $\ln \gamma_1^{(PO)}$  = 0.04145

No. of  $\gamma_1$  data = 7.0

Average deviation in  $\gamma_2^{(PO)}$  = 0.02289

Average deviation in  $\ln \gamma_2^{(PO)}$  = 0.02232

No. of  $\gamma_2$  data = 7.0

TABLE XXV (Cont'd)

Temperature = 200°C, Reference fugacity (1) = 11.12 atm., Reference fugacity (2) = 12.09 atm.

$x_2$	$y_2$	$\phi_2$	P, atm.	$\bar{V}_1^L$ , cc/mole	$\bar{V}_2^L$ , cc/mole	Poynting Correction for $\gamma_1$	Poynting Correction for $\gamma_2$	$\gamma_1$ (PO)	$\gamma_2$ (PO)	$\phi_1$	$\phi_2$
0.093	0.140	0.0786	15.49	119.88	131.29	1.0490	1.0538	1.0288	1.0252	0.8176	0.8757
0.209	0.279	0.1802	17.06	118.15	127.11	1.0533	1.0575	1.0628	0.9759	0.8008	0.8563
0.332	0.425	0.2925	18.75	116.99	123.37	1.0581	1.0614	1.0753	0.9999	0.7844	0.8357
0.438	0.535	0.3933	20.19	116.58	120.69	1.0625	1.0648	1.0903	1.0040	0.7713	0.8189
0.657	0.743	0.6144	23.19	117.74	116.81	1.0728	1.0723	1.0880	1.0171	0.7474	0.7860
0.761	0.835	0.7259	24.61	119.43	115.82	1.0786	1.0762	1.0444	1.0237	0.7377	0.7711
0.872	0.917	0.8500	26.12	122.29	115.46	1.0858	1.0808	1.0202	1.0166	0.7274	0.7558

 $\alpha_{12}$ , interaction constant of molecules (1) and (2) = 0.00019 mole/cc.

$x_2$	$\ln \gamma_1^{(PO)}$	Calc. $\ln \gamma_1^{(PO)}$	# $\Delta \ln \gamma_1^{(PO)}$	$\ln \gamma_2^{(PO)}$	Calc. $\ln \gamma_2^{(PO)}$	# $\Delta \ln \gamma_2^{(PO)}$	Calc. $\gamma_1^{(PO)}$	# $\Delta \gamma_1^{(PO)}$	Calc. $\gamma_2^{(PO)}$	# $\Delta \gamma_2^{(PO)}$
0.093	0.0284	0.0003	0.0281	0.0249	0.0341	-0.0092	1.0003	0.0285	1.0347	-0.0094
0.209	0.0609	0.0016	0.0593	-0.0244	0.0270	-0.0513	1.0016	0.0612	1.0273	-0.0514
0.332	0.0726	0.0041	0.0685	-0.0001	0.0201	-0.0202	1.0041	0.0712	1.0203	-0.0204
0.438	0.0865	0.0075	0.0790	0.0040	0.0148	-0.0108	1.0075	0.0828	1.0149	-0.0109
0.657	0.0844	0.0182	0.0662	0.0170	0.0060	0.0110	1.0184	0.0697	1.0060	0.0111
0.761	0.0435	0.0254	0.0180	0.0234	0.0030	0.0204	1.0257	0.0187	1.0030	0.0207
0.872	0.0200	0.0349	-0.0149	0.0165	0.0009	0.0156	1.0355	-0.0153	1.0009	0.0157

Average deviation in  $\gamma_1^{(PO)}$  = 0.04963Average deviation in  $\gamma_2^{(PO)}$  = 0.01995Average deviation in  $\ln \gamma_1^{(PO)}$  = 0.04772Average deviation in  $\ln \gamma_2^{(PO)}$  = 0.01978No. of  $\gamma_1$  data = 7.0No. of  $\gamma_2$  data = 7.0

$$\# \Delta \ln \gamma_i^{(PO)} = \ln \gamma_i \text{ (experimental)} - \ln \gamma_i \text{ (Calculated)} \quad (i = 1, 2)$$

$$\# \gamma_i^{(PO)} = \gamma_i \text{ (experimental)} - \gamma_i \text{ (calculated)} \quad (i = 1, 2)$$

for each point are also obtained.

It will be observed from Table XXV that the first round of least-squares fitting gave  $\alpha_{12} = 0.00054$  mole/cc at  $100^{\circ}\text{C}$ . The specified minimum mole fraction for x and y was 0.005, and since all the mole-fractions are larger than this value, all seven datum points in  $\gamma_1$  and  $\gamma_2$  are utilized in the first fitting. The percentage deviation in  $\ln \gamma_1^{(PO)}$ , which is also approximately the percentage deviation in  $\gamma_1^{(PO)}$ , is about 2.1 percent and that in  $\gamma_2^{(PO)}$  is 4.3 percent. The data are thermodynamically consistent since the difference in the average deviation of  $\gamma_1$  and  $\gamma_2$  is less than 3% (this is the criterion chosen, see the following section).

#### II(a). (II) Thermodynamic Consistency Test and Screening of Data

It is absolutely necessary to test the consistency of phase equilibrium data in terms of the rules of thermodynamics or in terms of the less rigorous yet well-established interproperty relations. The internal consistency of vapor-liquid equilibrium data are usually tested by the method proposed by Tao(214). The awkward data plotting procedure is replaced by a regression analysis. This also sets the error bound more precisely than any graphical procedure. The Redlich-Kister consistency criteria (215) have been extensively used in the literature. Therefore, it is necessary to make sure that the vapor-liquid equilibrium data satisfy the Gibbs-Duhem equation (see equation 44), which is the basis for most consistency tests. The high-pressure vapor-liquid equilibria present many difficulties, and many assumptions have to be made to simplify the requirements, for example, an equation of

state is used to calculate vapor-phase fugacity coefficients in the absence of volumetric data for vapor mixtures. Adler et al. (216) have proposed a method of testing the consistency when one of the components is above its critical temperature. They used Lewis' fugacity rule to calculate vapor-phase fugacities and since this introduces a large error Prausnitz et al. (115) have extended Redlich-Kister (215) and Herington's methods (217) to test the isothermal high-pressure data.

The average deviations of  $\gamma_1$  and  $\gamma_2$  are computed respectively at the end of the first round of fitting. If the experimental data are thermodynamically consistent, the average deviations of  $\gamma_1$  and  $\gamma_2$  are nearly equal in magnitude and generally small. If the data are inconsistent, the average deviation of  $\gamma$  for one component is generally much larger than that for the other; this happens because the less accurate set of data, say  $\gamma_1$ , scatters much more than the  $\gamma_2$  data, and the least-squares fitting, finding it impossible to fit the  $\gamma_1$  data any better, automatically fits better to the more accurate data for  $\gamma_2$ . If the average deviations of  $\gamma_1$  and  $\gamma_2$  data differ by more than 3%, the noise bound allowed in the computer program, the data may be considered as inconsistent. In such cases, the less reliable data are discarded, and the more reliable data are refitted after removing these individual points which have a percentage deviation larger than four times the average deviation of the more reliable data. In Table XXV, the second round of fitting would have removed any point in the  $\gamma_1$  or  $\gamma_2$  data, if such a point had a deviation greater than  $4 \times 0.021$  (in Table XXV, 0.021 is the smaller of the two average deviations in  $\ln \gamma$ ). Since

the consistency test is satisfied and none of the  $\gamma_1$  and  $\gamma_2$  datum points has this deviation, all the points are retained in the second round of fitting and same results are obtained. This second round of fitting is not included in Table XXV since for every isotherm the same results were obtained as in the first round of least squares fitting. Second round of fitting has been included only when some datum points have been screened (see Table XXVI).

II(a). (III) Analysis of the Binary System where  $T_{R_2} \geq 0.93$ .

Isotherms for which the reduced temperature of the lighter component exceeds 0.93, i.e. in the acetone (2) - benzene (1) system isotherms above 218.55°C, can be analyzed with the two-parameter dilated van Laar model using the unsymmetric convention for normalization (see page 56, Chapter I). The standard-state fugacity for component 2 (acetone) is Henry's constant of 2 in 1,  $H_{2(1)}^{(P0)}$  (see equation 43). This must be determined before the fitting can be carried out. Henry's constant is found with a program which contains a main program HENRYS and subroutines VOLPAR, PHIMIX and CUBEQN. The program calculates  $f_2^{(P)}/x_2$  for each point. Henry's constant is determined by plotting  $\ln f_2^{(P)}/x_2$  versus  $x_2$  and extrapolating to  $x_2 = 0$ , as shown in Figure 23. Correction of Henry's constant to zero pressure is performed in the fitting program. Figure 23 illustrates how Henry's constants are obtained from experimental data for several isotherms. In performing the extrapolation it is important to note that a plot of Henry's constant versus temperature is a smooth curve. Therefore, all the isotherms for the binary system benzene-acetone have been plotted on the same figure. The HENRYS program gives the following output:  $x_2, y_2, P, \bar{V}_1^L, \bar{V}_2^L, \phi_1$

TABLE XXVI

THERMODYNAMIC ANALYSIS OF THE SYSTEM BENZENE (1) - ACETONE (2) ABOVE  $T_{R2} = 0.93$

Temperature = 225.0°C, Reference Fugacity (1) = 15.164 atm., Saturation Pressure (1) = 20.921 atm.

Liquid Partial Molal Volume (1) at infinite dilution = 130.28 cc/mole,  $\bar{V}_2^\infty = 153.38$  cc/mole

T°C	$\frac{f_2}{x_2}$ atm.	(Total P - Sat.Press. of 1)atm.	$x_2$	$y_2$	P,atm.	Molal volume of saturated liquid mix. cc/mole	$\phi_1$	$\phi_2$	$\bar{V}_1^L$ , cc/mole	$\bar{V}_2^L$ , cc/mole	Corrected $T_R$ of liq. mixture
225.0	27.393	1.873	0.0930	0.1320	22.794	129.90	0.76792	0.84672	127.96	148.76	0.8942
225.0	30.500	4.186	0.2090	0.3100	25.107	129.53	0.74728	0.81901	125.76	143.80	0.9046
225.0	27.098	6.658	0.3320	0.4100	27.579	129.35	0.72489	0.79563	124.31	139.49	0.9159
225.0	27.548	8.785	0.4380	0.5250	29.706	129.42	0.70805	0.77368	123.85	136.56	0.9258
225.0	27.622	9.178	0.6570	0.7280	34.099	130.58	0.67599	0.73104	125.83	133.06	0.9468
225.0	27.852	15.265	0.7610	0.8235	36.186	131.91	0.66275	0.71128	128.71	132.91	0.9570
225.0	27.926	17.491	0.8720	0.9180	38.412	134.33	0.64891	0.69059	134.11	134.36	0.9678

Henry's constant at the saturation pressure of solvent determined graphically from above data = 25.517 atm.

$x_2$	$\phi_2$	Poynting Correction for $\gamma_1$	Poynting Correction for $\gamma_2$	(PO) $\gamma_1$	(PO) $\gamma_2$
0.0930	0.0786	1.0740	1.0865	1.0286	1.0687
0.2090	0.1802	1.0803	1.0924	0.9991	1.1836
0.3320	0.2925	1.0875	1.0987	1.0707	1.0455
0.4380	0.3933	1.0942	1.1043	1.0715	1.0575
0.6570	0.6144	1.1107	1.1174	1.0853	1.0478
0.7610	0.7259	1.1207	1.1249	1.0421	1.0496
0.8720	0.8500	1.1343	1.1346	0.9283	1.0434

$\alpha_{22}(1)$ , self-interaction constant of molecules 2 in the environment of molecules 1 = -0.00038 mole/cc.

$\eta_{2(1)}$ , dilation constant of solute 2 in solvent 1 = -0.41834.

TABLE XXVI (Cont'd)

$x_2$	$\ln \gamma_1^{(PO)}$	Calc. $\ln \gamma_1^{(PO)}$	$\neq$ $\Delta \ln \gamma_1^{(PO)}$	$\ln \gamma_2^{(PO)}$	Calc. $\ln \gamma_2^{(PO)}$	$\neq$ $\Delta \ln \gamma_2^{(PO)}$	Calc. $\gamma_1^{(PO)}$	$\neq$ $\Delta \gamma_1^{(PO)}$	Calc. $\gamma_2^{(PO)}$	$\neq$ $\Delta \gamma_2^{(PO)}$
0.093	0.0282	-0.0006	0.0288	0.0665	0.0124	0.0541	0.9994	0.0292	1.0125	0.0563
0.209	-0.0009	-0.0031	0.0022	0.1685	0.0263	0.1422	0.9969	0.0022	1.0267	0.1569
0.332	0.0684	-0.0076	0.0759	0.0444	0.0385	0.0060	0.9925	0.0783	1.0392	0.0062
0.438	0.0690	-0.0124	0.0814	0.0559	0.0462	0.0097	0.9877	0.0838	1.0473	0.0102
0.657	0.0819	-0.0197	0.1016	0.0467	0.0529	-0.0062	0.9805	0.1048	1.0544	-0.0066
0.761	0.0412	-0.0177	0.0589	0.0484	0.0522	-0.0038	0.9825	0.0596	1.0536	-0.0040
0.872	0.0744	-0.0067	-0.0677	0.0425	0.0499	-0.0074	0.9933	-0.0650	1.0511	-0.0078

Average deviation in  $\gamma_1^{(PO)} = 0.06041$

Average deviation in  $\ln \gamma_1^{(PO)} = 0.05949$

no. of  $\gamma_1$  data = 7.0

Second Round of Fitting

$\alpha_{22}(1) = -0.00022$  mole/cc.

Average deviation in  $\gamma_2^{(PO)} = 0.03541$

Average deviation in  $\ln \gamma_2^{(PO)} = 0.03277$

no. of  $\gamma_2$  data = 7.0

$\eta_{2(1)} = -0.20765$

$x_2$	$\ln \gamma_1^{(PO)}$	Calc. $\ln \gamma_1^{(PO)}$	$\neq$ $\Delta \ln \gamma_1^{(PO)}$	$\ln \gamma_2^{(PO)}$	Calc. $\ln \gamma_2^{(PO)}$	$\neq$ $\Delta \ln \gamma_2^{(PO)}$	Calc. $\gamma_1^{(PO)}$	$\neq$ $\Delta \gamma_1^{(PO)}$	Calc. $\gamma_2^{(PO)}$	$\neq$ $\Delta \gamma_2^{(PO)}$
0.093	0.0282	-0.0004	0.0285	0.0665	0.0072	0.0593	0.9996	0.0289	1.0072	0.0615
0.209	-0.0009	-0.0018	0.0009	0.1685	0.0155	0.1531	0.9982	0.0009	1.0156	0.1680
0.332	0.0684	-0.0047	0.0730	0.0444	0.0231	0.0213	0.9954	0.0754	1.0234	0.0221
0.438	0.0690	-0.0080	0.0771	0.0559	0.0285	0.0274	0.9920	0.0795	1.0289	0.0285
0.657	0.0819	-0.0166	0.0985	0.0467	0.0357	0.0110	0.9835	0.1018	1.0364	0.0114
0.761	0.0412	-0.0203	0.0616	0.0484	0.0373	0.0111	0.9799	0.0622	1.0380	0.0116
0.872	-0.0744	-0.0228	-0.0515	0.0425	0.0379	0.0046	0.9774	-0.0491	1.0386	0.0048

Average deviation in  $\gamma_1^{(PO)} = 0.05683$

Average deviation in  $\ln \gamma_1^{(PO)} = 0.05587$

No. of  $\gamma_1$  data = 7.0.

No. of  $\gamma_2$  data = 6.0.

QQXZ = -0.14546537, QQXY = 1.06316471, QQXX = 3.19300270

TABLE XXVI (Cont'd)

Temperature = 250°C, Reference fugacity (1) = 19.796 atm., Saturation pressure (1) = 29.470 atm.

Liquid partial molal volume (1) at infinite dilution = 142.27 cc/mole,  $\bar{v}_2^\infty = 184.34$  cc/mole.

T°C	$\frac{f_2}{x_2}$ atm.	(Total P - Sat.Press. of 1)atm.	$x_2$	$y_2$	P, atm.	Molal volume of saturated liquid mix. cc/mole	$\phi_1$	$\phi_2$	$\bar{V}_1^L$ , cc/mole	$\bar{V}_2^L$ , cc/mole	Corrected $T_R$ of liq. mixture
250.0	30.81	3.052	0.0930	0.1070	32.52	142.84	0.71103	0.82339	139.09	179.48	0.9391
250.0	32.25	5.880	0.2090	0.2400	35.35	144.09	0.68694	0.79446	135.92	175.01	0.9500
250.0	33.27	8.990	0.3320	0.3760	38.46	146.41	0.66228	0.76381	133.40	172.57	0.9619
250.0	33.68	11.73	0.4380	0.4850	41.20	149.86	0.64156	0.73820	131.58	173.31	0.9724
250.0	32.61	16.51	0.6570	0.6710	45.98	173.92	0.60808	0.69440	98.43	213.33	0.9946

Henry's constant at the saturation pressure of solvent determined graphically from above data = 30.756 atm.

$x_2$	$\phi_2$	Poynting Correction for $\gamma_1$	Poynting Correction for $\gamma_2$	(PO) $\gamma_1$	(PO) $\gamma_2$
0.0930	0.0786	1.1111	1.1457	1.0350	0.9923
0.2090	0.1802	1.1184	1.1550	1.0537	1.0303
0.3320	0.2925	1.1270	1.1672	1.0665	1.0517
0.4380	0.3933	1.1346	1.1810	1.0784	1.0522
0.6570	0.6144	1.1112	1.2567	1.2192	0.9574

Henry's constant at zero pressure = 27.10 atm.

$\alpha_{22}(1)$ , self-interaction constant of molecules 2 in the environment of molecules 1 = -0.00084 mole/cc.

$\eta_2(1)$ , dilation constant of solute 2 in solvent 1 = -2.66938.



TABLE XXVI (Cont'd)

$x_2$	$\ln \gamma_1^{(PO)}$	Calc. $\ln \gamma_1^{(PO)}$	# $\Delta \ln \gamma_1^{(PO)}$	$\ln \gamma_2^{(PO)}$	Calc. $\ln \gamma_2^{(PO)}$	# $\Delta \ln \gamma_2^{(PO)}$	Calc. $\gamma_1^{(PO)}$	# $\Delta \gamma_1^{(PO)}$	Calc. $\gamma_2^{(PO)}$	# $\Delta \gamma_2^{(PO)}$
0.093	0.0344	-0.0013	0.0357	-0.0077	0.0264	-0.0341	0.9987	0.0363	1.0267	-0.0344
0.209	0.0523	-0.0052	0.0575	0.0299	0.0494	-0.0195	0.9948	0.0589	1.0506	-0.0203
0.332	0.0644	-0.0058	0.0703	0.0505	0.0525	-0.0020	0.9942	0.0724	1.0539	-0.0021
0.438	0.0755	0.0080	0.0675	0.0509	0.0314	0.0195	1.0080	0.0704	1.0319	0.0204
0.657	0.1982	0.1656	0.0326	-0.0435	-0.0873	0.0438	1.1801	0.0391	0.9164	0.0410

Average deviation in  $\gamma_1^{(PO)} = 0.05540$

Average deviation in  $\gamma_2^{(PO)} = 0.02364$

Average deviation in  $\ln \gamma_1^{(PO)} = 0.05270$

Average deviation in  $\ln \gamma_2^{(PO)} = 0.02379$

No. of  $\gamma_1$  data = 5.0. No. of  $\gamma_2$  data = 5.0. QQXZ = 0.06979483. QQXY = 0.19190246. QQXX = 1.21501255

Temperature = 260°C, Reference fugacity (1) = 21.794 atm., Saturation Pressure (1) = 33.683 atm.

Liquid partial molal volume (1) at infinite dilution = 149.01 cc/mole,  $\bar{v}_2^\infty = 206.01$  cc/mole.

TOC	$\frac{f_2}{x_2}$ atm.	(Total P - Sat. Press. of 1) atm.	$x_2$	$y_2$	P, atm.	Molal volume of saturated liquid mix. cc/mole	$\phi_1$	$\phi_2$	$\bar{V}_1^L$ , cc/mole	$\bar{V}_2^L$ , cc/mole	Corrected $T_R$ of liq. mixture
260.0	34.05	3.138	0.0930	0.1050	36.82	150.57	0.68940	0.81900	145.24	202.53	0.9571
260.0	35.08	6.207	0.2090	0.2330	39.89	153.67	0.66375	0.78886	141.00	201.65	0.9682
260.0	35.14	9.518	0.3320	0.3560	43.20	159.80	0.63710	0.75869	135.53	208.63	0.9804
260.0	34.43	12.24	0.4380	0.4465	45.92	171.85	0.61514	0.73559	119.78	238.64	0.9912

Henry's constant at the saturation pressure of the solvent determined graphically from above data = 31.845 atm.

TABLE XXVI (Cont'd)

$x_2$	$y_2$	$\phi_2$	Poynting Correction for $\gamma_1$	Poynting Correction for $\gamma_2$	$\gamma_1$ (PO)	$\gamma_2$ (PO)
0.0930	0.1050	0.0786	1.1300	1.1859	1.0170	1.0565
0.2090	0.2330	0.1802	1.1372	1.2019	1.0358	1.0742
0.3320	0.3560	0.2925	1.1432	1.2288	1.0650	1.0525
0.4380	0.4465	0.3933	1.1340	1.2847	1.1256	0.9863

$\alpha_{22}(1)$ , self-interaction constant of molecules 2 in the environment of molecules 1 = -0.0017 mole/cc.

$\eta_2(1)$ , dilation constant of solute 2 in solvent 1 = -4.47296.

Henry's constant at zero pressure = 27.174 atm.

$x_2$	$\ln \gamma_1^{(PO)}$	Calc. $\ln \gamma_1^{(PO)}$	$\neq$ $\Delta \ln \gamma_1^{(PO)}$	$\ln \gamma_2^{(PO)}$	Calc. $\ln \gamma_2^{(PO)}$	$\neq$ $\Delta \ln \gamma_2^{(PO)}$	Calc. $\gamma_1^{(PO)}$	$\#$ $\Delta \gamma_1^{(PO)}$	Calc. $\gamma_2^{(PO)}$	$\#$ $\Delta \gamma_2^{(PO)}$
0.093	0.0169	-0.0025	0.0194	0.0550	0.0524	0.0026	0.9975	0.0195	1.0538	0.0027
0.209	0.0352	-0.0081	0.0432	0.0715	0.0871	-0.0156	0.9920	0.0438	1.0910	-0.0168
0.332	0.0629	0.0056	0.0574	0.0512	0.0550	-0.0039	1.0056	0.0594	1.0566	-0.0041
0.438	0.1183	0.0734	0.0449	-0.0137	-0.0497	0.0360	1.0761	0.0494	0.9515	0.0348

Average deviation in  $\gamma_1^{(PO)}$  = 0.04304

Average deviation in  $\gamma_1^{(PO)}$  = 0.01461

Average deviation in  $\ln \gamma_1^{(PO)}$  = 0.04122

Average deviation in  $\ln \gamma_2^{(PO)}$  = 0.01449

No. of  $\gamma_1$  data = 4.0

No. of  $\gamma_2$  data = 4.0

QQXZ = -0.01552030. QQXY = 0.03994685. QQXX = 0.57122391.

TABLE XXVI (Cont'd)

Temperature = 270°C, Reference fugacity (1) = 23.865 atm., Saturation Pressure (1) = 37.921 atm.

Liquid partial molal volume (1) at infinite dilution = 158.31 cc/mole,  $\bar{v}_2^\infty = 243.40$  cc/mole.

T°C	$\frac{f_2}{x_2}$ atm.	(Total P - Sat. Press. of 1) atm.	$x_2$	$y_2$	P, atm.	Molal volume of saturated liquid mix. cc/mole	$\phi_1$	$\phi_2$	$\bar{V}_1^L$ , cc/mole	$\bar{V}_2^L$ , cc/mole	Corrected $T_R$ of liq. mixture
270.0	35.16	3.378	0.0930	0.0960	41.30	162.10	0.66823	0.82476	153.30	247.88	0.9750
270.0	36.60	5.201	0.1510	0.1580	43.12	165.65	0.65201	0.81121	149.55	256.23	0.9807
270.0	37.19	6.759	0.2090	0.2190	44.68	171.00	0.63923	0.79426	143.68	274.38	0.9865

Henry's Constant at the saturation pressure of solvent determined graphically from above data = 33.615 atm.

$x_2$	$y_2$	$\phi_2$	Poynting Correction for $\gamma_1$	Poynting Correction for $\gamma_2$	$\gamma_1^{(PO)}$	$\gamma_2^{(PO)}$
0.0930	0.0960	0.0786	1.1527	1.2583	0.9999	1.0227
0.1510	0.1580	0.1289	1.1557	1.2814	1.0110	1.0453
0.2090	0.2190	0.1802	1.1550	1.3167	1.0231	1.0336

Henry's constant at zero pressure = 27.325 atm.

$\alpha_{22}(1)$ , self-interaction constant of molecules 2 in the environment of molecules 1 = -0.0011 mole/cc.

$\eta_2(1)$ , dilation constant of solute 2 in solvent 1 = -10.10114.

TABLE XXVI (Cont'd)

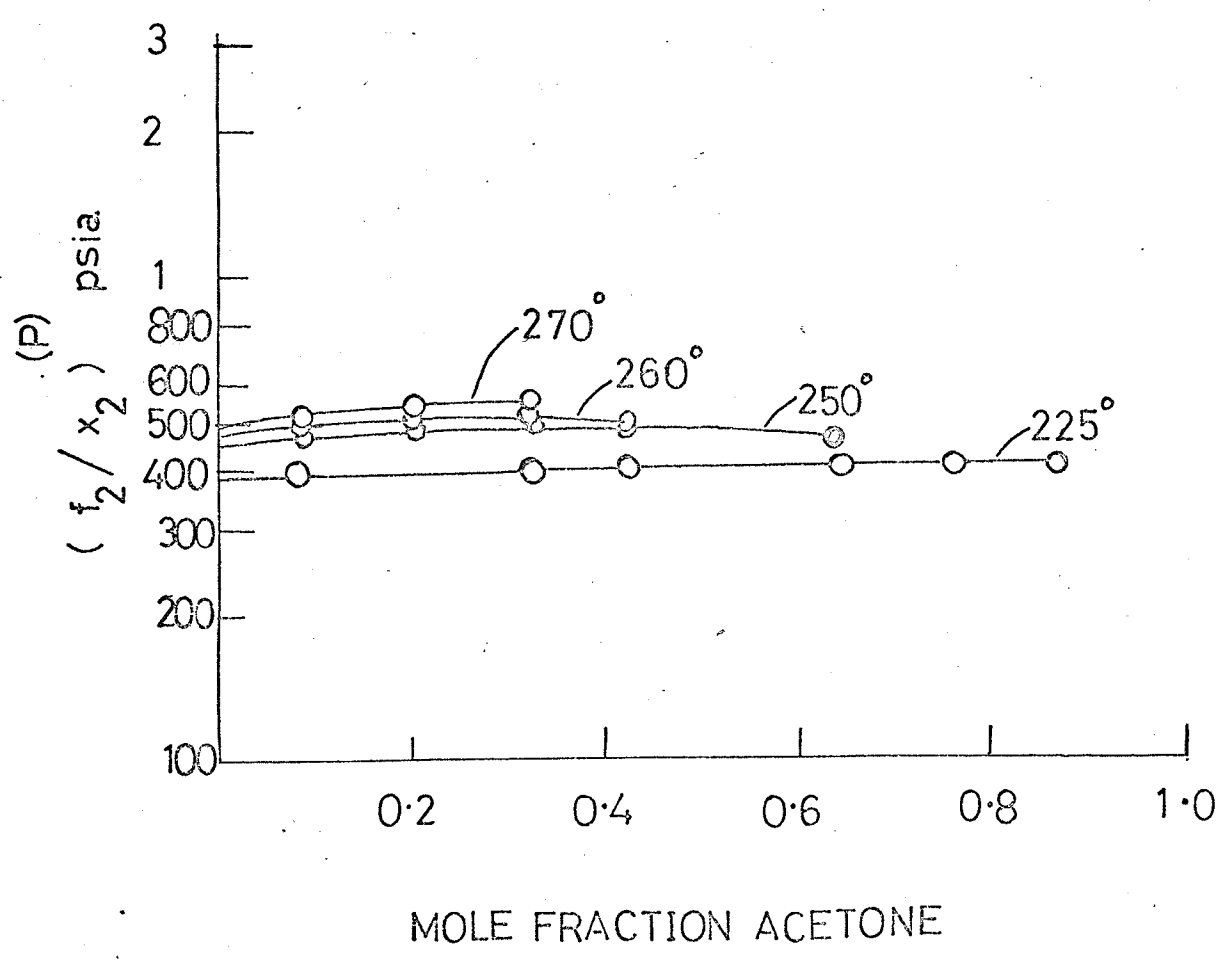
$x_2$	$\ln \gamma_1^{(PO)}$	Calc. $\ln \gamma_1^{(PO)}$	# $\Delta \ln \gamma_1^{(PO)}$	$\ln \gamma_2^{(PO)}$	Calc. $\ln \gamma_2^{(PO)}$	# $\Delta \ln \gamma_2^{(PO)}$	Calc. $\gamma_1^{(PO)}$	# $\Delta \gamma_1^{(PO)}$	Calc. $\gamma_2^{(PO)}$	# $\Delta \gamma_2^{(PO)}$
0.093	-0.0001	-0.0014	0.0013	0.0224	0.0315	-0.0091	0.9986	0.0013	1.0320	-0.0093
0.1510	0.0109	-0.0024	0.0133	0.0443	0.0388	0.0056	0.9976	0.0133	1.0395	0.0058
0.2090	0.0228	-0.0002	0.0229	0.0331	0.0294	0.0037	0.9998	0.0232	1.0298	0.0038
Average deviation in $\gamma_1^{(PO)}$ = 0.01262				Average deviation in $\gamma_2^{(PO)}$ = 0.00631						
Average deviation in $\ln \gamma_1^{(PO)}$ = 0.01251				Average deviation in $\ln \gamma_2$ = 0.00611						
No. of $\gamma_1$ data = 3.0				No. of $\gamma_2$ data = 3.0						
QQXZ = -0.01980372			QQXY = 0.00206222			QQXX = 0.13172585				

$$\# \Delta \ln \gamma_i^{(PO)} = \ln \gamma_i \text{ (experimental)} - \ln \gamma_i \text{ (calculated)} \quad (i = 1, 2)$$

$$\# \gamma_i^{(PO)} = \gamma_i \text{ (experimental)} - \gamma_i \text{ (calculated)} \quad (i = 1, 2)$$

FIGURE 23. Plot of Henry's Constant  $H_{2(1)}^{(P_1^S)}$  for Acetone (2) in Benzene (1) at 225°, 250°, 260°, and 270°C.

$(\ln \frac{f_2^{(P)}}{x_2} \text{ lb./sq. in. abs.})$  is plotted against  $x_2$  to evaluate Henry's constant,  $H_{2(1)}^{(P_1^S)}$ , by extrapolation to  $x_2 = 0$ . It may be observed that the absolute pressure has not been converted to atmospheres, since  $H_{2(1)}^{(P_1^S)}$  must be in p.s.i.a. for the FITTING program.)



and  $\phi_2$ , the saturation pressure of component 1, liquid partial molal volumes of both components at infinite dilution, reference fugacity of component 1 at zero pressure, molal volumes of the saturated liquid mixture for each concentration and the corrected reduced temperatures of the liquid mixture for each concentration. These can then be used in the FITTING program to evaluate the self-interaction constant,  $\alpha_{22(1)}$ , and the dilation constant  $\eta_{2(1)}$  in the dilated van Laar model. This fitting program has, like the SYMFIT program, a provision for testing thermodynamic consistency of experimental data and for screening of data.

In any two-parameter model, the two "best" parameters, as found by the computer are often not unique; considering experimental uncertainties, there are several sets of two parameters which may equally well represent the experimental data. Prausnitz et al. (116) have observed that  $\alpha_{22(1)}$  is more important and less uncertain than  $\eta_{2(1)}$  in the dilated van Laar model. The magnitude of the dilation constant shows a consistent and meaningful variation with respect to the temperature and the properties of the constituent components. As seen from Table XXVI, the dilation constants are larger for the isotherms approaching the critical temperature of benzene (the heavy component) i.e. they are larger at temperatures where the light component acetone is supercritical. This behavior of dilation constants is in agreement with their physical significance in the dilated van Laar model -- i.e., the liquid phase is dilated most when the subcritical heavy component itself is near its critical temperature, or when the light component is far above its critical temperature. Under these conditions the liquid

molal volume increases sharply with dissolved gas. The molal volume of the saturated liquid mixture at a temperature of 225°C and composition 0.093 mole fraction acetone is 129.9 cc/mole, which increases to 162.1 cc/mole at a temperature of 270°C, i.e. 35° above the critical temperature of acetone and about 19° below the critical temperature of benzene. Chueh et al. (116) have generalized  $\ln (\eta/\eta^*)^{1/2}$  in terms of  $T^*/T$  into a single reduced plot where  $\eta^*$  is a constant characteristic of the light component and  $T^*$  is a constant characteristic of the binary system. At a low temperature  $\eta_{2(1)}$  is small and because of lack of uniqueness,  $\eta_{2(1)}$  as determined from a least-squares fit may be a negative number. However, Chueh et al. (116) argue that a negative  $\eta_{2(1)}$  is not permitted by the solution model, and therefore a small positive  $\eta$  and a corresponding adjustment in  $\alpha$  will probably fit the experimental data equally well, within the experimental uncertainty. In any case, this was not found possible to do with my data. First of all negative values of  $\eta$  were not small in my case, and also the values of  $(\eta^*)^{1/2}$  for acetone could not be obtained. Chueh et al. have listed  $(\eta^*)^{1/2}$  values for various lighter gases in their publication (Figure 5, Reference 116) and I presume these values are selected on the basis of some available experimental data of the lighter components when dissolved in various solvents. The value for methane has been set equal to one for convenience and value for the quantum gases as zero. On this basis alone I have not been able to obtain any  $(\eta^*)^{1/2}$  value for acetone which I could use to get a positive value of  $\eta_{2(1)}$  for the binary system benzene-acetone. Chueh et al. (116) then give the following relation to obtain the  $\alpha_{22(1)}$  value, once  $\eta_{2(1)}$  is forced to become positive from the



generalized curve

$$\alpha_{22(1)} = \frac{1}{v_{c1}} \cdot \frac{QQXZ}{QQXX + 3n_{2(1)}QQXY} \quad (110)$$

where QQXZ, QQXX and QQXY are intermediate quantities in the least-squares program which are produced in the computer output of the FITTING program. Interestingly enough, the values for  $\alpha_{22(1)}$  are also negative, as obtained from my experimental data. The dilated van Laar model of Chueh and Prausnitz is based on the assumption that the nonideality of liquid mixtures is due to the interaction of solute molecules with each other in the environment of the solvent molecules and not because of interactions between the solute and solvent molecules (see page 56, this thesis). It is not quite clear whether such a model can be applied to benzene-acetone mixtures with advantage, especially in view of the fact that satisfactory results have not been obtained above the critical temperature of the lighter component (acetone). Acetone is definitely polar and the corresponding states theory of Scott (102), which is probably the most useful general theory for mixtures of simple non-polar liquids cannot be applied either. Scott has expressed the free energy of a liquid as a universal function of the reduced temperature and reduced pressure. The reducing parameters used by him are the characteristic intermolecular energy and molecular size. The free energy of a liquid mixture is then given by the same universal function using reducing parameters which are functions of composition. Thus, the excess free energy relative to an ideal gas at the same temperature and pressure, and the activity coefficients of the liquid mixture are easily found. Scott has proposed three different

ways by which the characteristic molecular parameters vary with the composition: (1) the liquid mixture consists of uniform cells all of the same size (the "single liquid solution"), (2) the liquid mixture consists of two kinds of cells, one for molecules of component 1 and one for molecules of component 2 (the "two liquid solution"), and (3) the liquid mixture has interactions of three kinds, the 1-1, 1-2, and 2-2 interactions (the "three liquid solution"). It is known that there is a close agreement of experimental results obtained at or near boiling points of mixtures with those predicted by Scott's "two liquid solution" theory. The "three liquid solution" theory does not apply to liquid mixtures very well and is valid for dilute gas mixtures only. Therefore, the activity coefficients of a liquid mixture at high pressures where one component is above its critical temperature should probably be best described by a theory which would be between "two liquid solution" and "three liquid solution" relationships. I presume the "two liquid solution" relation will give too high excess free energy and the "three liquid solution" will give too low value at conditions above the critical temperature of one of the components. Since at present there is no solution theory which will predict the correct activity coefficients under conditions considered here I hope this research will at least contribute to the experimental evidence needed to test possible future theories.

SUMMARY AND CONCLUSIONS

This thesis deals with the following physical and thermodynamic properties of the pure liquids acetone, benzene, chloroform and carbon tetrachloride and of mixtures of the binary system acetone-benzene in the whole concentration range and over the temperature range of 100°C to the respective critical points:- viz., orthobaric volumes, vapor pressure, critical constants, vapor-liquid equilibrium compositions.

The orthobaric volumes were obtained by means of a sealed tube technique and the critical phenomena were observed over a range of total volume which did not necessarily prove that the nose of the curve of orthobaric densities versus temperature was horizontal. The vapor pressure was measured by a closed air-manometer and the pressure was calculated from the equilibrium volume of compressed air, using van der Waals' equation. Other equations of state did not give markedly better results and variations were within the experimental error.

The critical temperatures of the pure compounds as well as those of mixtures were determined by the disappearance-of-the meniscus method. Critical densities of the pure compounds were obtained by the application of the law of rectilinear diameter, and the critical pressures by extrapolation of the log P versus 1/T line to the critical temperature.

In an effort to calculate the non-ideal behavior in each of the two phases in the vapor-liquid equilibria, an equation of state suggested by Redlich and Kwong was used for vapor-phase properties, and a modified van Laar equation for liquid-phase properties. The equation of Redlich and Kwong has been found to provide a simple method for calculation of fugacity coefficients. The dimensionless constants

$\Omega_a$  and  $\Omega_b$  have been re-evaluated from the saturated volumetric properties of each pure component as suggested by Chueh and Prausnitz. Redlich-Kwong equation, as modified by Chueh and Prausnitz, also has a binary interaction constant which significantly increases its accuracy for mixtures. Following the solution model of these authors, I attempted to account for the effect of composition on liquid-phase properties by a modified van Laar equation. There was little success above the critical temperature of acetone; but, the one-parameter model, when both components are below a reduced temperature of 0.93, was fairly successful. For showing the effect of pressure on liquid-phase properties, the partial molal liquid volumes were calculated using a liquid-phase equation of state coupled with an extension to mixtures of the corresponding-states correlation of Lyckman et al. The pressure correction (Poynting correction) to the activity coefficient in the liquid phase was then calculated from the partial molal volumes. The calculations are sensitive to the characteristic energy between two dissimilar molecules. These energies are known for a number of binary systems from either the second virial cross coefficients or the binary saturated liquid volumes. Since these are not known for acetone-benzene system, and generally for any mixture containing a polar compound, it cannot be definitely concluded as to what happens at high temperatures and pressures to such mixtures. Work is in progress in this laboratory to determine the saturated liquid volumes of certain binary systems containing polar components. Recently in a critical review of the phase behavior of mixtures Kay (218) has reiterated the importance of the interaction energies. While discussing the shape of

the critical locus curve of a mixture he says, "The shape of the critical locus curve is ultimately the result of the sum total of the potential energies of interaction between the molecules. However, we do not have sufficient knowledge of how molecules interact to evaluate these potentials, and hence we choose size, shape, and chemical nature of the molecules as practical parameters to distinguish between the different types of phase behavior exhibited by mixtures in the vapor and liquid states".

APPENDIX

The programs used in vapor-liquid equilibrium are given in "Appendix D" of the monograph by Prausnitz and Chueh (116). The title of the programs that I have used are given in Chapter V of this thesis -- they are the same as written by Chueh and Prausnitz.

The information for input data used in these programs was obtained as follows:

1) Pure component data -

$T_c$ ,  $P_c$ ,  $V_c$  for acetone and benzene were taken from the results obtained in this work. Acentric factors for these compounds were calculated from the vapor pressure data of the pure components using the equation given on page 46 ( $\omega$  for benzene = 0.211 and  $\omega$  for acetone 0.309). The dimensionless constants in the Redlich-Kwong equation of state were evaluated for each pure component by fitting equation (25) to the volumetric data of the saturated vapor and saturated liquid. They are slightly different from the universal values.

	Liquid Phase		Vapor Phase	
	$\Omega_a$	$\Omega_b$	$\Omega_a$	$\Omega_b$
Acetone	0.3900	0.0745	0.4600	0.0940
Benzene	0.4100	0.0787	0.4450	0.0904

The universal values are  $\Omega_a = 0.4278$  and  $\Omega_b = 0.0867$ . The coefficients for the reduced reference liquid fugacity of the two components at zero pressure which fitted the following equation

$$\ln \frac{f_{\text{pure}}^{(PO)}}{P_c} = C_0 + C_1/T_R + C_2/T_R^2 + C_3/T_R^3 + C_4/T_R^4 \quad (111)$$

were evaluated from the generalized table of Lyckman et al. (117).

In this table Lyckman et al. have tabulated the values of

$$\left( \log \frac{f_{\text{pure}}^{(PO)}}{P_c} \right)^{(0)} \quad \text{and} \quad \left( \log \frac{f_{\text{pure}}^{(PO)}}{P_c} \right)^{(1)} \quad \text{for different values of } T_R.$$

These values were fitted to equation (111) for each component by a

polynomial regression analysis and the following coefficients obtained

	<u>Acetone</u>	<u>Benzene</u>
$C_0 =$	-1.98432	0.69309
$C_1 =$	10.13478	2.68502
$C_2 =$	-11.89554	-4.62806
$C_3 =$	3.64036	0.70543
$C_4 =$	-0.45048	0.0

## 2) Vapor-phase and critical binary constants

The second virial coefficients of pure benzene and pure acetone are available in the literature up to 335° and 150° respectively (219). The cross coefficients have not been determined for this system beyond 90°C (139) and no experimental information is available about the saturated liquid volumes of this binary system. Therefore, the binary constant  $k_{12}$  which represents the deviation from the geometric mean for  $T_{c12}$  (see equation 36) was estimated ( $k_{12} = 0.01$ ) from interpolation.

The critical binary constant  $2\tau_{12}/(T_{c1} + T_{c2})$  was obtained from the experimental data of the critical temperatures of the binary mixture shown in Table XIII. Since the experimental volumetric data in the critical region were not available for the binary mixture, the correlating parameter for critical volumes  $2v_{12}/(v_{c1} + v_{c2})$  was

estimated from the generalized chart (p.41, ref. 116) given in the monograph. Parameters  $\tau_{12}$  and  $\nu_{12}$  are required only if  $T/T_{CM}$  is close to or larger than 0.93.



BIBLIOGRAPHY

1. de la Tour, C., Ann.Chim.Phys. (2) 21, 127 (1822)
2. Konig, W., Ann.Physik 11, 985 (1931)
3. Schmidt, G.G., Gilbert's Ann. 75, 343 (1823)
4. Andrews, T., Trans.Roy.Soc.London A159, 575 (1869)
5. Andrews, T., Proc.Roy.Soc. London A18, 42 (1869)
6. Andrews, T., Trans.Roy.Soc.London A166, 421 (1876)
7. Andrews, T., Trans.Roy.Soc.London A178, 45 (1887)
8. van der Waals, J.D., Doctoral Dissertation, Leiden, The Netherlands, 1873.
9. Kuenen, J.P., Die Zustandsgleichung (Vieweg, Braunschweig, 1907), Chapter V.
10. Bruhat, G., Chaleur et ind., 11, 263 (1930)
11. Clark, A.L., Chem.Rev. 23, 1 (1938)
12. Traube, I., Trans.Faraday Soc. 34, 1234 (1938)
13. Brescia, F., J.Chem.Education 24, 123 (1947)
14. Bakker, G., Z.Physik.Chem. 49, 609 (1904)
15. Mayer, J.E., Harrison, S.F., J.Chem.Phys. 6, 101 (1938)
16. Mayer, J.E., Mayer, M.G., "Statistical Mechanics", John Wiley & Sons, Inc., New York 1940, (Chapter 14)
17. Maass, O., Geddes, A.L., Trans.Roy.Soc. (London) A236, 303 (1937)
18. McIntosh, R.L., Dacey, J.R., Maass, O., Can.J.Research 17B, 241 (1939)
19. McIntosh, R.L., Maass, O., Can J. Research 16B, 289 (1938)
20. Naldrett, S.N., Maass, O., Can.J.Research 18B, 118 (1940)
21. Weinberger, M.A., Schneider, W.G., Can.J.Chem. 30, 422 (1952)
22. "Proceedings of the International Conference on Phenomena near Critical Points, Washington, 1965", NBS Misc. Publication No. 273, (1966).
23. "Symposium on Critical Phenomena in Magnetism", J.Appl.Phys. 37, No. 3, 1172 (1966)
24. Rowlinson, J.S., "Liquids and Liquid Mixtures", Butterworths Scientific Publications, London, 1959.
25. Rice, O.K., Chem.Rev. 44, 69 (1949)
26. Rice, O.K., "Thermodynamics and Physics of Matter", edited by F.D. Rossini, Princeton University Press, Princeton, N.J., 1955.

27. Kac, M., Uhlenbeck, G.E., Hemmer, P.C., J.Math.Phys. 4, 216, 229 (1963) and 5, 60 (1964)
28. Fisher, M.E., J.Appl.Phys. 38, 981 (1967)
29. Fisher, M.E., Rept.Progr.Phys. 30, 615 (1967) The Institute of Physics and Physical Society, London.
30. Heller, P., Rept.Progr.Phys. 30, 731 (1967) The Institute of Physics and Physical Society, London.
31. Kadanoff, L.P., Gotze, W., Hamblen, D., Hecht, R., Lewis, E.A.S., Palciauskas, V.V., Rayl, M., Swift, J., Rev.Mod.Phys. 38, 205 (1966)
32. Sengers, J.V., Levelt-Sengers, A., Chem.Eng.News 46, No.25, 104 (1968)
33. Green, M.S., Vicentini-Missoni, M., Levelt-Sengers, J.M.H., Phys. Rev.Letters, 18, 1113 (1967)
34. Onsager, L., Phys.Rev. 65, 117 (1944) and Physical Society Cambridge Conference Report, p.137 (1947)
35. Fisher, M.E., Burford, R.J., Phys.Rev. 156, No.2., 583 (1967)
36. Fierz, M., Helv.Phys.Acta., 24, 357 (1951)
37. de Boer, J., Changement de Phases, C.R. Deuxieme Reunion de Chimie Physique, Paris, p.8 (1952)
38. Fisher, M.E., Lectures in Theoretical Physics VII C (University of Colorado Press, Boulder) pp 1-159 (1965), Edited by W.E. Brittin
39. Essam, J.W., Fisher, M.E., J.Chem.Phys. 38, 802 (1963)
40. Widom, B., J.Chem.Phys. 43, 3898 (1965)
41. Kadanoff, L.P., Physics 2, 263 (1966)
42. Griffiths, R.B., Phys.Rev. 158, No.1, 176 (1967)
43. Lorentzen, H.L., "Statistical Mechanics of Equilibrium and Non-equilibrium", North-Holland Publishing Co., Amsterdam, 1965, p.262.
44. Lorentzen, H.L., Acta.Chem.Scand. 7, 1335 (1953)
45. Voronel<sup>†</sup>, A.V., Chashkin, Yu.R., Popov, V.A., Simkin, V.G., Soviet Phys. - JETP 18, 568 (1964)
46. Bagatskii, M.I., Voronel<sup>†</sup>, A.V., Gusak, V.G., Soviet Phys. - JETP 16, 517 (1963)
47. Amirkhonov, Kh.I., Gurvich, I.G., Dokl. Akad.Nauk. SSSR 91, 221 (1953); Chem.Abs. 48, 13363 g (1954)
48. Wentorf, R.H., J.Chem.Phys. 24, 607 (1954)
49. Rice, O.K., Thompson, D.R., J.Am.Chem.Soc. 86, 3547 (1964)
50. Rice, O.K., J.Phys. & Colloid Chem. 54, 1293 (1950)

51. Zimm, B.H., J. Phys. & Colloid Chem. 54, 1306 (1950)
52. Rice, O.K., and Rowden, R.W., "Changements de Phases", Comptes rendus, Societe de Chimie Physique, Paris, 1952.
53. Atack, D., Rice, O.K., Disc. Faraday Soc. 15, 210 (1953), J. Chem. Phys. 22
54. Rice, O.K., J. Chem. Phys. 23, 164 (1955) 382 (1954)
55. Chu, B., J. Am. Chem. Soc. 86, 3557 (1964)
56. Debye, P.J.W., J. Chem. Phys. 31, 690 (1959)
57. Scott, R.L., J. Phys. Chem. 62, 136 (1958)
58. Fisher, M.E., J. Math. Phys. 5, 944 (1964)
59. Widom, B., Rice, O.K., J. Chem. Phys. 23, 1250 (1955)
60. Davis, B.W., Rice, O.K., J. Chem. Phys. 47, 5043 (1967)
61. Dunlap, R.D., Furrow, S.D., J. Phys. Chem. 70, 1331 (1966)
62. Young, S., Z. Phys. Chem. 29, 139 (1899)
63. Young, S., Sci. Proc. Roy. Dublin Soc., New Series 12, 374 (1910)
64. Young, S., J. Chem. Soc. 59, 911 (1891)
65. Young, S., Edinburgh and Dublin Phil. Mag. & J. Sci. 50, 291 (1900)
66. Smith, J.M., "Introduction to Chemical Engineering Thermodynamics", p. 168, McGraw Hill Book Co., Inc., New York (1949)
67. Gibbs, J.W., Collected Works, Yale University Press, New Haven, 1928.
68. Lewis, G.N., Proc. Nat. Acad. Sci. U.S. 37, 49 (1901) and Z. Phys. Chem. 38, 205 (1901)
69. Pitzer, K.S., Lippman, D.Z., Curl, R.F. Jr., Huggins, C.M. and Peterson, D.E., J. Am. Chem. Soc. 77, 3433 (1955)
70. Riedel, L., Chemie-Ing-Tech. 26, 83, 259, 679 (1954); 27, 209, 475 (1955)
71. Wegscheider, R., Z. Physik. Chem. 99, 361, (1921) and 135, 362 (1928)
72. Wohl, A., Z. Physik. Chem. 87, 1 (1914) and 99, 207 (1921)
73. Neusser, E., Physik. Z. 35, 738 (1934)
74. Martin, J.J., Ind. Eng. Chem. 59, No. 12, 35 (1967)
75. Shah, K.K and Thodos, G., Ind. Eng. Chem., 57, No. 3, 30 (1965)
76. Redlich, O. and Kwong, J.N.S., Chem. Rev. 44, 233 (1949)
77. Benedict, M., Webb, G.B., and Rubin, L.C., J. Chem. Phys. 8, 334 (1940),  
ibid. 10, 747 (1942) and Chem. Eng. Progr. 47, 419 (1951)
78. Martin, J.J., Hou, C.Y., A. I. Ch. E. J., 1, 142 (1955)
79. a) Redlich, O., Ackerman, F.J., Gunn, R.D., Jacobson, M., Lau, S., Ind. Eng. Chem. (Fundamentals) 4, 369 (1965)  
b) Correction: Ind. Eng. Chem. (Fundamentals) 6, No. 4, 619 (1967)

80. Redlich, O., Dunlap, A.K., Chem. Eng. Progr. Symp. Ser. 59, 95 (1963)
81. Edmister, W.C. and Yarborough, L., A.I.Ch.E.J. 9, 240 (1963)
82. Ackerman, F.J. and Redlich, O., J. Chem. Phys. 38, 2740 (1963)
83. Wilson, G.M., Advan. Cryog. Eng. 9, 168 (1964)
84. Robinson, R.L., Jacoby, R.H., Hydrocarbon Process. Petrol. Refiner 44, No. 4, 141 (1965)
85. Barner, H.E., Pigford, R.L., Schreiner, W.C., Proc. Am. Petrol. Inst. (Division of Refining) 46, 244 (1966)
86. Estes, J.M., Tully, P.C., A.I.Ch.E.J. 13, 192 (1967)
87. Chueh, P.L., Prausnitz, J.M., Ind. Eng. Chem. (Fundamentals) 6, 492 (1967)
88. Joffe, J., Zudkevitch, D., Ind. Eng. Chem. (Fundamentals) 5, 455 (1966)
89. Chueh, P.L., Prausnitz, J.M., A.I.Ch.E.J. 13, 896 (1967)
90. Chueh, P.L., Prausnitz, J.M., A.I.Ch.E.J. 13, 1099 (1967)
91. Orentlicker, M., Prausnitz, J.M., Can. J. Chem. 45, 373 (1967)
92. Prausnitz, J.M., Gunn, R.D., A.I.Ch.E.J. 4, 430 (1958)
93. McGlashan, M.L., Potter, D.J.B., Proc. Roy. Soc. (London) A206, 448 (1951)
94. Hudson, G.H., McCoubrey, J.C., Trans. Faraday Soc., 56, 761 (1960)
95. Fender, B.E.F., Halsey, G.D., J. Chem. Phys. 36, 1881 (1962)
96. Dantzler, E.M., Knobler, C.M., Windsor, M.L., J. Phys. Chem. 72, 676 (1968)
97. Beattie, J.A., Chem. Rev. 44, 141 (1949)
98. Prausnitz, J.M., A.I.Ch.E.J. 5, 3 (1959)
99. Lewis, G.N., Randall, M., "Thermodynamics", McGraw-Hill, New York, 1923
100. Pitzer, K.S., J. Chem. Phys. 7, 583 (1939)
101. Longuet-Higgins, H.C., Proc. Roy. Soc. (London), A205, 247 (1951)
102. Scott, R.L., J. Chem. Phys. 25, 193 (1956)
103. Brown, W.B., Phil. Trans. A250, 175 (1957)
104. Prigogine, I., "The Molecular Theory of Solutions", Interscience, New York (1957)
105. Wojtowicz, P.J. et al., J. Chem. Phys. 27, 505 (1957)
106. Flory, P.J., J. Am. Chem. Soc. 87, 1833 (1965)
107. Stiel, L.I., Ind. Eng. Chem. 60, No. 5, 50 (1968)
108. Joffe, J., Ind. Eng. Chem. 40, 1738 (1948)

109. Leland, T.W., Chappellear, P.S., Gamson, B.W., A.I.Ch.E.J. 8, 482 (1962)
110. Leland, T.W., Chappellear, P.S., Ind.Eng.Chem. 60, No. 7, 15 (1968)
111. Pitzer, K.S., Lippman, D.Z., Curl, R.F., Huggins, C.M., Petersen, D.E., J.Am.Chem.Soc. 77, 3427, 3433 (1955)
112. O'Connell, J.P., Prausnitz, J.M., Ind.Eng.Chem.Process Design Develop. 6, 245 (1967)
113. Wohl, K., Trans.A.I.Ch.E. 42, 215 (1946)
114. Prausnitz, J.M., Chem.Eng.Sci. 18, 613 (1963)
115. Chueh, P.L., Muirbrook, N.K., Prausnitz, J.M., A.I.Ch.E.J. 11, 1097 (1965)
116. Quoted in Prausnitz, J.M. and Chueh, P.L., Ind.Eng.Chem. Vol. 60, No. 3, 34 (1968)  
Prausnitz, J.M., Chueh, P.L., "Computer Calculations for High-Pressure Vapor-Liquid Equilibria", Prentice-Hall, 1968. (Published since)
117. Lyckman, E.W., Eckert, C.A., Prausnitz, J.M., Chem.Eng.Sci. 20, 703 (1965)
118. Kay, W.B., Ind.Eng.Chem. 28, 1014 (1936)
119. Joffe, J., Ind.Eng.Chem. 39, 837 (1947)
120. Stewart, W.E., Burkhardt, S.F. and Voo, D., paper presented at A.I.Ch.E. Kansas City Meeting (May 18, 1959)
121. Pitzer, K.S., Hultgren, G.O., J.Am.Chem.Soc. 80, 4793 (1958)
122. Chueh, P.L., Prausnitz, J.M., A.I.Ch.E.J. 13, 1107 (1967)
123. Meissner, H.P., Sefarian, R., Chem.Eng.Progr. 47, 579 (1951)
124. Rowlinson, J.S., Trans.Faraday Soc. 51, 1317 (1955)
125. Smith, R.L., Watson, K.M., Ind.Eng.Chem. 29, 1408 (1937)
126. Kurata, F., Katz, D.L., Trans.Am.Inst.Chem.Engrs. 38, 995 (1942)
127. Mayfield, F.D., Ind.Eng.Chem. 34, 843 (1942)
128. Organick, E.I., Brown, G.G., Chem.Eng.Progr.Symp.Ser. No.2, 48, 97 (1952)
129. Organick, E.I., Chem.Eng.Progr.Symp.Ser. No. 6, 49, 81 (1953)
130. Davis, P.C., Bertuzzi, A.F., Gore, T.L., Kurata, F., J.Petrol.Technol. 6, 37 (1954)
131. Eilerts, C.K. et al., "Phase Relations of Gas-Condensate Fluids", Vol. 1, Monograph No. 10, U.S. Bureau of Mines (1957)
132. Grieves, R.B., Thodos, G., A.I.Ch.E.J. 6, 561 (1960)
133. Etter, D.O., Kay, W.B., J.Chem.Eng.Data 6, 409 (1961)
134. Grieves, R.B., Thodos, G., A.I.Ch.E.J. 9, 25 (1963)

135. Sutton, J.R., "Advances in Thermophysical Properties at Extreme Temperatures and Pressures", p.76, Am.Soc.Mech.Engrs., New York (1965).
136. Joffe, J., Zudkevitch, D., Chem.Eng.Progr.Symposium Ser. No.81, 63, 43 (1967)
137. Chatterjee, R.M., M.Sc. Thesis, Univ. of Manitoba, Wpg. September, 1965.
138. Campbell, A.N., Kartzmark, E.M., Chatterjee, R.M., Can.J.Chem. 44, 1183 (1966)
139. Abbott, M.M., Ph.D. Thesis, Rensselaer Polytechnic Inst., Troy, New York, August 1965.
140. Gieskes, J.M.T.M., Ph.D. Thesis, Uni. of Manitoba, Wpg. July, 1964.
141. Campbell, A.N., Kartzmark, E.M., Gieskes, J.M.T.M., Can.J.Chem. 41, 407 (1963)
142. Campbell, A.N., Gieskes, J.M.T.M., Can.J.Chem. 42, 186, 1379 (1964)
143. Campbell, A.N., Kartzmark, E.M., Can.J.Chem. 41, 1088 (1963)
144. Campbell, A.N., Kartzmark, E.M., Anand, S.C., Cheng, Y., Dzikowski, H.P., and Skrynyk, S.M., Can.J.Chem. 46, 2399 (1968)
145. Campbell, A.N., Kartzmark, E.M., Can.J.Chem. 45, 2433 (1967)
146. Rice, O.K., J.Phys.Chem. 66, 625 (1962)
147. Kuenen, J.P., Robson, W.G., Phil.Mag. 4, 121 (1902)
148. Herz, W.von, Neukirch, E., Z.Physik.Chem. 104, 433 (1923)
149. Fischer, R., Reichel, T., Mikrochemie ver. Mikrochim.Acta., 31, 102 (1943)
150. Rosenbaum, M., M.S. Thesis, University of Texas, Austin, Texas, August, 1951.
151. Kobe, K.A., Crawford, H.R., Stephenson, R.W., Ind.Eng.Chem. 47, 1767 (1955)
152. Harand, J., Monatsh. 65, 153 (1935)
153. Gornowski, E.J., Amick, E.H., Hixson, A.N., Ind.Eng.Chem. 39, 1348 (1947)
154. Bender, P., Furukawa, G.T., and Hyndman, J.R., Ind.Eng.Chem. 44, 387 (1952)
155. Connolly, J.F., Kandalic, G.A., J.Chem.Eng.Data., 7, 137 (1962)
156. Skaates, J.M., Kay, W.B., Chem.Eng.Sci., 19, 431 (1964)
157. Ambrose, D., Broderick, B.E., Townsend, R., J.Chem.Soc. 1967, Section A, 633.

158. Miller, D.G., *Ind. Eng. Chem.* 56, No. 3, 46 (1964)
159. Kobe, K.A., Lynn, R.E., *Chem. Rev.* 52, 117 (1953)
160. Rowlinson, J.S., "Handbuch der Physik", Edited by S. Flügge, Volume XII, Springer-Verlag, Berlin, 1958.
161. Sage, B.H., Reamer, H.H., *Chem. Eng. Progr., Symp. Ser.*, 48, (2), 3 (1952)
162. Everett, D.H., *Disc. Faraday Soc.* No. 15, 126 (1953)
163. Reilly, J., Rae, W.H., "Physico-Chemical Methods", Van Nostrand, New York, 1939.
164. Benedict, M., Solomon, E., Rubin, L.C., *Ind. Eng. Chem.* 37, 55 (1945)
165. Sage, B.H., Reamer, H.H., *Chem. Eng. Progr. Symp. Ser.*, 48, No. 2, 10 (1952)
166. De Priester, C.L., *Chem. Eng. Progr. Symp. Ser.* 49, No. 7, 1 (1953)
167. Boomer, E.H., Johnson, C.A., *Canad. J. Res. Section B* 16, 328 (1938)
168. Verschoyle, T.T.H., *Trans. Roy. Soc. (London)* A230, 189 (1931)
169. Reid, R.C., Sherwood, T.K., "Properties of Gases and Liquids", McGraw Hill, New York (1958)
170. Reid, R.C., *Chem. Eng. Progr.* 61, No. 12, 58 (1965)
171. Moritz, P., *Acta Chim. Hung. Tomus* 32, 97 (1962)
172. Thodos, G., *A.I.Ch.E.J.* (a) 1, 165 (1955), (b) 1, 168 (1955), (c) 2, 508 (1956), (d) 3, 428 (1957), (e) 4, 356 (1958), (f) 6, 206 (1960), (g) 8, 527 (1962)
173. Campbell, A.N., Chatterjee, R.M., *Can. J. Chem.* 46, 575 (1968)
174. Mathias, M.E., *Mem. Soc. Roy. Sci. Liege, Ser.* 3, ii (1899)
175. Cailletet, L., Mathias, E., *C.R. Acad. Sci., Paris* 102, 1202 (1886) and 104, 1563 (1887)
176. Guye, M., *Archives Sci. Phys. Nat., Ser* 3, Vol. xxxi (1894)
177. Gouy, R., *Compt. Rend.* 115, 720 (1892)
178. Guggenheim, E.A., *J. Chem. Phys.* 13, 253 (1945)
179. Zimm, B.H., *J. Chem. Phys.* 19, 1019 (1951)
180. Habgood, H.W., Schneider, W.G., *Can. J. Chem.* 32, 98, 164 (1954)
181. Landau, L.D., Lifshitz, E.M., "Statistical Physics", Pergamon Press, New York (1958)
182. Edwards, M.H., Woodbury, W.C., *Phys. Rev.* 129, 1911 (1963)
183. Widom, B., *J. Phys. Chem.* 41, 1633 (1964)
184. Gaunt, D.S., Fisher, M.E., Sykes, M.F., Essam, J.W., *Phys. Rev.* 14, 713 (1964)

185. Palmer, H.B., in "Molecular Theory of Gases and Liquids", by Hirschfelder, J.O., Curtiss, C.F., Bird, R.D., John Wiley, New York (1964)
186. Tisza, L., Chase, C.E., Phys. Rev. Letters, 15, 4 (1965)
187. Barieau, R.E., Bureau of Mines Report No. 6950, U.S. Department of Commerce (1967)
188. Myers, D.B., Smith, R.A., Katz, J., Scott, R.L., J. Phys. Chem. 70, 3341 (1966)
189. Goldhammer, D.A., Z. Physik. Chem. 71, 577 (1910)
190. Jüptner, H.v., Z. Physik. Chem. 85, 1 (1913)
191. Lowry, H.H., Erickson, W.R., J. Am. Chem. Soc. 49, 2729 (1927)
192. Cook, D., Trans. Faraday Soc. 49, 716 (1953)
193. Guggenheim, E.A., "Applications of Statistical Mechanics", Clarendon Press, Oxford (1966)
194. Kreglewski, A., Bull. Acad. Polon. Sci., Ser. Sci. Chim. 11, 91 (1963)
195. Michels, A., Blaisse, B., Michels, C., Proc. Roy. Soc., A160, 358 (1937)
196. Schröder, E., Z. Physik. Chem. 129, 79 (1927)
197. Mason, S.G., Naldrett, S.N., Maass, O., Can. J. Res. B18, 103 (1940)
198. Benson, S.W., Copeland, C.S., J. Chem. Phys. 23, 1180 (1955)
199. Fowler, R., Guggenheim, E.A., "Statistical Thermodynamics", Cambridge University Press, Cambridge (1949)
200. Ambrose, D., Division of Chemical Standards, National Physical Laboratory, Teddington, England, Private Communication, July 25, (1968)
201. Francis, A.W., Ind. Eng. Chem. 49, 1779 (1957)
202. Francis, A.W., Chem. Eng. Sci. 10, 37 (1959)
203. McMicking, J.H., Kay, W.B., Proceedings Amer. Petrol. Inst. (Div. of Refining) 45, (III), 75 (1965)
204. Geary, R.C., Leser, C.E.V., American Statistician, 22, No. 1, 20 (1968)
205. Thodos, G., Ind. Eng. Chem. 42, 1514 (1950)
206. Waring, W., Ind. Eng. Chem. 46, No. 4, 762 (1954)
207. Ambrose, D., Broderick, B.E., Townsend, R., J. Chem. Soc., Sec. A, 633 (1967)
208. Cox, E.R., Ind. Eng. Chem. 28, 613 (1936)
209. Cragoe, C.S., "International Critical Tables", Vol. III, p. 228, McGraw Hill Book Co., New York (1928)



210. Frost, A.A., Kalkwarf, D.R., J.Chem.Phys., 21, 264 (1953)
211. Counsell, J.F., National Physical Lab., Division of Chemical Standards, Teddington, Middlesex, England, "Private Communication", November 22nd, 1968.
212. Lyusternik, L.A., Yanpol'skii, A.R., "Mathematical Analysis", Pergamon Press, New York (1965)
213. Klaus, R.L., Van Ness, H.C., Chem.Eng.Prog., Symp.Ser., No. 81, 63, 88 (1967)
214. Tao, L.C., Ind.Eng.Chem. 56(2), 36 (1964)
215. Redlich, O., Kister, A.T., Ind.Eng.Chem. 40(2), 345 (1948)
216. Adler, S.B., Friend, L., Pigford, R.L., Rosselli, G.M., A.I.Ch.E.J. 6, 104 (1960)
217. Herington, E.F.G., Nature 160, 610 (1947)
218. Kay, W.B., Accounts of Chemical Research, 1, (11), 344 (Nov.1968)
219. Bottomley, G.A., Spurling, T.H., Aust.J.Chem. 20, 1789 (1967) and 19, 1331 (1966)